Tartaric acid biosynthesis in plants

By

Seth DeBolt (BSc. Ag. Hons)

A thesis submitted for the degree of
Doctor of Philosophy

School of Agriculture, Food and Wine, The University of Adelaide

Cooperative Research Centre for Viticulture

Department of Plant Pathology, University of California, Davis

TABLE OF CONTENTS

ABSTRACT

The biosynthetic pathway of L-tartaric acid (TA), the form most commonly encountered in nature, and its catabolic ties to vitamin C (AA), remain a challenge to plant scientists. Vitamin C and L-tartaric acid are plant-derived metabolites with intrinsic human value. In contrast to most fruits during development, grapes accumulate L-tartaric acid, which remains within the berry throughout ripening. Berry taste and the organoleptic properties and aging potential of wines are intimately linked to levels of L-tartaric acid present in the fruit, and those added during vinification. Research presented in this thesis begins with a study on the process of biomineralisation in the grape berry. Using ^{14}C tracer studies, it was found that AA has curious divergent pathways, on one hand TA is formed via C4/C5 cleavage of AA and on the other hand, oxalate via C2/C3 cleavage, all within a single plant species. Research then moved towards elucidating genes involved in TA synthesis. The use of transcriptional and metabolite profiling was employed to identify candidate cDNAs from genes expressed at developmental times and in tissues appropriate for L-tartaric acid biosynthesis in grape berries. Metabolic profiling provided the first broad scale screening of organic acids in the family Vitaceae. Enzymological analyses of one candidate confirmed its activity in the proposed rate-limiting step of the direct pathway from vitamin C to tartaric acid in higher plants. To this end, a novel plant protein, L-idonate dehydrogenase, was identified. Surveying organic acid content in *Vitis* and related genera, a non-tartrate forming species was identified in which this gene is deleted. This species accumulates in excess of three times the levels of vitamin C than comparably ripe berries of tartrate-accumulating species, suggesting that modulation of tartaric acid biosynthesis may provide a rational basis for the

production of grapes rich in vitamin C. Other genes isolated using transcriptional profiling were then tested for activity in the TA synthetic pathway. Characterisation of one candidate, encoding a putative homolog of transketolase, suggested a potential role in the cleavage of 5-keto D-gluconic acid to the 4-carbon precursor of TA Additionally, the enzyme showed activity against intermediates found within the oxidative pentose phosphate pathway, suggesting the need for further characterisation of its in vivo function. The focus of research then turned to experiments that were conducted with the intent of informing viticultural practices, where canopy management is used to modulate light penetration to individual clusters. Individual berry clusters were shaded from light and the results revealed that light played a significant role in TA accumulation and malic acid dissimilation in the grape berry. At the time of peak TA biosynthesis, organic acid levels and L-idonate dehydrogenase transcript levels were quantified. The results revealed a strong reduction in TA pools and corresponding decreases in L-IdnDH transcript, while levels of malate and oxalate were unaffected. To summarise, research presented in this thesis extends the understanding of grape berry metabolism by characterising dual metabolic fates for AA. Moreover, the success of combining transcriptional and metabolic profiling towards targeting a specific pathway in non-model plants was demonstrated. The key result of this research was the discovery of L-idonate dehydrogenase, which acts to oxidise L-idonate in the tartaric acid synthetic pathway. Furthermore a grape transketolase capable of carrying out a second step in the pathway was isolated and part characterised. Finally, these data present results of relevance to the applied practice of viticulture, because they reveal a differential impact of light on specific organic acids, relative to others.

STATEMENT OF AUTHORSHIP

The work contained in this thesis bears within no material which has been accepted for the award of any other degree or diploma in any University or other tertiary institution and, to the best of my knowledge and belief, contains no material previously published or written by another person, except where due reference is made in the text.

I give consent to copy this thesis and when deposited in the University library, being available for loan and photocopying.

Seth DeBolt

ACKNOWLEDGEMENTS

Firstly I would like to extend a massive thanks to my principle and external supervisors Christopher M. Ford and Douglas R. Cook whom had the greatest impact on my studies and also a big thanks to my third supervisor Steve Tyerman whom is an incredibly insightful scientist that I regret not having more time with from which to learn. Chris has shown me respect, been interested, thoughtful and kept my wayward ideas grounded at the same time as allowing me unlimited freedom to explore where my own interests lied. I think we make a great team. Doug too has been wonderful mentor. During the year I spent with his group at UC-Davis I gained confidence in many aspects of molecular biology. Doug was encouraging and insightful and has become a friend, and whether snowshoeing up Yosemite Valley or having a port and cigar, it has been great.

I also gratefully acknowledge my colleagues at UC Davis: Alberto Iandolino provided me with insight and berry samples, Francisco Goes da Silva with transcriptional profiling, Brendan Riley with molecular biology tips, Ben, Hong-Kyu, Varma and Ana are also thanked. In Adelaide, I thank Susan Wheeler for RNA samples, Patrick Iland and Renata Ristic for berry samples, Jim Hardie for photographs, Meg, Kate (2), Pat, Brent Kaiser for technical advice, Peter Høj and Dry as coordinators, Steve Clarke and Chris Day for wine tasting and wine making experience, Simon Robinson and Nicole Cordon for an RNA sample, and Bradley Geautrix for assistance with grinding berries and HPLC technical assistance in chapter 7. Thanks to Kandace Brooke my friend and fiancée. To my parents Tom and Linda DeBolt, I thank them for encouraging me to be happy, which somehow led me here.

ABBREVIATIONS

°C- degrees Celsius

^{14}C –carbon 14 isotope

5KG- 5-Keto D-gluconic acid

AA –Vitamin C, L-ascorbic acid

ATP- adenosine tri phosphate

bp- base pairs

BSA- bovine serum albumen

CaOxA- calcium oxalate

CaT- Calcium tartrate

cDNA- complimentary DNA

CO_2 - carbon dioxide

Contig- A gene or partial gene sequence based upon assembled overlapping ESTs

cv- cultivar

DAF- days after flowering

dH_2O- deionised water

DHA- dehydro ascorbic acid

DNA- deoxyribonucleic acid

EST- expressed sequence tag

FW- fresh weight

gm -grams

HCl- hydrochloric acid

HPLC- high performance liquid chromatography

K_2T- dipotassium tartrate

kb-kilobase

KHT- Potassium hydrogen tartrate

K_m - Michaelis constant

K_{sp}-solubility product

L- litre

LC-MS- liquid chromatography mass spectrometry

L-IdnDH- L-idonate dehydrogenase

MP- Mehler Peroxidase reaction

mg- milligrams

mM- millimolar

MM- Michealis Menten

mRNA- messenger RNA

NAD^+- nicotinamide adenine dinucleotide (oxidized form)

NADH- nicotinamide adenine dinucleotide (reduced form)

$NADP^+$- nicotinamide adenine dinucleotide phosphate (oxidized form)

NADPH- nicotinamide adenine dinucleotide phosphate (reduced form)

OPPP- oxidative pentose phosphate pathway

ORF- open reading frame

OxA- Oxalic acid

P- phosphate

PAGE- polyacrylamide gel electrophoresis

PCA- principle component analysis

PCR- polymerase chain reaction

pK_{1-} dissociation constant

PSI- photosystem one

PSII- photosystem two

PV- pre veraison

PVP- poly vinyl pyrrolidone

RQ- respiratory quotient

RNA- ribonucleic acid

RNAi- ribonucleic acid interference

RTPCR- reverse transcriptase PCR

SEM- scanning electron microscopy

TA- L-Tartaric acid [(*2R, 3R) 2*,3-dihydroxybutanedioic acid, ($HO_2CCHOHCHOHCO_2H$)]

Taq- *Thermus aquatica*

TC- tentative consensus sequence

TCA- tri carboxylic acid / trichloroacetic acid

TEM- transmission electron microscopy

ThA- Threonic acid

Tris- *tris*(hydroxymethyl)aminomethane

V_{max} – maximal velocity

w/w –weight per weight

µL- micro litre

PUBLICATIONS

Parts of the work described in this thesis have been published or submitted for publication in the following:

Experimental

DeBolt, S., Hardie, J., Tyerman S.D. and Ford, C.M. (2004) Composition and synthesis of raphide and druse crystals in berries of *Vitis vinifera* L. cv. Cabernet Sauvignon: the role of ascorbic acid as the biosynthetic precursor of both oxalic and tartaric acids is revealed by specific radio labelling studies. *Aust. J. Grape Wine Res.* **10,** 134-142.

DeBolt, S., Cook, D.R. & Ford, C. M. (2006) L-Tartaric acid synthesis from vitamin C in higher plants. *Proc. Natl. Acad. Sci..* USA. **103,** 5608-5613.

DeBolt, S., Iandolino, A., Cook, D. R. and Ford, C. M. Analysis of grapevine transketolase I for activity in the OPPP and tartaric acid synthesis. Manuscript in preparation

DeBolt, S., Ristic, R., Iland, P. & Ford, C. M. Light interference affects organic acid synthesis in berries of the grapevine *Vitis vinifera* cv. Shiraz. Manuscript in review

Patent

DeBolt S. Cook D.R. and Ford, C.M. **(2005)** Provisional patent 503479. Invention Title: Tartaric acid biosynthesis in plants: Involved cloning and characterisation of key gene and protein involved in tartaric acid synthesis and its knockout to create grape rich in vitamin C.

Review

DeBolt, S., Melano,V. and Ford, C. M. Vitamin C catabolism to tartaric and oxalic acids in higher plants. *Annals of Botany*, requested and in preparation

Conference papers

2003 DeBolt S, Tyerman, S and Ford CM Biosynthesis of organic acids in the grapevine, **Combio,** Melbourne, Australia

2004 DeBolt S, Ford CM. Towards and understanding of tartaric acid biosynthesis in the grapevine berries, **7th International Symposium for Grapevine Physiology and Biotechnology**. Paper: Session 1. The University of California, Davis

2004 DeBolt S, Goes da Silva, F, Iandolino A, Choi, H, Ford CM and Cook DR. In silico analysis of the grapevine transcriptome: identification of candidate genes for tartaric acid biosynthesis, **Plant and Animal Genome** XIII Conference Poster session

2004 DeBolt S, Goes da Silva, F, Iandolino, A, Choi, H, Ford, CM, Tyerman, S and Cook, DR. In silico analysis of the grapevine transcriptome: identification of candidate genes for tartaric acid biosynthesis. Poster presentation, **Combio**, Perth, Australia

2004 DeBolt S., Hardie J., Tyerman S., and Ford CM. Composition and synthesis of raphide and druse crystals in berries of *Vitis vinifera* L. cv. Cabernet Sauvignon: the role of ascorbic acid as the biosynthetic precursor of both oxalic and tartaric acids is revealed by specific radio labelling studies. **The Australian Journal of Grape and Wine Research**. 10. 2 pp. 135-142.

2005 DeBolt S, Goes da Silva, F, Iandolino A, Choi, H, Cook DR, and Ford CM Sour grapes indeed - the first molecular and biochemical step in the tartrate biosynthetic pathway in Eukaryotes, Paper **1st International Grape Genomics Symposium**, St Louis, Mo

2005 DeBolt S. Towards understanding tartaric acid synthesis in plants. **Cooperative Research Centre for Viticulture Symposium**. Paper, session on grapevine genomics, chair Prof. Simon Robinson

2005 DeBolt S Cook, DR, and Ford CM. Combining transcriptional and metabolic profiling towards novel gene discovery. Paper: **Combio,** Adelaide, Australia

2006 DeBolt S Cook, DR, and Ford CM. Tartaric acid biosynthesis in higher plants. Paper. **PAGXIV**

LIST OF TABLES

LIST OF FIGURES

LIST OF EQUATIONS

Chapter 1

General Introduction

1.1 Introduction

During their development, grape berries accumulate substantial levels of organic acids (Ruffner, 1982). The most abundant of these, tartaric acid (TA) and malic acid (MA) (Terrier and Romieu, 2001), play important roles in grape and wine quality specifications, providing a combination of low pH conditions that protect juice, must and wine from oxidative and microbial spoilage, and organoleptic properties that contribute to palate and flavour expression of the wine (Jackson, 2000).

In the developing grape berry, TA has been shown to accumulate rapidly pre-veraison, and thereafter to remain at constant levels (w/w), while MA, although also synthesised pre-veraison, is rapidly broken-down at the onset of berry ripening and utilised as a metabolic substrate via the TCA cycle (Iland and Coombe, 1988). Unlike MA, TA is not a substrate for the normal catabolic processes of the cell, nor is it degraded during vinification by malo-lactic bacteria. Consequently, it is an ideal and vital component of wine; adjustments of acid levels for pH management and specific wine-style outcomes are made by the addition of exogenous TA. Tartaric acid is therefore an economically important compound, a rough estimate based on an across-Australia average addition level of 4g TA per litre of juice or must processed and a cost of $8 per kg TA suggests that for the 2001 vintage, the Australian wine industry spent $AU 32 M on the addition of TA. At times during the 2001 vintage, the price for TA was approximately 50% greater than that quoted here, so in total the cost may have exceeded $AU 40 M.

The famous French scientist Louis Pasteur began his illustrious career at the age of 26, with an investigation of the crystallography of TA, and thus was the first to demonstrate the existence of optical isomers (Pasteur, 1860). The biosynthesis of TA and its catabolic ties to vitamin C have since posed significant challenge to plant scientists (Stafford 1958, 1959, Loewus and Stafford, 1958, Hale, 1962, Saito and Kasai, 1969, 1984, Ruffner, 1982, Iland and Coombe, 1988, DeBolt *et al.*, 2004, Green and Fry, 2005). The aim of the research described in this thesis is to further extend the understanding of this metabolic pathway, at a fundamental scientific level, and more intriguingly, to seek an answer to how and why grape berries accumulate this rare organic acid. Basic interest in the biochemistry of TA has lagged far behind

its industrial and oenological importance. Since a brief but productive period of interest between the late 60's and early 70's, TA biochemistry has commonly been a side pocket in research programs- a matter of interest linked to its stereochemical properties and catabolic ties to vitamin C (AA) (Loewus and Stafford, 1958, Saito and Loewus 1989, summerised in a review by Loewus, 1999 and recently Green and Fry, 2005).

Three pathways have been proposed for TA biosynthesis in plants. Two of these arise from AA and one from gluconic acid (Saito and Kasai, 1969, 1984, Saito and Loewus, 1989a,b). In the formation of TA from AA, a six carbon intermediate is cleaved either between either position C2/C3 or C4/C5 in specific plant species. The former pathway yields oxalic acid and TA, the latter yields TA and 2-carbon glycoaldehyde that is cycled to hexose metabolism (Saito and Kasai, 1984). In *Vitis vinifera,* ripening berries use the C4/C5 route, with TA biosynthesis occurring exclusively in the period of development between anthesis and veraison (Malipiero *et al.,* 1987, DeBolt *et al.*, 2004). A very minor component of the total TA in the grape berry (approx. 5 %) is synthesised via the gluconic acid pathway (Saito and Kasai, 1984). All pathways are discussed in detail further in this chapter.

Little is known about the processes by which TA is made during grape berry development, its role in the cell or the mechanisms that control its accumulation. Work carried out in the 1980s showed that viticultural management, particularly of canopy architecture and the consequences for bunch shading (Jackson, 1986, 2000) had significant impact on levels of TA via elevated potassium ion (K^+). This research however did not address the processes underlying TA biosynthesis; rather it addressed the fate of existing TA. The biochemical pathway by which TA is made in the grapevine has been inferred from the detection of specific intermediate compounds following feeding experiments using radioactively labelled substrates (Saito and Kasai, 1969, 1984, Saito and Loewus, 1979); no data exists concerning the enzymes involved in its synthesis or dissimilation nor the genes that encode them. The primary objectives of this thesis are to address long standing questions regarding the pathway to TA synthesis in the grapevine. In this review, relevant research is surveyed to provide insight into physiological, biochemical and viticultural aspects of TA accumulation, and to highlight what is known, what is hypothesised and what is unknown about TA synthesis.

1.2 Tartaric acid

Nomenclature

L-Tartaric acid, *(2R, 3R) 2*,3-dihydroxybutanedioic acid ($HO_2CCHOHCHOHCO_2H$) in its pure form occurs as a white crystalline dicarboxylic acid. As discovered in Louis Pastuer,s famous publication of 1860, TA occurs as three distinct isomers and one racemic mixture, the *dextro-, levo-,* and *meso-* forms, and the DL form. The *dextro-* and *levo-* forms are optically active; the *meso-* form is optically inactive, as is racemic acid, a mixture of equal parts of the *dextro-* and *levo-* forms (Pasteur, 1860) (Figure 1.1). The two isomers of TA that occur in nature are primarily the *levo* and *dextro,* the levo form occurring in many plants (Stafford, 1958) and the *dextro* form occurring in several microrganisms (Stafford, 1957). TA is one of the strongest organic acids, with a first dissociation constant (pK1) of 2.98 (Table 1.1); the extent of its dissociation is dependent on the pH of the surrounding aqueous solution (Figure 1.2). Conventionally *(2R, 3R) 2*,3-dihydroxybutanedioic acid is referred to as L-TA, but the more formal L-threarate is also used in some literature (Green and Fry, 2005ab). It is referred to as tartaric acid or TA in the present review. The use of 'TA' in oenological circles encodes titratable acidity; in this review 'TA' encodes tartaric acid only.

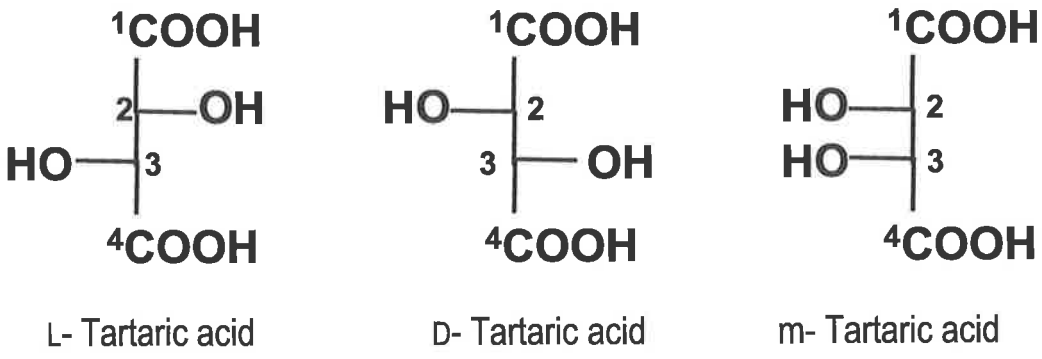

Figure 1.1 Tartaric acid occurs as a four carbon dicarboxylic acid in three isomeric forms, *levo, dextro* and *meso*: D and L are optically active and m is optically inactive.

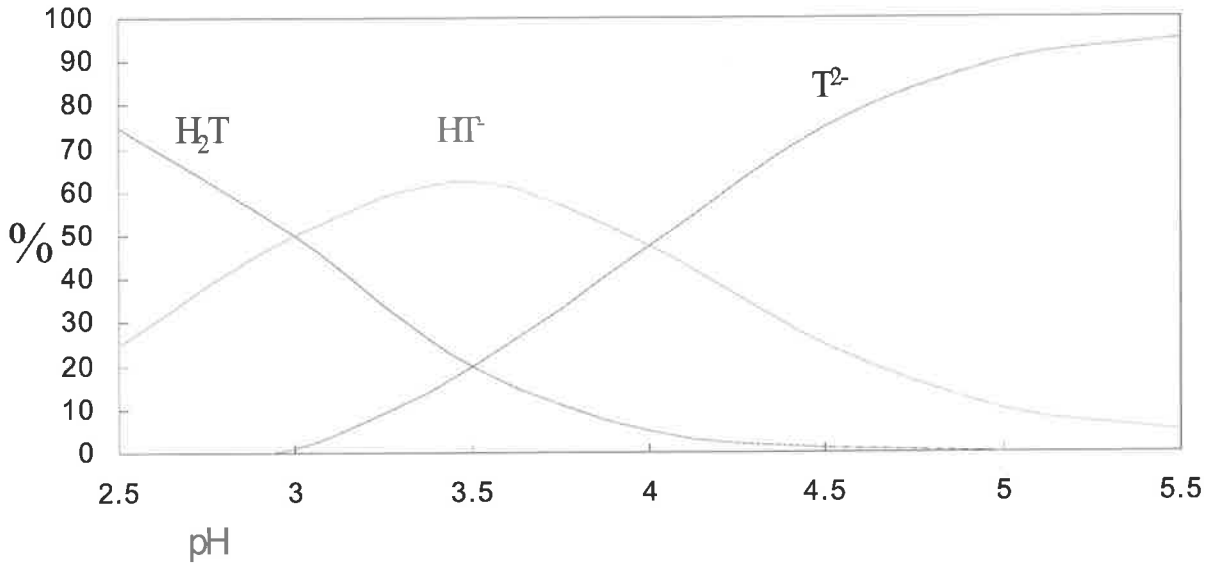

Figure 1.2 Dissociation of L (+) tartaric acid at various pH levels (Mattick *et al.,* 1980 *Am. J. Eonol. & Vitic*, Iland, 1984 (Masters Thesis))

Table 1.1 Dissociation constants (K) and pK values for L (+) tartaric acid

	Step 1	Step 2
Tartaric acid (TA)	$H_2T \rightleftharpoons H^+ + HT^-$	$HT^- \rightleftharpoons H^+ + T^{2-}$
	K_1 1.04×10^{-3}	K_2 4.55×10^{-5}
	pK_1 2.98	pK_2 4.34

The biosynthesis of tartaric acid in plants

Compared to the major organic acids found in plants, such as malate (Famiani *et al.*, 2000, 2005), citrate, succinate, ascorbate (Smirnoff, 2001), fumarate and oxalate (Franchesci and Nakata, 2005), little attention has been paid to the formation of TA. In a survey of TA accumulation in angiosperms (Stafford, 1958), it was shown that the grapevine was the most economically significant plant crop to accumulate this rare organic acid. TA is practically resistant to metabolic breakdown (Iland and Coombe, 1988) making it a key quality attribute of wine. Other organic acids occurring in the grape, such as malate and citrate, are metabolised in the grape during the latter stages of development as well as during primary and secondary fermentation, whereas TA remains inert, able to stabilise pH and influence the organoleptic properties of wine.

In the grape vine, TA is proposed to be a metabolic derivative of L-ascorbic acid (AA) or gluconic acid (Saito and Kasai, 1969, 1982, 1984, Saito and Loewus, 1989ab, DeBolt *et al.* 2004, Green and Fry, 2005). Understanding AA in the grapevine is therefore important to understanding TA. AA is perhaps the most important regulator of the redox potential of the cell (Smirnoff, 2001), making the highly active catabolic pathway of TA formation of great interest at a cellular level. Vitamin C in plants has been linked to cell division, cell expansion, photosynthesis and many stress related responses (Smirnoff, 1996). Its biosynthesis in plants has only recently been solved, and involves oxidation of L-galactose to galactono-lactone, which is further oxidised form the ascorbate molecule (Wheeler *et al.* 1998). This is considered the 'non-inversion' pathway (Loewus and Loewus, 1987), since in the conversion from D-glucose, there is conservation of the hydroxymethyl group at C6 and an epimerisation at C5 to form AA.

In the plant, AA is an extremely important metabolite, it is initially synthesised during plant germination and continues to be formed in regions of active growth throughout the life span of the plant (Loweus, 1999). Shown to be translocated, AA can readily travel from leaves to floral and fruiting parts of *Arabidopsis* (Franchesci and Tarlyn, 2002), but no such research on transport or site of synthesis has occurred in the grapevine, with on site AA formation in the berry the most likely pathway to synthesis. Ascorbic acid functions in plants as an enzyme cofactor (Smirnoff, 2000), in the detoxification of reactive oxygen species (Conklin,

2001, Francisco *et al.,* 2002), and is associated with photoprotection (Smirnoff, 2000) and protection against wounding and insect herbivores (Conklin, 2001). The metabolism of ascorbic acid within the apoplast (ie the extracytoplasmic spaces within cell walls) has been proposed to have a significant role in cell wall expansion and elasticity (Green and Fry, 2005a, b) and more directly associated signalling, cell expansion and division (Smirnoff, 1996). The importance of AA extends to an intrinsic human value as a vital micronutrient. We as humans lack the necessary enzymes responsible for its biosynthesis (Nishikimi *et al.*, 1994) making it necessary for us to acquire it externally, therefore understanding its accumulation and metabolism in plants will help scientists towards maximising nutritional composition of plants. Moreover, as humans are rarely deficient in dietary AA, it should be noted that the importance of AA is strongly associated with plant growth and protection.

Hough and Jones (1956) first suggested that TA was a product of AA metabolism rather than primary oxidative metabolism of sugars. This inference led to Loewus and Stafford (1958), using 6-^{14}C-AA, to test the loss of C1 and C2 of ascorbic acid and the oxidation of the terminal carbons of the C4 fragment to form TA in a detached grapevine leaf. They unfortunately found that virtually none of the ^{14}C radiolabel appeared in TA from grape leaves, and concluded that there was negative evidence for a direct pathway from AA to TA. Saito and Kasai (1968) subsequently showed that grape berries were able to fix ^{14}C-labeled CO_2 into TA within 8 hours of exposure in the dark. This led to the conclusion that TA was being made from sugars formed by photosynthetic activity (Saito and Kasai, 1968). These authors subsequently tested various sugars for their ability to support TA biosynthesis and found that none were effective. Sugar derivatives were then tested, and uniformly labelled glucurono-1,4-lactone and AA were found to incorporate a considerable amount of radiolabel through to TA (Saito and Kasai, 1969). In a perhaps brilliant insight, 1-^{14}COOH AA, rather than 6-^{14}C AA, was tested and found to be highly effective, with 72% of the radioactivity appearing in TA; the results of this experiment were reported in what has become the decisive paper in TA biosynthesis (Saito and Kasai, 1969). Further work using [1-^{14}C] and [6-^{14}C] AA, confirmed that a product of AA metabolism was cleaved between carbons 4 and 5 (C4/C5), with the 4-carbon (C4) fragment being converted to TA (Figure 1.3)(Wagner *et al.,* 1975, Saito and Kasai, (1982, 1984), Saito and Loewus, 1989). The identities of the intermediate compounds between AA and TA were determined by Saito and Kasai (1982, 1984),

who discovered by the addition of iodoacetic acid, which acts to modify cysteine residues and thereby inhibit enzyme activity, three intermediates between AA and TA containing radiolabel. The three intermediates compounds are D-xylo-2-hexulosonic acid (2-keto-L-gulonic acid), L -idonic acid and D-*xylo*-5-hexulosonic acid (5-keto- D-gluconic acid (5KG)) (Figure 1.3). Saito and Kasai (1989b) showed that in the bean plant (*Phaseolus vulgaris*), the accumulation of 5KG was the limiting factor controlling synthesis of TA. In cultivars that were not accumulating TA in appreciable amounts, when 5-KG was added there was up to 200 fold increases in formation. Malipiero *et al.* (1987) effectively used a time course study of 14C-AA conversion to TA in *vivo* to show that the oxidation of idonate to 5-keto gluconic acid is the regulatory step. Their data showed high relative percentages of radioactivity arresting in idonate, both in TA synthesizing tissue (10 %) and in tissue past its biosynthetic peak (25 %), compared with the rapid ^{14}C interconversion kinetics seen between the other intermediates.

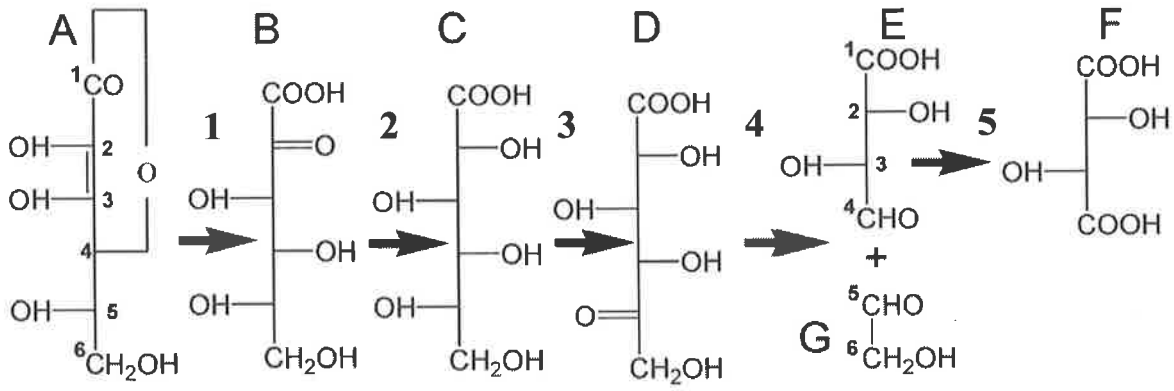

Figure 1.3 The primary biosynthetic pathway for tartaric acid formation in Vitaceous plants the conversion from idonate [C] to 5 keto gluconate [D] is the only the enzyme characterised (3) as discussed in chapter 3, 4 and 5. A ascorbic acid, B 2-keto L-gulonic acid, C idonic acid, D 5-keot D gluconic acid, E tartaric acid semi aldehyde, G putative glycoaldehyde and F tartaric acid

In the formation of TA from AA, a second pathway exists but occurs only in the family *Geraniaceae* (summarised by Banhegyi and Loewus, 2004). Ascorbic acid is cleaved at the C2/C3 (2/3) position, yielding oxalic acid (OxA) and threonic acid (ThA), which is further oxidised at the fourth carbon to form TA (Wagner and Loewus, 1973, Saito and Loewus, 1992) (Figure 1.4).

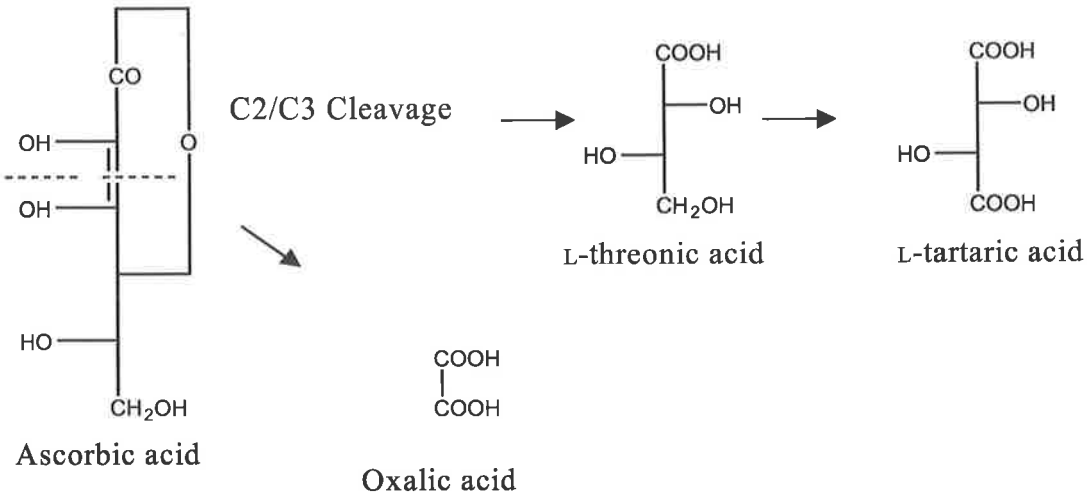

Figure 1.4 Biosynthetic pathways for tartaric acid formation in Geraniaceous plants. Note that although oxalate-accumulating plants use this pathway up to the formation of L-threonic acid, this compound is not always oxidised to form TA. Recently, details of this pathway have been revised in the family Rosaceae (Green and Fry, 2005)

The third pathway to TA does not include AA (Figure 1.5). Instead it utilises the C1-C4 of the glucose molecule to form to D-gluconic acid, 5-KG and finally TA (Figure 1.5) (Saito and Loewus, 1989c). Species of legume (*Bauhinia reticulata, Phaseolus vulgaris*) occur that synthesise TA in the leaf (Stafford, 1959, Saito and Loewus, 1989c). This pathway was confirmed to be the biosynthetic pathway for TA accumulation in legumes when Saito and Loewus (1989c) showed that TA accumulating cultivars of *P. vulgaris* (bean plant) followed the D-gluconic acid

pathway (Saito and Loewus, 1989b and c). This AA non inclusive pathway also functions in the grapevine, but only to a very small extent (Saito and Loewus, 1989a), with between 2 and 9 % of the TA formed via this mechanism. This pathway and its importance in the grapevine need to be reconfirmed due to a new pathway for AA biosynthesis (Wheeler *et al.,* 1998) influencing the method of calculating relative amounts of TA.

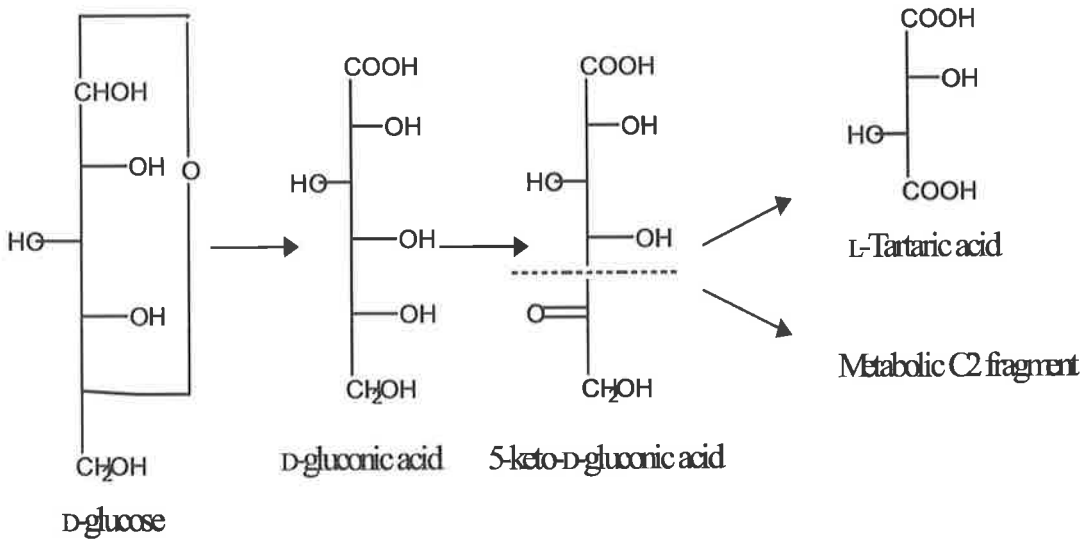

Figure 1.5 The minor pathway for TA biosynthesis in grapevines and major pathway for TA synthesis in leguminous plants

The question of why and how TA is accumulated via more than one pathway in the grape remains unclear and needs further investigation. Its relationship to photosynthesis inferred by the findings of Saito and Kasai (1969) suggests clues to the proposed direction of further studies in this area. Furthermore, two additional pathways for AA biosynthesis have been proposed recently. Agius *et al.* (2003) engineered increased vitamin C levels in *A. thaliana* by over-expressing a D-galacturonic acid reductase cloned from strawberry fruit. *Myo*-inositol is also proposed as a new intermediate in L-ascorbic acid biosynthesis (Lorence *et al.,* 2004). If these pathways apply to the grape vine, there may be at least three pathways of AA

formation, whose expression and activities are likely to involve temporal and spatial differences. Whether these three pathways pool the AA or whether AA from the different pathways has a different catabolic fate has not been tested.

Dissimilation of tartaric acid

Little has been reported on the metabolism of tartrate, as its concentrations in the berry remain fairly constant after veraison. Stafford (1957) reported the activity of an enzyme TA dehydrogenase, but this acts on the *meso* form only. Subsequently, Peynaud and Maurie (a French paper, as translated and reported by Ruffner, 1982) suggested metabolism of tartrate, based on high respiratory quotient values in the ripening grape, particularly at high temperatures. Then Takimoto *et al.* (1976) provided some strong conjecture by the use of ^{14}C radiolabelled CO_2 studies, and showed that TA may not completely be biochemically inert in the grape berry. But critically, confusion in the Takimoto paper may exist between loss due to metabolism and formation of insoluble KHT and CaT complexes.

Enzymes of tartaric acid biosynthesis

The cleavage of 5-KG to yield TA is common to both the D-gluconic acid and AA pathways of TA biosynthesis in grapevine tissue (Wagner *et al.*, 1975, Saito and Kasai, 1984) (Figure 1.3 and 1.5), but interestingly is the only common interconversion among the two pathways. Saito and Kasai (1984) suggested that the C4/C5 cleavage of 5KG is a non-enzymic step. Furthermore, Saito and Loewus (1989b) found that the presence of 5KG was the limiting step for TA formation in the bean plant. Malipiero *et al.* (1987) performed a comprehensive time-course analysis of the pulse feeding radiolabelled AA to grape berries and concluded that it is unlikely to be non-enzymic. Furthermore, they report that L-idonate oxidation is likely to be the rate-limiting step in the pathway. They further showed via kinetic analysis that ascorbate loss in the system was highly correlated with L-idonate and TA accumulation. In a more recent and conclusive report Saito *et al.* (1997) incorporated $^{18}O_2$ and ^{14}C into grape tissue and via stoichiometric calculation showed that in fact

the final reaction of the pathway converting 5-KG to TA is highly likely to be enzymatic, involving a hydrolase reaction. This thesis was further supported when a group from Finland, working on metabolism in *Gluconobacter suboxidans* suggested the involvement of a transketolase in the catalytic mechanism for a similar conversion based on preliminary enzymatic data (Salusjarvi *et al.*, 2004). Transketolases are common proteins in the oxidative pentose phosphate pathway (Caillau and Quick, 2005). The fact that the breakdown of 5KG is common to two pathways may suggest the use of a common plant protein such as a transketolase to carry out the reaction. Although not investigating plant metabolism, Salusjarvi *et al.* (2004) also suggested that an aldehyde dehydrogenase might be responsible for the conversion of TA semi aldehyde to TA in the grape. Much remains unknown in the biosynthesis of TA and understanding the enzymes involved in the pathway would go a long way to elucidating the functional roles of this pathway and its impact on the cell.

1.3 Other grape organic acids

The combined concentration of MA and TA makes up more than 90% of total berry acidity (Terrier and Romieu, 2001). Other organic acids such as citric, fumaric, succinic, formic, acetic, glycolic, lactic, aconitic, quinic, shikimic and mandelic acids occur in very small amounts (summarized by Ruffner, 1982)(Figure 1.6). In the grape berry, organic acid accumulation occurs between anthesis and veraison (Iland and Coombe 1988). At veraison, acid accumulation ceases and sugars are translocated into the grape berry (Kliewer, 1966). In the grape MA is metabolised post veraison; Iland and Coombe (1988) showed an 81 % decrease in MA post veraison. It must be noted that some of this decrease was attributable to grape volume increase. TA on the other hand remains inert, excluding the effect on concentration of berry volume increase post veraison (Kliewer, 1966, Iland and Coombe, 1988). Maximum TA accumulation occurs in the first 20 to 30 days post anthesis, whereas maximum MA accumulation occurs just prior to verasion at 40 to 60 days post anthesis (Possner and Kleiwer, 1985, Terrier and Romieu, 2001)(Figure 1.7). The studies that were performed to determine the time of maximum organic acid synthesis measured levels of acid using HPLC but failed to show where and how these acids were made.

I

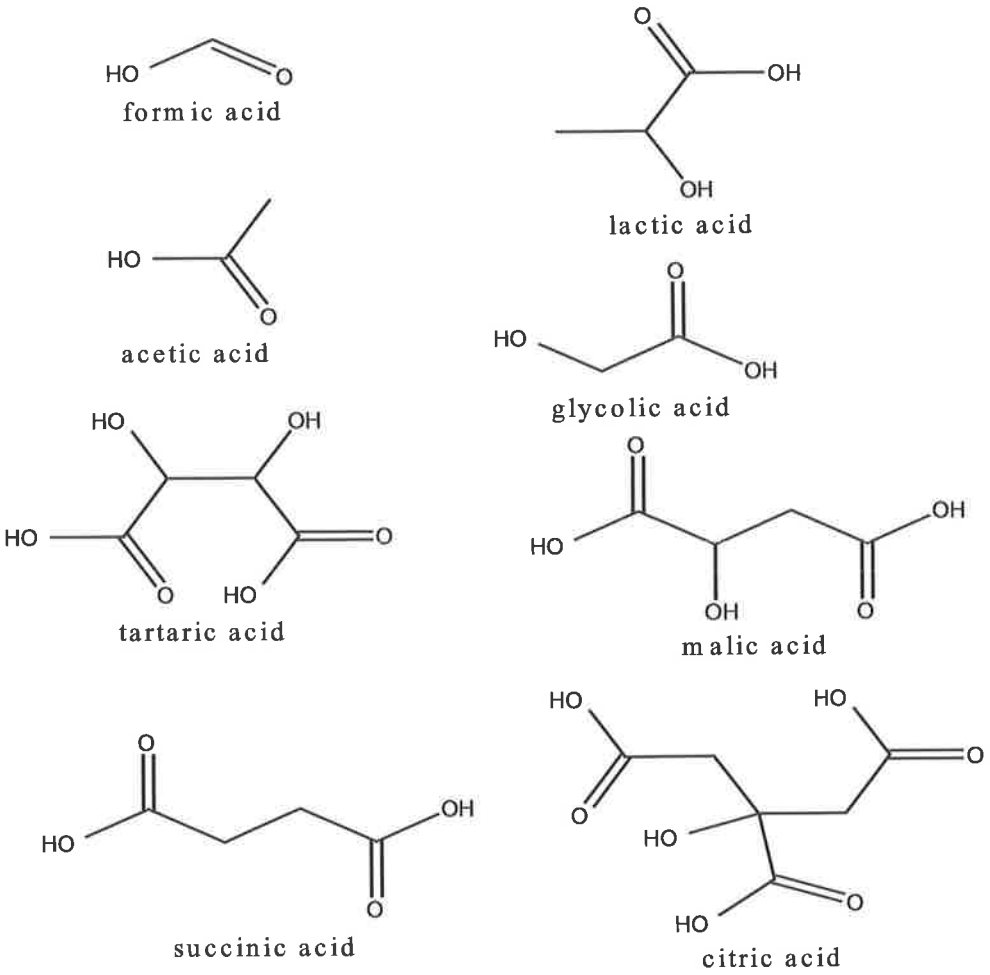

Figure 1.6 Chemical structures of the common grape organic acids

As in many fruits the MA and citric acid content decreases with ripening, it has been suggested that the two-tiered cycle of acid then sugar accumulation in grape berries is due to co-evolution with birds (Hardie, 2000 although first suggested by van der Pijl, 1982). Accumulation of acid before the seed is developed makes the berry

unpalatable to willing avian dispersers, but after veraison sugar accumulation along with colour change indicates the seed is ready to be dispersed.

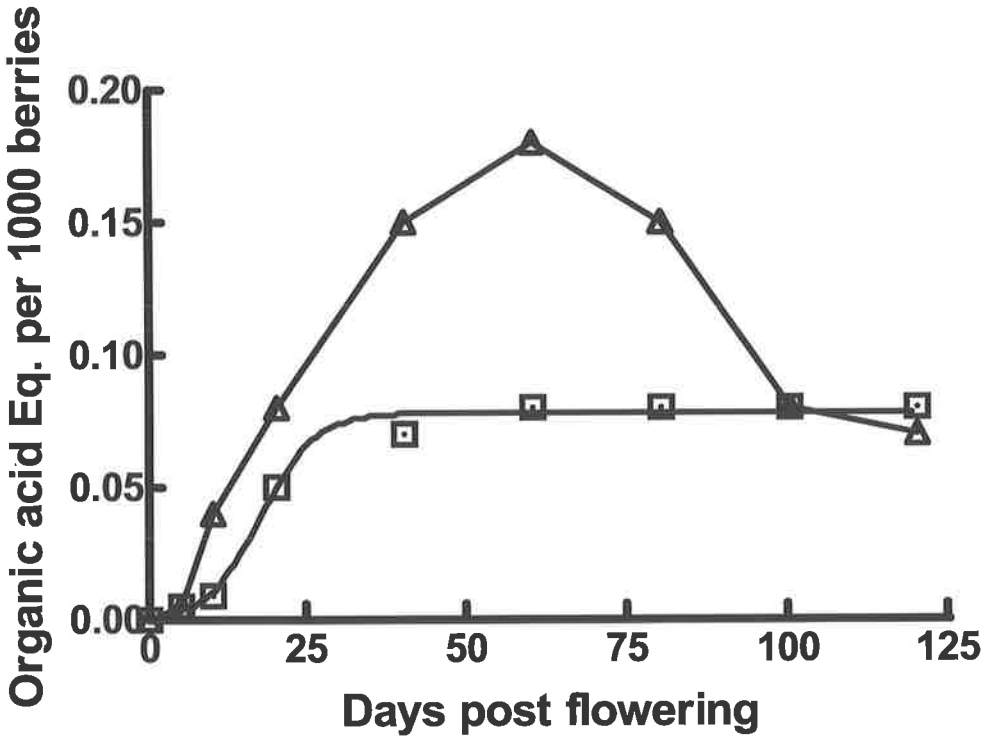

Figure 1.7 Synthesis of malic and tartaric acid in the developing grape berry (adapted from Terrier and Romieu, 2001), the open squares represent tartaric acid and the open triangles indicate malic acid

1.4 Tartrate transport and location in the grape

Early research into organic acid accumulation in the grape berry by Peynaud and Maurie, (1958), translated by Ruffner, (1982), suggested that TA was translocated from leaves to the berry (also put forward by Winkler *et al.,* 1974). But translocation-blocking experiments by Hale (1962) and ^{14}C labelled TA experiments by Malipiero *et al.* (1987) showed that a large proportion, if not all of the TA in grape berries was synthesised locally. The relatively low photosynthetic ability of the grape berry,

compared with leaves, means that it relies on imported assimilates, sucrose being the main translocated substance (Ruffner, 1982). Therefore, the conclusion was drawn that organic acids are synthesised in the berry from imported carbohydrates. According to Terrier *et al.* (1998), grape berry organic acids are synthesised in the cytoplasm. It must be noted however that the excision of the berry from the peduncle as performed in these experiments may create a stress response associated with TA synthesis

When the grape berry is green in its pre-veraison stage, berry cells accumulate an enormous amount of acid in their vacuoles, estimated by Ruffner, (1982) at 0.45 eq. L^{-1} of fully protonated MA and TA. Early in berry formation large vacuoles are present in the pericarp (Harris *et al.,* 1968), and cell division is occurring rapidly (Terrier and Romieu, 2001); after this initial cell division stage and until approximately 4 weeks post flowering, cells no longer divide and the increase in berry volume is due to cell expansion. Terrier *et al.* (1998) looked in detail at the vacuolar changes associated with transport of organic acids in grapes. They showed that transport rates for organic acids are not summative, and that acids are most likely transported to the vacuole across the tonoplast via an organic acid channel (Terrier and Romieu, 2001). The dicarboxylic acid channel has been characterised for malate in Arabidopsis (Emmerlich *et al.*, 2003). This channel is coupled with the activity of pyrophosphatase (V-PPase) during pre veraison stage and via V-Adenosine triphosphatase (V-ATPase) during ripening (Figure 1.8), which creates a cationic charge gradient inside the vacuole needed to pull anions from the cytoplasm to the vacuole (Terrier *et al.,* 1998). Storage of malic, tartaric and citric acids as major osmotica leads to the large increase in mean volume of the pericarp cells between anthesis and ripening (Terrier and Romieu, 2001).

Concentrations and compartmentation of TA in the grape berry have been previously studied (Hale, 1977, Possner and Kliewer, 1985, Iland and Coombe 1988). Possner and Kliewer (1985) demonstrated the location of acids in grape by dividing the grape berry into four concentric zones and showed that the posterior end (furthest from the pedicel) accumulates 35% less TA than the anterior end. Further results of this research showed that MA and TA have opposing concentration gradients. Malic acid increased in concentration from the periphery to the seed, whereas TA increased from the seed to the periphery. Tartrate accumulates in grape berries pre-veraison, and subsequently remains at constant levels per berry throughout ripening. Tartrate in the

berry tends to be converted to soluble salt forms as ripening progresses, furthermore as berries approach ripeness relative amounts of tartrate increase in the skin compared

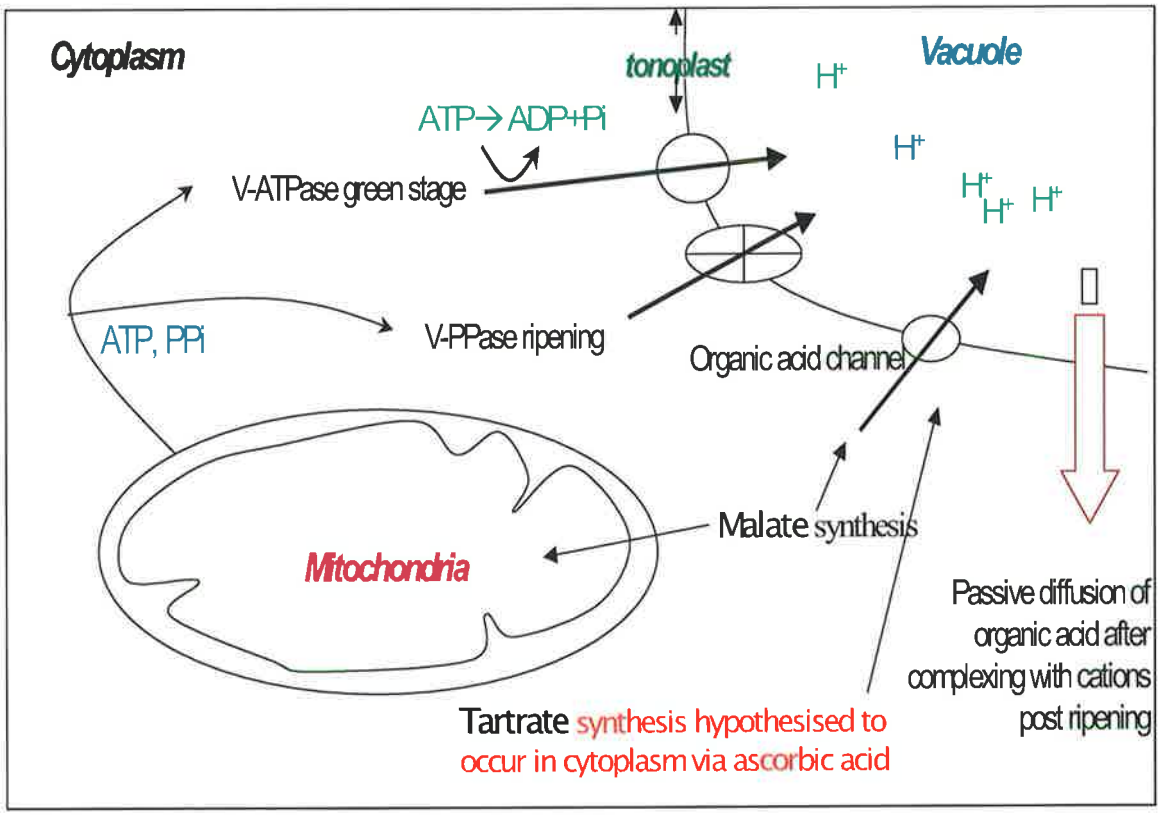

with the flesh (w/w) (Iland and Coombe, 1988).

Figure 1.8 Proposed transport of malate and tartrate in and out of the vacuole (Adapted from Terrier and Romieu, 2001), whereby pre veraison, organic acids synthesised in the cytoplasm are transported across the tonoplast by an electrochemical gradient created by hydrogen ions being pumped into the vacuole by VVpase and ATPase pumps. After which, during post veraison ripening, passive diffusion of organic acids leaving the vacuole destined to be remetabolised in the mitochondria, by the TCA cycle, complex with potassium or calcium which facilitate the movement out of the vacuole, as the tonoplast becomes leaky (Tyerman *et al.*, 2004).

1.5 The physiological role of tartaric acid

The occurrence of TA in the plant kingdom, particularly in angiosperms, is quite common (Stafford, 1959, Ruffner, 1982), but its synthesis in significant amounts is rare. TA is present throughout the grape vine (*V. vinifera*), with exception of the roots (Kliewer, 1966, Ruffner, 1982), but is accumulated to its highest concentrations in the berries and leaves. There is little knowledge regarding the physiological role of TA in the grape vine, whereas other organic acids have defined functions in cellular metabolism, TA has no metabolic or energetic gain associated with it. The formation of more common fruit organic acids such as MA and citric acid occurs via well-characterised pathways and intermediates (Buchanan *et al.,* 2000). Much is known about the physiological roles of these acids, including roles in providing pH balance and counter ion activity for the transport of cations in the xylem (Stumpf and Burris, 1979, Israel and Jackson, 1982).

Ascorbic acid, the precursor to TA in grape berries, is known to have antioxidant activity. The oxidation of the AA molecule to dehydroascorbic acid may be a biochemical signal for the synthesis of TA in the grape, although simply looking at EST data from the grape sequencing project shows that dehydroascorbate and monohydroascorbate oxidase enzymes are transcribed in post veraison cDNA libraries. Green and Fry (2005) recently postulated that vitamin C breakdown occurs in the apoplast, and that is oxidative interaction creates a level of cell wall expansion, but they did not carry on to look into pathways occurring inside the cell, neither did they look at the grapevine as a model species. Photoinhibition and photo-oxidation are events caused by low light acclimated leaves being exposed to increased levels of light intensity. According to Smirnoff (2000), to acclimatise, the tissue must produce antioxidant and photoprotectant systems. Gatzek *et al.* (2001) conclusively showed that ascorbate pools increase in high light acclimation conditions; whether this increase in AA is carried through to increased TA accumulation is unclear. Furthermore, immature grape berries may be hypoxic since numerous waxed platelets (Jackson, 2000 pp. 68) are present and it is postulated that they are needed to limit water loss and subsequent gas exchange at this early stage of development, combined with the rapid cell division and subsequent large need for oxygen. Hypoxic regions in fruit are linked to the formation of active oxygen species such as peroxide (H_2O_2)(Blokhina *et al.,* 2001), which if occurring in the young grape berry would lead

to an increased need for antioxidant systems. Research is needed to test the potential involvement of TA biosynthesis in such an antioxidant system.

A potential role for TA is in balancing the effect of excess calcium and potassium ions (counter ions) in the berry (proposed by Ruffner, 1982), to maintain electrical neutrality and appropriate osmotic pressure (Jackson, 2000 pp. 149). Ruffner (1982) suggested potassium and calcium as natural counter ions for TA in the grape berry. Further tests on effect of TA on charge balance could greatly increase the understanding in this area.

Within the vacuole of the grape the pH is relatively low, often between 2.5 and 3.3 (Ruffner, 1982). The inert nature of TA suggests a role in maintaining this low vacuolar pH; its dissociation constants reveal that it has a low pK_1 of 2.98, which makes it an excellent buffer for maintenance of low pH. If MA was used, having a pK_1 of 3.54, it would for less effective for maintenance of pH, not to mention it is readily utilised as a metabolic substrate.

1.6 The effect of temperature on grape berry acidity

Temperature plays a considerable role in mediating the acid content of the grape berry. Under continuous warm conditions acid synthesis in the pre veraison berry is decreased (Buttrose *et al.*, 1971). Furthermore, malate utilization is increased post veraison, particularly at temperatures above 30 °C (Ruffner and Hale, 1976) (Figure 1.9). The consequence for warm climate Australian grapevine growers is low acidity in ripe grape berries, which results in a flat wine, prone to microbial spoilage, unless pH can be adjusted with TA.

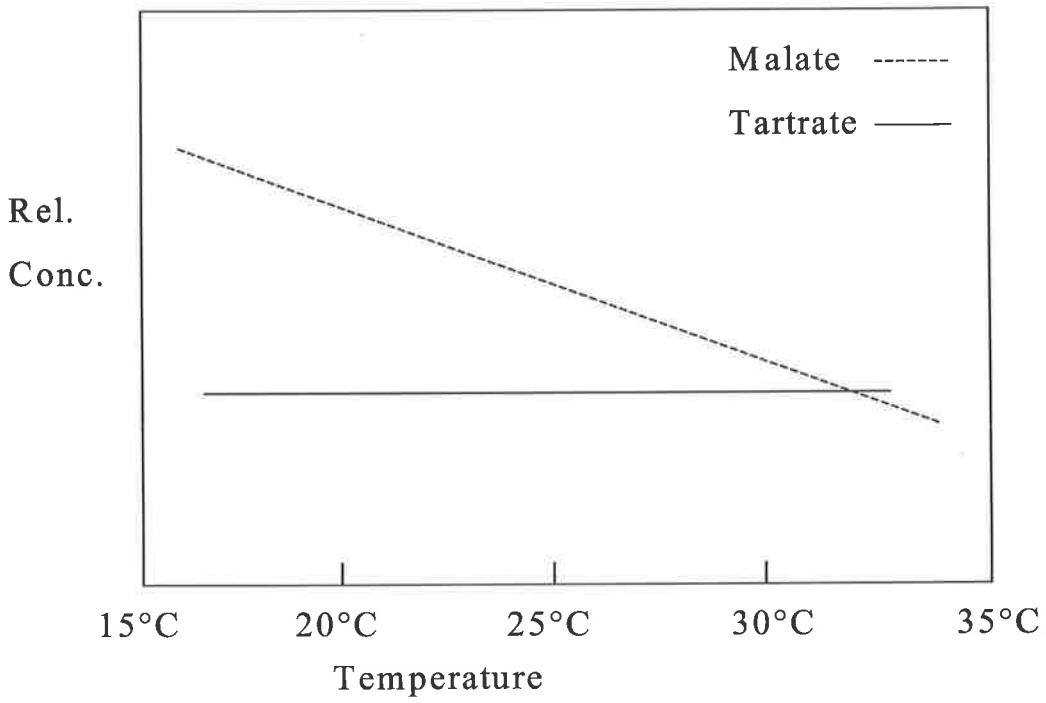

Figure 1.9 Summary of the effects of temperature on acid accumulation in the grape berry (adapted from Coombe, 1987, Jackson, 2000)

The difference between the effect of sunlight and temperature is somewhat unclear on grape berry TA accumulation as sunlight is a combination of visible and infrared (heat) radiation. Some evidence exists that sun exposure has positive effects on TA accumulation in the grape berry compared to shaded fruit (Smith *et al.,* 1988, reported by Jackson, 2000). Saito and Kasai (1969) showed that in the light, radioactivity was immediately found in TA after $^{14}CO_2$-fixation, whereas the same experiment, repeated in the dark, showed that radioactivity was detected in TA only after a delay of 480 min post $^{14}CO_2$-fixation. Yet, further supporting the positive correlation between light and TA is the observation of maximal TA synthesis occurring in parts of the plant where high rates of photosynthesis and cell division are taking place, such as young leaves and young berries (Stafford, 1959, Kliewer 1965).

The influence of light may not be directly increasing TA, rather so its precursor AA, which may then provide a concentration gradient for the increase in TA. It has recently been shown that increased AA pool size occurs when *Arabidopsis*

thaliana leaves were exposed to high light acclimation (Gatzek *et al.,* 2001). Yet, Kasahara *et al.* (2002) reports that when plants are exposed to higher light levels than required for photosynthesis, increased reactive oxygen species are generated in the chloroplasts, and chloroplast avoidance movement occurs to reduce the light intensity reaching chloroplast. During PSI, peroxide is produced via the electron transfer from PSI to oxygen, which forms superoxide leading to peroxide formation by the activity of superoxide dismutase (Allen, 1977), this process has been correlated with a light dependant reduction of dehydroascorbate, a well characterised mop for reactive oxygen species (Anderson *et al.*, 1983). Moreover, Demmig *et al.* (1987) correlated the high light inducible conversion between violaxanthin and zeaxanthin, and its increase suggested as a mechanism for protecting PSII against high light.

The MP- reaction, which acts as an electron acceptor in PSI (Mehler, 1951), whereby ascorbate peroxidase (APO) catalyses the conversion of peroxide to water, is followed by regeneration of ascorbate by the glutathione coupled DHA system, allows electron flow from PSII to PSI to proceed without net oxygen transfer (Neubauer and Yamamoto, 1992). Neubaurer and Yamamoto (1992) present a model, which intrinsically links the AA pool to photosynthesis and the impact of excess light. Photosynthetic activity in fruit during the early stage of development when grape berries are tiny, hard, green (6 mm diameter) structures would be largely affected due to the small surface area to cell density. Moreover, the relative anoxia of immature berries combined with the substantial rate of cell division and metabolic activity may drive the production of active oxygen species, as anoxia and peroxidation have previously been linked (Biemelt *et al.*, 1998). An idea worthwhile testing therefore, is whether the young grape berries are vulnerable to high light conditions, and how the AA pool contributes to changes in TA synthesis? We already know that TA synthesis places a high demand on AA pools, reaching 7-10 mg. gm^{-1} berry weight (Iland and Coombe, 1988), but fundamental answers tying TA in with phenotypic events is needed to understand the positive evolutionary effect of retaining TA biosynthesis and sequestration.

1.7 K^+ and Ca^{2+} and their equilibrium with tartaric acid in the grape

Potassium and calcium uptake occurs primarily post veraison, and is accumulated in the skin, where 30-40% of the potassium and calcium are found (Ruffner, 1982, Iland and Coombe, 1988). Jackson (2000) and Terrier and Romieu (2001) both suggest that cation levels increasing in the vacuole produce a dynamic equilibrium whereby greater permeability in the tonoplast occurs. Acid salt complexes then passively diffuse from the vacuole to the cytoplasm where they are utilized as metabolic substrates. In this way cations act to neutralise organic acids.

Ascorbic acid catabolism in grape vines occurs via cleavage either at C4/C5 or C2/C3 positions respectively. Calcium ions (Ca^{2+}) and to a lesser extent potassium ions (K^{+}) complex with organic acids to form crystalline structures called raphides in highly specialised cells called idioblasts (Ruffner, 1982, Webb *et al.,* 1995). There are differing views as to whether raphides are Ca or K oxalate salts; Winkler *et al.* (1974) stated that they are potassium salts while Ruffner (1982) suggested that they are calcium salts. Furthermore the chemical nature of the organic component is unclear, in a comprehensive paper Webb *et al.* (1995) showed using X-ray powder diffraction that the crystals in *Vitis lambrusca* leaves contain oxalic acid; in the berry, tartrate is the main organic acid and crystals in the berry have been reported to contain tartrate (Ruffner, 1982, Storey, 1987), but X-ray diffraction evidence was missing. Hardie (2000) provided an interpretive paper regarding the adaptive aspects of the *Vitis* genera and explained the occurrence of needle like, calcium oxalate raphides as a plant defence mechanism, accumulated to physically deter ingestion by insects. This hypothesis has not yet been conclusively tested in *Vitis vinifera.* Nor has the amount of organic acid sequestered in raphides been quantified.

1.8 The oenological importance of tartaric acid

Harsh, unfinished characters mark the organoleptic properties of high acid wine and conversely low acid levels lead to flat wines that lack structure. Acid in wine provides low pH conditions that protect juice, must and wine from oxidative and microbial spoilage. Moreover the pH and acid structure of a wine is intimately linked to the aging potential. Low pH in wine also allows the maximum effect of SO_2 additions, which is the primary antimicrobial agent used in winemaking, and also acts by inhibition of polyphenol oxidase activity in juice (Jackson, 2000), which causes premature browning. SO_2 is subject to the following pH dependant equilibrium [SO_2 +

$H_2O \Leftrightarrow HSO_3^- \Leftrightarrow SO_3^{2-}$] (Jackson, 2000). Ultimately, optimal pH has broad importance as a key quality attribute of wine.

The proportion of TA that deprotonates is dependant on the pH of the surrounding solution (see Figure 1.1, Table 1.1). In wine TA is the preferred acid to add because much less needs to be added to achieve the desired pH change (pK_1 2.98). In addition, TA is relatively inert to oxidative and microbial consumption during primary and secondary fermentation (Ruffner, 1982, Terrier and Romieu, 2001). The main problem being as wine ages, dissolved TA complex and crystallise and have the tendency to precipitate out of solution as a bitartrate salt generally covalently bound with potassium. This precipitate is undesirable for the consumer and is arduously avoided by the winemaker who uses cold stabilisation to reduce the potential of spontaneous precipitation in finished wine.

1.9 Conclusion and general aims

The inherently chiral nature of TA has intrigued, amused and entertained generations of scholars, yet the biosynthetic origin of the chiral form most often encountered in nature, TA, and its catabolic ties to vitamin C, has remained a challenge to plant scientists. In contrast to most fruits, grapes accumulate L-TA during development. Moreover, berry taste and the organoleptic properties and aging potential of wines are intimately linked to levels of TA present in the fruit and added during vinification. Elucidation of the intermediates relating TA to vitamin C catabolism showed that they proceed via L-idonic acid, the proposed rate-limiting step in the pathway. As yet neither enzymes, nor the genes that encode them are known for any step in the pathway for TA biosynthesis. Moreover the recalcitrance for facile gene manipulation and transformation in the grapevine makes forwards genetics a difficult proposition. The aims of this thesis are to explore the cellular process of TA biosynthesis, which despite the agricultural, oenological and scientific importance of TA, is uncharacterised at a biochemical level. Deficiencies exist in our understanding of temporal and spatial aspects of its synthesis, the impact of various biotic and abiotic stresses on formation, its presence as crystals or salts and importantly the transcriptional regulators of TA biosynthesis. Due to the woody perennial nature of the grapevine, mutant analysis through T-DNA insertion lines and reverse genetics are

not feasible in search for components of the TA pathway. Moreover the pathway of interest is limited to the grape (Loewus, 1999). Therefore a more creative hypothesis-driven approach is needed to strive towards elucidating the genes involved in biosynthesis. Characterising the transcriptome during times when and where TA biosynthesis occurs has not previously been undertaken. Aims of this study are to provide an understanding of the transcriptional events controlling early fruit development and critically isolate candidate genes for TA biosynthesis. Transcriptional profiling will occur in combination with a thorough characterization of the metabolic profile of grapes from the family Vitaceae; aims of this study are to discover significant variation in TA levels to correlate candidate genes expression with biosynthesis. Therefore PCR based validation of candidate gene will occur across templates, which demonstrate significant variation in TA biosynthesis. Discovery of genes will lead to recombinant protein over expression in *vitro* using prokaryotic expression systems, and subsequent molecular and biochemical characterisation of proteins involved in TA biosynthesis.

In addition to molecular and biochemical answers several other aspects of TA in grapes call for attention. Understanding the impacts of various viticultural factors, in particular light interference will aim to test the hypothesis that TA biosynthesis which maximally occurs in young leaves and berries is associated with regions of high metabolic and photosynthetic activity. A fundamental understanding of the role as well as the biochemistry behind TA biosynthesis is missing from the metabolic ontology. Therefore a clear aim is to develop and test hypothesese towards an understanding of TA synthesis in plants.

Chapter 2

Composition and synthesis of raphide crystals and druse crystals in the berry of *Vitis vinifera* L. Cabernet Sauvignon: L-Ascorbic acid is a biosynthetic precursor to both L-tartaric acid and oxalic acid as revealed by specific radioisotope tracer studies

2.1 Introduction

The biosynthesis and accumulation of organic acids characterises fruit development in many plant species. Malic and citric acids are the most common forms of fruit acids; however, in berries of the grapevine (*Vitis vinifera* L.), significant biosynthesis and accumulation of L-tartaric acid ((2*R*-3*R*)-2,3-dihydroxybutanedioic acid) occurs. Levels of tartaric acid and its salts may reach 7 mg per berry (Iland and Coombe, 1988), significantly greater than either malate or citrate. Grape berry development follows a double sigmoidal pattern with distinct phases of cell development and expansion (Coombe and McCarthy, 2000). Tartaric acid biosynthesis occurs during the early stages of berry growth, levels of the acid remaining constant on a per-berry basis during the later periods of sugar accumulation and berry softening (Terrier and Romieu, 2001).

Although the enzymology and molecular biology of tartaric acid biosynthesis, and the mechanisms used for its transport within the developing grape berry remain unknown, it was shown over 30 years ago that the predominant precursor of tartaric acid in grape berries is ascorbic acid (3 oxo-L-gulofuranolactone; Saito and Kasai, 1969, 1984). Ascorbic acid is successively oxidised and cleaved between carbon atoms 4 and 5, ultimately yielding tartaric acid and a two-carbon fragment presumed to enter the respiratory catabolic pathway (Saito and Loewus, 1989). In other plant species, ascorbate is cleaved between carbon atoms 2 and 3, ultimately yielding tartaric acid from carbon atoms 3 to 6, and oxalic acid from carbon atoms 1 and 2 (Loewus, 1999).

Given the importance of tartaric acid equilibria in wine production, controlling for example acidity, pH and tartrate stability, one fundamental aspect of tartrate metabolism that requires clarification is whether it is involved in biomineralisation in the fruit of *V. vinifera*, the species used predominantly for wine. In *Vitis*, and species of related genera eg *Cissus*, *Ampelocissus* and *Parthenocissus*, biomineralisation occurs in various tissues including leaves, roots, fruits, seeds and stems (Haberlandt, 1914, Esau, 1965, Arnott and Pautard, 1970, Pratt, 1971, Antcliff, 1990, Webb, 1999, Nakata, 2003), and gives rise to two crystalline forms: raphides, bundles of needle-like crystals, and druses, star-shaped crystal aggregates (Esau, 1965, Webb, 1999).

Within the fleshy pericarp of the fruit, raphide forms occur in idioblasts, specialised cells distributed throughout the exocarp, while druses are found in the cells of the endocarp surrounding the developing seed (Hardie *et al.*, 1996) (Figure 2.1). However, in regard to the composition of both crystal types, the literature remains equivocal, having been largely reliant for identification on morphological appearance or similarity to forms seen in other plants. Druses have generally been considered as crystalline aggregations of calcium oxalate (Hardie *et al.*, 1996). Despite an early report of calcium oxalate raphides in grapevine tissues (Haberlandt, 1914), some confusion has arisen concerning the composition of raphide crystals. Winkler *et al.*, (1962), in the textbook "General Viticulture" described crystalline deposits near the skin of the grape as "cream of tartar" ie potassium hydrogen tartrate, a description retained in the subsequent edition (Winkler *et al.*, 1974). Ruffner (1982) concluded that the description appeared to have its basis in the abundance of both potassium and tartaric acid in the grape but reported that calcium, rather than potassium, was the mineral moiety. Storey (1987) confirmed that the mineral moiety was calcium, although expressing uncertainty about the organic component of crystalline material. More recently, in a study of crystal formation and composition in the leaves of *V. labrusca,* raphide crystals were shown to consist of calcium oxalate monohydrate (Webb *et al.*, 1995). Raphide crystals isolated from stems of *V. vulpina* have also been shown to be composed of calcium oxalate (Nelson, 1993 (M.S. thesis), reported by Webb *et al.*, 1995) and recently raphide crystals found in the apical meristem of *V. vinifera* roots were described as calcium oxalate (Storey *et al.*, 2003). Therefore it is clear that some confusion exists, particularly regarding the composition of grape berry raphide crystals from *V. vinifera*, where tartrate is the major accumulated organic acid.

Additional confusion exists in the published literature regarding the counter cation of grape berry crystals, which has been proposed to be calcium or potassium. Winkler *et al.* (1974) and Boulton *et al.* (1998) consider that potassium forms the counter ion in berry crystals; these latter authors moreover report that crystals of potassium bitartrate have been observed in grape berry cells. Alternatively, Ruffner (1982), Storey (1987), and Arnott and Webb (2000) suggest that the counter ion in berry crystals is calcium, and a similar conclusion was reached also for the crystals observed in the roots of *V. vinifera* (Storey *et al.*, 2003).

Grape berry skins contain higher concentrations of potassium ions than are found in the flesh (Iland and Coombe, 1988). The presence of calcium in grape berry crystals was determined using dispersive X-ray analysis by Ruffner (1982). Calcium is present in all plant cells as it is a vital plant micronutrient, but in high cytosolic concentrations is toxic to plant cells (White and Broadley, 2003). Moreover, cellular calcium levels can differ significantly between mesophyll and epidermal cell types (Leigh and Storey, 2004). Recently, the function of oxalate accumulation in grapevine roots was suggested to fulfil a role in the sequestration of excessive levels of calcium ions (Storey *et al.* 2003). Furthermore, a candidate matrix protein that seeds crystal precipitation has been isolated from idioblast cells in *Lemna minor* and *Pistia stratiotes*, and may indicate the mechanism whereby high capacity calcium sequestration is achieved in these cells (Li *et al.*, 2003, Mazen *et al.*, 2003).

In preliminary experiments designed to provide quantitative data regarding the levels of organic acids accumulating in berries during development, a compound with HPLC elution characteristics suggestive of oxalic acid was extracted from pre-veraison berries. Oxalate invariably accumulates only as insoluble salts, most usually of calcium. This suggested the intriguing possibility that in berries of *V. vinifera*, crystals previously described in the literature as composed of tartrate salts, may in fact contain oxalate as the organic component. As mentioned above, the known pathways for oxalate and tartrate formation in plants are both via the metabolism of ascorbate (Saito and Kasai, 1969, Kostman *et al.*, 2001, Kostman and Koscher, 2003). The consequence of oxalate and tartrate being formed respectively from carbon atoms 1 and 2 and 1 to 4 of ascorbate indicates that cells within the mesophyll of the grape berry are capable of using ascorbate for at least two distinct biosynthetic outcomes. This is in agreement with Kostman *et al.* (2001) who suggest that idioblasts are 'physiological compartments independent of adjoining cells'.

In this chapter the extensive examination of grape berry (*V. vinifera*) crystals is presented, including microscopic examination of crystal occurrence and localisation in developing berries. In addition, an adapted extraction method is presented for crystal isolation from berries of *V. vinifera* and evidence provided by X-ray powder diffraction studies shows that the crystals of *V. vinifera* grape berry raphides and druses to be composed of calcium oxalate monohydrate. Furthermore, it is demonstrated via radioisotope tracer studies that both tartaric acid and oxalic acid are derived from ascorbic acid within berries of *V. vinifera*.

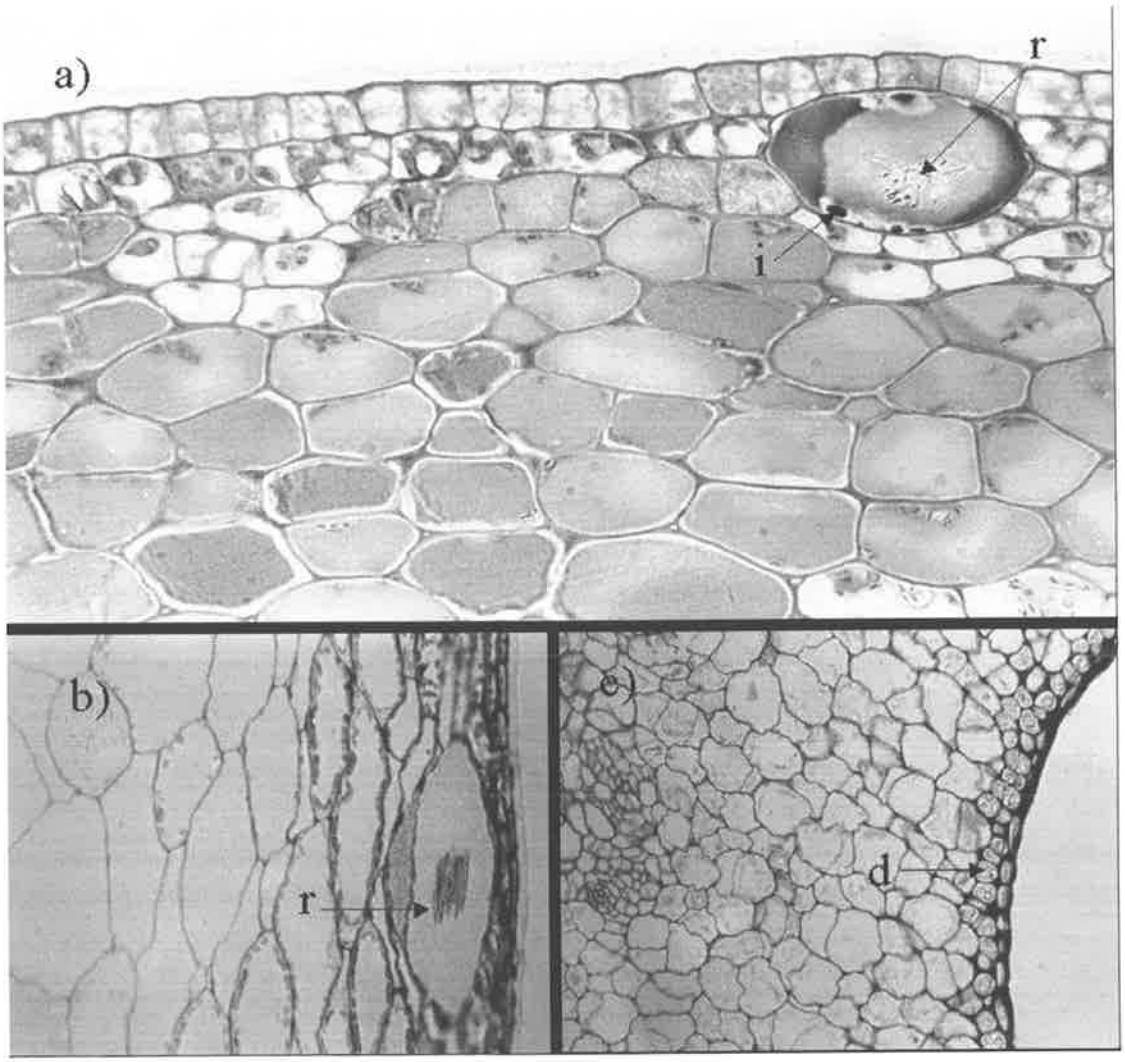

Figure 2.1 Two types of crystalline deposit occur in the grape berry. Figure **2.1a**: Light microscopy of an immature berry of grapevine cultivar Traminer showing an idioblast cell (i) containing raphide crystals (r) (Bar = 10 μm). Figure **2.1b**: As Figure 1a, showing a longitudinal view of a bundle of raphide crystals (Bar = 15 μm). Figure **2.1c**: As Figure 1a, showing a layer of druse crystals (d) adjacent to the seed endocarp (Bar = 60μm). SEM microscopy and photography displayed in Figure 1 was prepared by and provided with permission of Dr. Jim Hardie.

2.2 Methods and Materials

Chemicals

All chemicals and reagents used were of analytical grade or higher. Authentic samples of organic acids and their salts were obtained from Sigma, Fluka, Riedel den Haan and BDH as applicable.

Plant material

For crystal isolation and compositional analyses, and for feeding studies using radiolabelled ascorbic acid, grapevine plants, *V. vinifera* cv. Cabernet Sauvignon, were grown in a temperature-controlled glasshouse, with a photoperiod of 16h light, 8h dark. Prior to the radio-labelling experiment, leaves from the bottom half of the plant had approximately 1/3 of their leaf surface removed to simulate herbivory in an effort to boost crystals production in line with methods developed by Molano-Flores (2001).

Crystal extraction and purification

Grape berries of grapevine cultivar Cabernet Sauvignon were used for crystal isolation. The extraction method was adapted from those described by Webb *et al.* (1995) and Kostman *et al.* (2001). Plant material (16.5 g) was homogenised in a Waring blender for 3 min at high speed in a fume hood using an extraction mixture comprising 100 ml of methanol: chloroform (2:1). The homogenate was filtered through 6 layers of cheesecloth and allowed to settle overnight at ambient temperature, following which the supernatant was removed. The pellet was washed with a 1% (w/v) solution of SDS to remove proteinaceous contamination, and left to settle for 4 h at room temperature. The supernatant was again removed and the pellet was left overnight in a solution of cellulase (1.2 % w/v), pectolyase (0.12 % w/v), BSA (0.5 % w/v), $CaCl_2$ (1.0 mM), PVP40 (0.5 % w/v) and 10 mM MES (pH 6). The supernatant was removed and the pellet fraction washed in ethanol and left to settle for 4 h. The resulting crystal fraction was used for TEM and X-ray powder diffraction analysis.

TEM analysis

A Philips CM200 transmission electron microscope fitted with an EDAX DX4 energy-dispersive X-ray system (Adelaide Microscopy, The University of Adelaide) was used for all determinations. The microscope was operated at an accelerating voltage of 200 kV. The energy-dispersive x-ray system was used to show the presence of Ca, O and C.

X-ray powder diffraction analysis

X-ray diffraction patterns were recorded with a Philips PW1800 microprocessor-controlled diffractometer operating at 40 kV and 60 mA using Co K-alpha radiation, variable divergence slit, and graphite post diffraction monochromator (CSIRO Division of Soils, Adelaide, South Australia). The diffraction patterns were recorded in steps of 0.05° 2 theta with a 3.0 second counting time per step over the angle range 3-80° 2 theta, and logged to data files for analysis using the CSIRO developed program XPLOT.

HPLC analysis of berry composition

Following incubation with radiolabelled ascorbic acid, ca 5g fresh weight of grape berries was homogenised in a mortar and pestle with 5 ml of 0.5 M H_3PO_4 pH 1.5. The slurry was transferred to a 10 ml polypropylene centrifuge tube, the volume adjusted to 10 ml with the same solvent and placed on a rotating mixer at room temperature for 2 h to ensure that all crystals were fully dissolved. After this time a 2 ml aliquot was removed and placed into a 2 ml microcentrifuge tube, centrifuged at 14,000 rpm for 2 min at room temperature, passed through a 45 µm filter and the organic acids separated using HPLC. The loading volume was 20 µl, loaded via an autosampler (Beckman System Gold, Model 507e) onto an HPLC column (Prevail OA organic acid 4.5 x 250 mm, Alltech Associates) fitted with a guard cartridge of the same material. The mobile phase used was 25 mM KH_2PO_4 adjusted to pH 2.0 with phosphoric acid, at a flow rate of 0.5 ml/min (Beckman System Gold, Model 126NM). Detection of the organic acids including oxalic, tartaric, and malic was by UV absorbance at 210 nm using a diode array detector (Beckman System Gold,

Model 168) by comparing peaks with elution times and absorbance spectra of known standards.

Bunch feeding experiments and analysis

Glasshouse-grown vines (cultivar Cabernet Sauvignon) were used for these experiments. Ascorbic acid labelled with ^{14}C in position 1, (13.0 μCi $mmol^{-1}$, Amersham Biosciences) was administered at a concentration of 1 μ Ci per dose via an unbleached, non-waxed cotton thread and passed through the bunch stem of a single bunch of immature grape berries (approximately 4 weeks post anthesis, with berries still green and hard) (Figure 2.2) in 4 doses over a 96-hour period. At other times the thread was maintained in a moistened state with water. A light/dark regime of 16 hrs and 8 hrs respectively was followed. At the completion of the time course, berries were removed from the bunch and extracted with 0.5 M H_3PO_4 as detailed earlier. Aliquots of the post-column eluate were collected and assayed in triplicate by liquid scintillation counting in a Canberra Packard TriCarb 2100. The bunch feeding experiment was repeated using a second vine. To further clarify results, purified crystals from one radiolabelled grape berry bunch were assayed by liquid scintillation counting.

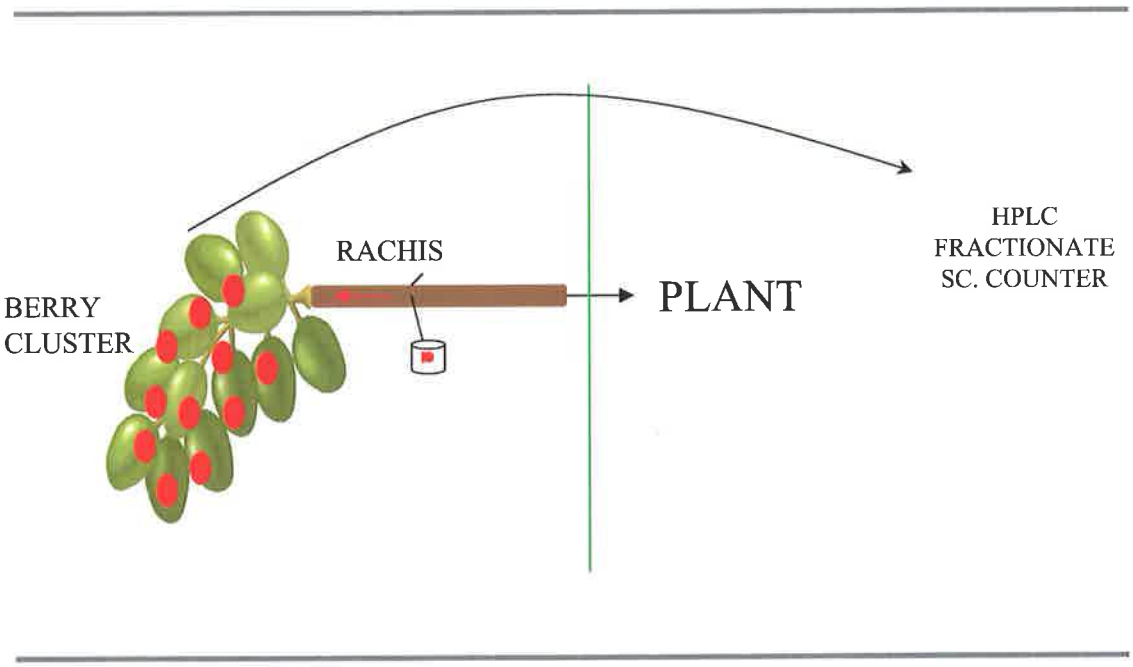

Figure 2.2 A schematic diagram of the bunch feeding experimental design whereby a cotton thread was placed through the rachis and capillary action used to feed the dissolved radio-labelled ascorbic acid into the developing berry cluster whilst still on the plant to provide the best conditions for observing normal in *vivo* metabolism

2.3 Results

2.3.1 Crystal isolation and purification

Examination by light microscopy of protoplasts extracted from a *V. vinifera* berry showed a number of needle-like crystals similar to those previously reported (data not shown). These punctured the tonoplast and plasma membranes and were visible by light microscopy as independent structures. A method was therefore developed to further isolate pure crystals from larger amounts of berry tissue to determine their composition. In this way it was possible to prepare from ca 16.5 g of berries sufficient crystals to coat the surface of the mounting disc of the X-ray diffraction apparatus. These crystals were essentially free from contamination by proteins and lipids, although minor amounts of cellular debris remained (Figure 2.3a). The extraction protocol used a treatment with cellulase to remove traces of cell wall material from the preparation. This reagent was incubated with the crystal preparation in a solution containing among other components, 1.0 mM $CaCl_2$, which could readily form an insoluble precipitate if there were any traces of oxalic acid present. No traces of crystals other than in the form of raphides or druses were evident in the final preparations, indicating that non-specific formation of calcium oxalate had not occurred. In many cases intact crystal bundles were clearly distinguishable under the light microscope (Figure 2.3b).

The extraction procedure was aimed at maintaining the integrity of all possible crystal structures, for instance potassium hydrogen tartrate, calcium tartrate and calcium oxalate. Calcium tartrate ($CaC_4H_4O_6$) and calcium oxalate (CaC_2O_4) are insoluble in alcohol; calcium tartrate is sparingly soluble in water (solubility quoted at 2 gL^{-1} at 85^0C in the Merck Index), while the same reference suggests that calcium oxalate is 'practically insoluble in water'. However, potassium hydrogen tartrate ($KC_4H_5O_6$) is soluble in water, requiring 162 ml per gram at 25^0C. The extraction and isolation procedure used in this research aimed not to dissolve these crystals. When 1 g of pure potassium hydrogen tartrate (Sigma Aldrich), was placed in 100 ml of 2:1 methanol-chloroform extraction buffer or aqueous 1 % SDS, KHT remained insoluble. Potassium tartrate ($K_2C_4H_4O_6$) is extremely soluble in water, and would not be expected to form crystals under physiological conditions.

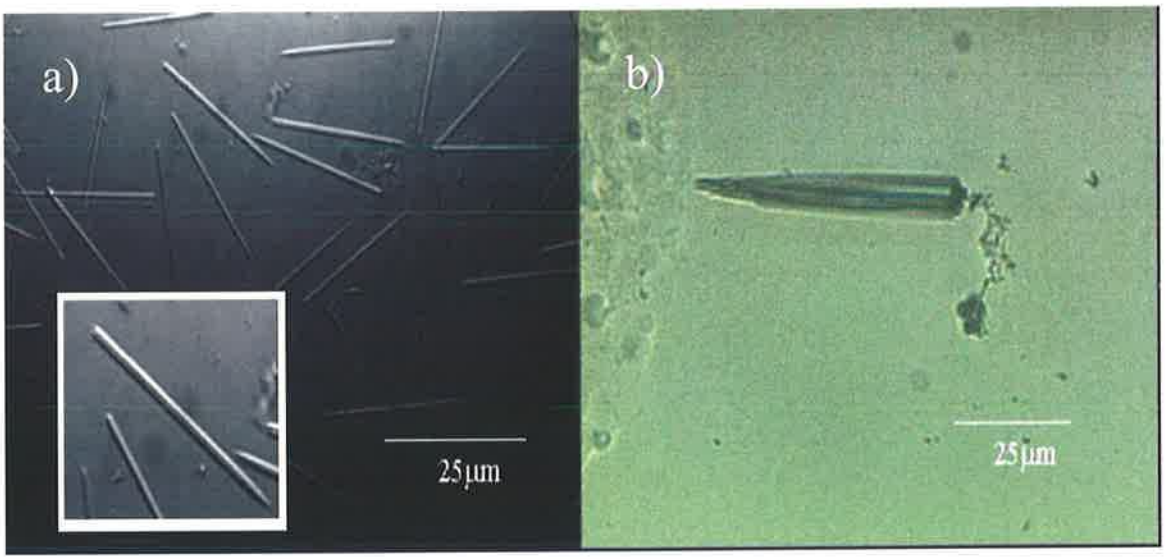

Figure 2.3 Light microscopy of raphide crystals from *V. vinifera* berries. Figure 2.3a shows a sample of crystals observed in an extract prepared from berries of cultivar Cabernet Sauvignon. Inset shows that many of the crystals are composed of twinned raphides as described by Arnott and Webb (2000). Figure 2.3b: A berry extract prepared as in Figure 2a, illustrating an intact bundle of raphide crystals.

2.3.2 TEM analysis

An enriched sample of raphides from grape berries was obtained by slicing the berry with a scalpel and allowing crystal raphides to move out of the berry cells in the juice. These crystals were used to determine the structural form of the needle crystals using TEM. Out of 6 scans of individual crystals, 5 diffraction patterns matching calcium oxalate monohydrate structure, and 1 unknown were obtained (Figure 2.4). Normally in a TEM analysis the 3D crystal repeat structure would be determined using one crystal to take a series of diffraction patterns at a number of different angles. This was not possible with raphides from the grape berry. Each diffraction pattern required approximately 1 minute recording time, during which period the crystals were melting due to heating caused by the electron beam.

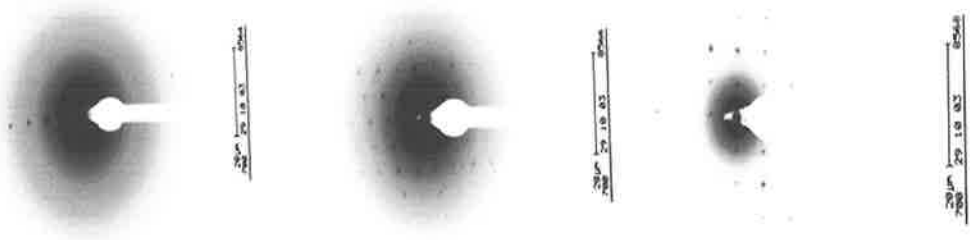

Figure 2.4 Analysis of two of the three crystals using TEM resulted in diffraction patterns matching that of calcium oxalate; the signal was weak and did not give conclusive results regarding the structure as the crystals were breaking down too early under the electron beam

2.3.3 X-ray powder diffraction

Standard crystal diffraction patterns for calcium oxalate, calcium tartrate, dipotassium tartrate and potassium hydrogen tartrate were compared to the patterns obtained with crystals isolated from the grape berry (Figure 2.5). The diffraction pattern given by the sample of crystals purified from the grape berry gave a distinctive pattern matching that of calcium oxalate hydrate (Figure 2.6a). The X-ray powder diffraction analysis would have shown as little as 2% of the crystals present in berries as CaT (2.6b), KHT (2.6d) or K_2T (2.6c). No signals indicative of the presence of these compounds were detected in crystal preparations derived from grapevine berries.

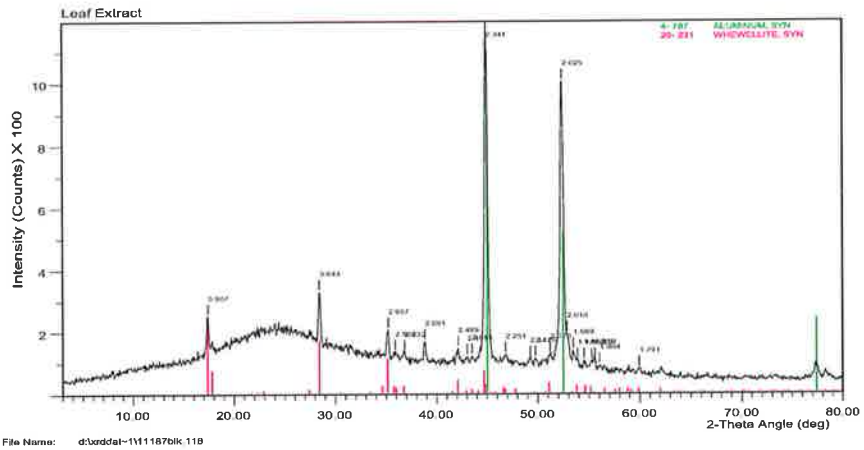

Figure 2.5 Leaf crystals were also purified and showed by powder X-ray diffraction to be composed of calcium oxalate hydrate. The two large peaks seen in the central right are representative of the diffraction pattern of the aluminium disk, which the isolated crystals were placed upon for X ray analysis

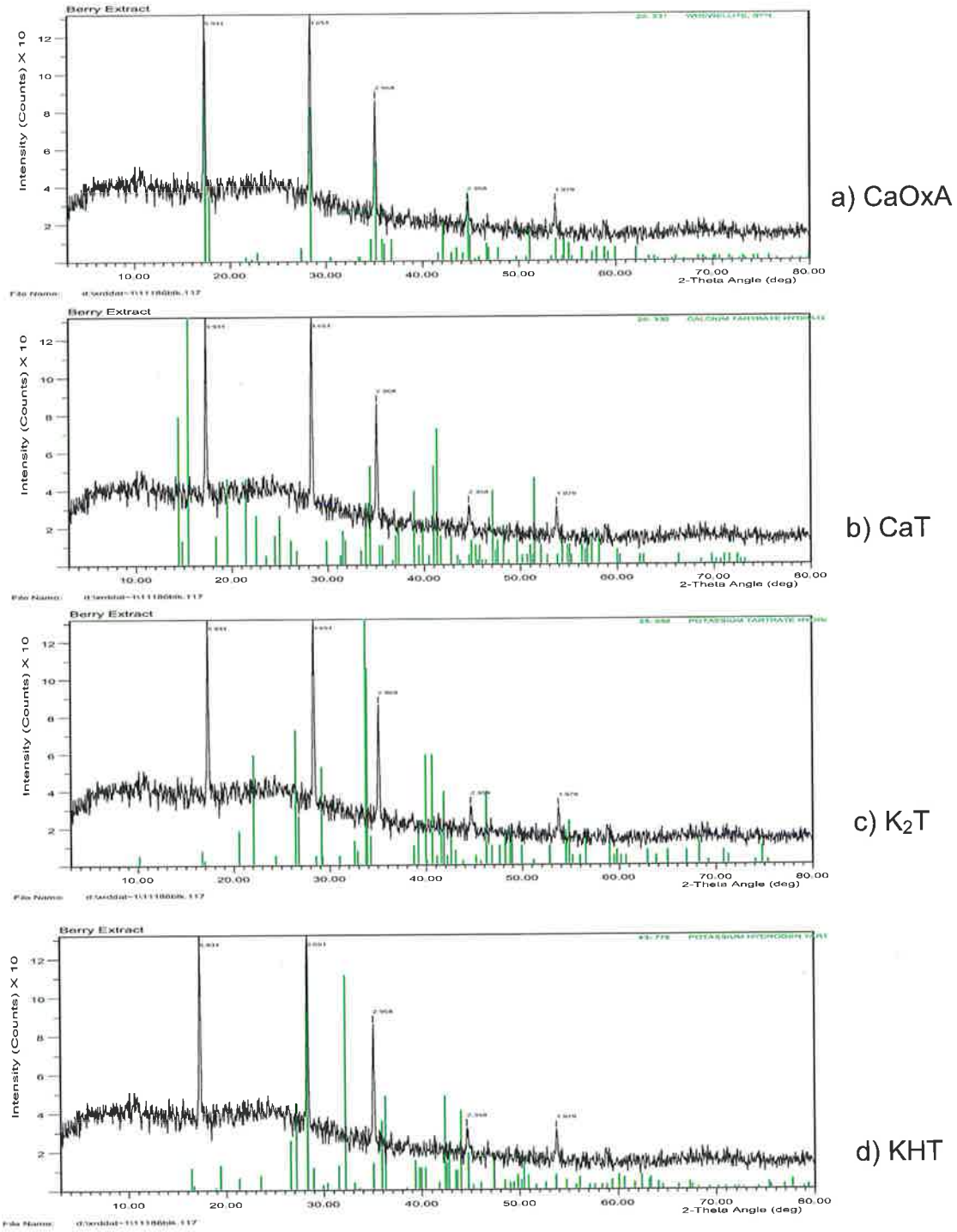

Figure 2.6 X ray powder diffraction patterns of the crystals of the *V. vinifera* grape berry compared to standard diffraction patterns of pure crystal compounds. Figure **2.6a**: the diffraction pattern of crystals isolated from berries of grapevine cultivar Cabernet Sauvignon, overlaid onto the diffraction pattern of calcium oxalate monohydrate (Whewellite); Figures **2.6b, c** and **d** are the standard diffraction patterns of calcium tartrate, potassium hydrogen tartrate and potassium tartrate respectively,

each overlaid onto the experimentally determined diffraction pattern obtained from grape berry crystals. An exact match is seen for calcium oxalate monohydrate; none of the other standard diffraction patterns are evident in the sample isolated from grapevine berries.

2.3.5 Bunch feeding with 1-[^{14}C]-Ascorbic acid and analysis of radiolabelled product formation

The metabolic origin of oxalic acid in many plants has been proposed to be ascorbate (Loewus, 1999 and references therein). Ascorbate has also been proposed as the precursor to tartaric acid biosynthesis in grapevine berries. To test the fate of ascorbate, and to determine the likely mode of its cleavage, berries of *V. vinifera* were fed with ascorbic acid labelled with ^{14}C at position 1. Of the radiolabel fed into the grape berry cluster, 52 ± 5 % ended up in tartrate, 21 ± 3 % in oxalate, 3 % remained as labelled ascorbic acid and 24 % was detected in the tube and capillary after pulse radiolabel feeding experiments had occurred for 4 days with 2 days of water flushing. HPLC analysis of berry extracts and comparison of the elution times of the major radioactive peaks with those of authentic samples of oxalic and tartaric acids chromatographed under identical conditions confirmed the identity of the products formed following bunch-feeding with ascorbate (Figure 2.7). No radioactivity was found in the peak corresponding to the malate eluted from the berry, further confirming the very different biosynthetic processes used for the two major grape acids. Purified crystals from the radio labelled grape berry bunch were assayed by liquid scintillation counting: the data obtained showed that approximately 20 % of the initial radioactivity fed to the bunch could be recovered in the crystals. This result mirrored the radioactivity detected for oxalate when using the HPLC assay.

Experimental problems were experienced in the HPLC analysis of oxalic acid as it consistently co-eluted with fructose. Although there is no known pathway by which ascorbate may be metabolised to fructose, a further experiment was performed to ensure that in detecting radioactivity from chromatographic fractions eluted from the HPLC column we were measuring oxalate and not fructose. HPLC analysis of

grape juice extracted using 80% (v/v) ethanol (Iland and Coombe, 1988) was compared with juice produced using extraction in 0.5 M phosphoric acid as described earlier. Only in the latter extraction conditions would we expect to see solubilisation of calcium oxalate crystals. The area of the mixed oxalate plus fructose peak was increased in the sample prepared using acid extraction, suggesting that the extraction process had solubilized oxalate crystals (data not shown).

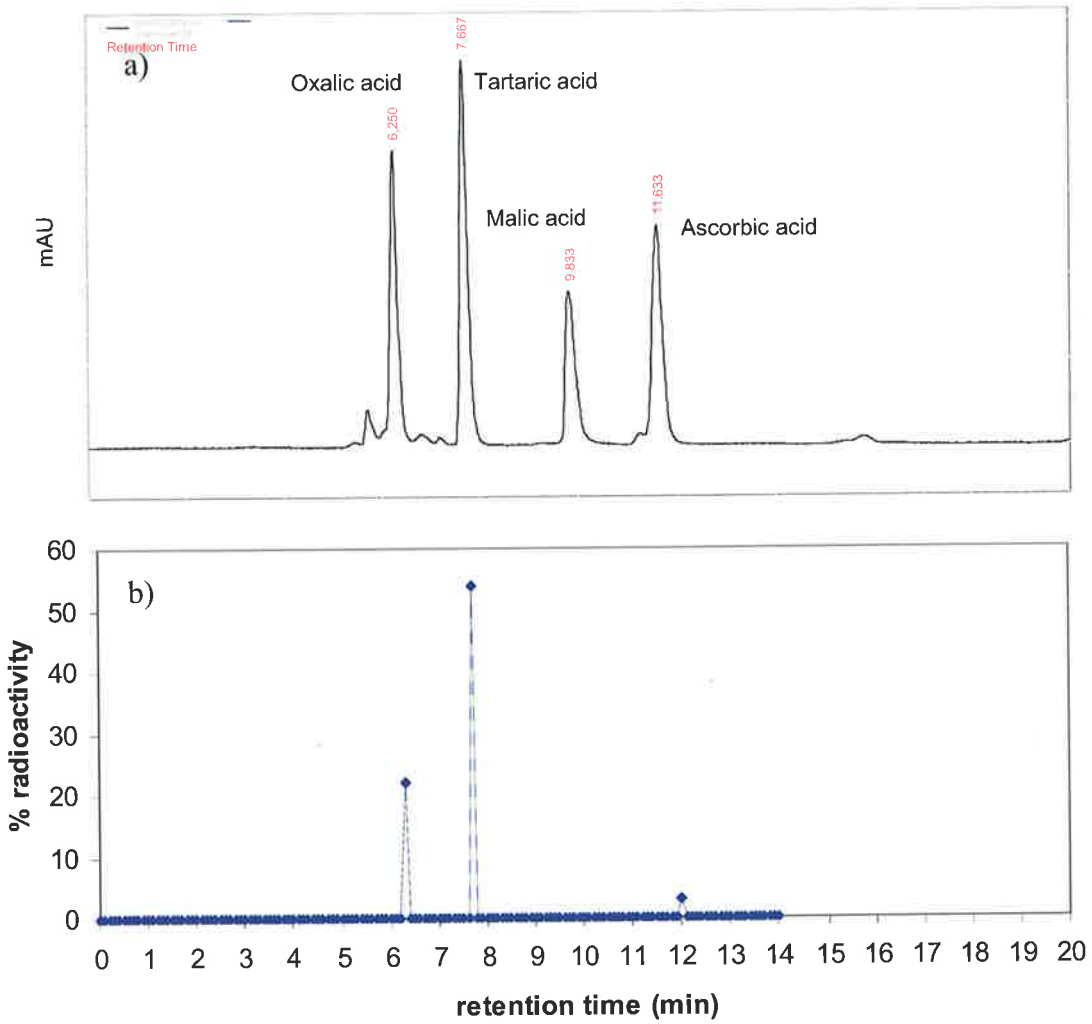

Figure 2.7 Grape berries fed with 1-[^{14}C]-ascorbic acid accumulate radiolabel in tartaric and oxalic acids. Figure **2.7a**: HPLC chromatogram of authentic oxalic, tartaric, malic and ascorbic acids. Figure **2.7b**: The corresponding fractions of HPLC eluants prepared by acid extraction of ^{14}C-labelled ascorbic acid-fed grape berries analysed by liquid scintillation counting. Retention times are equivalent for both parts of the figure. In Figure **2.7b**, the amount of radioactivity found in each compound is expressed as a proportion of the starting material.

3.4 Discussion

In many instances (Winkler *et al.*, 1962, 1974, Ruffner, 1982, Storey, 1987, Hardie *et al.*, 1996, Boulton *et al.*, 1998, Hardie, 2000) the composition of raphide crystals observed in berries of the grapevine *V. vinifera* has been accepted as salts of tartaric acid, either calcium or potassium. The initial reasoning was based largely on tartaric acid being the main organic acid accumulating in grape berries, and the known insolubilities of its salts at elevated concentrations. In contrast, studies into the phenomena of biomineralization in plants have identified calcium oxalate as the constituent of crystals identified in many oxalate-accumulating plants (Arnott and Pautard, 1970, Nakata, 2003). While not generally considered an oxalate-accumulating plant, various species of grapevine were examined in the context of crystal formation in leaves and fruits (Webb *et al.*, 1995). It was demonstrated that the needle-like raphide crystals found in leaves of *V. labrusca* were composed of calcium oxalate hydrate, moreover a later report of twinning in oxalate raphides suggested that they may be isolated from fruits of the grapevine species *V. mustangensis* (Arnott and Webb, 2000).

Data presented in the current chapter indicated no evidence for tartrate in crystals isolated from *V. vinifera* berries (Figure 2.5 and 2.6). Conversely, it was found that these crystals were composed of calcium oxalate monohydrate, in line with the findings of Webb *et al.* (1995) and Arnott and Webb (2000) for other species of the genus *Vitis*. Raphides and druses are the only two crystalline structures observed in ultra-structural studies of the grape berry, presented as a schematic in Figure 2.8. Potassium hydrogen tartrate isolated from wine forms orthorhombic crystals (Rodriguez-Clemente and Correa-Gorospe, 1988), no such crystals were seen by microscopic examination of grape berry extracts. The identity of crystals purified from berries of *V. vinifera* cv Cabernet Sauvignon was confirmed by TEM and X-ray powder diffraction analyses, with authentic samples of tartrate salts also subjected to analysis by X-ray powder diffraction to provide a clear distinction from the diffraction patterns obtained from grape berry crystals (Figure 2.6). These data substantiate the results of earlier investigations into the composition of crystals from various tissues of a number of species of *Vitis* (Webb *et al.*, 1995, Arnott and Webb, 2000). In addition they pose the question that, given the relatively high concentrations of potassium (K^+) and tartrate found in the developing berry (1500-2500 mg/L and 2-6 g/L respectively,

Dunsford and Boulton, 1981), why is no KHT found in the crystalline state? These levels are in excess of the solubility product K_{sp} of potassium hydrogen tartrate in aqueous solution, (0.417×10^{-6} mol^2L^{-2} at 20^0C; Berg and Keefer, 1958). The insolubility of ionic salts is controlled by the solubility product K_{sp}, defined for potassium hydrogen tartrate (KHT) as: $K_{sp} = [K^+] \times [HT^-]$ (Berg and Keefer 1958). Solutions in which the product of $[K^+]$ and $[HT^-]$ exceeds K_{sp} are defined as supersaturated, or unstable, and it may be expected that given favourable conditions for nucleation events to occur, crystals will be formed. Until this point, the solution contains only high (supersaturating) concentrations of the constituent ions that together *will* constitute the salt; it contains no KHT in the absence of the formation of crystals. The absence of crystals of KHT from *intact* grape berry cells when the K_{sp} has been exceeded may be explained by a consideration of the compartmentation of the anions and cations involved. Organic acids including tartrate are translocated by as-yet unknown carriers to the vacuole, where conditions of low pH are established as a consequence (Ruffner, 1982). Potassium accumulates predominantly in the cytoplasm, where levels are approximately 10-times those found in the vacuole (see Mpelasoka *et al.*, 2003 for a recent review of potassium in grape berries). Conversely, calcium levels in the vacuole may reach millimolar concentrations, one thousand-fold higher than attained in the cytoplasm (Storey *et al.*, 2003). This would suggest that, given appropriate conditions, the formation of calcium salts of organic acids would be more likely than the corresponding potassium salts. Calcium tartrate and calcium oxalate are each practically insoluble in aqueous solutions, and we may therefore ask the question: "why do we detect only raphide and druse crystals of calcium oxalate in extracts of berries?" The answer we suggest lies in the fact that *in vivo* crystal formation is a directed process, (see below), and that in the absence of specific modes of crystal growth control, these forms of calcium oxalate crystals would not be formed. A simple test using compounds known to inhibit crystal formation supported this argument (data not shown). The addition of levels of metatartaric acid, carboxymethylcelluose or soluble tannin sufficient to prevent the formation of crystals of potassium bitartrate from a supersaturated solution, to a solution prepared by mixing 20 mg L^{-1} of calcium chloride with an equal volume of 0.5 gL^{-1}oxalic acid, did not prevent the formation of crystals of calcium oxalate over a 24 hour period at 4^0C (the solubility of calcium oxalate in cold water is 0.0067 g L^{-1}). Examination of these crystals by light microscopy revealed their morphology to be neither raphide nor

druse, but rather the mix of irregular forms reported by Webb (1999). Calcium oxalate is approximately 550-times less soluble in aqueous solutions than potassium bitartrate, and it could therefore be expected that in the absence of specific control of crystal formation *in vivo*, masses of these small non-raphide, non-druse crystals would be seen. The absence of such crystal forms from grape berry idioblasts strongly supports the hypothesis that crystal formation *in vivo* occurs by directed processes.

Table 2.1 Composition and localisation of crystals detected from the grapevine (NR – not recorded, ND – no data)

Species	*Tissue*	*Crystal form*	*Composition*	*Reference*
Vitis sp.	Leaf	Raphide	Calcium oxalate	Haberlandt (1914)
Vitis sp.	NR	NR	Calcium tartrate	Tunmann (1913, cited in Arnott and Pauchard 1970)
Vitis sp.	Leaf	Raphides, others	Calcium oxalate	Metcalfe and Chalk (1950)
Vitis sp.	Leaf	NR	Calcium tartrate	Netolitzky (1929, cited in Metcalfe and Chalk, 1983)
Vitis sp.	Berry	NR	Potassium hydrogen tartrate	Winkler et al.(1962, 1974)
Vitis sp.	Berry, leaf and shoot	ND	Calcium tartrate	Ruffner (1982)
Vitis vinifera	Berry	Raphides	Calcium tartrate	Storey (1987)
Vitis labrusca	Leaf	Raphides	Calcium oxalate	Webb et al. (1995)
Vitis vinifera	Berry	Raphides (R) and druses (D)	(R) Calcium tartrate (D) Calcium oxalate	Hardie et al. (1996); Hardie (2000)
Vitis sp.	Berry	NR	Potassium hydrogen tartrate	Boulton et al. (1998)
Vitis vinifera	Root	Raphides	Calcium oxalate	Storey et al. (2003)

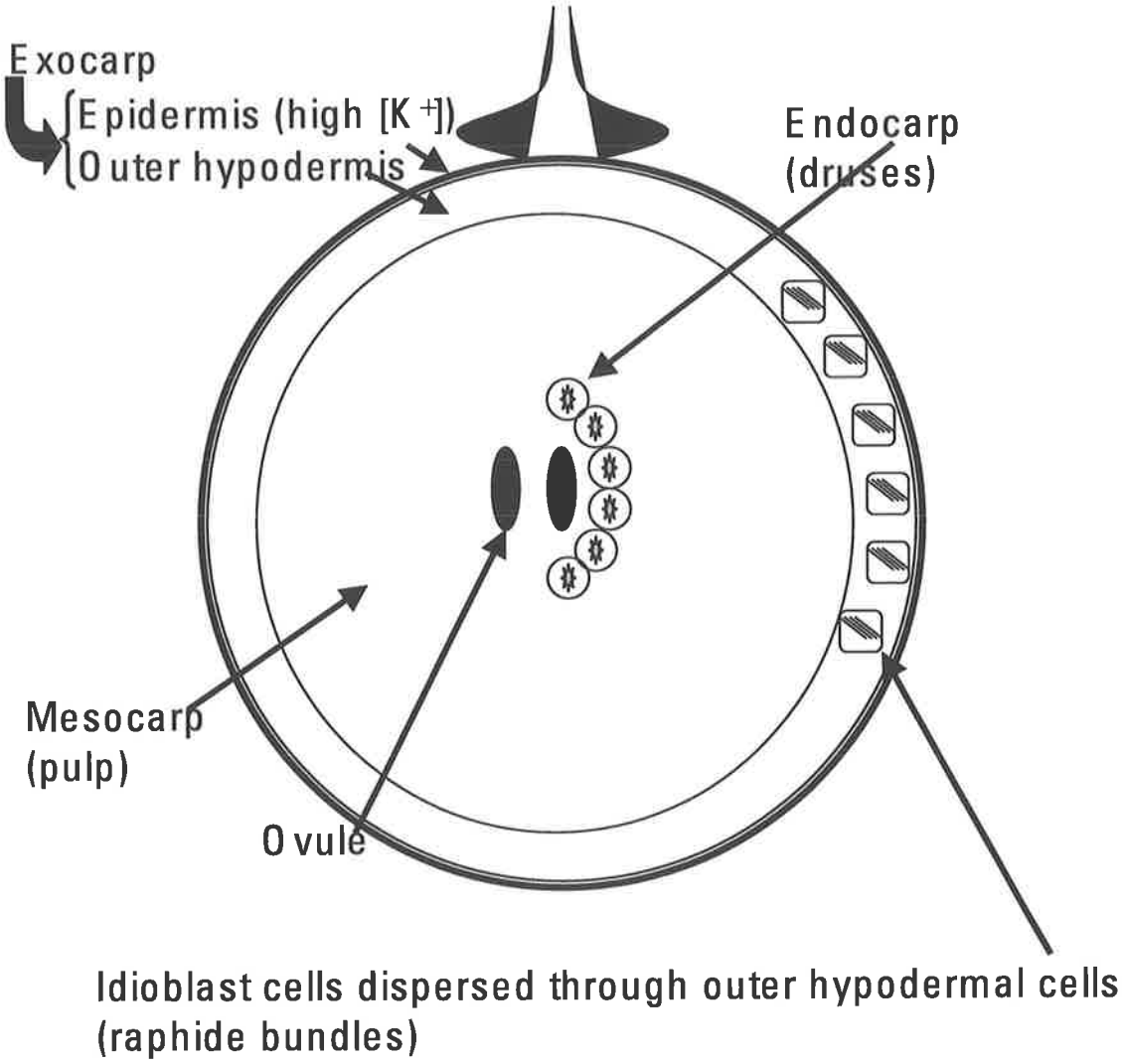

Figure 2.8 A schematic diagram of a grape berry, illustrating the three tissue types that constitute the pericarp and the crystal forms known to occur in them (drawing not to scale)

Where crystal formation does occur within plant cells, there is much evidence to suggest that it is not a spontaneous process, but rather is restricted to vacuoles of cell types specialised for this purpose, and promoted by the presence of specific proteins (Nakata, 2003). Crystal idioblast cells appear to be specialised for the synthesis and accumulation of crystals of calcium oxalate, possessing several features including large amounts of endoplasmic reticulum and a vacuolar organisation that results in the formation of crystal chambers, within which nucleation occurs (Webb, 1999). Calcium sequestration in idioblasts is perhaps the most physiologically important role proposed for these cells. The role of calcium oxalate crystals observed in the apical meristem of grapevine roots has been suggested to be calcium sequestration (Storey *et al.*, 2003); a similar role may be postulated to exist in the grape berry. In the grape berry, xylem transport is much diminished at veraison due to stretching of tracheids and broken segments of tracheid membranes where the vascular bundles enter the berry (Coombe and McCarthy, 2000). Calcium is still needed for essential cell functions such as cell signalling, cytoplasmic streaming and as an important component of cell walls (Storey *et al.*, 2003). A hypothesis is, that in the grape berry, randomly dispersed crystal idioblasts may facilitate large scale calcium storage compartments from which remobilisation can proceed at specific developmental stages. A similar mechanism of calcium modulation has been proposed for the crystal idioblasts of *Lemna minor* (Mazen *et al.*, 2003).

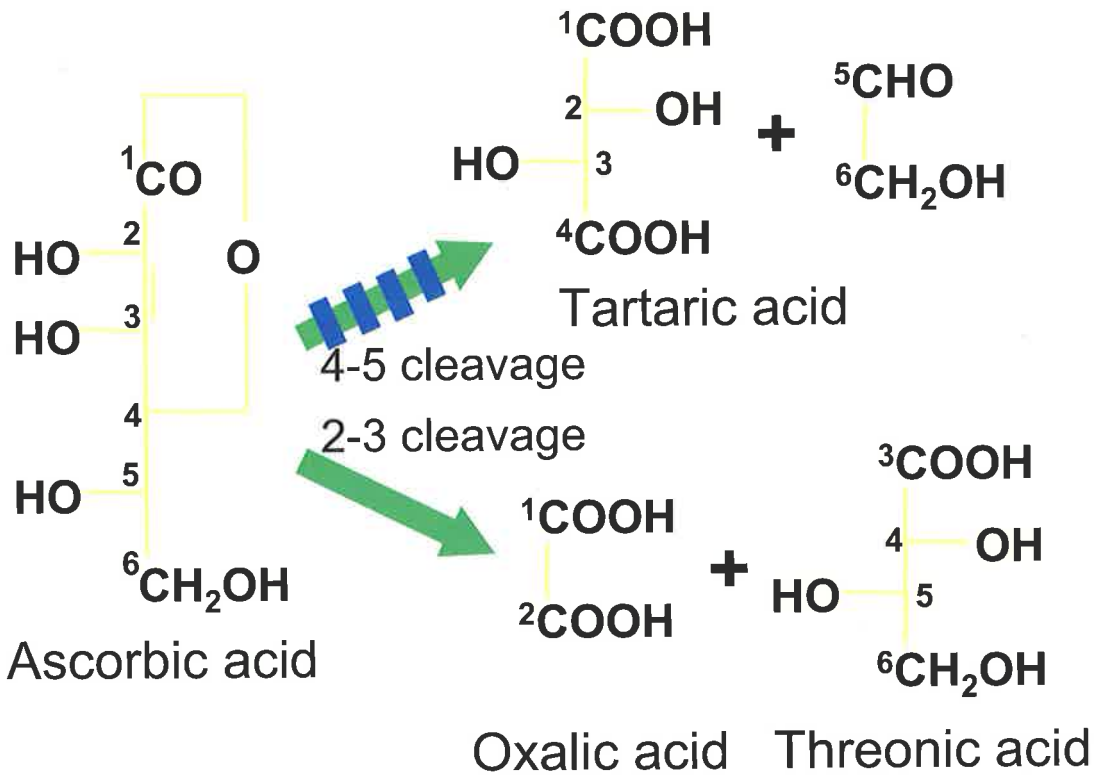

Figure 2.9 Shows a proposed model for the metabolism of ascorbic acid in the grape berry based on the 1-carbon labelled ascorbate being detected in both tartaric and oxalic acid. Based on the data, which shows that purified crystals contained the same percentage of radiolabel as solubilized oxalic acid, our model proposes that crystal forming cells are metabolically independent of surrounding cells for ascorbate metabolism.

The clear demonstration of the presence of oxalic acid salts in developing berries of *V. vinifera* has important implications for our understanding of grape berry organic acid synthesis and accumulation. In earlier reviews of grape berry organic acids (Ruffner, 1982, Terrier and Romieu, 2001), oxalic acid was not identified as a significant component of the berry. The lack of detection of oxalate may have been due to measurements being made on free acids in juice rather than aiming to dissolve insoluble salts of organic acids. Similarly, the experiments of Saito and Loewus (1989), in which the biosynthetic precursor of tartaric acid in grape berries was

investigated, did not use acid extraction of total berry organic acids and thus may have not detected the formation of oxalates. In regards to oxalate metabolism Hardie *et al.* (1996) reported the disappearance of druses in the grape berry seed endocarp as the berry approached physiological ripeness. The liberation of oxalate associated with crystal breakdown has not previously been discussed. Oxalate is broken down by oxalate oxidase to release carbon dioxide and peroxide (Loewus, 1999): the presence of peroxide could lead to a subsequent oxidation of seed coat phenols which would provide a mechanism for seed coat browning seen at this stage of berry development.

These results pose an important question regarding the role of ascorbate as a biosynthetic precursor in the grape berry. Kostman *et al.* (2001) showed that crystal-containing idioblast cells are able to independently synthesise oxalate from ascorbate in *Pistia stratiotes,* most probably via a cleavage between positions 2 and 3 of the 6-carbon ascorbate molecule. Our experimental data using ascorbic acid radiolabelled at the 1-position showed clearly that both oxalic acid and tartaric acid were synthesised by intact berries (Figure 2.9). With the extraction methods used in the present work, it was not possible to determine from which cell type the individual organic acids were isolated. Instead of converting ascorbate to tartaric acid via a cleavage between carbon atoms 4 and 5 to form tartrate and a metabolic 2-carbon fragment (the reaction proposed to occur within the mesocarp cells of the grape berry; Saito and Kasai, 1969, 1984), idioblast cells within the mesocarp may use ascorbate to form oxalic acid via a cleavage between carbons 2 and 3, although this remains to be tested experimentally in the grape. If, as our data suggests, the biosynthesis of oxalic acid occurs via ascorbate metabolism, an intriguing level of differential expression must occur between idioblasts and the surrounding mesocarp cells of the grape berry, resulting in one case in 4,5 cleavage to yield tartaric acid, and in the other the 2,3 cleavage-mediated formation of oxalic acid (see Figure 2.9 for a model of AA degradation in the grape berry). This is in agreement with the thesis presented by Kostman *et al.* (2001) that idioblasts are in fact independent of adjacent cells for ascorbic acid and oxalic acid formation. Literature search reveals (Table 2.1) that the evidence presented here represents the first evidence of these two fates for ascorbate within a single physiological tissue. The possibility that tartrate is metabolised to form oxalate cannot be completely dismissed, but *in vivo* breakdown has not previously been suggested and is yet to be tested.

Chapter 3

The isolation of candidate genes for tartaric acid biosynthesis: combining transcriptional and metabolic profiling in a targeted approach

3.1 Introduction

The enormous undertaking of many laboratories around the world to gain deeper understanding of model plant system genomes, such as Arabidopsis, Medicago and rice, using expressed sequence tag (EST) and contig (assembled ESTs) analysis, microarrays and characterisation of pathways via biochemical approaches, proteomics, point and deletion mutants (forwards genetics) has paved the way for gaining an understanding of gene expression in higher plants. Focus on higher plants has cleverly been aimed at species that rapidly reproduce, have small genomes and can be easily grown in glasshouses such as rice, maize and Arabidopsis, but emphasis has yet to be placed on many of the world's important horticultural crops. Molecular genetic approaches such as forward genetics, which are effective for Arabidopsis, are ineffective for plants such as the grapevine. In lieu of genetic analysis a more creative process is needed: the use of transcriptional profiling to focus on a single biochemical event in a specific spatial and temporal location is described in this chapter.

Fruit provides essential nutrition for much of the world's population, yet much is still to be learned at the basic biochemical level regarding fruit development. The grape is one of the most economically important fruit crops in the world, producing table grapes, dried fruits, wine and fruit juice. Many biochemical pathways are regulated by as yet unknown genes, and many more still are completely uncharacterised. The concentrated efforts of an international consortium of laboratories have successfully facilitated progress towards EST sequencing of the grape transcriptome (University of California, Davis; CSIRO Australia; University Instituto Agrario di San Michele all'Adige (IASMA), Italy; University of Nevada-Reno; USA, Institut National de la Recherche Agronomique France)(Iandolino *et al.*, 2004). These efforts have been made public, with data deposited in the GENBANK, TIGR and UC-Davis plant genome annotation databases. The availability of these large data sets has triggered a recent surge of interest into the grapevine, and provided opportunities for characterising areas of metabolism, for instance transcriptional profiling of the grapevine (Goes da Silva *et al.*, 2005, Terrier *et al.*, 2005), and genes associated with specific processes such as stress response and cell walls (Davies and Robinson, 2000), isolation of transcripts for improved flowering and fruitfulness

(Boss *et al.*, 2001, Boss *et al.*, 2002, Boss and Thomas, 2002, Boss *et al.*, 2006), grape colour (Kobayashi *et al.*, 2004) and acidity (DeBolt *et al.*, 2006).

Research described in this and the next chapter describes the outcomes of combining transcriptional data and metabolic profiling, respectively, for the identification of candidate TA biosynthetic genes from berries of the cultivated grapevine *V. vinifera.* This chapter will focus on transcriptional profiling, with the aim to identify tentative consensus sequences (TCs, which are aligned ESTs that form putative genes) differentially expressed when and where TA is maximally being made, using high throughput sequencing data as a psuedo quantitative indicator of gene expression. Transcriptional profiling has been applied to several EST data-sets for the identification by differential expression analysis of gross trends in an organism's transcriptome (Sketel *et al.*, 1999). Plants studied in this way include *Medicago* (Federova *et al.*, 2002), rice (Ewing *et al.*, 2000), tomato (Moore *et al.*, 2005, Van der Hoeven *et al.*, 2002), potato (Ronning *et al.*, 2003), and recently grape (Goes da Silva *et al.*, 2005). These papers often describe a snapshot of the genes, which cluster as ESTs arising from cDNA libraries from specific spatially distinct cell types, but EST data-sets have rarely been used to target uncharted areas of plant metabolism. The use of publicly available array data has been used for coordinated expression analysis of known cellulose synthesis genes to discover novel genes (Persson *et al.,* 2005). Combining large scale transcript and metabolite profiling with the selection of candidates expressed when and where TA synthesis occurs, and using PCR to validate their differential expression, is a logical method of gene discovery. By correlating gene expression data with natural variation in the synthesis of TA, the aim was to provide candidate genes that could be further tested via over-expression and characterisation of enzymatic activity.

The grapevine has clear and well-defined plant ontology, with both vegetative and reproductive growth cycles fully documented (Coombe and Dry, 1988, Coombe and McCarthy, 2000). Therefore, when EST sequencing was proposed, the isolation of mRNA from as many developmental stages and tissues of the grapevine as possible would not only represent the way to gain maximum genome coverage, but with the appropriate annotation of each clone, could be related back to defined phenotypic characteristics. Further rigour was introduced by the preparation and complete DNA sequencing of multiple cDNA libraries derived from tissues in each phase of development. In this way it has been possible to capture maximal transcriptome

coverage because cDNA arising from different areas of the plant and developmental stages have markedly different gene expression (Goes da Silva *et al.*, 2005, Terrier *et al.*, 2005). Statistical methods used to isolate differentially expressed transcripts from EST sequencing data are complicated by the occurrence of highly expressed transcripts, whose sequences are represented multiple times within the derived datasets (Ewing *et al.*, 2000). To overcome this limitation, the sequence representation of housekeeping genes and ubiquitously expressed transcripts within each cDNA library was removed from the tables of differentially expressed genes, and normalisation of cDNA libraries was achieved (Sketel *et al.*, 1999). The problem with normalisation is that it eliminates analysis of an individual transcript's abundance in the cDNA library from which it was sequenced, a layer of information that can potentially provide researchers with a list of highly up-regulated genes. To overcome this, the researcher must identify differentially expressed transcripts through the above mentioned pipeline, then go back to the original data set and look at the number of ESTs per contig: sequencing depth ratio (Federova *et al.*, 2002).

In the grapevine, pre veraison berry development is the ideal spatial and temporal location for isolation of TA synthetic genes, as TA accumulation has been shown to occur during pre veraison development and to be switched off post veraison (Iland and Coombe, 1988). Pre veraison or stage 1 of berry growth is characterised by an initial period of rapid cell division followed by a subsequent period of growth and development of the seed embryo, at the same time as biochemical events such as tannin and organic acid biosynthesis are taking place (Coombe 1960, Coombe and McCarthy, 2000). The intermediate compounds involved in TA biosynthesis were elucidated using radioisotope tracer studies, with enzyme activity stopped using iodoacetic acid (Saito and Kasai, 1969, 1978, 1984). The inter-conversions identified suggested that oxido-reductase type activity catalysed at least three of the four steps, but despite considerably efforts (data not published: K. Saito pers. comm. and FA. Loewus, pers. comm.) no enzymes involved in the pathway were identified. Experiments using radioisotope tracer data provided clues as to the type of enzymes that may be involved in TA biosynthesis. In this context, understanding the interconversions facilitates the search for conserved domains and motifs (strings of amino acids which contain homology to characterised enzymes of the proposed function) likely to be involved in TA biosynthesis among a defined list of candidate

genes. In this chapter a list of 10 differentially expressed candidate genes are identified by in silico analysis of the grapevine transcriptome.

3.2 Methods and materials

Transcriptional data

Publicly available *Vitis vinifera* sequence data (including ESTs, expressed transcripts as well as other available DNA sequences in the NCBI database) were extracted from GenBank with Batch Entrez at NCBI (http://www.ncbi.nlm.nih.gov/) (provided by Francisco Goes da Silva, The University of California, Davis) and used for all analyses presented within this chapter. To briefly describe the processing of transcriptional data, vector-derived sequences were removed from grape cDNA sequence data as well as *E. coli*, mitochondria, chloroplast and low quality sequences using platform independent in-house PERL programs (Goes da Silva *et al.*, 2005). According to the methods described by Goes da Silva *et al.* (2005), sequences that were used in this analysis were clustered into contigs with the TIGR Gene Indices Clustering Tools (TGICL at http://www.tigr.org/tdb/tgi/software/). All singletons were removed from the dataset because they are unsuitable for statistical comparison. Genes were annotated according to tBLASTx constraints (Altschul *et al.*, 1997). These data were compiled at the College of Agricultural and Environmental Sciences (CAES) Genomics Facility (http://cgf.ucdavis.edu/) (by Ana Leslie, The University of California, Davis). Raw data tables comprising the annotated TCs, a list of the number of ESTs that comprised each TC, information detailing the source cDNA library for each EST and a count of the total number of ESTs per TC were provided by Anna Leslie and Francisco Goes da Silva.

In silico identification of pre-veraison expressed transcripts

Differential expression analysis was used to restrict the TCs to candidates from cDNA libraries (56 cDNA libraries were used in the analysis) prepared from tissues in which TA biosynthesis maximally occurs (Stafford, 1959, Iland and Coombe, 1988, Saito and Loewus, 1989, Terrier and Romieu, 2001). 10 out of the 56 cDNA libraries met this criterion, these were 9 pre veraison berry cDNA libraries and 1 pre veraison leaf cDNA library (Table 3.1). The other 46 cDNA libraries represented flower, root, leaf, stem, bud, veraison and post veraison berry transcripts (cgf.ucdavis.edu); transcripts from the 10 cDNA libraries selected as meeting the TA

synthetic criteria can then be determined differentially expressed relative to the other 46 cDNA libraries. The method described by Goes da Silva *et al.* (2005) for 693 differentially expressed transcripts was modified to allow greater numbers of TCs into the analysis to increase genome coverage. Specifically, for a TC to be classified as differentially expressed, it must comprise more than 5 ESTs, drawn from across the 10 libraries tested, and the number of times ESTs comprising a selected TC are present in the correct subset of cDNA libraries must be greater than 80 %.

Further cross referencing was achieved by individually examining TCs to assess if ESTs comprising each TC were present in several of the 10 libraries or arose from a single cDNA library. Standardisation and normalisation of data set was achieved by multiplying the number of ESTs encoding part of an individual TC found within a single cDNA library by 100, then dividing this number by the total number of ESTs sequenced in that cDNA library. This standardised the data for variation between per library sequencing depth, which differed between ~28,000 and 300 ESTs. For each TC, these values were summed across all cDNA libraries to give a relative percentage value (the % expression of a given TC in each library relative to all other libraries). Data was transformed (normalised) according to the relative percentage value of each TC by multiplying the standardised value by 100 and dividing by the relative percentage (Sketel *et al.*, 1999, Ewing *et al.*, 2000, Goes da Silva *et al.*, 2005).

Motif searching among candidate genes

Candidate unigenes identified by transcriptional profiling of EST data were analysed to identify putative protein functional domains and motifs not necessarily identified in a tBLASTx analysis (Altschul *et al.*, 1990, 1997). Sequences encoding candidate TCs were further examined using PFAM, NCBI, BRENDA and Interpro gene structure and protein domain BLAST interfaces (Mulder *et al.*, 2002, 2005). Specifically, domain architecture associated with oxido-reductase enzyme activity was sought in the candidates, since the sequence of intermediate compounds in the formation of TA from ascorbic acid implicated the involvement of this class of enzymes at a number of steps.

3.3 Results

3.3.1 In silico analysis of the grapevine transcriptome: identification of cDNAs derived from genes whose expression is limited to the developmental period and tissues associated with tartaric acid biosynthesis

Due to the grapevine having well-defined plant ontology, cDNA libraries were categorised to include the developmental stages at which sampling of material for RNA extraction and cDNA library synthesis occurred (pre veraison, veraison, post veraison)(recorded for all tissues under metadata at the UC Davis website cgf.ucdavis.edu/grape). These classifications, recorded by the database compilers at cgf.ucdavis.edu/grape, made it possible to determine those libraries most likely to contain sequences from which cDNAs associated with TA biosynthesis would be found. In screening the literature, it was determined that TA maximally occurs in the pre-veraison berry, and in early stages of leaf development (Terrier and Romieu, 2001). 10 cDNA libraries represented in the IGGP cDNA library collection matched the specificities of maximal TA synthesis (Table 3.1).

In silico analysis was applied to identify differentially expressed TCs from TA-biosynthetic cDNA libraries relative to the other 46 libraries from non-TA synthetic tissue (cDNA library information is available at cgf.ucdavis.edu/grape). The total TC count (containing more than 1 EST per TC, therefore emitting singletons) is approximately 13,500 genes comprising (at the time of analysis) 131,586 sequenced ESTs. For statistical validity, a TC selection criterion was based on a TC containing at least 6 ESTs per TC. This parameter reduced the number of TCs from 13500 TCs containing more than one EST to 3640 TCs containing at least 6 ESTs. When TCs that were derived from the 10 TA-synthetic cDNA libraries only and contained greater than 5 ESTs were selected (meaning 100 percent frequency) a total of 8 transcripts were present. UC Davis contig number and BLAST results providing putative function to each of these genes are as follows:

1. 1030770: C96833 hypothetical protein F18B13.24 [imported] - Arabidopsis thaliana
2. 1030850: PII protein [Ricinus communis]

3. 1032452: xanthine dehydrogenase, putative [Arabidopsis thaliana]
4. 1032387: p27KIP1-related-protein 1 [Lycopersicon esculentum]
5. 1031240: prolylcarboxypeptidase -related [Arabidopsis thaliana]
6. 1029451: invertase/pectin methylesterase inhibitor - related [Arabidopsis thaliana]
7. 1031325: expressed protein [Arabidopsis thaliana]
8. 1029591: seed specific protein Bn15D18B [Brassica napus]

Table 3.1 Describes the list of cDNA libraries identified as TA synthetic tissues used in differential expression analysis

#	cDNA library description
1	Green Grape berries Lambda Zap II Library
2	Green Grape Berries Lambda Triplex2 Library
3	Green Grape (harvested at 5 p.m.) Pedicles Lambda Triplex2 Library
4	Green Grape (harvested at 9 a.m.) Pedicles Lambda Triplex2 Library
5	Cabernet Sauvignon Berry Stage I - CAB3
6	Grape Inflorescence pSPORT1 Library
7	CabSau Berry Preveraison Stage 32 (PREu0032)
8	CabSau Berry Fruit Set Stage 28 (PREu0028)
9	Green Grape Berry Skins Lambda Triplex2 Library
10	Cabernet Sauvignon Pre veraison Leaf -CA12LI

Therefore, to extend the analysis and capture more differentially expressed genes, TCs that contained at least 80 % of their ESTs derived from TA synthetic cDNA libraries were used; for example if 10 ESTs comprised a TC, then 8 must arise from TA synthetic cDNA libraries (Table 3.1). By loosening the parameters for differential expression, the number of TCs differentially expressed in TA synthetic tissue was extended from 8 to 87 candidate genes (Table 3.2). If the minimum number of 6 ESTs per TC is eliminated, the data is more prone to false positives because a lower number of ESTs could by chance arise from the same cDNA library. If no limitation is placed upon the number of ESTs per TC a total of 565 TCs are differentially expressed in TA synthetic tissue (data not shown).

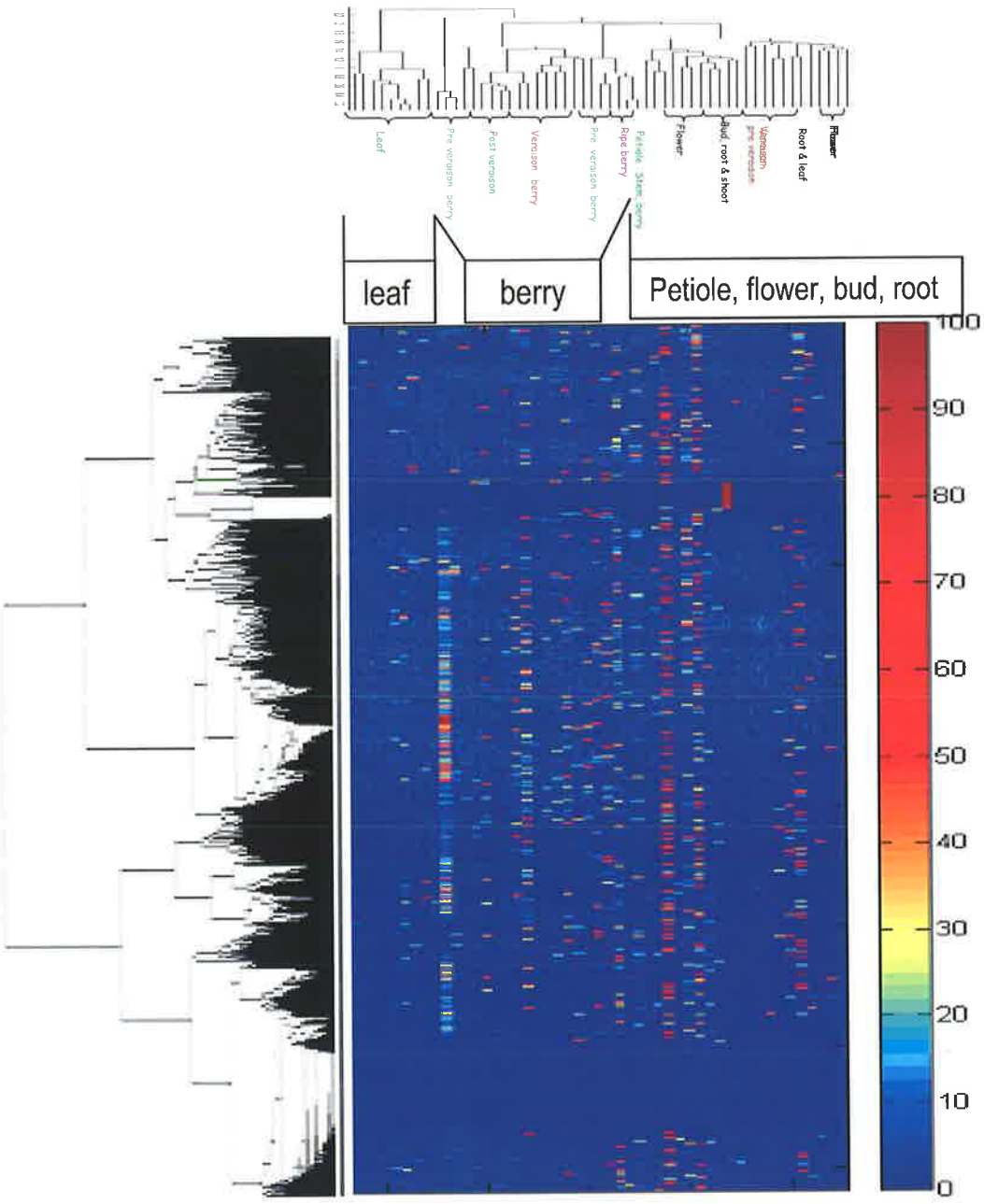

Figure 3.1. 2-Dimensional hierarchical clustering of 3640 TCs that meet the selection criteria of 6 ESTs per TC versus 56 cDNA libraries. Within the matrix the degree to which a TC is expressed in any library is expressed as a colour, which is a percentage of the total ESTs per TC (for example 100% is encoded by the colour red). Each endpoint in the cDNA hierarchical tree is representative of a single cDNA library.

A 2 dimensional hierarchically cluster analysis was applied (Figure 3.1) utilizing a correlation matrix (statistical program: Matlab ®, Simulink and Stateflow Inc.) to group cDNA libraries based on EST abundance in TCs. In the analysis, TCs composed of ESTs from similar cDNA libraries were grouped, this result basis gene expression as a function of spatial and temporal plant development. Clustering analysis provided a snapshot of cDNA libraries that had similar ESTs derived from them, showing that certain tissues cluster together (Figure 3.1), for instance leaf libraries clustering in the same branch of the hierarchical tree shown in the upper dimension of the 2D hierarchical clustergram (Figure 3.1).

Pre veraison berry cDNA libraries, which were the aim of this study, however, clustered in non-regimented order (also noted by Goes da Silva *et al.*, 2005). In several locations on the hierarchical tree pre veraison berry libraries shared similar ESTs and therefore gene expression patterns with non-pre veraison berry libraries. In one case pre veraison berry libraries clustered with a 'berry specific super-branch' on the hierarchical tree, including post veraison and veraison libraries. In another case pre veraison libraries tending to group with areas of rapid cell division such as shoot, bud and root libraries.

3.3.2 Gross trends in pre veraison specific transcripts

EST per TC values varied greatly among the data set (Figure 3.2), with the 88 % of TCs containing between 6 and 20 EST per TC. Of the 87 putative genes identified as differentially expressed during early berry development, several TC annotations provided by tBLASTx were suggestive of metabolic processes. Gene candidates grouped in either metabolism or no function comprised more than 50% of the 87 differentially expressed transcripts (Figure 3.3). Glucosyltransferase protein homologs and the oxido-reductase family of proteins were both well represented, with 5 and 9 annotated unigenes for each family respectively. Genes encoding putative proteins, annotated as having no significant homolog, were most abundant among the pre veraison candidate list, with 6 "no hit" genes, 3 genes annotated as similar to an unknown protein and 16 genes annotated as "expressed proteins" (meaning a homolog exists, which in every case was derived for sequenced Arabidopsis genome, itself with no known function). These data show that the transcriptional events occurring during the early stages of fruit development are not well characterised. Genes annotated as

common microtubule binding protein, kinases, auxin related protein and ubiquitin proteins were present, as well as a suite of, signalling, nuclear and ribosomal proteins (Table 3.2). Only 1 transporter appeared to be differentially expressed in pre veraison berries, a gene annotated as a homolog to a 34 kDa outer mitochondrial membrane protein porin (voltage-dependent anion-selective channel protein). Other annotations to protein homologs of interest were 2 ripening related proteins, a hydrolase, flavanone isomerase, dehydration induced protein, ATPase and 2 transcription factors.

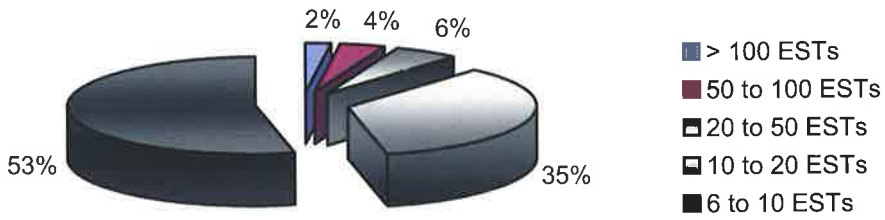

Figure 3.2 Pie chart summarizing the number of ESTs per TC used in the differential expression analysis (displayed per grouping as a percentage of the total number of TCs used)

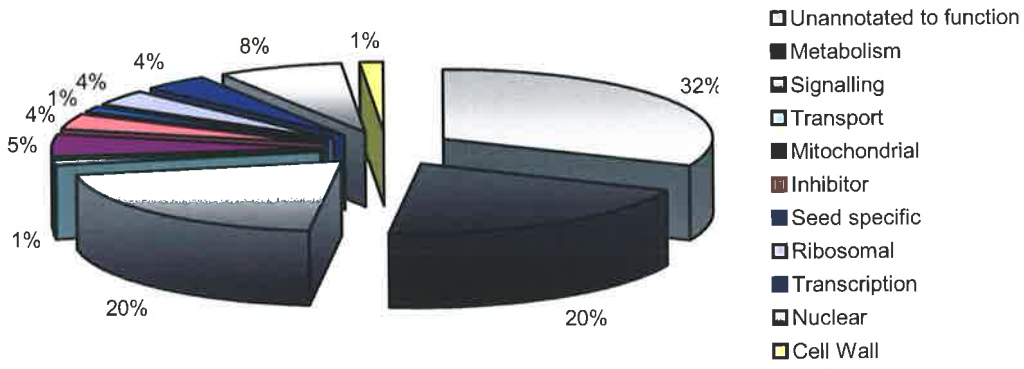

Figure 3.3. Displays the grouping of the 87 candidate genes in Table 2 into global gene function based on annotations provided by tBLASTx analysis

Table 3.2 Annotations and contig numbers for the 87 differentially expressed unigenes

Candidate	Contig number	Annotation
1	1030770	C96833 hypothetical protein F18B13.24 [imported] - Arabidopsis thaliana
2	1030850	PII protein [Ricinus communis]
3	1032452	xanthine dehydrogenase, putative [Arabidopsis thaliana]
4	1032387	p27KIP1-related-protein 1 [Lycopersicon esculentum]
5	1031240	prolylcarboxypeptidase -related [Arabidopsis thaliana]
6	1029451	invertase/pectin methylesterase inhibitor - related [Arabidopsis thaliana]
7	1031325	expressed protein [Arabidopsis thaliana]
8	1029591	seed specific protein Bn15D18B [Brassica napus]
9	1028225	expressed protein [Arabidopsis thaliana]
10	1029391	glycosyltransferase family [Arabidopsis thaliana]
11	1028683	26S proteasome regulatory particle triple-A ATPase subunit2b [Oryza sativa (japonica cultivar-group)]
12	1030372	putative RING zinc finger protein [Arabidopsis thaliana]
13	1031466	AF190634_1 UDP-glucose:salicylic acid glucosyltransferase [Nicotiana tabacum]
14	1029209	ribosomal protein L5p family [Arabidopsis thaliana]
15	1027309	T03958 heat shock protein 18p - common tobacco
16	1030567	No hit
17	1029130	L-iditol 2-dehydrogenase (sorbitol dehydrogenase), putative [Arabidopsis thaliana]
18	1030564	expressed protein [Arabidopsis thaliana]
19	1027959	AF133894_1 glutathione S-transferase [Persea americana]
20	1030574	expressed protein [Arabidopsis thaliana]
21	1030007	diaminopimelate epimerase - like protein [Arabidopsis thaliana]
22	1029436	expressed protein [Arabidopsis thaliana]
23	1030712	P0489B03.9 [Oryza sativa (japonica cultivar-group)]
24	1031738	No hit
25	1028186	transcription initiation factor IIB (TFIIB) [Arabidopsis thaliana]
26	1027721	lectin [Glycine max]
27	1030231	transducin / WD-40 repeat protein family [Arabidopsis thaliana]
28	1031227	P0439E11.8 [Oryza sativa (japonica cultivar-group)]
29	1027029	phenylalanine ammonia lyase [Populus balsamifera subsp. trichocarpa x Populus deltoides]
30	1030571	MPPA_SOLTU Mitochondrial processing peptidase alpha subunit, mitochondrial precursor
31	1029186	Methylenetetrahydrofolate dehydrogenase (NADP) (EC 1.5.1.5) - garden pea
32	1027807	expressed protein [Arabidopsis thaliana]
33	1030059	A86205 hypothetical protein [imported] - Arabidopsis thaliana
34	1029008	emb|CAB71043.1~gene_id:MCA23.10~strong similarity to unknown protein [Arabidopsis thaliana]
35	1030995	AF402605_1 homeodomain leucine zipper protein HDZ2 [Phaseolus vulgaris]
36	1029472	subtilisin-like serine protease [Arabidopsis thaliana]
37	1029157	CFI_VITVI Chalcone–flavonone isomerase (Chalcone isomerase)
38	1029358	expressed protein [Arabidopsis thaliana]
39	1031493	expressed protein [Arabidopsis thaliana]
40	1030432	pre protein translocase SECYprotein -related [Arabidopsis thaliana]
41	1031884	MCT-1 protein-like [Oryza sativa (japonica cultivar-group)]
42	1030009	unknown protein [Arabidopsis thaliana]
43	1029697	auxin-regulated protein [Zinnia elegans]
44	1028880	OSJNBa0022H21.13 [Oryza sativa (japonica cultivar-group)]
45	1029419	ubiquitin family [Arabidopsis thaliana]
46	1028948	dihydropyrimidinase [Arabidopsis thaliana]
47	1029344	histone H2A, putative [Arabidopsis thaliana]
48	1030682	expressed protein [Arabidopsis thaliana]
49	1030595	No hit
50	1028096	succinate-semialdehyde dehydrogenase, putative (SSDH) [Arabidopsis thaliana]

Candidate	Contig number	Annotation
51	1030766	expressed protein [Arabidopsis thaliana]
52	1031158	No hit
53	1030192	AF481952_1 hairy meristem [Petunia x hybrida]
54	1028618	No hit
55	1028904	putative ripening-related P-450 enzyme [Vitis vinifera]
56	1028742	GDSL-motif lipase/hydrolase protein [Arabidopsis thaliana]
57	1031746	AF429384_1 mevalonate kinase [Hevea brasiliensis]
58	1030458	putative U4/U6 snRNP-associated 61 kDa protein [Oryza sativa (japonica cultivar-group)]
59	1030503	expressed protein [Arabidopsis thaliana]
60	1032050	auxin-induced (indole-3-acetic acid induced) protein family [Arabidopsis thaliana]
61	1030426	microtubule bundling polypeptide TMBP200 [Nicotiana tabacum]
62	1030778	expressed protein [Arabidopsis thaliana]
63	1030704	aminopropyl transferase [Oryza sativa (japonica cultivar-group)]
64	1028137	ubiquitin-conjugating enzyme 13 (UBC13) [Arabidopsis thaliana]
65	1029378	putative coatmer beta subunit (beta-coat protein) (beta-COP) [Oryza sativa (japonica cultivar-group)]
66	1031350	bZIP protein, G/HBF-1-related [Arabidopsis thaliana]
67	1032464	expressed protein [Arabidopsis thaliana]
68	1031121	cyclophilin [Pseudotsuga menziesii]
69	1030997	34 kDa outer mitochondrial membrane protein porin (Voltage-dependent anion-selective channel protein)
70	1028715	A84902 auxin-regulated protein GH3 homolog At2g46370 - Arabidopsis thaliana
71	1030870	small nuclear ribonucleo protein D2 -related [Arabidopsis thaliana]
72	1031032	No hit
73	1029468	expressed protein [Arabidopsis thaliana]
74	1030166	AF197330_1 calcineurin-like protein [Eucalyptus grandis]
75	1028615	dehydration-induced protein-related [Arabidopsis thaliana]
76	1028440	NADH-ubiquinone oxidoreductase 20 kDa subunit, mitochondrial precursor
77	1030738	glutathione S-transferase [Pisum sativum]
78	1029639	40S ribosomal protein S25 [Glycine max]
79	1031001	expressed protein [Arabidopsis thaliana]
80	1028060	40S ribosomal protein S9 (RPS9C) [Arabidopsis thaliana]
81	1030370	NUAM_SOLTU NADH-ubiquinone oxidoreductase 75 kDa subunit, mitochondrial precursor
82	1030695	T07926 probable starch synthase (EC 2.4.1.-) (clone CD192) - Chlamydomonas reinhardtii (fragment)
83	1030215	transcription factor Hap5a, putative [Arabidopsis thaliana]
84	1030449	expressed protein [Arabidopsis thaliana]
85	1029144	cytochrome P450, putative [Arabidopsis thaliana]
86	1030038	ribosomal protein S21 - like [Arabidopsis thaliana]
87	1030922	WD-repeat protein GhTTG2 [Gossypium hirsutum]

In order to determine if transcripts sharing homology with oxido-reductase proteins are found throughout the grapevine and not skewed towards pre veraison berry development, an assessment of the *in silico* expression patterns of various annotated and characterised oxido-reductase transcripts was performed (Table 3.3). The results showed that oxido-reductase protein homologs are broadly found

throughout the grapevine both temporally and spatially (Figure 3.4). These data show certain genes are linked to parts of the plant and times at which cDNA libraries were made and aim to provide clues as to the role of each gene. For instance, C3 is expressed in abiotically stressed berries only, suggestive of its role in stress response. Further, the data showing expression of oxidoreductase protein homologs throughout the grapevine rules out the chance that the TCs isolated in pre veraison berry cDNA libraries are representative of false positives.

Table 3.3 Annotated oxidoreductase protein homologs sourced from the grapevine.

ID	Annotation
C1	AF194174_1 alcohol dehydrogenase 2 [Vitis vinifera]
C2	AF195867_1 alcohol dehydrogenase 7 [Vitis vinifera]
C3	AF349916_1 putative short-chain type alcohol dehydrogenase [Solanum tuberosum]
C4	AF195867_1 alcohol dehydrogenase 7 [Vitis vinifera]
C5	putative NADH dehydrogenase [Oryza sativa (japonica cultivar-group)]
C6	short-chain dehydrogenase/reductase family protein [Arabidopsis thaliana]
C7	Methylenetetrahydrofolate dehydrogenase (NADP) / methenyltetrahydrofolate cyclohydrolase- garden pea
C8	6-phosphogluconate dehydrogenase -related [Arabidopsis thaliana]
C9	oxidoreductase, 2OG-Fe(II) oxygenase family [Arabidopsis thaliana]
C10	aldo/keto reductase family [Arabidopsis thaliana]

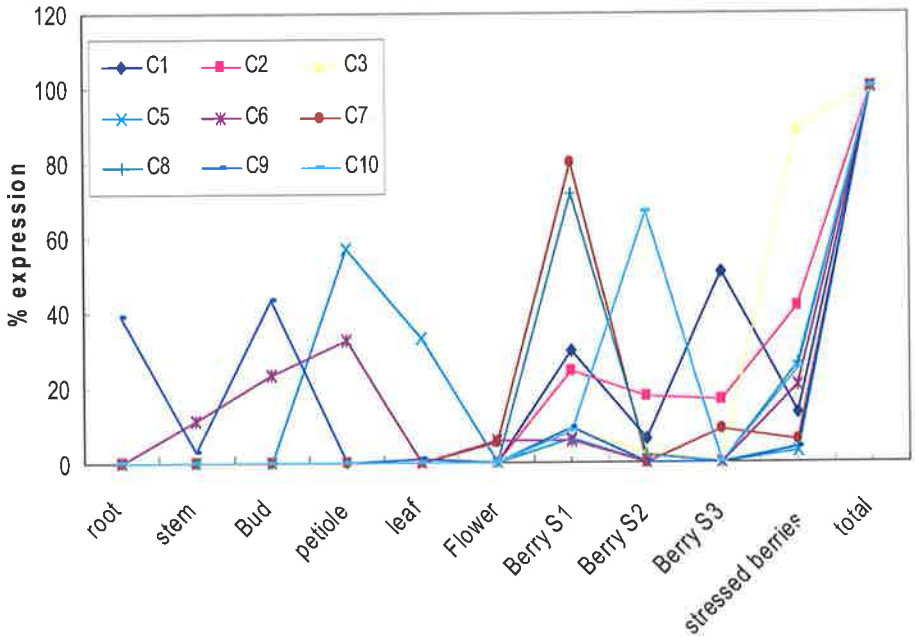

Figure 3.4 Oxidoreductase protein homologs from Table 3.3 and their expression pattern in various tissue specific cDNA libraries. Total represents that percentage expression in all genes is out of 100 %

3.3.3 Motif and domain analysis of putative candidate genes

Clearly, not all the genes identified as being expressed in pre veraison berries were of interest as potential candidates for TA synthesis. Cross-referencing transcripts encoding candidate sequences with domain architecture suggesting involvement in the reactions between ascorbic acid and TA with the correct expression profile provided a powerful tool to further refine the list of candidate genes. Web-based BLAST interfaces (PFAM, InterPro, BRENDA, BLASTp) were used as guidance tools for further cross-referencing and candidate selection.

Finally, a set of candidate genes was selected based on these combined expression and protein homology criteria. This set of candidates included genes encoding 4 oxido-reductase proteins and 4 genes differentially expressed in pre veraison berries (Table 3.4). Four genes with predicted functions not associated with oxidoreductase reactions but with matching in silico expression data were selected as control genes, to validate the process. Two other genes were subsequently added to the candidate list, they were two transcripts which shared homology to plant transketolases (Bernacchia *et al.*, 1995). Neither of these genes had been characterised in the grape. A full list of candidate genes are described below and the internal primers used to amplify each gene is listed in Table 3.4.

Table 3.4 Candidate genes identified via in silico analysis for PCR validation

Candidate genes	contig #	domain	forwards primer	reverse primer
1	1030770	Glyoxalase, Predicted ring cleavage motif	GAGTGTAGGCAGTGGGTGGT	TGAAGGAAATGGGAATGGAG
2	1031325	Eukaryotic proteins of unknown function	GAGCTGCAAGATTCACCACA	TTGACATGGGATGATGCACT
3	1032330	Oxidoreductase	CAGCTCTCTCATGGTGTCCA	CCCTCTACAGCGACAAGGAG
4	1032452	Xanthine dehydrogenase	CTTGCACAAATGCTCCTTCA	CCTTTCGGCTCATGGATTTA
5	1029130	Oxidoreductase	AAGTTTGCCTTGTGGGTTTG	AAGGCTTCCTCCACATCCTT
6	1028096	Succinate aldehyde dehydrogenase	CACCATTGACAGCCTTAGCA	CAGGTCTGCATCGTCAAAGA
7	1038692	Ferric reductase	CTTGAACCAGGCAACCATCT	TTCTGTTTTGGGCTCTTGCT
8	1027918	Translation regulation	CCACCCAGGTAGTCTCTGGA	CTCCAGGGTCTGCTGAAAAG
9	1028716	Transketolase	CTGTCGATAGACGCAGTGGA	CACTTCAACCCCAGGTGTCT
10	1012153	Transketolase	AGAAGAGCGCAATGTCAGGT	TCTCCAAGCCCAATTGAATC

Gene candidate 1 did not have strong homology to known proteins, yet was selected based on a glyoxalase motif and a putative extradiol ring cleavage motif found at the N terminus end of the ORF. It is a short ORF of only 511 bp most similar to a glyoxalase enzyme (Singla-Pareek *et al.*, 2003), which when over expressed has the potential to alleviate salt stress. Differential expression when and where TA synthesis occurs, was the basis for selection. Motif selection was based upon its putative role in cleaving the lactone ring of the ascorbate molecule, which is a classic lactone sugar acid and the first committed step in TA synthesis in plants (Saito and Kasai, 1969). The low homology of this candidate gene to characterised proteins suggests that its catalytic activity could vary from homologs and make this candidate worthwhile exploring for alternative function.

Gene candidates 2, 3 and 4 were pre veraison expressed transcripts with candidates 3 and 4 having oxido-reductase motifs suggestive of function in several of the interconversions in the pathway for tartrate synthesis (reviewed in Loewus, 1999).

Gene candidate 5, which was subsequently found to encode the enzyme responsible for the key step in TA biosynthesis, had 77% amino acid homology to a plant L-iditol dehydrogenase. When the sequence was aligned against the sequences held on protein databases, matches to several interesting conserved motifs were identified. The N-terminal domain of alcohol dehydrogenase-like proteins has a GroES-like fold, the C-terminal domain having a classical Rossman-fold. Proteins

sharing homology included alcohol dehydrogenase, which contains a zinc-finger subdomain within the GroES-like domain, ketose reductase (sorbitol dehydrogenase), formaldehyde dehydrogenase, quinone oxidoreductase and 2,4-dienoyl-CoA reductase. The high homology of this gene to known proteins was a deterrent against its further characterisation, but sheep sorbitol dehydrogenase was also found to be similar to a characterised idonate dehydrogenase found in *E. coli* (Bausch *et al.*, 1998).

Gene candidate 6 displayed significance in that it encoded a homolog to succinic semialdehyde dehydrogenase from plants, which has been suggested to potentially have, in addition to its widely recognised role, a second metabolic function in oxidising TA semi aldehyde to TA (Salusjarvi *et al.*, 2004) and was among the highest candidate genes differentially expressed in the PV berry. In the pathway of TA formation it was determined by careful radioisotope tracer studies that tartaric semi aldehyde is the penultimate compound before TA is formed (Loewus, 1999).

Gene candidates 7 and 8 were small chaperone like proteins, one shared homology to a cytochrome B561 protein and had a ferric reductase motif; Asard *et al.* (2002) implicated a similar protein in controlling ascorbate metabolism.

Candidate genes 9 and 10 shared homology with transketolase sequences (Flechner *et al.*, 1996, Mendel *et al.*, 1996, Bouvier *et al.*, 1998); both were isolated from the grapevine BLAST option at TIGR (www.tigr.org/grapevine) and shared 86% identity at the amino acid level. Their importance to this study lies in the implication of a transketolase being able to cleave the 5-keto-D-gluconic acid molecule in bacteria (Salusjarvi *et al.*, 2004). No proof of this has yet been demonstrated, but biochemically it would make a great deal of sense. Transketolase enzymes are functional, primarily in plastids, in many aspects of cell metabolism, although they are potentially promiscuous enzymes, actively utilising many substrates (Schenk *et al.*, 1998). Within chapter 6 of this thesis, research is described in which real time PCR was used to measure its transcript levels during berry development and the putative transketolase enzyme was expressed as a recombinant protein in bacteria to provide enzymological evidence for its role in TA synthesis.

3.4 Discussion

Transcriptional profiling has provided a set of 10 candidate genes that fit a selection criterion based on expression profile and annotated protein homology to domains and motifs that provide potential for involvement in TA biosynthesis (Table 3.4). The ability to characterise transcriptional events during a particular time of plant development is a powerful tool towards understanding basic cellular processes (Van der Hoeven *et al.*, 2002) and in this case critical to pinpointing gene(s) involved in the pathway for TA synthesis.

Global gene expression patterns provide a snapshot of the pre veraison berry specific transcripts. But correlating these genes with well understood biochemical and cellular events known to take place at this time of development is essential to validate the experimental design. For instance, pre veraison berry development is characterised by the berry developing from cap fall to the developing fruit (Coombe and McCarthy, 2000), a rapid period of cell division, organic acid synthesis, photosynthesis, formation of the embryo, and preparing the anatomy, physiology and metabolism for ripening, which are to follow post veraison. When looking at pre veraison transcripts differentially expressed during this time, enzymes involved with aspects of metabolism (Figure 3.3) dominated the profile of annotated proteins. Considering that rapid cell division (occurring in the root apical meristem, bud and shoot formation), photosynthesis (occurring in leaves) and organic acid synthesis (occurring in nearly all areas of the plant (Kleiwer, 1965)) are occurring at this time, to find that a large proportion of expressed genes were likely involved in metabolism was not unexpected (Figure 3.3). To challenge this point, nearly 30 % of all transcripts were unannotated, which may suggest that the reason a lot of genes associated with metabolism were highlighted is because these genes fall under popular areas of research. Genes related to ripening fruit (Contig numbers 1028904, 1032387), seed formation (contig number 1029591) and TA formation (putative, later shown to be 1029130), which are restricted to this stage of development, were also found in the list of differentially expressed genes (Table 3.2). Therefore, it may be assumed that by searching for differentially expressed genes, housekeeping genes and those not associated with processes commonly occurring in the rest of the plant were successfully removed from the data set by the chosen statistical parameters (similar to that used by Goes da Silva *et al.*, 2005, but the data set was different in that a

minimum of 6 ESTs per TC was chosen). Ultimately, if a gene is expressed in other areas of the plant, but the vast majority of ESTs encoding the genes of interest are found in the pre veraison berry we can safely assume it is differentially expressed (Ronning *et al.*, 2002). For this reason a cut-off value was used, requiring that greater than 80% of ESTs must be derived from TA synthetic cDNA libraries for any TC considered to be differentially expressed (adapted from the R-statistic used by Sketel *et al.*, 1999 and Goes da Silva *et al.*, 2005). The result of this experiment was the identification of several genes of interest, such as a seed specific protein homolog, several glucosyltransferase protein homologs that beckon characterisation, ripening related protein, transcription factor, a chalcone flavanone isomerase which is a key step in flavonoid biosynthesis (Dixon and Steele, 1999), many dehydrogenases and 22 genes with no clear protein homologs. Numerous genes with no function suggest that this part of plant development is wide open to study, and that workhorse experimental plants such as Arabidopsis do not necessarily contain the same suite of genes.

In a broad sense, the process of annotating candidate sequences based on homology has many flaws, including mis-annotation and natural variability. That is, only a few hundred lines of descent for proteins and protein domains occur (Gerlt and Babbit, 2000). The rest is evolution, whereby small changes in amino acid structure can influence protein interactions (Gerlt and Babbit, 2000). A suggested approach for further work is cloning and prokaryote over expression of all unknown proteins, upstream sequencing for functional clues hidden within promoter sequences and microarray experiments towards linking transcription with various physiological responses and stress responses. Moreover, reverse genetics via RNAi knockout of genes may provide further evidence towards candidate TCs role in fruit ripening. Many other genes that were eliminated in this analysis because there were too few ESTs per TC (5 and less) were highly differentially expressed (data not shown). Genes within this subset, although having limited statistical significance, are likely to encode key genes in the ripening process and TA formation. To this end, it is important that groups continue to deposit sequenced ESTs into the public domain to create the potential to mine the entire transcriptome.

Concluding this chapter, the hypothesis that bioinformatics could be effectively used to isolate genes by searching for those composed of ESTs from 10 cDNA libraries of pre veraison berries compared to the 46 cDNA libraries from the rest of the grapevine as a background subtractive, combined with a detailed

understanding of putative biochemical conversions involved in TA synthesis, provided us with a set of candidate genes to further test and validate as candidates. In the past 5 years a large amount of infrastructure has been poured into EST sequencing projects in non-model species creating enormous databases of genomic data, but as yet little of this data has been utilised to its full potential. Transcriptional profiling in plants, which is generally undertaken by groups associated with the sequencing, provides a gross overview of trends in transcriptional structure (Sketel *et al.*, 1999, Ewing *et al.*, 2000, Van der Hoeven *et al.*, 2002, Ronning *et al.*, 2003 and Goes da Silva *et al.*, 2005, Achnine *et al.*, 2005, Alba *et al.*, 2005). The research described in this chapter used genomic data to mine for genes expressed when and where TA biosynthesis maximally occurs. The success of this approach was due to a combination of understanding the uncharacterised pathway at a basic level (thanks to many detailed radioistope tracer studies by Kazumi Saito and coworkers between 1968 and 1994), a well-defined plant ontology in the grapevine (Jackson, 2000 describes both spatial and temporal developmental stages), and EST sequencing of cDNA libraries from all physiological locations of the vine at various developmental stages (IGGP). These data, combined, provide a means whereby the cDNA sequencing datasets could be interrogated and thus prompted to reveal hitherto hidden information, this method offers an alternative to common forward and reverse genetic approaches available in model plants. The following chapters (chapter 4, 5 and 6) describe research that utilised the framework provided in this chapter to test for correlation of candidate genes with changes in the biosynthesis of TA and characterisation of candidate TCs.

Chapter 4

Isolation of TA synthetic candidate genes using large scale metabolic profiling to assess variation in TA and subsequent correlation of gene expression with biosynthesis using rtPCR

4.1 Introduction

Biosynthesis and accumulation of organic acids are key steps in fruit ripening and development (Seymour *et al.*, 1993). In many species, malic acid or citric acid are the predominant acids found in the fruit, with lesser amounts of succinic, lactic, acetic and ascorbic acids also commonly found. In apples, malic acid is the most common form of organic acid contributing to pH and flavour of the fruit, whereas in the orange, citric and ascorbic acids dominate the organic acid profile. Grapevines, from species within the family Vitaceae, are unique among crops under broad cultivation (the only other example being the tamarind, *Tamarindus indica*) in which the major organic acid accumulating within the fruit is TA (Buchs, 1957, cited by Stafford, 1959). Plants possessing the necessary enzymes to form TA and the genes encoding them occur in a remarkably narrow botanical distribution (Amerine 1956, Stafford 1957, 1959, Loewus 1999), most notably within the Vitaceae.

An early review (Stafford, 1959) reported the distribution of TA in the leaves of angiosperms, using paper chromatography. Leaves were chosen for this study because at the time it was thought that TA biosynthesis occurred in the leaves and was transported to the fruiting and flowering parts of the plant. This was subsequently disproved by translocation blocking experiments by Hale (1962), which showed TA biosynthesis could take place in an excised grape berry. Using paper chromatography Stafford (1959) showed that the distribution of TA was limited to three main families, Vitaceae (*Vitis vinifera*: 318 μmoles per leaf), Geraniaceae (*Pelargonium hortorum*: 41 μmoles per leaf) and Leguminocae (*Phaseolus vulgaris*: 18 μmoles per leaf) with by far the largest concentrations accumulating in the Vitaceous plants, up to 494 μmoles per leaf in *V. lubruscana*. Several genera including *Parthenocissus, Cissus, Ampelocissus, Ampelopsis* and the most agronomically important genus, *Vitis*, used for table grape and wine production worldwide occur within this family. *Vitis* and *Parthenocissus* have both been used as model plants to demonstrate the ability to accumulate TA via ascorbic acid catabolism (radioisotope tracer studies summarised by Loewus, 1999).

Individual cultivars of *V. vinifera* accumulate malic and TA in different ratios, for instance cultivars Carnigane, Malbec and Pinot noir have proportionally higher relative concentrations of malic acid (Ruffner, 1982) whereas other cultivars such as

Riesling, Semillon, Merlot, and Grenache have higher TA:malic acid ratios (Kliewer *et al.,* 1967). Significant variation has previously been noted also between seasons as well as cultivars (Winkler *et al.,* 1974). It must be noted that the measurement of these ratios will necessarily always reflect not only the accumulation of individual acids through their biosynthesis and translocation into the vacuole, but in the case of malic acid, its catabolism during later stages of berry ripening. In a recent study of a fleshless grape mutant it was found that the ratio of malic to TA was particularly skewed to TA accumulation compared to the wildtype vine (Fernandez *et al.,* 2006). Moreover, malic acid metabolism increases with increasing temperature (Coombe, 1987) particularly at temperatures greater than 30°C (Ruffner and Hale, 1976). Iland and Coombe (1988) measured greater than 80% consumption of malic acid in the latter stages of development.

Interestingly, despite relatively detailed knowledge of TA to malic acid levels within a few species of *Vitis spp*, comparative data regarding the inter-generic and inter-species variation within the family Vitaceae is lacking. A species showing aberrant levels of TA accumulation, either much greater than commonly found within species of *Vitis*, or much less, or one in which TA was totally absent, would provide a powerful means to validate the candidate TA biosynthetic genes isolated as described in Chapter 3. Elevated TA levels may be linked to increased candidate gene expression, or conversely, a species lacking TA may show reduced or zero expression of a candidate gene.

In the present chapter, the level of accumulation of four organic acids during berry development was studied. A total of 28 members of the family Vitaceae, originating from different geographical locations were used and acids measured were tartaric, oxalic, malic and succinic acid. Wide variability was shown among grape species, and critically, one species was identified in which TA did not appear to accumulate. The transcription of candidate TA-biosynthetic genes (from Chapter 3) was compared between the non-TA accumulator and the TA-accumulating species. In this way, one candidate gene was identified with an expression pattern consistent with TA biosynthesis.

4.2 Methods and Materials

Chemicals

Refer to the list of suppliers of authentic chemicals in Chapter 2

Plant material

Berries from species within the family Vitaceae were grown at the University of California grape germ plasm experimental vineyard, (part of the National Clonal Germplasm Repository for Fruit and Nut Crops), Winters CA. Species were chosen originating from 4 continents (Table 4.4). Samples were collected pre veraison (denoted as stage 1), veraison (stage 2) and post veraison (stage 3). Stage 1 was defined as the developmental period prior to colour change and sugar accumulation. Samples were collected when berries were 4-6 weeks post anthesis. Post veraison or stage 3 sampling was carried out when berries were at physiological ripeness, having passed through colour change and sugar accumulation, and were collected between 14-16 weeks post anthesis (Coombe and McCarthy, 2000).

Sampling

Sampling took place over two growing seasons, the 2003 and 2004 seasons. Samples were collected in a population of a minimum of 2 vines, which are genotypically identical. Multiple bunches were collected and samples randomised by mixing thoroughly, then 3 samples of 5 berries were selected at random for extraction of acids and their analysis by HPLC. The remaining samples were stored at -20^0C for further HPLC analysis and -80^0C for RNA extraction. Post veraison berries were sampled in summer 2003 (August, by Dr. Alberto Iandolino), and based on the greatest variation in results of these post veraison samples, species were selected for pre veraison berry organic acid measurements, which were taken in spring (May, by the author) 2004.

Sample preparation

Refer to the acid extraction method described in Chapter 2.

Quantification of organic acid content by HPLC

Detection of the organic acids including oxalic, tartaric, and malic was by UV absorbance at 210 nm using an ultra violet detector fitted to a HP 1100 series HPLC (Agilent Technologies Inc., Palo Alto, CA). This instrument was coupled to a refractive index detector (RID) used to quantify glucose and fructose content. Twenty micro litres of the berry extract was injected into the HPLC, which comprised two back to back Aminex HPX-87H columns (7.8x300 mm, Bio-Rad Laboratories Inc., Hercules, CA), protected by a cation H+ cartridge guard column (Bio-Rad Laboratories Inc., Hercules, CA) at a flow rate of 0.6 ml min^{-1}. The column temperature was maintained at 50 °C for the entire separation. The 30 min. isocratic run used a 1.5 mM aqueous sulfuric acid (H_2SO_4) solution as the mobile phase (Frayne, 1996). Peak identity and quantification were determined using a set of standard solutions. The HP Chemstation® A.10.02 software was used for instrument operation, peak identity, manual integration and quantitation of results.

Malic acid assay

Roche BOEHRINGER MANNHEIM Enzymic Bioanalysis was used to quantify malic acid in the *Ampelopsis* species for malic acid in addition to HPLC due to a substantial peak of ascorbic acid interfering with accurate integration of the HPLC chromatogram. The method was achieved as described in the BOEHRINGER MANNHEIM kit (Cat. No. 10 139 068 035) and samples were read on a spectrophotometer at 340 nm.

Principle component analysis

Principle component analysis (PCA) and ordination plots were compiled in the software program SAS (SAS Institute Inc. NC, USA) and used to elucidate the relationships between species and the profile of organic acids.

Comparative method of analysis

The statistical program MATLAB® (Simulink and Stateflow Inc) was used to create a two dimensional hierarchical cluster of organic acid data based on a similarity relationship between all 28 grape species used and their organic acid profile of malic, tartaric, oxalic and succinic acids.

PCR validation of gene expression

Total RNA from *Vitis vinifera, V. californica, Ampelopsis brevipedunculata* and *A. acontifolia* was extracted from washed grape berries and leaves as described (Iandolino *et al.*, 2004). RNA was made into single strand cDNA using standard protocol (StrataGene®). Genomic DNA was extracted (MoBio®) from *V. vinifera, A. acontifolia* and *P. tricuspifolia*. For candidate genes, internal 18-22mer primers were designed with annealing temperatures approximately 55°C (Table 4.1) and for gene candidate 5, 3 additional sets of internal primers spanning the ORF were designed. Ubiquitin and actin sequences were used for amplification controls due to transcription of this gene occurring throughout berry development. RT-PCR reactions comprised 1.5 pmol of each primer, 0.5µl Taq DNA polymerase, 0.5µl dNTPs, 1µl MgCl (25 mM), 1µl (500 ng.μl^{-1}) template mRNA (cDNA), 2µl 10× (Mg free) buffer, to 20 µl with dH_2O. A three minute heating at 95°C followed by 32 cycles of 95 °C (30 sec) denaturation, 55-60 °C (30 sec) annealing temp and between 45 and 270 sec extension followed by a final extension of 5-7 minutes.

Table 4.1 Internal primers used to amplify each candidate gene

Candidate		Primers (internal)
1	*Forwards*	GAGTGTAGGCAGTGGGTGGT
	Reverse	TGAAGGAAATGGGAATGGAG
2	*Forwards*	GAGCTGCAAGATTCACCACA
	Reverse	TTGACATGGGATGATGCACT
3	*Forwards*	CAGCTCTCTCATGGTGTCCA
	Reverse	CCCTCTACAGCGACAAGGAG
4	*Forwards*	CTTGCACAAATGCTCCTTCA
	Reverse	CCTTTCGGCTCATGGATTTA
5	*Forwards*	AAGTTTGCCTTGTGGGTTTG
	Reverse	AAGGCTTCCTCCACATCCTT
6	*Forwards*	CACCATTGACAGCCTTAGCA
	Reverse	CAGGTCTGCATCGTCAAAGA
7	*Forwards*	CTTGAACCAGGCAACCATC
	Reverse	TTCTGTTTTGGGCTCTTGCT
8	*Forwards*	CCACCCAGGTAGTCTCTGGA
	Reverse	CTCCAGGGTCTGCTGAAAAG
9	*Forwards*	CTGTCGATAGACGCAGTGGA
	Reverse	CACTTCAACCCCAGGTGTCT
10	*Forwards*	AGAAGAGCGCAATGTCAGGT
	Reverse	TCTCCAAGCCCAATTGAATC

4.3 Results

4.3.1 Development of HPLC analysis of berry organic acid profiles

HPLC chromatography was able to discriminate between most of the organic acids surveyed. Malic and ascorbic acids co-eluted from the column system used; an enzymatic kit based on malate dehydrogenase activity was used to measure malic acid, which could then be subtracted from the peak to obtain an approximate measure of ascorbic acid concentration. Ascorbic acid was not quantitatively measured due to rapid degradation and sample storage. In the berries of *Ampelopsis spp.*, levels were measurable but not considered accurate. To a lesser extent an overlap occurred also between the elution times of authentic standards of citric and oxalic acids. In this case, retention times were separated by ca 0.2 min., which was sufficient to allow discrimination. Citric acid was not detailed in this study because it is not associated with the focus of this research and concentrations in Vitaceous fruit are very low (Stafford, 1959). Berries ground in acidic extraction buffer displayed a peak at the correct retention time for oxalate, when berries were ground under non-acidic conditions the peak was substantially smaller (DeBolt *et al.,* 2004).

4.3.2 Pre veraison measurements of grape berry organic acids

Pre veraison collection of berries was less extensive than post veraison collection due to tissue availability, with 10 species and 25 species sampled respectively. Data for TA revealed that one species, A. *aconitifolia* contained no detectable TA. Its closest related species A. *brevipedunculata* contained measurable amounts of TA. Species of *Vitis* surveyed all contained large amounts of TA as did species of *Parthenocissus*. The greatest accumulator of TA was *V. riparia*, which contained ca 17 $mg.g^{-1}$ FW. But it must be noted that species of *Vitis* except *V. californica* and *V. champinii* contained greater than 10 $mg.g^{-1}$ FW (Table 4.2). Malic acid was present in all species surveyed, as was succinic acid and oxalic acid. Succinate was consistently found to occur in substantial concentrations in pre veraison fruit (Table 4.2). Ascorbic acid was not present in all species, in fact was only detectable in the *Ampelopsis* species (Table 4.2).

Table 4.2. Average and standard deviation data for organic acid levels in berries of all species screened during pre veraison development. TA,MA and OxA levels expressed as mg acid per g fresh weight berry tissue; AA and SU levels expressed as mg acid per 100 g fresh weight berry tissue.

Pre veraison Family	TA		MA		OxA		SU		AsA	
Genus Species	Av	Std Dev.	Av	Std Dev.	Av	Std Dev.	Av	Std Dev.	Av	Std Dev.
Asia										
A. acontifolia	0	0	6	0	0.8	0.3	48.8	7.3	6.5	2.4
A.brevipedunculata	0.6	0.3	6	0	1.4	0.2	68	12.4	8.5	3.6
Vitis jaquomontii	11.3	0.4	10.4	1.2	0.4	0	4.9	0.8	0	0
Vitis amerensis	11.9	0	7.1	0.3	0.2	0	1	0.1	0	0
Americas										
Vitis californica	9.6	0.9	14.5	1	0.2	0.1	7.7	0.7	0	0
Vitis bloodworthiana	16.5	1.1	14.1	1.8	0.6	0.1	6.2	1.6	0	0
Vitis acerifolia	16.9	3	11.7	0.9	0.5	0.2	1.6	1	0	0
Vitis champinii	9.5	3.9	8.9	2.2	0.1	0	2.2	0.8	0	0
France										
Vitis vinifera	12.8	2.5	11.6	0.5	0.2	0	15.2	1.1	0	0
Vitis riparia	17.7	2.4	14.8	1.4	0.6	0.1	1	1.1	0	0

4.3.3 Post veraison measurements of grape berry organic acids

Analysis of TA levels in post veraison fruit showed that again one species, *A. aconitifolia*, contained no TA (Figure 4.1). As observed in pre veraison fruit, all the Vitis species made substantial amounts of TA. The species that were maximal TA pre veraison, although maintaining substantial amounts of TA, were not necessarily the greatest accumulators in the post veraison fruit (Table 4.2 and Table 4.3). There was no great reduction in TA content of grape berries seen between pre and post veraison fruit. Comparing average pre veraison with post veraison measurements of berry organic acid content in berries from species of the genus *Vitis* did however demonstrate a gross trend of reduction in malate and succinate post veraison, displaying much higher average values in pre veraison fruit (Table 4.2 and 4.3). Oxalate concentrations were not seen to change significantly between pre and post veraison. Three other grape specimens were measured for post veraison accumulation but were not added to Table 4.3. A further species of *Parthenocissus, P. tricuspifolia,*

was identified in the Adelaide Botanical Gardens and measured for TA content. The Adelaide Botanical Gardens also provided a second *A. aconitifolia* vine, which again made no TA. Moreover, the genus *Muscadinia* was represented by berries collected from *M. rotundafolia* which accumulated 8.84 ± 0.94 mg. gm^{-1} FW TA and 14.25 ± 1.53 mg. gm^{-1} FW malic acid.

Table 4.3 Average and standard deviation all species screened during post veraison berry development. TA,MA and OxA levels expressed as mg acid per g fresh weight berry tissue; AA and SU levels expressed as mg acid per 100 g fresh weight berry tissue.

Post veraison										
Family	**TA**		**MA**		**OxA**		**SU**		**AsA**	
Genus Species	**Av**	**Std Dev.**	**Av**	**Std Dev.**	**Av**	**Std Dev.**	**Av**	**Std Dev.**	**Av**	**Std Dev**
Asia										
A. acontifolia	0.0	0.0	1.9	0.6	1.8	0.9	2.2	0.6	0.3	0.0
A.brevipedunculata	0.8	0.9	1.0	0.8	1.0	0.3	14.9	2.3	0.5	0.2
A.vitifolia	0.61	0.22	2.37	0.42	2.35	0.71	18.90	4.51	0.0	0.0
V. thunbergii	12.2	1.1	8.2	0.8	0.4	0.1	0.0	0.0	0.0	0.0
V. jaquomontii	7.8	1.6	7.5	1.9	0.3	0.1	0.5	0.5	0.0	0.0
V. ficifolia	16.8	1.8	5.1	0.7	0.4	0.6	0.4	0.1	0.0	0.0
V. amerensis	17.5	0.9	4.9	2.5	0.3	0.0	0.0	0.0	0.0	0.0
Americas										
V. californica	11.6	1.5	6.1	1.1	0.2	0.2	0.2	0.2	0.0	0.0
V. bloodworthiana	10.3	0.6	7.1	2.0	1.0	0.3	0.0	0.0	0.0	0.0
V. biformis	16.9	2.1	23.7	2.9	0.7	0.3	1.5	0.4	0.0	0.0
V. acerifolia	14.2	1.6	10.3	2.0	0.6	0.3	0.7	0.4	0.0	0.0
V. champinii	10.8	1.6	5.1	0.9	0.2	0.1	0.4	0.3	0.0	0.0
V. cinerae	11.6	2.2	10.7	0.2	0.6	0.3	0.0	0.0	0.0	0.0
V. treleaseii	8.6	1.9	8.9	1.8	0.3	0.4	0.3	0.1	0.0	0.0
P. quinquefolia	6.8	1.0	4.1	0.9	0.4	0.4	1.2	0.7	0.0	0.0
V. tilifolia	14.7	0.6	20.7	1.2	2.2	0.5	0.6	0.1	0.0	0.0
V. labrusca	11.7	2.6	8.1	2.3	0.3	0.1	1.7	0.09	0.0	0.0
V. arizonica	8.7	0.6	7.7	0.7	1.0	0.5	0.4	0.1	0.0	0.0
V. nesbittiana	8.1	0.5	8.2	0.5	0.1	0.2	0.4	0.1	0.0	0.0
V. monticola	9.4	1.6	7.1	0.4	0.3	0.1	0.3	0.3	0.0	0.0
V. girdiana	13.0	1.4	11.2	1.3	1.4	0.7	0.5	0.1	0.0	0.0
V. palmata	13.6	1.2	13.1	1.9	0.3	0.5	0.3	0.0	0.0	0.0
V. vulpina	15.1	1.3	14.3	3.3	0.0	0.0	0.4	0.1	0.0	0.0
France										
V. riparia	9.5	1.9	6.9	1.1	0.4	0.2	1.7	2.0	0.0	0.0
V. vinifera	6.3	0.7	5.6	0.4	0.2	0.0	0.3	0.2	0.0	0.0

4.3.4 Distribution of TA in the family Vitaceae

A large shift in TA profile was measured between the *A. aconitifolia* (Figure 4.1B) and *V. vinifera* (Figure 4.1A), the species *A. acontifolia* makes no TA, whilst two others in the same genus *A. brevipedunculata* and *A. vitifolia* make TA in small amounts (under a $mg.g^{-1}$). The identification of a species of TA deficient grape was the primary discovery of this survey and pertains to the latter parts of this chapter for isolation of candidate TA synthetic genes.

Parthenocissus (2n=40) and *Muscadinia* (2n=40) both displayed a similar profile to the *Vitis* genus with TA measured as the greatest accumulating organic acid post veraison. There is significant variation between post and pre veraison measurements, which were taken in consecutive seasons. In the pre veraison data set, accumulation patterns showed *V. riparia, V. acerifolia, P. tricuspifolia* and *V. bloodworthiana* had the greatest TA concentrations (Table 4.2). Conversely in post veraison fruit that were collected in the previous growing season, *V. ficifolia, V. amerensis* and *V. biformis* (Table 4.3) had the greatest concentrations of TA. *V. acerifolia* consistently had the highest concentrations across the two growing seasons with 16.9 and 14.2 $mg.g^{-1}$ FW respectively.

Of the 25 species collected in the measurement of post veraison TA concentrations (Figure 4.2A, shows the TA concentration of species which align with those in Table 4.4) a range of 0 in *A. aconitifolia* to 17.5 $mg.g^{-1}$ FW in *V. amerensis* was observed (Figure 4.2B). Two out of the three species of the genus *Ampelopsis* accumulated less than 5 $mg.g^{-1}$ FW TA, with *A. brevipedunculata* and *A. vitifolia* both displaying a small peak that had the same elution profile as TA. In the genus *Vitis, Muscadinia* and *Parthenocissus*, all species accumulated greater than 5 $mg.g^{-1}$ FW.

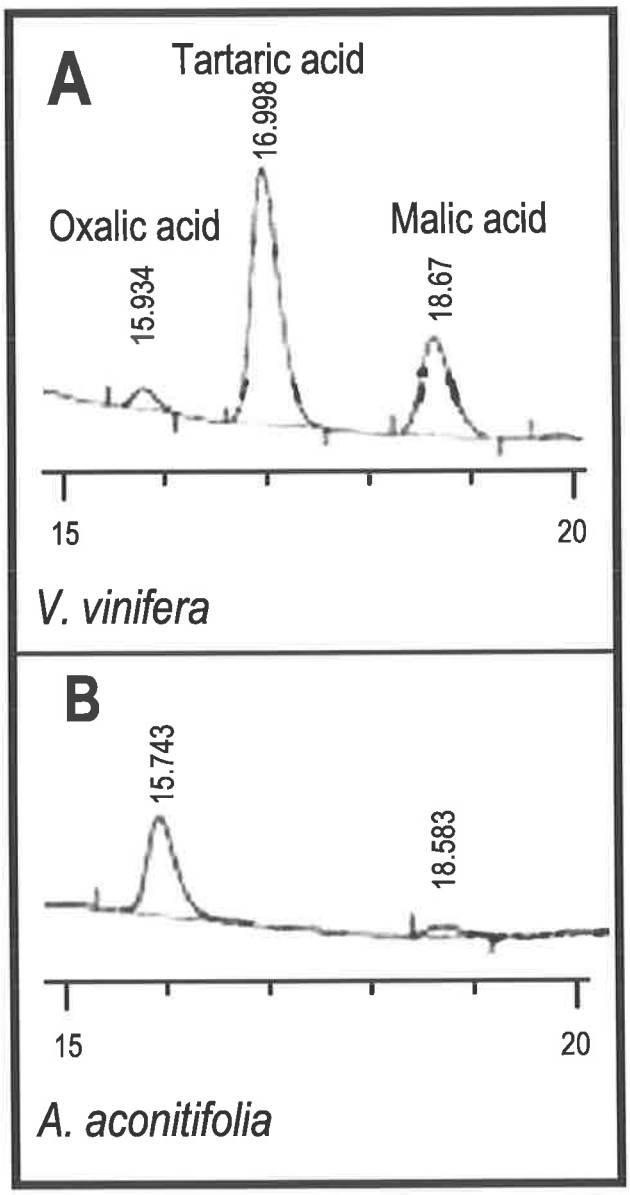

Figure 4.1 HPLC chromatogram and elution profile of the TA forming species *Vitis* (A) versus the non-TA forming species *Ampelopsis aconitifolia* (B)

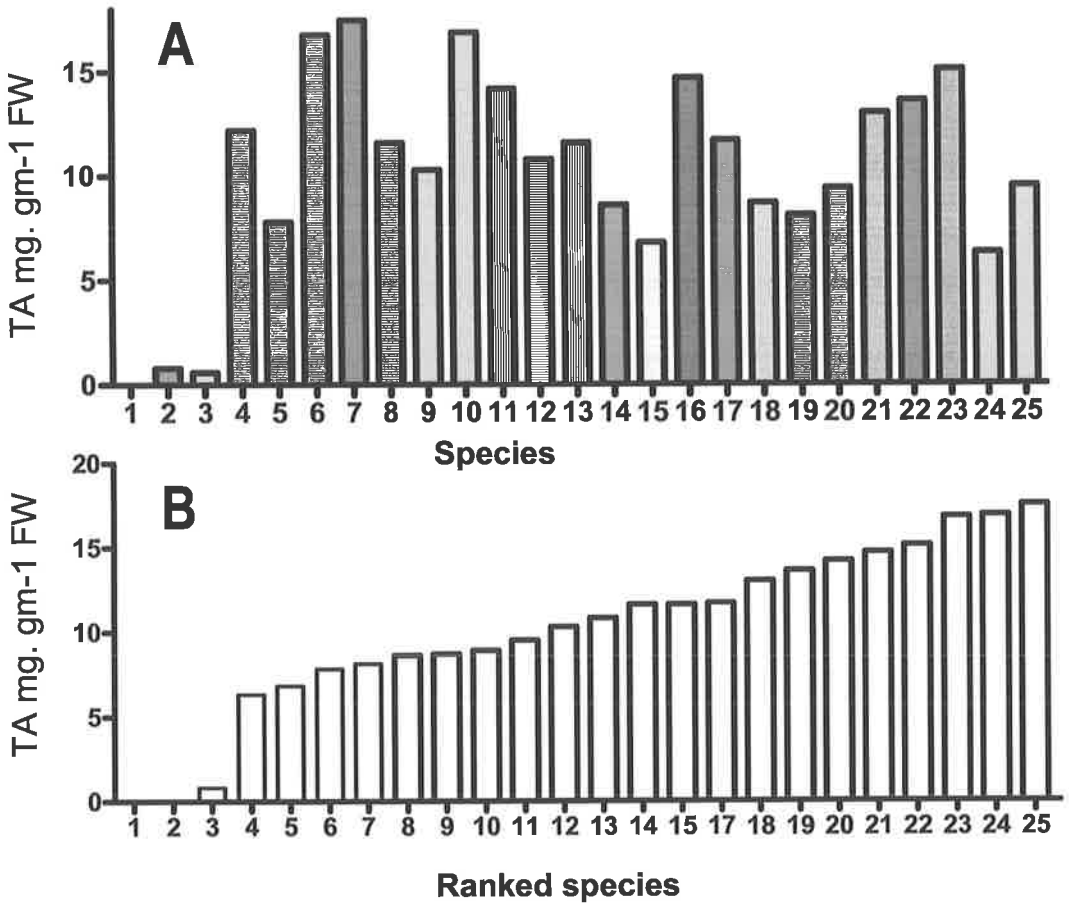

Figure 4.2 A. Profile of TA among 25 species of family Vitaceae (numbers correspond to species listed in Table 4.4). B. Ranked TA levels among the 25 species listed in A. Classification 1-25 in panel B does not correspond to that in panel A.

Table 4.4. Grapevine genus and species used in this study the continent of origin and a tentative linkage based upon organic acid profile and average berries per gram fresh weight

ID Number	Genus	Species	Origin	Tentative genetic linkage	Berries per gram
		Asia			
1	*Ampelopsis*	*aconitifolia*	China/Korea	13	3
2	*Ampelopsis*	*brevipedunculata*	China/Japan	13	4
3	*Ampelopsis*	*vitifolia*	Asia	13	4
4	*Vitis*	*jacquemontii*	Pakistan	12	0.7
5	*Vitis*	*ficifolia*	China	10	6
6	*Vitis*	*thunbergii*	Asia	9	7
7	*Vitis*	*amurensis*	China	9	1.3
		Americas			
8	*Vitis*	*bloodworthiana*	Mexico	2	4
9	*Parthenocissus*	*quinquefolia*	USA	14	7
10	*Vitis*	*cinerae*	USA	7	4
11	*Vitis*	*acerifolia*	USA	2	2
12	*Vitis*	*arizonica*	Mexico	1	3
13	*Vitis*	*nesbittiana*	Mexico	1	0.7
14	*Vitis*	*girdiana*	USA	1	3
15	*Vitis*	*monticola*	USA	6	2
16	*Vitis*	*tiliifolia*	Brasil	10	7
17	*Vitis*	*palmata*	USA	2	4
18	*Vitis*	*vulpina*	USA	2	2.5
19	*Vitis*	*labrusca*	USA	3	0.85
20	*Vitis*	*biformis*	Mexico	4	7
21	*Vitis*	*champinii*	USA	4	0.9
22	*Vitis*	*californica*	USA	1	0.8
23	*Muscadinia*	*rotundafolia*	USA	4	0.8
		France			
24	*Vitis*	*vinifera*	France	11	0.5
25	*Vitis*	*riparia*	France	2	5

4.3.5 Distribution of other organic acids in the family Vitaceae

In addition to TA: malic acid, oxalic acid and succinic acid were measured under acidic conditions via HPLC. Malic acid was accumulated to measurable quantities in all species surveyed (Figure 4.3). The range of malic acid accumulation was greatest post veraison and varied from 1 $mg.g^{-1}$ FW in *A. brevipedunculata* to 23.2 $mg.g^{-1}$ in *V. biformis* (Table 4.3).

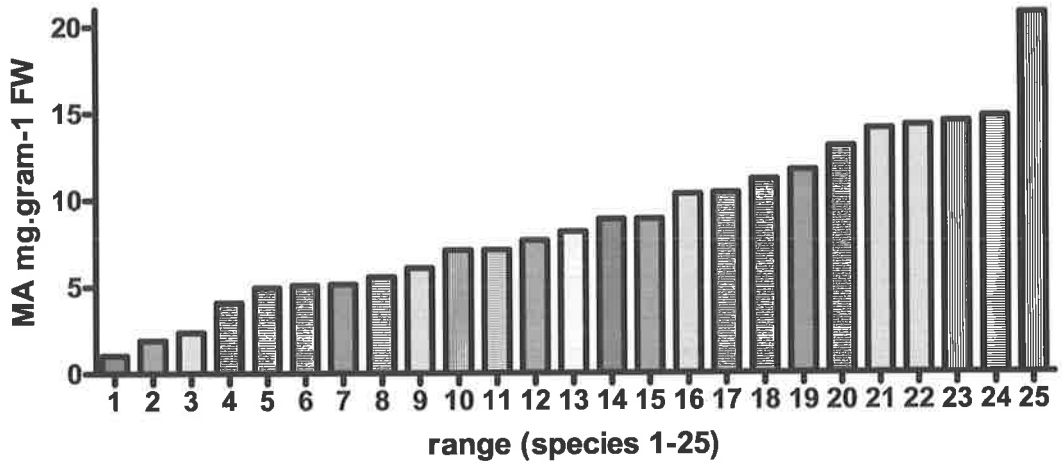

Figure 4.3 Represents the post veraison range of malic acid accumulated in the family Vitaceae

In both pre and post veraison berries, species within the genus *Ampelopsis* not only accumulated the least TA but also accumulated greater amounts of succinic acid than any other genus. *A. acontifolia* and *A. brevipedunculata* make 48.8 and 68 $mg.g^{-1}$ FW of succinic acid respectively (Table 4.2) and several species of *Vitis* accumulated no succinic acid post veraison (Figure 4.4). During pre veraison berry development all species of *Vitis* screened accumulated succinic acid. Those species that accumulated substantial amounts of succinic acid were *V. vinifera* (14.2 $mg.g^{-1}$ FW), *V. californica* and *V. bloodworthiana* all of which accumulated greater than 5 $mg.g^{-1}$ FW (Table 4.2). Post veraison measurements revealed than only species in the genus *Ampelopsis* maintained accumulation of succinic acid greater than 5 mg. g^{-1} FW, whereas all species of *Vitis* and *Parthenocissus* screened had less than 2 $mg.g^{-1}$ FW (Table 4.3).

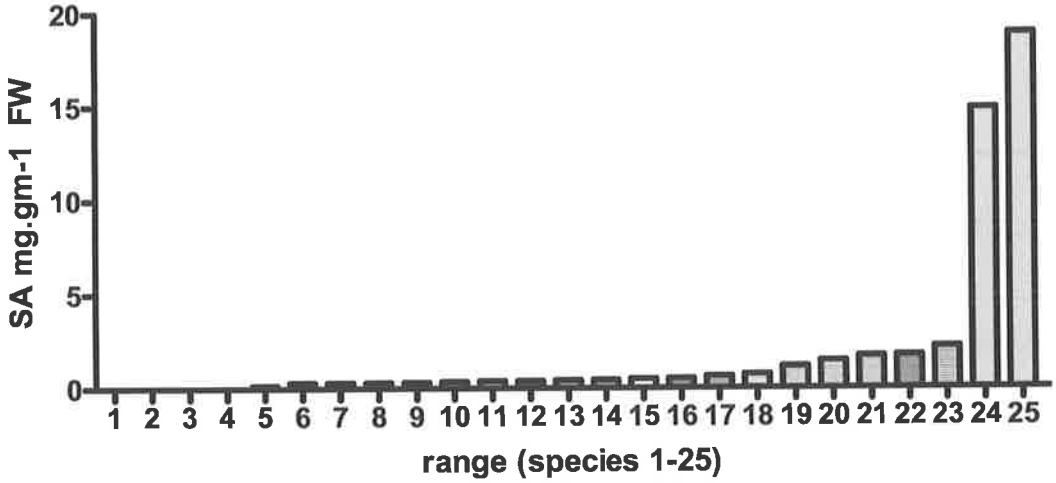

Figure 4.4 Represents the post veraison range (from lowest to highest) of succinic acid accumulated in the family Vitaceae

The accumulation of oxalic acid across the surveyed species was under 3 $mg.g^{-1}$ FW (Figure 4.5). Species that accumulated greater concentrations of oxalic acid were the species of *Ampelopsis*, however several species of *Vitis* also including V. *bloodworthiana*, *V. champinii* and *V. tillifolia*. One species of grape lacked oxalic acid from its berries, that being *Muscadinia rotundifolia*.

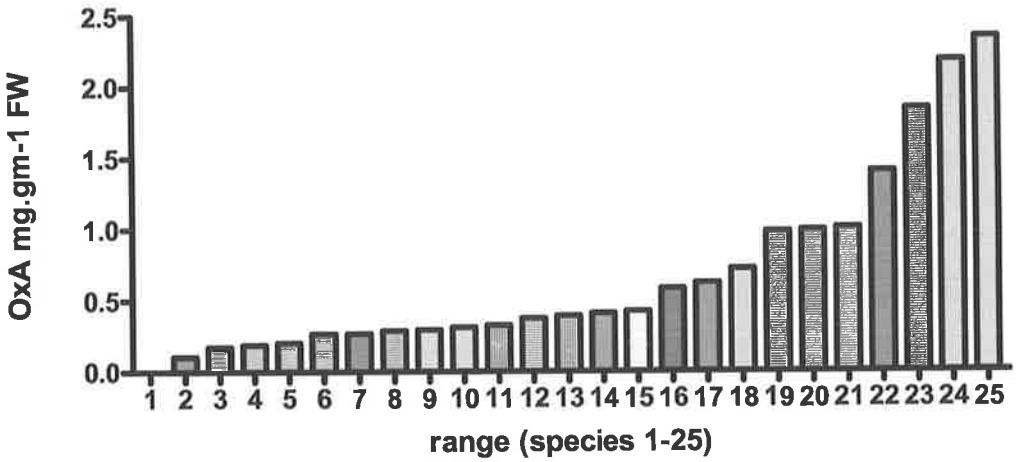

Figure 4.5 Represents the post veraison range of oxalic acid accumulated in various species the family *Vitaceae*

4.3.6 PCR validation of gene expression

Validation of pre veraison expression of candidate genes as well as correlating candidate expression with the species of grape making no TA (*A. aconitifolia*) was achieved for candidate genes (Table 4.1). TA biosynthesis maximally occurs during stage 1 of berry development, which is depicted by the inset photograph of a pre veraison berry (Figure 4.6).

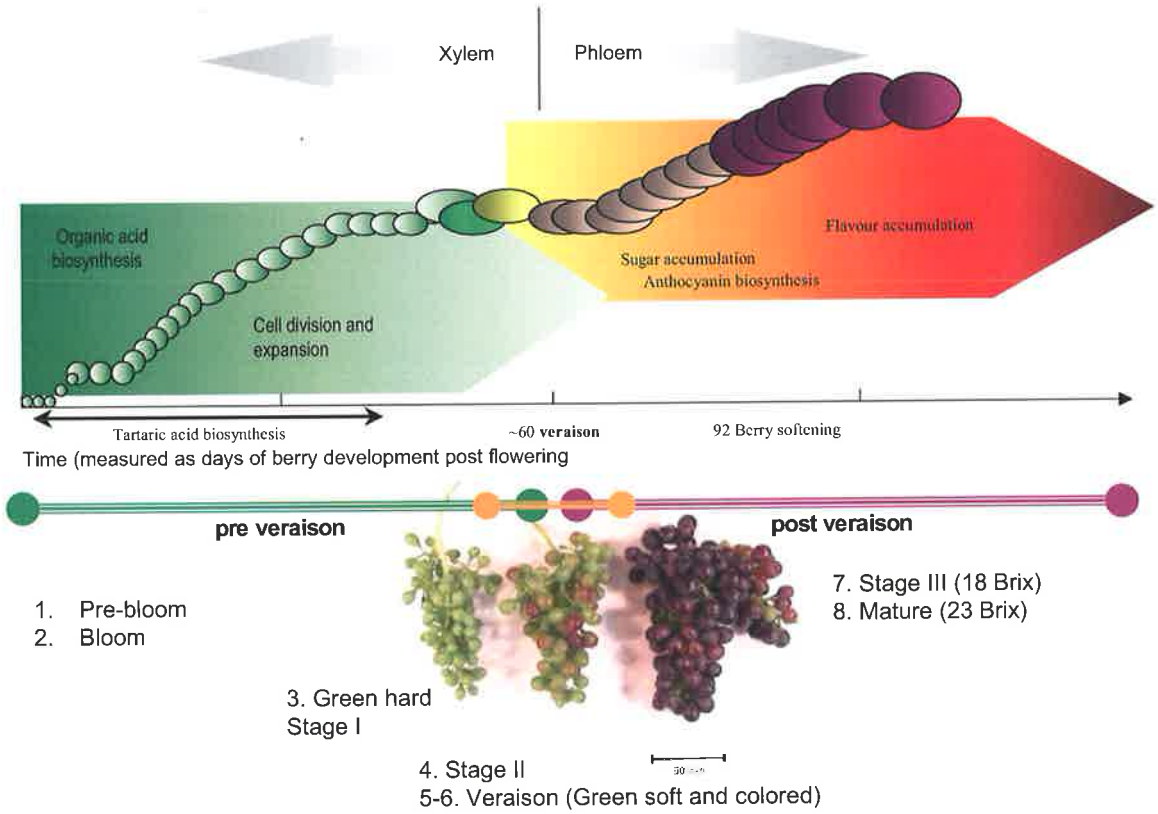

Figure 4.6 A schematic diagram of berry development, with inset pictures to provide the reader with an appreciation for the developmental stages discussed. The time at which TA biosynthesis occurs is indicated along the x-axis (adapted from Iland and Coombe, 1988, Coombe and McCarthy, 2000 and DeBolt *et al.*, 2004) (grape photographs courtesy of Dr. Cassandra Collins)

mRNA was extracted every two weeks post flowering and used to assess whether the transcriptional events identified *in silico* matched those occurring in *vivo* (RNA was standardised to 500 ng.μL^{-1} for PCR data). Candidates 1 to 8 were amplified as described in the Methods and Materials, and showed a general trend of pre veraison transcription for all 8 candidates, without using real time quantitative PCR, which was used for individual candidate genes of greatest interest (Chapters 5 and 6). Candidate genes 9 and 10 were analysed individually; results are described in Chapter 6 and are not discussed in this Chapter. Results showed that no candidates could be ruled out based on a lack of expression during pre veraison, measured as amplification of internal primers in cDNA template extracted from stage 1 berries (Figure 4.7).

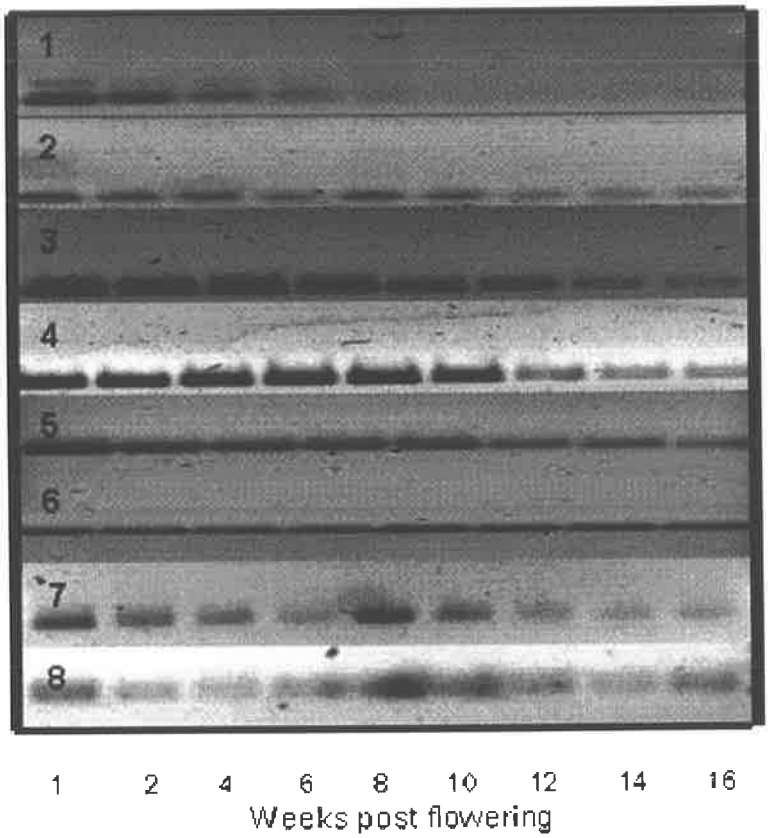

Figure 4.7 Candidate gene transcription across *V. vinifera* berry development, measured in weeks post flowering, using mRNA extracted at each time point and then standardised at 500 ng.μL^{-1}. Candidates are listed 1-8 in the top left hand corner of

each PCR amplification block. All amplicons matched the molecular weight size of the designed internal PCR product 260 bp.

Analysis of candidate gene amplification between messenger RNA from TA forming species (*V. vinifera*) versus non-TA forming species (*A. aconitifolia*)

Results showed that out of the 8 candidates amplified from mRNA template, extracted from TA forming (*V. vinifera*) and non-TA forming (*A. acontifolia*) species, that all but one were amplified in both species (Figure 4.8). Lane 5 contains the amplicon that was successfully amplified in the *V. vinifera* (1) mRNA and did not amplify in the *A. acontifolia* (2) mRNA. Lane 9 in both cases is a molecular weight DNA ladder. Lane 4 did not amplify under any annealing temperatures or extension times tested, it is most likely that lane 4 contains a chimeric clone, which are common in EST contig assembly.

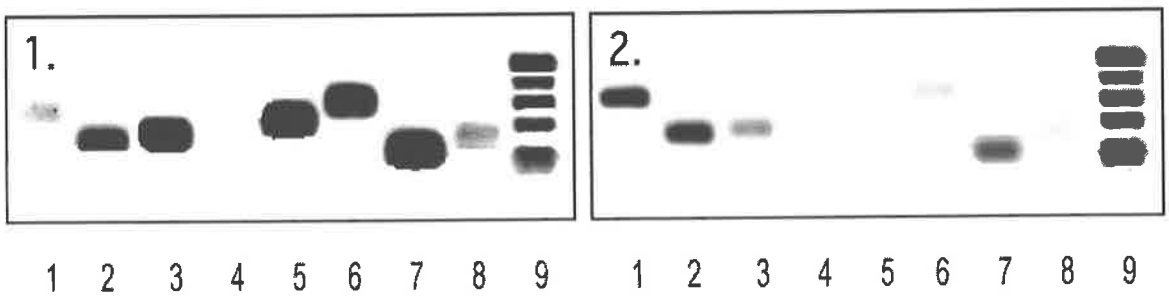

Figure 4.8 Amplification of candidate genes from mRNA as template of *V.vinifera* (1) and *A. acontifolia* (2). No amplification was observed for candidate gene in lane 5 from *A. acontifolia* templates. Minor bands in both panel gels (ca 50 bp) are primer dimer PCR amplification artefacts. The ladder is a 100 bp ladder and increases in the following order: 100, 200, 300, 400 and 500 bp.

A series of internal primers spanning more than 50 % of the ORF were amplified from gDNA extracted from *Vitis* (Figure 4.9A) and *Ampelopsis* (Figure 4.9B), further demonstrating a lack of amplification in the species of *Ampelopsis* lacking the ability to form TA.

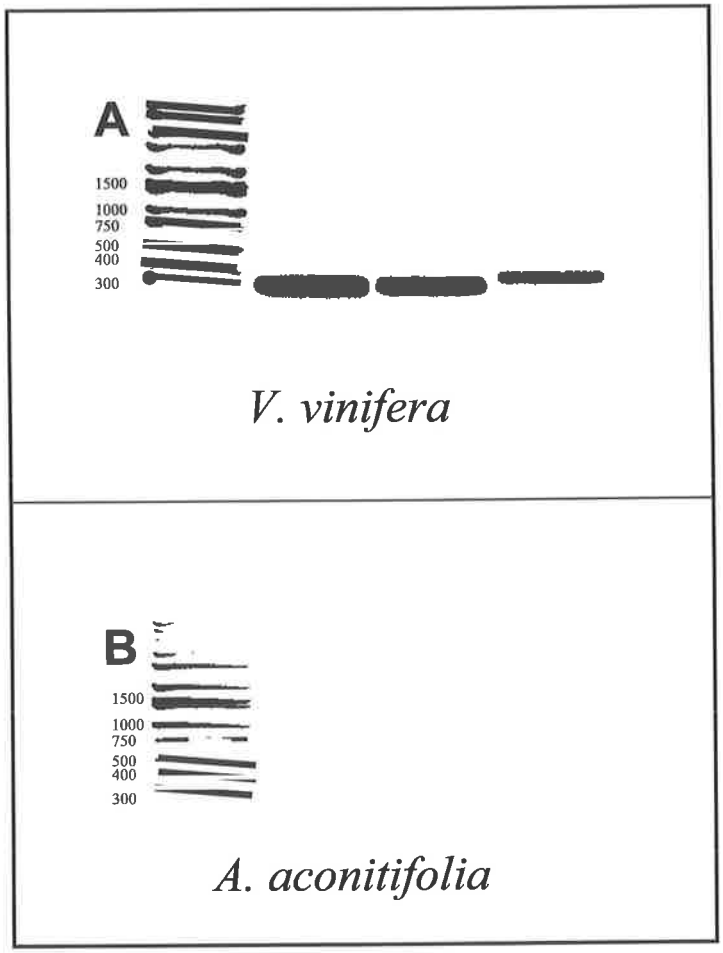

Figure 4.9 Amplification of L-IdnDH using three different sets of internal primers designed to amplify products between 200 and 350 bp in size in *V. Vinifera* (A) and *A. acontifolia* (B)

Analysis of candidate gene amplification between genomic DNA isolated from TA forming species versus non-TA forming species

Results using genomic DNA as a template confirm that the gene candidate five was unable to be amplified in the non TA forming species (*A. aconitifolia*) but crucially was able to be amplified from several TA forming species (*V. vinifera, V. californica, P. tricuspifolia, A. brevipedunculata*)(data not shown). Using genomic DNA as a template showed that amplification of candidate genes 1, 2, 3, 6 (very faint

in (1)), 7 and 8 are all successfully amplified in both templates, but importantly shows that the same primers that amplified a 300 bp PCR product from mRNA (which is identical to the size for which the primers were designed to amplify) for candidate 5, amplify a band close to 600 bp in genomic DNA showing the presence of an intron in the ORF. To test for the intron size more accurately, the full length primers designed to amplify the 1101 bp ORF of candidate 5 were used on the gDNA template resulting in a 1900 bp product, and indicating that there is most likely two introns in the ORF of a total size of 800 bp (Figure 4.10).

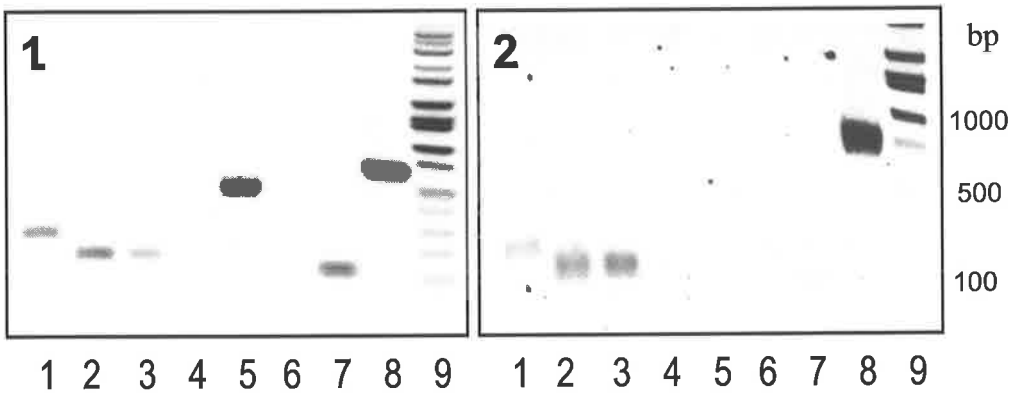

Figure 4.10 Amplification of candidate genes from gDNA as template of *V. vinifera* (1) and *A. acontifolia* (2). No amplification was observed for candidate gene in lane 5 from *A. acontifolia* templates. Lanes 1-8 encode candidate genes and lane 9 is a Hi Lo molecular weight DNA ladder.

4.4 Discussion

Data in the grapevine transcriptome has provided the ability to extract clues as to the nature of the genes that are differentially expressed when and where TA formation occurs in the grapevine. Over 135,000 ESTs sequenced from all parts of the grape and times of development provided the data for maximal genome coverage, but also created the potential for a genomic *in silico* northern (Chapter 3). It is a considerable challenge to then link genomic data to TA biosynthesis as the grapevine is a slow growing perennial vine crop where no mutant analysis is available. Access to grape specimens from the germplasm repository (UC Davis) and Adelaide Botanical gardens, South Australia, provided an opportunity to screen, via HPLC analysis, for variability in TA levels in grapevine species from all over the world (Table 4.4). Modern metabolomic methods use NMR, LC-UV, GC-MS, LC-MS, LC-LIF and CE-LIF to search deeper into the metabolome of an organism (Summer *et al.*, 2003). In this chapter HPLC-UV was effective to isolate and identify TA from the grape organic acid profile. Metabolic profiling has been used to fingerprint a plant family for classification of species (Gorinstein *et al.*, 1995) or to look for new epitopes or conjugates of a compound (Hunman and Sumner, 2002), but the aim of this chapter was to identify significant variation in TA biosynthesis to correlate biosynthesis with expression of candidate genes isolated via transcriptional profiling of EST data (Chapter 3). In addition to successfully achieving the desired outcome, this work provides the first thorough screen of organic acids in the family Vitaceae.

It was found that considerable difference in TA biosynthesis occurred between species and genus (Figure 4.2). Significant differences were expected as large differences have been reported between cultivars of *V. vinifera* (Kliewer *et al.*, 1967, Ruffner, 1982). Importantly it was discovered that *A. aconitifolia* makes no TA and *A. brevipedunculata* and *A. vitifolia* make very little TA compared with *Vitis, Parthenocissus and Muscadinia* species (Table 4.3). Therefore, the lack of TA in *A. aconitifolia* allowed the testing of candidate gene amplification in TA forming and non-TA forming species. In support of the two genomes (both Vitaceous plants) remaining well conserved and being able to support amplification of genes designed from Vitis sequencing data, 10 candidate genes, in addition to control genes ubiquitin and actin amplified in both *A. aconitifolia* and *V. vinifera.* The only gene that could not be amplified from both *Ampelopsis* and *Vitis* cDNA templates was candidate 5,

which encoded a putative L-iditol 2 dehydrogenase, with domains suggestive of NAD dependant dehydrogenase activity acting on the CH-OH groups of the donor substrate (Chapter 3). These data suggest that the two genomes remain somewhat conserved, if albeit on a small number of genes screened. In agreement with these data, the gene candidate 5 amplified from template prepared from several other grape species including *Parthenocissus tricuspifolia* (gDNA), *V. californica* (mRNA and gDNA) and *V. labrusca* (gDNA)(data not shown). Experiments have been performed estimating genome conservation between model legumes and legume crops and among related species of grass with considerable phylogenetic distance (Bennetzen and Freeling, 1995, Devos and Gale, 2000, Choi *et al.*, 2004). Using differential expression analysis to isolate candidate genes would expectedly weed out common transcripts, therefore the amplification of all but one gene across all templates tested suggests some degree of conserved genome synteny in the grape family. These data are in agreement with the thesis of Delseny (2004).

Within the genus *Ampelopsis* two of the three species screened contained TA in small amounts in consecutive seasons. *A. brevipedunculata* and *A. vitifolia* contained 0.6 and 0.8 $mg.g^{-1}$ fresh weight respectively and *A. acontifolia* no TA in the pre and post veraison samples. The genus *Ampelopsis* originates in Asia, and more specifically is found in Japan, Korea and China (Figure 4.11)(all species were collected at UC Davis grape germ plasm repository and Adelaide Botanical Gardens, Australia); many species of *Vitis* also originate in Asia (Table 4.4)(information from UC Davis, grapevine germplasm repository database). In all *Vitis* species from Asia, TA is a major contributor to vacuole organic acid content (Table 4.2 and 4.3). Considering TA formation as a genetic trait, no geographical localisation of this trait can be shown. Although of the three species of *Ampelopsis* screened in this study, only one formed TA, in all *Ampelopsis* species succinic acid was the major organic acid present in pre veraison berries, with 48 and 68 $mg.g^{-1}$ fresh weight. Succinic acid was almost entirely consumed as a metabolic substrate during berry development, post veraison berries containing 2.2 and 14.9 $mg.g^{-1}$ fresh weight. Importantly, succinic acid is not considered a major organic acid in the grape berry (Ruffner, 1982), data in Table 4.2 shows that in all *Vitis* species surveyed pre veraison, succinic acid was present in substantial quantities. A comparative metabolomic study between *Vitis* and *Ampelopsis*, similar to the approach of characterising fruit development

(Aharoni *et al.,* 2002) may help reveal the physiological differences that occur between the two grape genera.

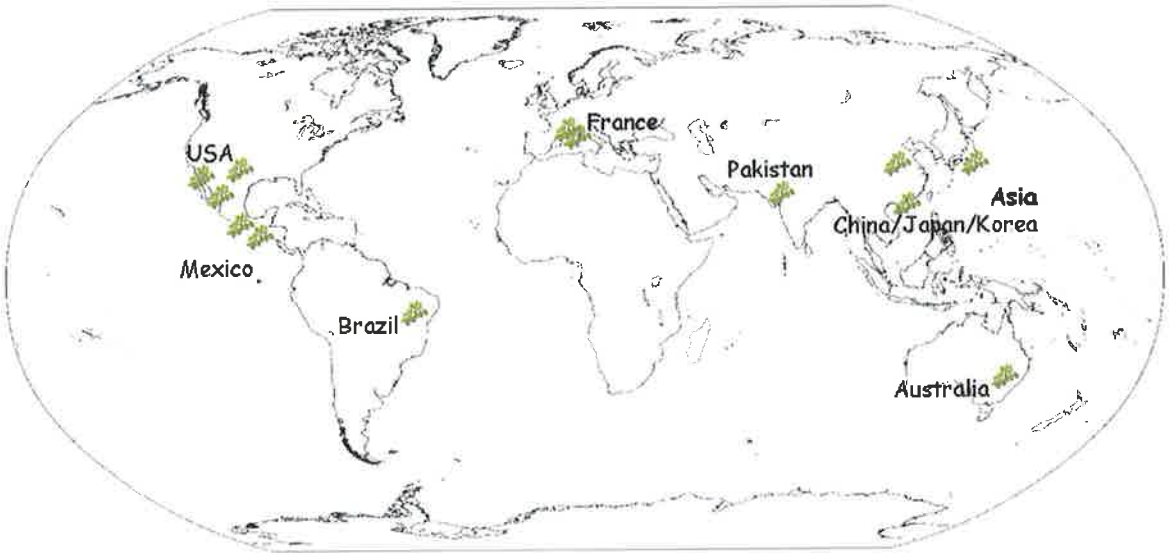

Figure 4.11 Examples of the global distribution of grape berries used in this study. Species allocated to Australia were not used in this study although are noted to contain both TA and oxalic acid (author's observation); the genera *Cissus* and *Ampelocissus* are the most noteworthy native Australian grapes.

Ascorbic acid does not absorb well at 210 nm, it absorbs maximally at 244 nm (Davey *et al*, 1997), and therefore, in this study sensitivity was severely limited because 244 nm data was not obtained. Combine low absorbance with the fact that ascorbic acid readily breaks down upon freeze thawing and cellular disruption (Davey *et al.* 1997) and only species containing a substantial quantity of ascorbic acid would result in detection. Levels of ascorbic acid in *Ampelopsis* were still quantifiable, suggesting that significantly more ascorbic acid was present in the fruit of this genus.

Characterising natural variation in organic acids in *Vitis* species was highly correlated with what is known of the genetic relationships within these species (Prof

Andy Walker, UC Davis pers. comm., data not published as of the date of thesis preparation). A comparative method of analysis was adopted to gain an understanding of the gross trends in data between species based on organic acid profiles. A 2 dimensional hierarchical cluster analysis was used to draw relationships based on similarity between species (Figure 4.12). The hierarchical cluster was broken into two main subgroups. Tartaric and malic acid levels were the best indicators of subgroup 1 (the first main branch in the tree) and of subgroup 2, succinic and ascorbic acid were the best indicators for the observed branching (Figure 4.12A). PCA was effectively utilised to confirm these results, statistically demonstrating that species in the genus *Ampelopsis* clustered in with succinic acid and species of *Vitis* clustered with TA, accounting for a total of 83 % of the variance in the data (data not shown). This breaks the family *Vitaceae* into two main groups of organic acid accumulators, those that make substantial amounts of TA, and those that do not. A tentative phylogenetic tree was formed from this data and what is known from genetic mapping (Figure 4.12B).

High TA accumulators, identified by significantly greater concentrations than the mean, in pre veraison berries were the species *V. acerifolia* and *V. riparia.* However, in post veraison berries, *V. ficifolia, V. vulpina V. biformis*, and *V. amerensis* contained significantly greater amounts of TA than the mean (Table 4.2). Pre and post veraison data sets do not correlate positively, suggesting seasonal influence as well as inter-species differences. Abiotic factors such as water application and temperatures will impact on the organic acid content between seasons (identified in all major viticultural texts, for instance Jackson, 2000, and chapter 7). Berry fresh weight is still the most uniform method of comparing samples, rather than a per berry measurement, as an enormous difference was observed in berry size (Table 4.4). The dependency of warm climate wine regions on the addition of exogenous TA to balance pH and organoleptic qualities of wine may warrant investigation into a beneficial cross between *V vinifera* (used for wine making) and a species such as *V. amerensis* or *V. acerifolia. V. amerensis* is a species originating in the north of China where is tolerates temperatures of less than negative 40 degrees Celsius (Zhang *et al.,* 1990). Understanding of grapevines as a plant family may hold possibilities to opening up new wine regions suited to different climatic and stress conditions.

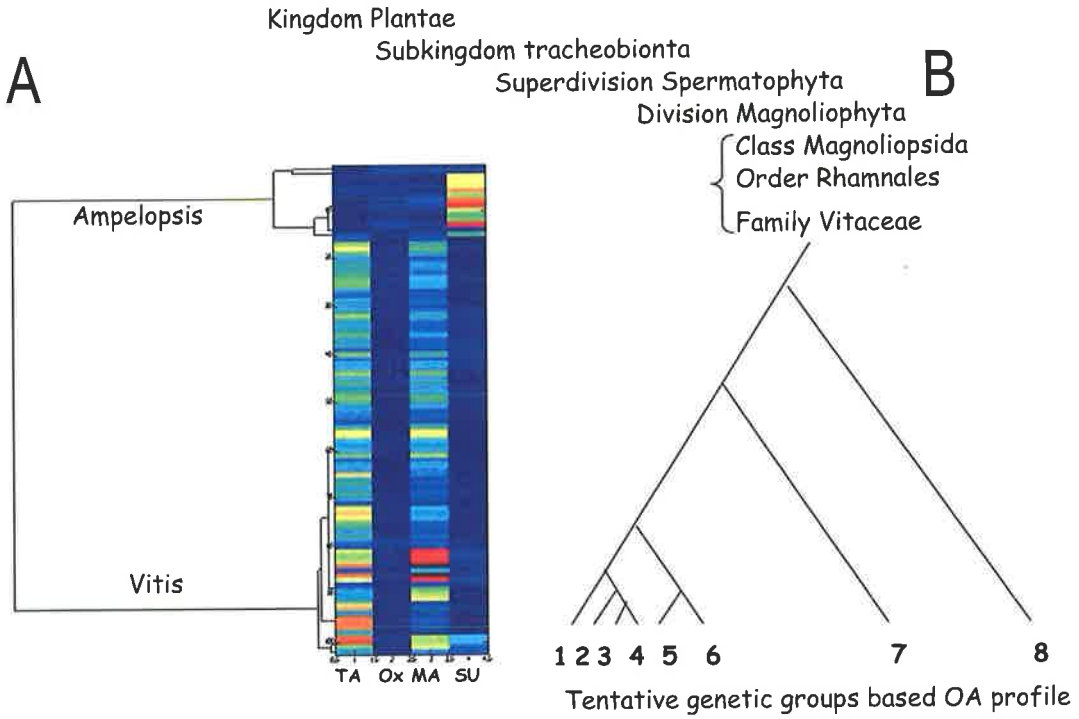

Figure 4.12 A) 2D hierarchical cluster grouping species based on organic acid profile. B) Phylo-organic acid mapping based variability in the organic acid profile correlated with phylogenetic estimates derived by the lab of A. Walker (UC Davis); refer to Table 4.4 for the species corresponding to groups 1 to 8.

Both malate and succinate are accumulated pre veraison then are readily consumed as metabolic substrates post veraison. The vacuole is the subcellular compartment responsible for storage of organic acids, which are synthesised in the cytoplasm and transported to the vacuole via ATPase and VVpase proton pumps which drive an electrochemical gradient (Terrier and Romieu, 2001). The tonoplast is hypothesised to become leaky and organic acids binding with cations such as calcium passively leave to vacuole destined to provide an addition carbon source for energy production in the latter stages of berry ripening (Terrier and Romieu 1998, 2001). Data in this chapter reflects this scenario in the majority of species characterised, however a number of species still had high levels of malate at post veraison collection. *V. biformis* and *V. tillifolia* are the two greatest accumulators of malate late in development, having 23.7 and 20.7 $mg.g^{-1}$ fresh weight respectively. Moreover, in

the *Ampelopsis* species, which favoured succinic acid as the major pre veraison organic acid, post veraison data shows that nearly all the succinic acid was consumed. The A*mpelopsis* berries contained much less water, instead they were more of a milky consistency, and the lack of water was obvious when extracting mRNA from the berries. Osmotic potential was not measured, but water transport into the berry of *Vitis* species can be correlated to the formation of TA, a strong organic acid and therefore a more powerful counter ion. Oxalic acid accumulation did not demonstrate a clear pattern of accumulation, with both pre and post veraison development displaying similar levels (below 3 $mg.g^{-1}$ FW). In all but one species oxalic acid was a component of the berry organic acid profile. This is in agreement with previous radio labelling studies performed in chapter 2 (DeBolt *et al.* 2004, Green and Fry, 2005ab). Assuming that oxalate content is directly proportional to crystal raphide production (DeBolt *et al.*, 2004) this may simply indicate that these plants were more stressed or under attack by herbivores as this has been shown to influence raphide formation in other plants (Mores-Flores, 2001, Nakata, 2003, Fransceschi and Nakata, 2005).

Metabolite profiling is a powerful tool in combination with transcriptional profiling in moving towards forward genetics in species where classical reverse genetic approaches such as gene silencing and gene knockouts are not available. Previously it has been shown by paper chromatography and subsequent radioisotope tracer studies, that many species of *Vitis* and the related genus *Parthenocissus* contain TA (Stafford 1957, 1959, Saito and Loewus, 1989). It was assumed that all plants in the family Vitaceae would carry this trait. Of our screened population 27 out of 28 species contained detectable amounts of TA using HPLC. But in *A. acontifolia*, both pre and post veraison berries in two consecutive seasons contained no TA. The use of this natural mutant has allowed isolation of a single candidate gene correlated with TA biosynthesis, which will be characterised in the following chapter.

Chapter 5

Cloning, heterologous expression, substrate specificity and enzyme kinetics of the novel plant enzyme L-idonate dehydrogenase

5.1 Introduction

Research described in previous chapters has identified a TA biosynthetic candidate that is not expressed in the non-TA accumulating grape, this chapter will describe research to isolate and characterise the candidate gene. To briefly recapitulate previous experiments; faced with a lack of homologous proteins for any steps in the biosynthetic pathway of TA, combined transcriptional and metabolic profiling were used to target a key gene in the biosynthesis of TA in grapevines, hitherto a pathway whose occurrence was postulated but for which no enzymological or molecular evidence existed. Transcriptional profiling has been used widely in combination with metabolite analysis (Suzuki *et al.*, 2002) in the search for glucosyltransferase activities in *M. truncatulata* (Achnine *et al.*, 2005), and during fruit development in tomato (Alba *et al.*, 2005). Recent work provided a method for the interrogation of transcript data from a large collection of sequenced and catalogued grapevine cDNAs (Goes da Silva *et al.*, 2005); this resource was used to refine the search for candidate genes expressed in tissues known to be active in TA biosynthesis. Likely involvement in TA biosynthetic reactions was further tested by examining the domain architecture of deduced protein sequences for evidence of oxidoreductase-type reaction domains. A number of potential candidates were identified by this combined approach. To further test each of these candidate genes and in the absence of a simple transgenic assay system in grapevines, we surveyed the organic acid profiles of 28 members of the family Vitaceae. Considerable differences in the accumulation of tartaric, oxalic, malic and succinic acids were observed, suggesting that the full metabolomic analysis of grape berry composition will reveal numerous metabolite differences within this plant family. Crucial to the present investigation, one species, namely *Ampelopsis aconitifolia*, was identified in which TA could not be detected. PCR analysis of berry messenger RNA and genomic DNA indicated that one candidate gene was absent from the *A. aconitifolia* genome.

Although biochemical evidence has remained unknown, elucidation by radioisotope tracer studies of the intermediates relating TA to AA catabolism in the direct pathway (Saito and Kasai, 1969, DeBolt *et al.*, 2004, Saito and Kasai, 1982, Saito and Kasai, 1984, Malipiero *et al.*, 1987, Saito and Loewus, 1989, Saito, 1992) showed that they proceed via 2-keto L-gulonic acid to L-idonic acid (Saito and Kasai, 1984, Malipiero *et al.*, 1987), which is oxidised to form 5-keto D-gluconic acid (Saito and Kasai, 1982, Saito and Kasai, 1984, Malipiero *et al.*, 1987). 5-Keto D-gluconic acid is subsequently cleaved between carbon atoms 4 and 5 to form the 4-carbon L-threo-tetruronate (Saito, 1992), which is oxidised to form TA. It is proposed that a glycoaldehyde is formed from the remaining 2-carbon fragment (Saito and Loewus, 1979). The oxidation of idonate to 5-keto D-gluconic acid is considered to be the regulatory step (Malipiero *et al.*, 1987, Saito *et al.*, 1984, Loewus, 1999), due to high percentages of radioactivity arresting in idonate, both in TA synthesizing tissue (10 %) and in tissue past its biosynthetic peak (25 %), compared with the rapid ^{14}C interconversion kinetics seen between the other intermediates (Malipiero *et al.*, 1987). Cleavage of 5-keto D-gluconic acid was proposed to be non enzymatic due to its close kinetic correlation with respect to ^{14}C conversion into TA (Saito and Kasai, 1984). These data were refuted when ^{18}O tracer experiments suggested the cleavage mechanism to involve a putative hydrolase (Saito, 1992). More recently, it has been shown that in *Gluconobacter suboxidans*, 5-keto D-gluconic acid can be used as the substrate for a dedicated transketolase (Salusjarvi *et al.*, 2004). These authors speculated that further oxidation of the resulting 4-carbon semialdehyde by a succinate semialdehyde dehydrogenase homolog could result in formation of TA. These combined experiments provide a list of likely substrates that the candidate gene may utilise. Within this chapter, the cloning of the TA-biosynthesis candidate sequence whose identification was described in Chapters 3 and 4 is presented. The expression and purification of the encoded protein, identified as L-idonate dehydrogenase (L-IdnDH), previously unreported in plants, is described. Furthermore,

enzymological experiments using a broad range of substrates that confirm the role of L-IdnDH in TA biosynthesis are detailed.

5.2 Methods and materials

Chemicals

See chapter 2 for a list of authentic chemical suppliers

Analysis of amino acid sequences by motif and domain BLAST searching

The conceptual amino acid sequence encoding the key candidate gene was analysed by BLAST (Altschul *et al.*, 1990). The deduced protein sequence was analysed to identify putative domains and motifs via PFAM, NCBI, BRENDA and Interpro protein domain BLAST interfaces (Mulder *et al.*, 2005) to provide further clues of function.

Plant material

Berry and foliar samples were from vines grown in Winters, northern California, and Adelaide, South Australia. Sampling occurred in the 2004 and 2005 growing seasons. Multiple bunches of berries were collected and three 5-berry sub-samples were selected from a random 50-berry sample for HPLC analysis in the developmental series. Berry and foliar samples were collected from these same plants for isolation of RNA and DNA.

HPLC measurements

Grape berries (ca 5g) were homogenised in a mortar and pestle with 5 ml of 0.5 M H_3PO_4 pH 1.5. The slurry was transferred to a 10 ml polypropylene centrifuge tube, the volume adjusted to 10 ml with the same solvent and placed on a rotating mixer at room temperature for 2 h. After this time a 2 ml aliquot was removed and placed into a 2 ml microcentrifuge tube, centrifuged at 14,000 rpm for 2 min at room temperature, passed through a 45 µm filter and the organic acids separated using HPLC. The loading volume was 20 µl, loaded via an autosampler (Beckman System Gold, Model 507e) onto an HPLC column (Prevail OA organic acid 4.5 x 250 mm, Alltech Associates) fitted with a guard cartridge of the same material. The mobile phase used was 25 mM KH_2PO_4 adjusted to pH 2.0 with phosphoric acid, at a flow rate of 0.5 ml/min (Beckman System Gold, Model 126NM). Detection of TA was by UV absorbance at 210 nm using a diode array detector (Beckman System Gold, Model 168).

PCR amplification of the candidate sequence

Full length putative candidate sequence was amplified using primers F'-GGGCATATGATGGGGAAAGGAGGCAACTCTG and R'-CCGGATCCTTAGAGATTAAACATGACCTTG which contains a sticky end BamHI site and HinDIII site for directional cloning into the pET expression system, described below. A further five sets of internal primers amplifying 600 bp, 525 bp, 300 bp, 200 bp and 260 bp PCR products throughout the open reading frame were used in the analysis (Table 5.1). Sequencing analysis was performed on all cloned amplicons using M13 Forward and Reverse primers in the cloning vector (either pGEMT-Easy or TOPO2.1), the BIG-DYE reaction mix and isopropanol DNA cleanup. Sequencing involved a five minute heating at 95°C followed by 25 cycles of 95 °C (15 sec) denaturation, 50°C (15 sec) annealing followed by a 60°C (4 min) extension. For all

PCR reactions, either ubiquitin or actin sequences were used to design primers for amplification controls. RT-PCR reactions were composed of 1.5 pmol of each primer, 0.5µl Taq DNA polymerase, 0.5µl dNTPs, 1µl MgCl (25 mM), 1µl (500 ng.µl^{-1}) template mRNA, 2µl 10× (Mg free) buffer, to 20 µl with dH_2O. A three minute heating at 95°C followed by 32 cycles of 95 °C (30 sec) denaturation, 55 °C (30 sec) annealing temp, extension times followed 1 min per Kb product size, followed by a final extension of 5 minutes. Quantitative RT PCR was conducted using 10 µl of BioRad® real time PCR reagent, 1µl (500 ng.µl^{-1}) template cDNA, 8.4 µl dH_2O and , 0.6 µl (1.5 pmol) F/R primer. Internal primers were as follows: forward primers AAGTTTGCCTTGTGGGTTTG and reverse primer AAGGCTTCCTCCACATCCTT. Standard curve for expression of putative L-IDNDH was formed by cloned and sequenced putative L-IDNDH used as template at a series of known log scale concentrations. Relative expression is based on a correction factor, which is a calculated based upon the expression of the ubiquitin control gene in all templates.

Molecular cloning and recombinant protein formation of L-IdnDH

Full-length putative L-IdnDH was amplified from *V. vinifera* RNA obtained from berries sampled 4 weeks post anthesis and cloned via pTOPO2.1(In*vitro*gen) into pET14b (Novagen) for prokaryotic expression. Sequencing at each cloning step was used to check orientation and alignment. The sequence verified construct was transformed into *E. coli* BL21 (DE3) plysS (Novagen) for induction. Transformants (50 ml in 250 mL Erlenmeyer flask) were grown in TerrificBroth supplemented with ampicillin (100 µg.mL^{-1}) and chloramphenicol (34 µg.mL^{-1}). Once the culture reached an optical density of 0.9 at 600 nm the expression of L-IdnDH was induced by addition of 0.4 mM IPTG. Cells were harvested by centrifugation 3h post induction and resuspended in sonication buffer (4 ml/g wet cell paste; Clontech) containing 10 mM 2-mercaptoethanol, followed by three freeze-thaw cycles in liquid nitrogen.

Protease cocktail (Roche) was added and cells disrupted by reciprocation through a 20g needle followed by centrifugation at 13,500 *g* for 10 min at 4°C, and divided into soluble and insoluble fractions. Final purification of soluble material was achieved using Talon resin (Clontech).

Enzyme assay and substrate specificity for recombinant L-IdnDH

Assays (150µL) contained 15 µL purified protein extract (ca 0.09 mg/mL) pre-equilibrated to 30°C in 100 mM Tris HCl pH 8, 330 µM NAD^+ or NADH, in a glass cuvette zeroed at A_{340} nm before addition of substrate to a final concentration of 33 mM. The forward and reverse reactions (L-idonate to 5-keto D-gluconic acid and 5-keto-D-gluconic acid to L-idonate respectively) were followed by change in absorbance at A_{340}nm. HIS-TAG purified protein was used in all assays; therefore untransformed *E. coli* reactions are not presented in the data. Controls included, no enzyme, boiled enzyme, no substrate (dH_2O), reaction stopped with TCA, no added NAD^+ and/or no added NADH. Substrates tested included L-idonate (supplied as the monosodium salt), 5-keto D-gluconic acid (supplied as the monopotassium salt), 2-keto-L-idonic acid, L-ascorbic acid, D-sorbitol and D-gluconic acid. Reactions were stopped with 50 µL 1 M HCl, centrifuged at 13,500 *g* for 5 min. and the supernatant (20 µL) loaded onto an HPLC column (Prevail OA 4.6 x 250 mm, Alltech Associates). The mobile phase was 25 mM KH_2PO_4 adjusted to pH 2.0 with phosphoric acid, at a flow rate of 0.5 mL/min. Detection of the organic acids including L-idonate and 5-keto D-gluconic acid was by UV absorbance at 210 nm.

Characterising the catalytic activity of L-IdnDH

K_m values of the recombinant L-IdnDH were determined for the donor substrate 5-keto-D-gluconic acid and the reverse reaction from L-idonate.

Additionally V_{max} was determined for the combination of forwards and reverse reactions. Conditions of the reaction were as described above, using ca 0.09 mg/mL purified protein and varying concentrations of substrate. The recombinant protein used in kinetic assays was frozen once at –80°C before use. The Biorad ® benchtop spectrophotometer was programmed to measure kinetics of enzyme activity, set at A_{340} nm, measuring ΔA_{340} nm every 5 seconds for 100 seconds. The K_m and V_{max} data were calculated using transformed data and plotted as Lineweaver-Burke graphs. V was calculated as nkatal equivalents, nmoles of NAD sec^{-1} mg $protein^{-1}$. Freezing and thawing stability of the protein was tested as activity over time. The variation of activity with pH was studied for the acceptor substrates, to calculate the ideal pH for L-IdnDH, oxidation and reduction reactions were measured between pH 5.4 and 8.5 using the following buffers: MES, pH 5.4-6.2; PIPES, pH 6.2-6.6; TRIS, pH 6.5-8.5. Standard assays were carried out as described, with the buffer concentration fixed at 100 mM throughout.

Precursor feeding experiments

Authentic L-idonate and 5 keto gluconate (100 mM in dH_2O) were added to sliced berries from *A. aconitifolia* and *V. vinifera.* Individual berries were, within an hour of removal from vines, hand sliced using a razor blade into sections ca 1 mm thick. Aqueous solutions of each substrate at concentrations of 100 mM were administered until all berry slices were submerged. Measurements of TA content (n=3 per time point) were made hourly from 0-3 hours via HPLC and the identity of the reaction products confirmed by LC-MS.

Polyclonal antibody formation, berry protein isolation and western blotting

Polyclonal antibody production was provided as a fee for service by Adelaide University Laboratory Animal Services. Following a pre-immune test bleed (10 ml) an initial immunisation of ca 400µg of IMAC-purified L-IdnDH (500 µL) was

presented intramuscularly in an equal volume of Freund's complete adjuvant (Sigma Chemical Company). Second and third immunisations were administered at approximately 4-week intervals using similar levels of protein in an equivalent volume of Freund's incomplete adjuvant (Sigma Chemical Company). Following a test bleed that confirmed the presence of cross-reacting antibody, ex-sanguination via a terminal cardiac bleed was performed. Serum was collected from the blood after 24 hr storage at 4^0C.

Total protein was extracted from berries using TCA-acetone precipitation. Five berries to an average starting weight of approx 3 grams were crushed into a fine powder using chilled mortar and pestle in the presence of liquid nitrogen. Following grinding, 150mg of ground grape extract was placed into a 2 mL microcentrifuge tube and exactly 1mL of extraction buffer (XB) added (XB consisted of 80% (v/v) acetone, 12.5% w/v TCA and 28mM β-mercaptoethanol (B-ME)), followed by brief vortexing. A further 1mL XB was then added and a brief vortex was completed. The preparation was placed at -20° C for 2 hours, after which was centrifuged at 4° C for 20 min at maximum speed. Supernatant was decanted and discarded. The pellet was washed twice in 80% acetone to remove all TCA and air dried for 5-10 minutes. TCA was made fresh for each protein preparation, and B-ME was added to the XB last.

The protein pellet was resuspended in 500-700 µL of lysis buffer 1 (LB1 was composed of: 9.5M Urea, 2% w/v CHAPS, 0.2% v/v carrier ampholyte pH 5-8, 0.3% v/v carrier ampholyte pH 3-10, 65mM DTT). To break up the pellet the protein preparation was vortexed for 1 hour then centrifuged at room temperature for 10 min at maximum speed. Supernatant was then decanted and label as cytsolic protein. The protein pellet was resuspended in 1 mL of LB1, followed by 5 minutes centrifugation at 3500g, following centrifugation the supernatant was collected and added to cytsolic fraction. This step minimises the chance of protein overlap between the two cytosolic and membrane bound fractions. The pellet was resuspended in the same volume of lysis buffer 2 (Lysis Buffer 2 (LB2) contains: 7M Urea, 2M Thiourea, 4% w/v CHAPS, 0.2% v/v carrier ampholyte pH 5-8, 0.3% v/v carrier ampholyte pH 3-10, 65mM DTT both lysis buffers are prepared to 10mL with 5mL of milli q water added last). After addition of LB2, the protein pellet was broken up using an end over shaker at 4 C for 1 hour. The preparation was then centrifuged for 10 minutes at high speed.

Finally, the supernatant was removed and labelled as membrane bound fraction, or insoluble protein.

Western blotting was performed according to Lane and Harlow (19xx), using a 1:5000 dilution of the primary antibody stock.

5.3 Results

5.3.1 Sequence analysis and cloning of a full length cDNA encoding the novel plant enzyme L-idonate dehydrogenase (L-IdnDH)

The nucleotide sequence and conceptual translated amino acid sequence were obtained from UC Davis clone number 1029130, which was sequenced as part of the grapevine EST sequencing project. Contig 1029130 encoded a full length open reading frame (ORF) of 1101 bp, and was utilised to design primers for the successful amplification of putative L-IdnDH from messenger RNA extracted from pre veraison *Vitis vinifera* ca. Cabernet Sauvignon grape berry tissue as a template. BLAST analysis of contig 1029130 reveals several homologs from plants such as *Lycopersicon esculentum* (tomato) and Arabidopsis 2-iditol dehydrogenase (sorbitol dehydrogenase) type proteins. ClustalW sequence comparison reveals that although much of the sequence remains identical (77 % at the amino acid level), there are several strings of amino acids, which are unique to the grape sequence (Figure 5.1).

An 1101 bp PCR fragment was cloned and sequenced from berry (*V. vinifera* ca. Cabernet Sauvignon) tissue and sequence analysis revealed only 5 bases differed between the clone 1029130 (Figure 5.2a) and the sequenced gene isolated from the grape. No amino acid changes resulted from any of the nucleotide differences between the clone and the PCR product from the grape berry template (Figure 5.2b). Sequencing of the putative IdnDH isolated from *Parthenocissus tricuspifolia* showed just one amino acid change in the ORF, where at amino acid 313, a cysteine replaced a tyrosine (Figure 5.2c). As described in the previous chapter, a species of grape making no TA was discovered and used as a 'subtractive' for candidate gene validation. To address the possibility that a point mutation or frame-shift caused the

lack of amplification of the candidate cDNA sequence from RNA isolated from the non TA accumulator, a series of internal primers was amplified across the ORF; none of these resulted in amplification (data not shown).

The deduced protein encoded by L-IdnDH contains 366 amino acids, with a putative mass of 40.1 kDa. A search of the InterPro, PFAM and NCBI sequence motif databases (Mulder *et al.*, 2005) revealed several areas of conserved sequence. A motif sharing similarity to the only known homologous reaction, that being an *E. coli* protein which catalyses the reversible oxidation of L-idonate to 5-keto D gluconic acid was identified. The N-terminal domains of both proteins share an alcohol dehydrogenase-like backbone that has a GroES-like fold, and the C-terminal domain having a classical Rossman-fold. Also, the bacterial protein contains domains associated with alcohol dehydrogenase, with a zinc-finger subdomain within a GroES-like domain, ketose reductase (sorbitol dehydrogenase), formaldehyde dehydrogenase, quinone oxidoreductase and 2,4-dienoyl-CoA reductase. Not all of these domains are found in the grape berry homolog. The grape sequence lacks a predicted RNA methylase motif, but it maintains the alcohol dehydogenase backbone and a zinc-finger subdomain within the GroES-like domain. Additional to the *E. coli* protein, the putative grape L-IdnDH contains a putative methylase-associated domain proposed to be involved in ubiquinone/menaquinone biosynthesis (coenzyme metabolism) identified in the domain search as UbiE. The proposed catalytic activity of the idonate dehydrogenase in the grape is L-idonate + $NAD^{(+)}$ ←→ 5-keto gluconic acid + NADH. Both enzymes belong to the zinc containing alcohol dehydrogenase family and share several conserved motifs. Yet interestingly, although many homologous motifs were shared between the two L-IdnDH genes, they only contain 31 % identity at the amino acid level. Using a simple NCBI amino acid sequence BLAST of the grape L-IdnDH sequence reveals that IDNd from *E. coli* does not appear in the first 100 hits.

```
Tomato          MGKGGS-----------DENMAAWLLGVNTLKIQPFNLPALGPHDVRVRMKAVGICGSDV 49
Arabidopsis     MGKGGMSQGEGS--KVEEENMAAWLVGINTLKIQPFLLPSVGPHDVRVRMKAVGICGSDV 58
IDN             MGKGGNSEDAVSSKEHGEENMAAWLLGIKTLKIQPYILPSLGPHDVKVRIKAVGICGSDV 60
                ***** :..  ::..  :*******:*::******: **::*****:**:**********

Tomato          HYLKTMRCADFVVKEPMVIGHECAGIIEEVGGEVKTLVPGDRVALEPGISCWRCNLCKEG 109
Arabidopsis     HYLKTMRCADFVVKEPMVIGHECAGIIEEVGEEVKHLVVGDRVALEPGISCWRCNLCREG 118
IDN             HHFKTMRCANFIVKKPMVIGHECAGIIEEVGSEVKNLVVGDRVALEPGISCNRCSLCRNG 120
                *::*******:*:**:**************** *** ** ************ **.**::*

Tomato          RYNLCPEMKFFATPPVHGSLANQVVHPADLCFKLPDDISLEEGAMCEPLSVGVHACRRAN 169
Arabidopsis     RYNLCPEMKFFATPPVHGSLANQVVHPADLCFKLPENVSLEEGAMCEPLSVGVHACRRAE 178
IDN             QYNLCREMKFFGSPPTNGSLANQVVHPSNLCFKLPDNVSLEEGAMCEPLSVGIHACRRAN 180
                :**** *****.:**.:**********::******:::***************:******:

Tomato          VGPETNILVLGAGPIGLVTLLAARAFGAPRIVIVDVDDYRLSVAKKLGADDIVKVSINIQ 229
Arabidopsis     VGPETNVLVMGAGPIGLVTMLAARAFSVPRIVIVDVDENRLAVAKQLGADEIVQVTTNLE 238
IDN             VGPETNVLIMGSGPIGLVTMLAARAFGAPRIVLVDVDDQRLAIAKDLGADDIIRVSTNIQ 240
                ******:*::*:*******:******..****:****: **::**.****:*::*: *::

Tomato          DVATDIENIQKAMGGGIDASFDCAGFNKTMSTALGATRPGGKVCLVGMGHHEMTVPLTPA 289
Arabidopsis     DVGSEVEQIQKAMGSNIDVTFDCAGFNKTMSTALAATRCGGKVCLVGMGHGIMTVPLTPA 298
IDN             DLDEEVAKIQSTMVTGVDVSLDCVGFNKTMSTALNATRAGGKVCLVGLAQSEMTVPLTPA 300
                *:  :: :**.:*  .:*.::**.********** *** ********:.:  ********

Tomato          AAREVDVIGIFRYKNTWPLCLEFLRSGKIDVKPLITHRFGFSQEEVEEAFETSARGGDAI 349
Arabidopsis     AAREVDVVGVFRYKNTWPLCLEFLTSGKIDVKPLITHRFGFSQKEVEDAFETSARGSNAI 358
IDN             AAREVDIVGIFRYRNTWPLCLEFLRSGKIDVKPLITHRFTFSQKDVEEAFETSARGGNAI 360
                ******::*:***:********** ************** ***::**:********.:**

Tomato          KVMFNL 355
Arabidopsis     KVMFNL 364
IDN             KVMFNL 366
                ******
```

Figure 5.1 Clustalw sequence comparison between the two most homologous proteins (Tomato protein accession number BAE47038 and Arabidopsis protein ascension number NP 974925), and the consensus sequence for the grape L-IdnDH (IDN)

A

MGKGGNSEDAVSSKEHGEENMAAWLLGIKTLKIQPYILPSLGPHDVKVRIKAVGICG
SDVHHFKTMRCANFIVKKPMVIGHECAGIIEEVGSEVKNLVVGDRVALEPGISCNRCS
LCRNGQYNLCREMKFFGSPPTNGSLANQVVHPSNLCFKLPDNVSLEEGAMCEPLSV
GIHACRRANVGPETNVLIMGSGPIGLVTMLAARAFGAPRIVLVDVDDQRLAIAKDLGA
DDIIRVSTNIQDLDEEVAKIQSTMVTGVDVSLDCVGFNKTMSTALNATRAGGKVCLVG
LAQSEMTVPLTPAAAREVDIVGIFRYRNTWPLCLEFLRSGKIDVKPLITHRFTFSQKDV
EEAFETSARGGNAIKVMFNL*

B

ATGGGGAAAGGAGGCAACTCTGAGGATGCTGTTTCAAGCAAGGAGCATGGAGAAGAGAACAT
GGCAGCTTGGCTTCTGGGCATCAAGACCCTCAAGATTCAACCCTACATTCTCCCTTCTCTGGG
CCCCCATGATGTTAAAGTTAGGATCAAAGCTGTAGGGATATGTGGAAGTGATGTTCATCACTT
CAAGACAATGAGGTGCGCAAATTTTATTGTGAAGAAGCCAATGGTGATAGGCCATGAGTGTGC
TGGTATCATAGAAGAAGTTGGGAGTGAAGTGAAGAATCTTGTAGTAGGTGACCGGGTTGCTCT
GGAGCCCGGTATTAGCTGTAACCGATGCAGTCTTTGCAGGAATGGTCAATACAATCTATGCAG
AGAAATGAAGTTTTTTGGATCTCCTCCAACCAATGGTTCTCTAGCTAACCAGGTGGTCCATCCT
TCAAATCTTTGTTTCAAGCTACCTGACAATGTGAGCTTGGAGGAAGGAGCAATGTGTGAGCCG
CTCAGTGTCGGCATCCATGCTTGTCGCCGTGCTAATGTTGGCCCTGAGACCAACGTACTGAT
CATGGGATCAGGCCCCATCGGCCTTGTCACAATGCTGGCTGCTCGTGCTTTTGGAGCGCCGA
GGATTGTCCTTGTGGACGTAGATGATCAGCGACTAGCTATTGCAAAAGATCTTGGCGCAGAC
GATATTATCCGGGTTTCAACGAATATTCAGGATCTAGATGAAGAAGTGGCAAAAATACAAAGC
ACAATGGTTACTGGAGTTGATGTGAGCTTGGACTGTGTCGGCTTCAACAAAACCATGTCAACA
GCTTTGAACGCGACTCGAGCAGGCGGCAAAGTTTGCCTTGTGGGTTTGGCCCAGAGTGAGAT
GACTGTTCCTCTCACTCCAGCTGCTGCCAGGGAGGTCGATATTGTTGGCATATTCCGCTATAG
GAACACATGGCCGCTCTGCCTTGAGTTTTTGAGGAGTGGCAAGATTGATGTTAAACCCCTGAT
AACCCACAGGTTTACTTTCTCACAGAAGGATGTGGAGGAAGCCTTTGAAACCAGTGCTCGTG
GGGGTAATGCTATCAAGGTCATGTTTAATCTCTAA

C

MGKGGNSEDAVSSKEHGEENMAAWLLGIKTLKIQPYILPSLGPHDVKVRIKAVGICGSDVHHFKTMRCANFIVKKP
MVIGHECAGIIEEVGSEVKNLVVGDRVALEPGISCNRCSLCRNGQYNLCREMKFFGSPPTNGSLANQVVHPSNLC
FKLPDNVSLEEGAMCEPLSVGIHACRRANVGPETNVLIMGSGPIGLVTMLAARAFGAPRIVLVDVDDQRLAIAKDLG
ADDIIRVSTNIQDLDEEVAKIQSTMVTGVDVSLDCVGFNKTMSTALNATRAGGKVCLVGLAQSEMTVPLTPAAARE
VDIVGIFR[redacted]RNTWPLCLEFLRSGKIDVKPLITHRFTFSQKDVEEAFETSARGGNAIKVMFNL*

Figure 5.2 A) Amino acid sequence (top enclosed) and B) nucleotide sequence (bottom enclosed) for *Vitis vinifera* grapevine L-IdnDH C) Encodes the *Parthenocissus* grapevine L-IdnDH with a single amino acid change at aa 313.

5.3.2 Real time PCR analysis of L-IdnDH shows transcription matches exponential increase in tartaric acid biosynthesis

Internal primers were used to amplify a 260 bp amplicon from mRNA (*V. vinifera* ca. Cabernet Sauvignon), which was subsequently cloned and sequenced,

with 100 % sequence match to grape L-IdnDH (1029130), to ensure results reflected the transcription pattern of L-IdnDH. This amplicon was used in serial dilution (1:10 in log increments to 1:10000) to make a standard curve for amplification scaling. Then, using RNA extracted every two weeks post flowering until physiological ripeness (measured as 18 weeks post flowering); L-IdnDH was amplified in triplicate reactions using each template mRNA sample. Ubiquitin primers amplified in each template provided a correction factor that was no larger than 4 at any time point. Results showed a clear and distinct peak in transcription 4 weeks post flowering (Figure 5.3A). Transcription if L-IdnDH is maximal between 2 and 6 weeks post flowering, after which it drops dramatically and by 10 weeks post flowering, just after veraison, there is no transcription of L-IdnDH. The transcriptional profile is clearly pre veraison specific.

HPLC measurements of TA were made from fresh tissue of *Vitis vinifera* cv. Cabernet Sauvignon berries collected fortnightly post flowering, during the course of berry development as described above (Figure 5.3B). TA biosynthesis begins slowly, for the first two weeks post flowering, then increases at an exponential rate between 2 weeks and 6 weeks post flowering, with a peak in biosynthesis measured at approximately 4 weeks post flowering. These data are consistent with previously published accounts of TA accumulation in the developing berry (Iland and Coombe, 1988, Terrier and Romieu, 2001). Indeed, the critical result of this experiment was to observe the correlation between TA biosynthesis and transcription of putative L-IdnDH. Transcription of the candidate sequence and the accumulation of TA are positively correlated, providing an excellent example of molecular events matching *in vivo* activity. During the latter stages of berry development, there is no change in TA concentration on a weight per weight measurement, indicating the low probability of continued biosynthesis, which is also consistent with transcription ending at veraison. Critically, coordinated expression data, now shows that gene candidate 1029130 is expressed when and where TA is synthesised in *V. vinifera*, and not expressed in the grape lacking the ability to form TA (Chapter 4, Figure 4.4).

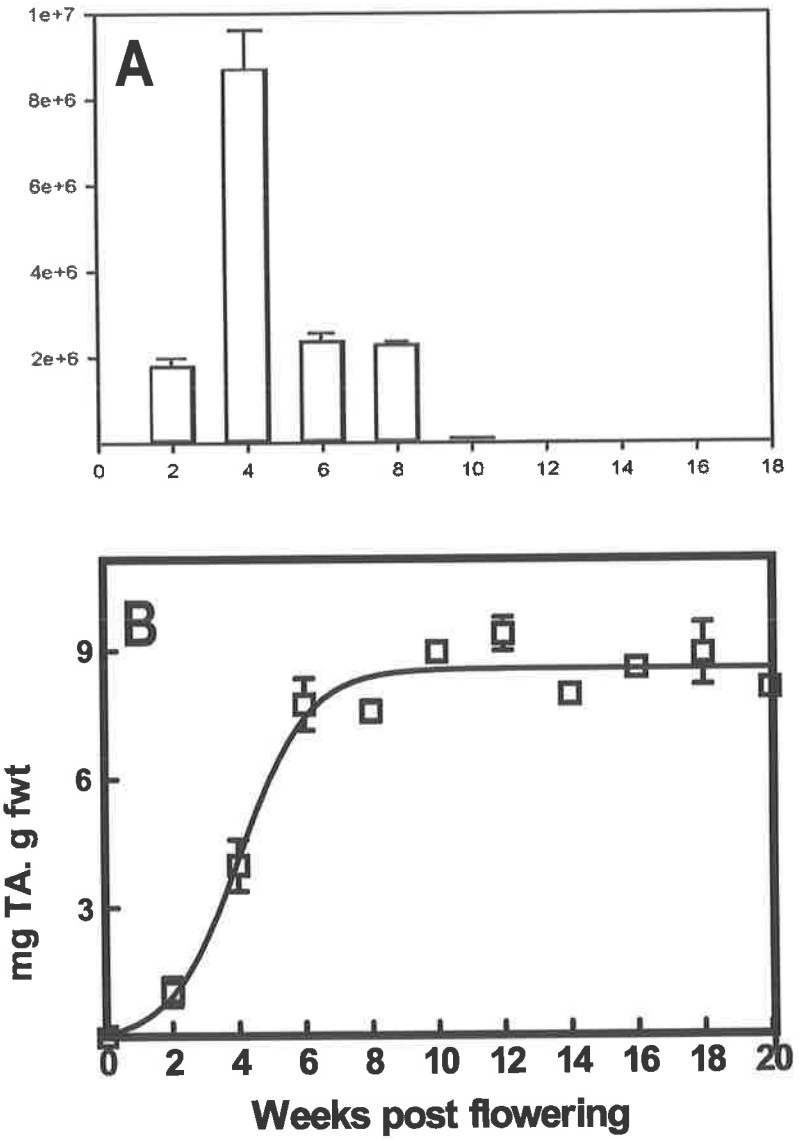

Figure 5.3 A) Quantitative rt-PCR analysis of candidate gene transcription during berry development compared with ubiquitin expression to create a correction factor for each template. **B)** Accumulation of TA during berry development (*V. vinifera* ca. Cabernet Sauvignon). Bars = standard error, n=3.

5.3.3 Functional over-expression in *E. coli* (strain BL21-DE3-plysS), HIS-TAG purification, analysis of the recombinant protein and characterisation of substrate specificity

Active soluble recombinant L-idonate dehydrogenase protein was translated in *E. coli* after transformation with pET14b vector containing the full length gene insert and induction with IPTG (Figure 5.4). Induction temperature of 37 °C was adequate to make substantial amounts of soluble protein, inductions at 32 and 28 °C were more time consuming and did not yield better results (data not shown). To confirm that the HIS-TAG bound protein was the protein identified on the Coomassie blue-stained gel, western blotting using a proprietary anti his-tag monoclonal antibody was used (data not shown).

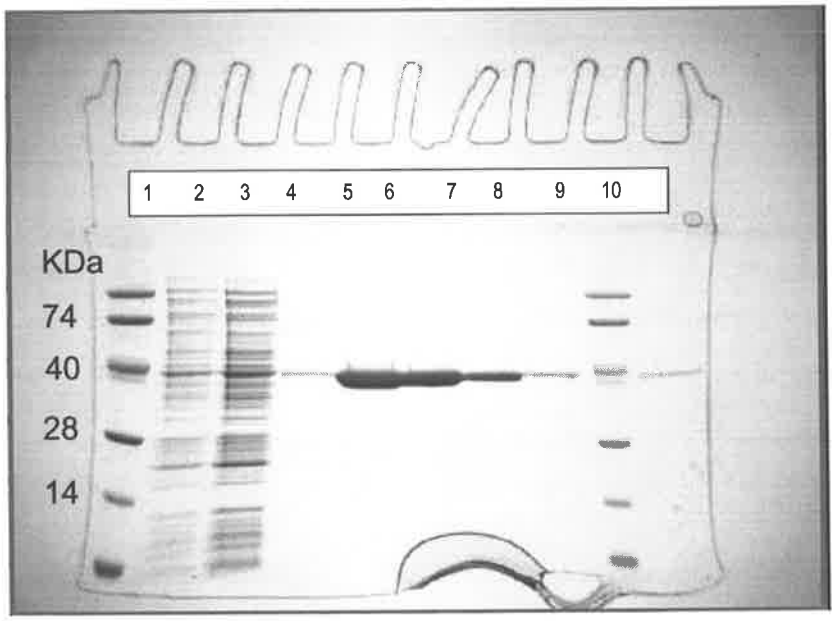

Figure 5.4 Purification and yield of soluble HIS-TAG purified idonate dehydrogenase. Lane 1 and 9 are molecular weight ladders, lane 2 and 3 are wash elutions from the talon column lane 4-5, 6, 7, 8 and 10 are 5 µl of a 200 µl protein elution containing the HIS-TAGGED idonate dehydrogenase.

Activity of the recombinant protein was tested in a simple NAD^+ coupled reaction and showed high substrate specificity and catalytic activity for L-idonate and, in the reverse reaction, 5-keto D-gluconate (Figure 5.5 and 5.6). HPLC was used to separate the reaction mix, and a single peak, formed in the reverse reaction (reaction shown in figure 5.7), co-chromatographed with authentic L-idonate and was absent in all controls (Figure 5.7). LC-mass spectrometry (MS) was used to confirm that the mass of the reaction product matched that of authentic L-idonate (data not shown). As stated above, L-IdnDH is highly similar to 2-iditol dehydrogenase (sorbitol dehydrogenase); when sorbitol was tested, NAD^+ reduction occurred but at very low rate. D-gluconic acid and 2-keto L-gulonic acid and L-ascorbic acid were also tested as substrates with NAD^+ and NADH as cofactors; all displayed none to very low rates of NADH or NAD^+ formation (Figure 5.6AB). Therefore, it is suggested that L-IdnDH belongs to the sorbitol dehydrogenase family of alcohol dehydrogenases (oxidoreductase), with principal activity against L-idonate, and is therefore the first characterised enzyme associated with TA biosynthesis in higher plants. While annotation based on homology is a guide to the nature of this protein, within the 23% variation between L-IdnDH and the plant Arabidopsis, apple, and loquot sorbitol dehydrogenases, substrate specificity and catalytic activity are markedly different.

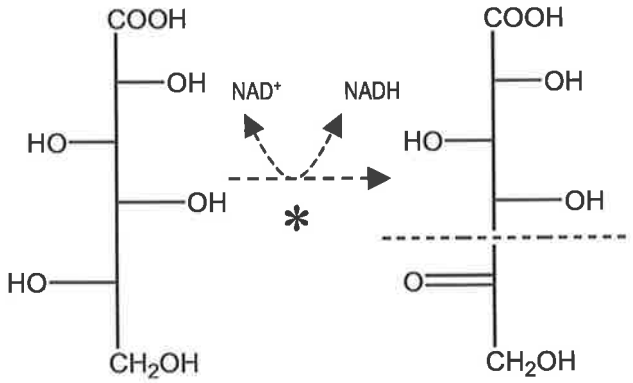

L-idonic acid 5-keto D-gluconic acid

Figure 5.5 The activity of L-idonate dehydrogenase acts on the 5th carbon of the L-idonate intermediate, oxidising the hydroxyl to form a ketone group and subsequently changing the molecule to 5-keto D-gluconic acid. NAD^+ is absolutely required as a cofactor for the enzyme. L-Idonate dehydrogenase acts reversibly to reduce the ketone group on carbon 5 using NADH as a cofactor.

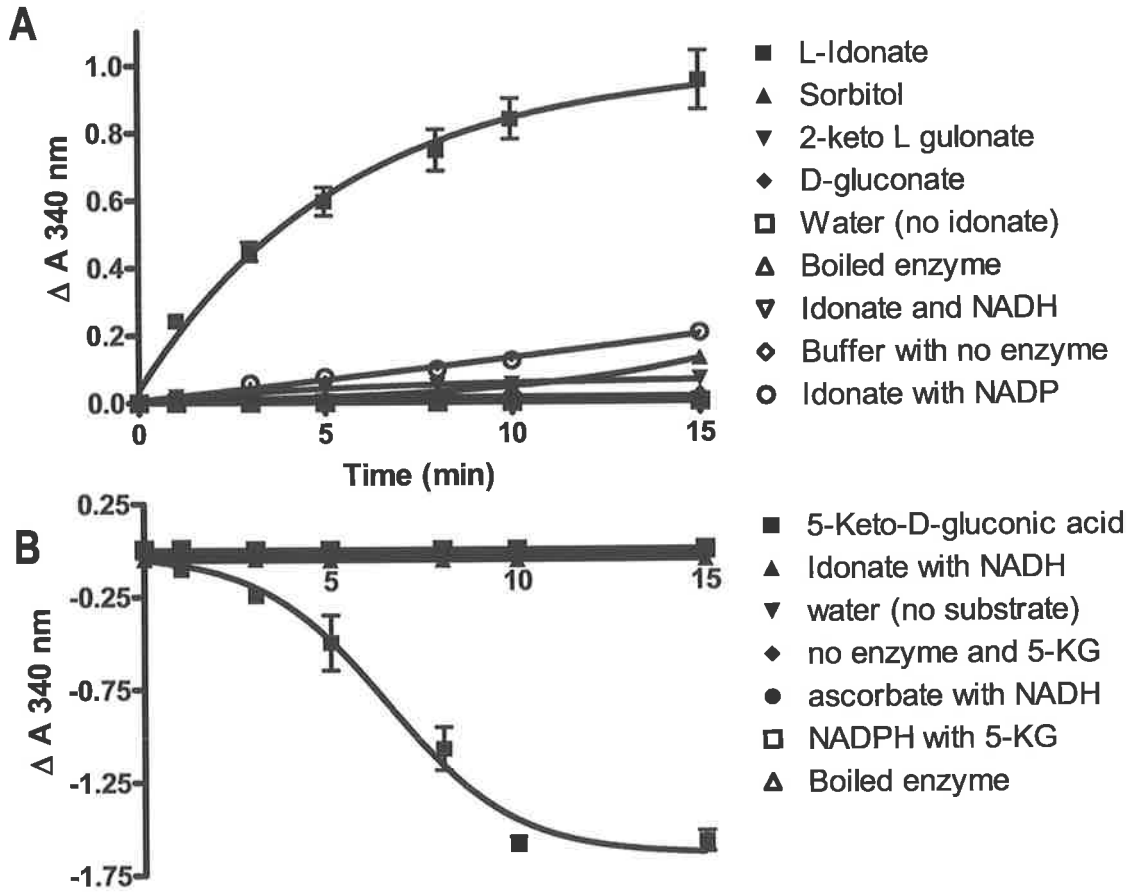

Figure 5.6 Characterising the substrate specificity and activity of recombinant *V. vinifera* idonate dehydrogenase. **A** The filled square indicates the complete forward reaction L-idonate to 5-keto D-gluconate (see methods and materials). **B** Filled squares also denote the complete reverse reaction from 5-keto D-gluconate to L-idonate (see methods and materials). Reactions were followed by change in absorbance at 340nm. Bars = standard error, n=3. Substrate specificity was measured along with various controls as shown on the right hand column; all reactions were measured under the same pH and temperature conditions.

Mass spectrometry confirmed that the product of the reduction of 5-keto D-gluconic acid by L-IdnDH matched the mass of authentic L-idonate (data not shown), and therefore clearly identified the novel plant enzyme idonate dehydrogenase. Initial tests were carried out at room temperature, which yielded some activity. Equilibrating enzyme, buffer and all reagents at 30°C prior to adding substrate increased overall

activity. A pH range from 5.5 to 8.5 was tested for the activity of L-IdnDH, it was determined that buffering the pH at 8 with 100 mM Tris-HCl gave maximal activity (data not shown). Trichloroacetic acid (TCA) is a potent inhibitor of protein activity; addition of TCA stopped reduction of NAD^+ at various time points during catalysis (data not shown).

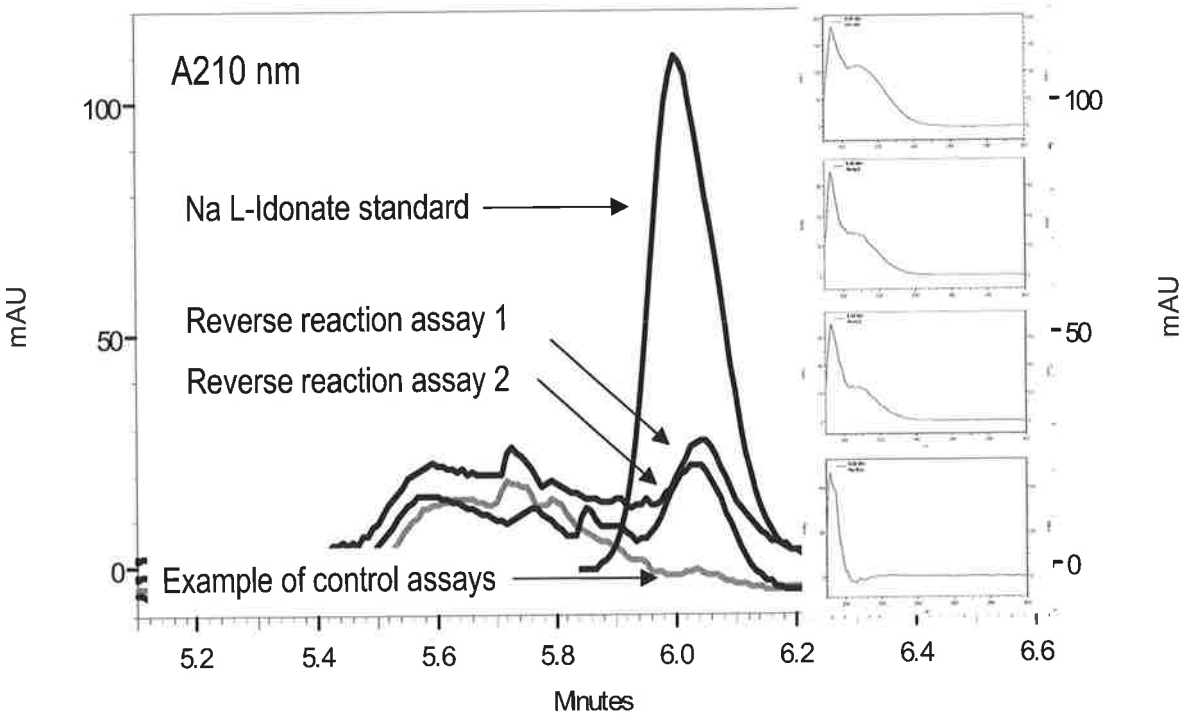

Figure 5.7 Shows the HPLC chromatograms of the reverse L-IdnDH reaction mix over a 15 minute time frame under conditions described in the methods and materials. Standard Na-L-idonate elutes at 6.02 minutes and has a distinct absorbance spectrum, (top right-inset) with absorbance maxima at 190 and 210 nm. A reaction mix using 300 mM substrate showed the formation of a product with retention time and absorbance spectrum (middle two insets) matching authentic L-idonate. A control assay stopped with TCA at time 0, shows that no peak is formed and no matching absorbance spectrum occurs.

5.3.4 Characterising the catalytic activity of L-IdnDH

Initial-rate determinations of L-IdnDH activity plotted against concentration for the substrates of forward and reverse reactions were fitted to hyperbolic saturation curves, indicative of Michaelis Menten (MM) kinetics operating in both directions of the reaction catalysed by the enzyme. K_m values of the recombinant L-IdnDH were determined from these curves for the forward and reverse reactions to be 2.8 mM and 12.2 mM respectively (Figure 5.8). With forward reaction defined as the conversion of idonate to 5-keto gluconic acid. Additionally V_{max} calculated for 5-keto-D-gluconic acid and L-idonate showed 188 (nkatals mg-1) and 772 (nkatals mg-1) respectively (Figure 5.8). Transformation of the experimental data to double reciprocal (Lineweaver-Burk) plots, the standard approach for determination of basic kinetic parameters, suggested that an alternative mechanism of action may in fact be occurring in at least one direction of the enzyme's activity.

Interestingly, when the initial rate data for the reverse reaction 5-keto-D-gluconic acid to L-idonate was fitted to a sigmoidal model, the fit obtained was closer than for the hyperbolic curve (Figure 5.9). The graphing program PRISM4® calculated (P value 0.0001) that the sigmoidal curve was the preferred fit, suggesting that some form of cooperativity or allosterism may be occurring. The reaction kinetics for the cooperative model were not substantially different, K_m values for reverse reaction catalysing the conversion of 5-keto-D-gluconic acid to L-idonate were 9 mM (Figure 5.12) compared to 12 mM for MM kinetics. V_{max} calculated using the allosteric model in the same order as above was 582 (nkatals 0.01mg-1).

Differences in the fitted allosteric and MM models are primarily due to a delayed initial exponential increase in substrate consumption (Figure 5.10), which does not ideally fit the one site binding hyperbola in the MM model. Alternatively, values at 1 mM to 5 mM displaying a low increase in substrate consumption, which when converted into a double reciprocal (1/v over 1/s) plot skews the data in the reverse reaction and are suggestive of a limiting value in substrate concentration of 5 mM, after which the reaction runs at a maximal rate.

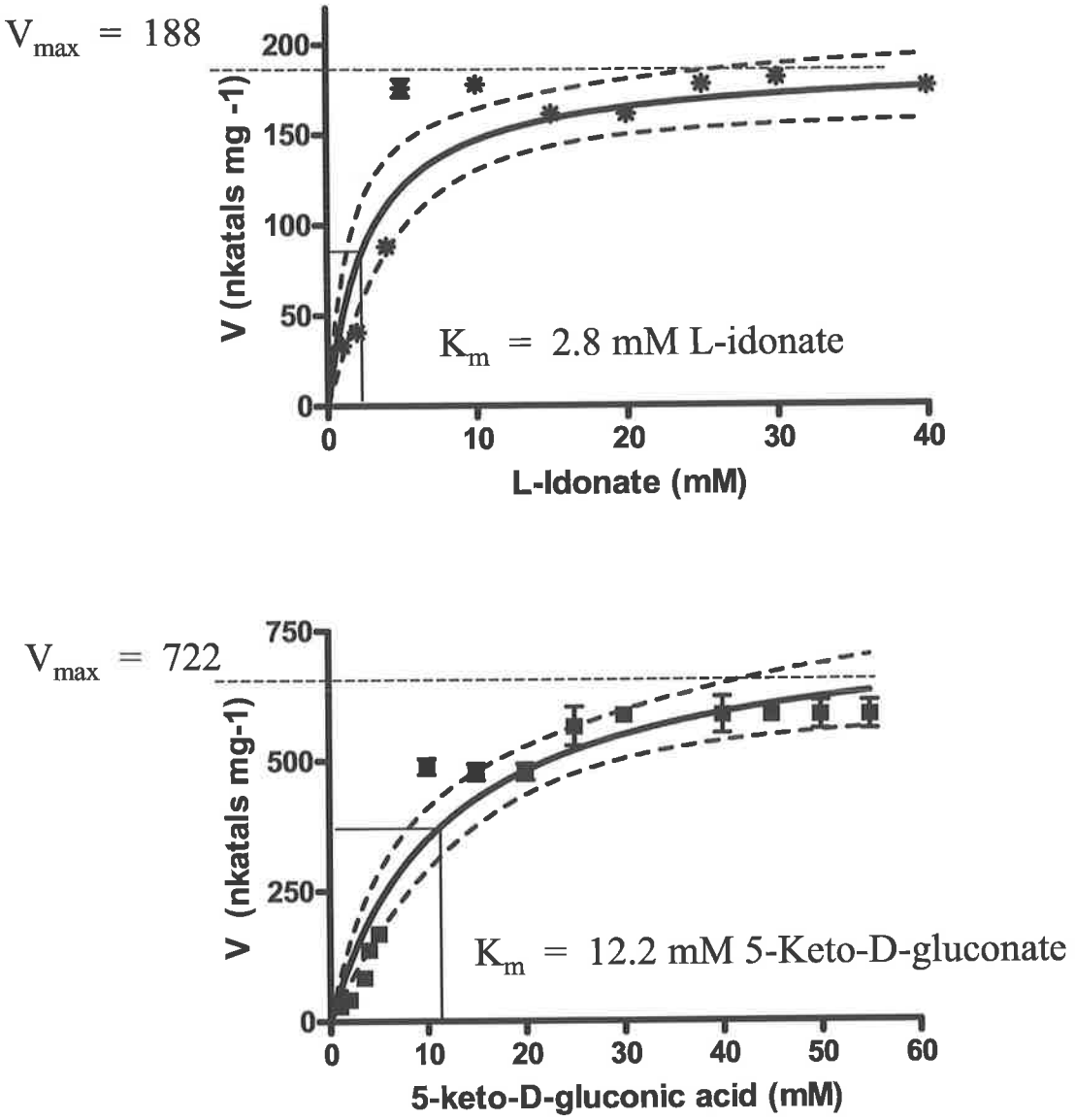

Figure 5.8 Enzyme kinetics plotted using Michaelis Menten kinetics for L-idonate in the forwards reaction (top) and 5-keto-D-gluconic acid in the reverse reaction (bottom) and the calculated Km and Vmax values.

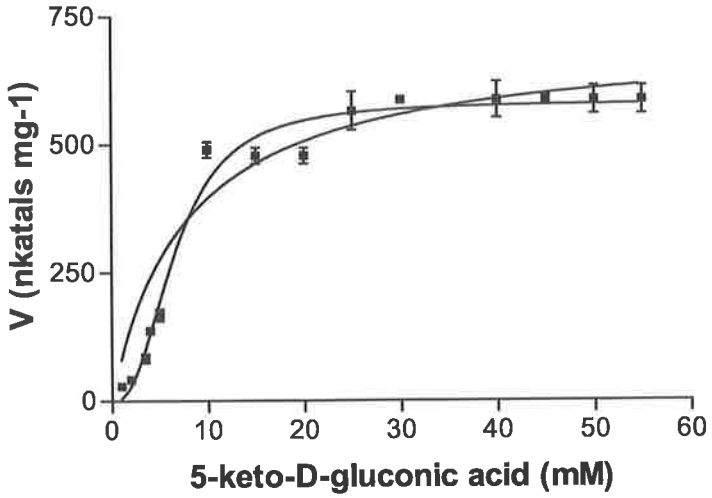

Figure 5.9 The difference between the allosteric model and Michaelis Menten model plotted to the reverse reaction data in V (as nmoles of NAD per second per mg of protein) over concentration of donor substrate

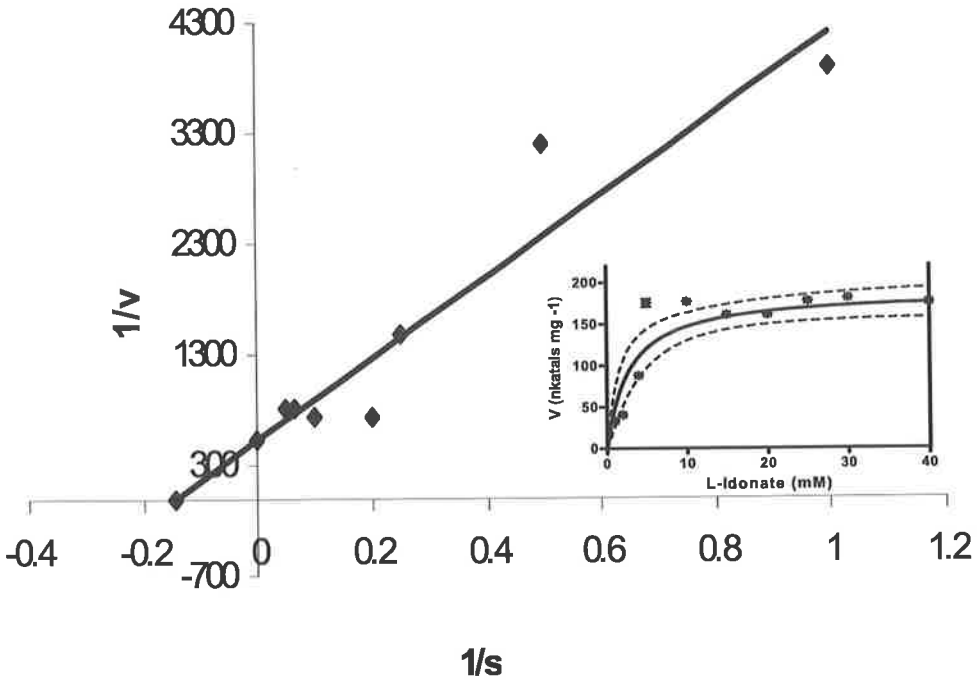

Figure 5.10 A double reciprocal plot of the forwards reaction fit to Michaelis Menten kinetics

5.3.5 Berry slice feeding experiments: *in planta* addition of substrates involved in the reaction chemistry of L-IdnDH

Evidence from radioisotope tracer studies in grape berries, showed that ^{14}C radiolabel on either idonate or 5-keto D-gluconate is incorporated into TA (Saito and Kasai, 1984). To investigate and further confirm the involvement of idonate and 5-keto D-gluconate in TA synthesis, slices of grape berries from *V. vinifera* and *A. aconitifolia* were incubated in each substrate and the resulting formation of TA compared with control incubation data. This resulted in rapid increase in berry TA concentration, in *V. vinifera* and crucially no formation of TA in *A. aconitifolia* (data not shown). The negative control treatment (water only) showed no increase in TA concentration for *V. vinifera* grapes (Table 5.1); after three hours of incubation uptake of water resulted in dilution of the initial berry TA level. Over a three hour period, more than 10 mg greater TA was formed after addition of the substrate 5-keto D-gluconate compared to the control without substrate addition (H_2O) (Table 5.1). Moreover, adding L-idonate to berry slices also significantly increased the level of TA accumulation compared to the control (Table 5.1). These data, combined with specific radioisotope tracer studies, confirm the capacity of L-IdnDH to catalyse the reaction chemistry critical to TA formation and demonstrate the high activity of this metabolic pathway. These data demonstrate the rapid rate of catalytic reaction turnover from L-idonate and 5KG to TA conversion in *vivo*.

Table 5.1 Berry slice feeding experiments: TA accumulation measured in mg per gram FW in *V. vinifera* berry slices incubated with 100 mM L-idonate, 5-keto-D-gluconate or water *

Time (hr)	Control (H_2O)	L-idonate (100mM)	5-keto gluconate (100mM)
0	0.0 mg	0.0 mg	0.0 mg
1	0.0 ± 0.8 mg	3.4 ± 1.3 mg	1.9 ± 1.3 mg
2	0.2 ± 0.4 mg	4.0 ± 0.2 mg	4.1 ± 0.3 mg
3	-3.9 ± 0.6 mg	6.2 ± 2.2 mg	11.1 ± 5.6 mg

* substrate additions to *A. aconitifolia* did not stimulate the formation of tartaric acid

5.3.6 *In planta* measurements of ascorbic acid in tartaric acid accumulating and non accumulating species

To answer the possibility that in the absence of a functional pathway for TA formation AA would accumulate, measurements of AA in TA accumulating and non accumulating species were made. As detailed in Chapter 4, measurements of frozen samples had shown that a difference in AA was likely. Using fresh berries ground in phosphoric acid and loaded immediately onto the HPLC column to avoid any oxidative degradation, AA levels were up to five times greater in non TA accumulating vines compared to TA accumulating vines at the same developmental stage (Figure 5.11).

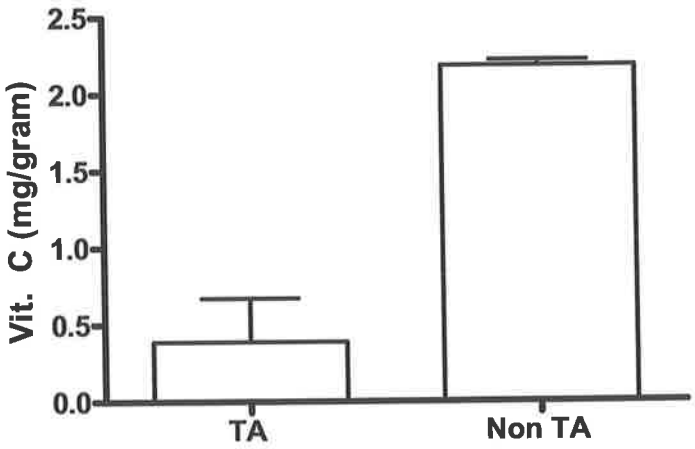

Figure 5.11 Vitamin C measured in ripe berries of *V. vinifera* and *A. aconitifolia*. 5 berries were sampled per replicate. Bar = standard error, n=3).

5.3.7 Polyclonal antibody formation, berry protein isolation and western blotting

Primary antibody (blood serum) was collected and used against protein extracted from the pre veraison berry with good success, with western blot analysis

revealing L-IdnDH to be present in both the cytosolic fraction and insoluble protein fractions (Figure 5.12), however further studies revealed some degree of cross reactivity (data not shown).

Figure 5.12 Western blot analysis using polyclonal antibody to the grapevine L-IdnDH. Lane 1 is a molecular weight ladder, lane 3 to demonstrates the reactivity of the antibody to cytosolic protein, and lane 2 demonstrates the reactivity of L-IdnDh antibody to insoluble protein fraction isolated from pre veraison grape berries (4 weeks post flowering). The band in lane 3 corresponds with a 40 kDa band in the molecular weight ladder.

Discussion

Despite their structural similarity, markedly different biochemical processes form TA and L-malic acids, which accumulate to high levels in grape berries during ripening. TA accumulation occurs in a very small number of plant species, the most significant of these being the cultivated grapevine *V. Vinifera* (Stafford, 1959). TA levels within grape berries confer organoleptic properties important in the palatability of table grapes, but more importantly, provide the basis for the control of pH that is crucial during the production of wine. Data within this chapter demonstrates enzymatic activity for a key component (L-idonate dehydrogenase) of the formerly uncharacterised TA biosynthetic pathway AA (vitamin C) in grapevine *V. vinifera*. Previous chapters have described the use of a combination of transcript and metabolite analyses in Vitaceous species to identify and correlate candidate gene expression with TA formation towards isolating the L-IdnDH gene.

Preliminary biochemical investigations to identify TA-biosynthetic specific enzyme activity in soluble protein extracts prepared from immature grape berries were unsuccessful (data not shown). It is suggested that despite the use of extraction buffer systems designed to maximise the recovery of enzymatic activity from these tissues (Ford and Høj, 1998), the combination of high organic acid and high phenolic conditions was refractory to the recovery of a measurable amount of soluble protein. Earlier work (data not shown) to isolate glucosyltransferase enzymes from similar tissues was likewise unsuccessful, with only one tenth to one fortieth of the yield of protein observed in extractions from mature berries compared to leaves (Ford and Høj, 1998). Although the ease of transformation in model plant systems such as *Arabidopsis* provides researchers with reverse genetic tools to link genes to phenotypes, many non-model systems, including the grapevine, display recalcitrance to facile transformation. Consequently, despite their undisputed economic and cultural importance, the biology of these species remains largely unexplored.

Enzymological evidence confirmed the capacity of the encoded enzyme to complete a key step in TA biosynthesis, the conversion of L-idonate to 5-keto D-gluconic acid, providing the first evidence for a biochemical component of this pathway. The product of the 'reverse reaction', L-idonate, was identified by HPLC-mass spectrometry, confirming the specificity of the enzyme for its postulated

substrate. The lack of measurable activity with other substrates further supported the specific role proposed for the enzyme. An L-idonate dehydrogenase also occurs in the gluconate II pathway of *E. coli*, where gluconate is utilized as an energy source in the human gut (Bausch *et al.*, 1998, Bausch *et al.*, 2004). It is also likely that the reduction of 5-keto D-gluconate to L-idonate in *Fusarium sp.* No. 125 reported in the early 1960's may also have been catalysed by a similar enzyme (Takagi, 1962A, Takagi, 1962B). Interestingly, the identity between *E. coli* L-idonate dehydrogenase and grapevine L-IdnDH is only 31% at the amino acid level, although both share a zinc-binding alcohol dehydrogenase backbone. The grapevine protein is more similar to sequences encoding NAD^+-linked 2-iditol dehydrogenases from a number of plants including *Arabidopsis thaliana*, *Malus domestica* (apple), *Eriobotrya japonica* (loquat) and *Lycopersicon esculentum* (tomato). In addition to the classical C-terminal Rossman fold characteristic of $NAD(P)^+$ dehydrogenases, these enzymes contain a predicted ketose reductase domain associated with sorbitol dehydrogenase activity. The divergence of paralogous genes due to small changes in amino acid sequence has been reported to alter the specificity and catalytic activity of enzymes (Broun *et al.*, 1997, Henikoff *et al.*, 1997); the origin of the unusual substrate specificity possessed by L-IdnDH may be explained by a similar series of events.

The absence of the L-IdnDH paralog, specifically from *A. aconitifolia* but not from related TA-forming species, is consistent with a gene deletion in *A. aconitifolia* as an underlying cause of a lack of TA accumulation in this species. The discovery of a grape lacking TA synthesis (a naturally occurring mutant) was paramount to the current study, as has been shown in other pathways studied such as cellulose synthesis where all the genes for proteins directly involved in cellulose synthesis have been identified by mutant analysis (Somerville, 2006). The desirability of strengthening the argument for *in vivo* function by furthering the correlation between TA production and transcript abundance was addressed in *V. vinifera*. *V. vinifera* is arguably the best system for such analysis (relative to *Aconitifolia* spp, for example) because of the strong correlation between the accumulation of L-IdnDH transcript and TA (Figure 5.3A and 5.3B), and because biochemical studies in *V. vinifera* implicate the conversion of idonate to 5-keto gluconate as the rate-limiting step (Saito and Kasai, 1984, Malipiero *et al.*, 1987). In an experiment described in detail in Chapter 7, individual berry clusters were shaded from light. At the time of peak TA biosynthesis, organic acid levels (Figure 7.6A) and L-IdnDH transcript levels (Figure

7.6B) were quantified. To this end, reduction in the TA pools correlated with corresponding decrease in L-IdnDH transcript levels, while levels of malate and oxalate were unaffected (Figure 7.6C).

Berry slices prepared from immature *V. vinifera* tissue exhibited a high rate of TA biosynthesis when fed L-idonate or 5-keto D-gluconic acid; moreover this activity was absent from berries of the non-TA accumulating species *A. aconitifolia*. L-idonate could at first glance be expected to accumulate in berries of this species, but this was not the case. Instead, it was observed that berries of *A. aconitifolia* possess significantly higher levels of ascorbate, the biosynthetic precursor of TA (Saito and Kasai, 1969) and an abundant organic acid in many fruit. Moreover, the possibility that L-idonate or 5-keto-gluconic acid may feedback inhibit the conversion of ascorbic acid to 2-keto-L gulonic acid may explain why ascorbic acid accumulates in *A. aconitifolia*. In spite of the scientific advances made in the production of AA and its biocatalytic intermediates, there remains a need for methods for the production of AA. Additionally, many of the methods utilized for the production or synthesis of AA fail to be cost-effective so as to be commercially viable. The discovery of a new, cost-effective and relatively simple method for the production of AA would be advantageous. This suggests the intriguing possibility that *in planta* deletion of components of the TA biosynthetic pathway may lead to increased amounts of AA within the developing berry, lending additional support to the conclusion that L-IdnDH is a key component of the pathway converting vitamin C to TA.

Assessment of the enzyme kinetics (Figure 5.8, 5.9 and 5.10) showed that L-IdnDH in the reverse direction demonstrated a sigmoidal response rather than fitting a classical Michaelis Menten kinetic model. Sigmoidal enzyme kinetics are indicative of allosteric enzymes (Campbell, 1999). Allosteric is a word derived from two Greek words: 'allo' meaning other and 'steric' meaning place or site; allosteric means other site and an 'allosteric enzyme' is an enzyme with two binding sites. These enzymes commonly have more than one subunit, such as dimers or tetramers (Smith *et al.*, 1994). Allosterism can have positive or negative results for the enzyme's ability to utilise substrate; in the case of L-IdnDH the enzyme appears to display positive cooperativity. Enzymes displaying positive cooperativity have sigmoidal kinetics

reflecting the very large increase in intial rate (V_o) with increasing substrate over a very narrow range of substrate concentration (Figure 5.8B). Broadly, this result may fit in with the finding reported in Chapter 7, namely that large amounts of AA are synthesised early in berry development, providing a concentration gradient at the time in which TA synthesis is occurring. The role of AA in controlling and regulating the oxidative burst associated with photosystem I has been shown in plants (Anderson *et al.*, 1983). In the grape the use of AA for TA formation correlates well with increased sequestration, hypothetically a clear correlation can be drawn.

If TA production in *A. aconitifolia* were to be solely due to lack of the gene encoding L-IdnDH, then it could be also expected that exogenously added 5-keto-D-gluconate would restore TA formation to berries of *A. aconitifolia*. Our results showed that the addition of 5-keto-D-gluconate to berry slices of *A. aconitifolia* did not have this effect (Table 5.1), indicating that additional factors may contribute to the lack of TA accumulation in this species. Further investigation of candidate genes encoding additional TA-biosynthetic steps, including the characterisation of gene knock-out and knock-down phenotypes produced by RNA interference technology may serve to answer these questions (discussed in Chapter 8, future directions).

The present work provides biochemical and molecular evidence for the proposed rate-limiting step in formation of TA in the grapevine and demonstrates the utility of combining molecular, metabolic and biochemical approaches to resolve otherwise intractable biosynthetic phenomena. Biochemical data supports the proposed function of L-IdnDH in the conversion of L-idonate to 5-keto D-gluconate *in vitro* and, by virtue of the identification of a grapevine species lacking the gene encoding this enzyme, *in vivo* also. Furthermore, evidence provided from the examination of precursor uptake experiments allows for the first time in any plant species a glimpse into the intricacies of the role of L-ascorbic acid as a biosynthetic precursor, and suggests a rational basis to design grapes, already the world's most important fruit crop, containing elevated levels of the vital human micronutrient vitamin C.

Chapter 6

Candidate genes VvTKl and TSAD: Cloning, heterologous expression and enzymatic assays towards their involvement in tartaric acid biosynthesis

6.1 Introduction

Chapter 7 will describe research into the involvement of two new candidate genes (VvTKI, TSAD and LC1) in TA biosynthesis. Previous chapters have described the methods used to isolate candidate genes by transcriptional profiling (Chapter 3), implicate genes by PCR analysis (Chapter 4) and research in chapter 5 showed methods of prokaryote over-expression and enzymatic assays to provide biochemical data demonstrating recombinant protein function. Of the candidate genes isolated in Chapter 3, the key candidate, which was characterised as the novel plant protein L-idonate dehydrogenase, was accompanied by a further set of genes that did not correlate exactly with TA biosynthesis in the subtractive genome of *A. aconitifolia* (Chapter 4). They did however display the appropriate tissue and developmental expression patterns in *V. vinifera*. Because it is unclear how or why *A. aconitifolia* lacks the ability to form TA, it is important to explore candidate genes in more detail. The two genes share global gene homology with plant transketolase and aldehyde dehydrogenase proteins. In the following introduction, literature relating primarily to the transketolase will be explored with mention to the aldehyde dehydrogenase limited because biochemical characterisation of this protein was less successful.

Transketolase

Salisjarvi *et al.* (2004) presented an insightful paper into aspects of gluconate metabolism in bacteria, and although not the main thrust of the publication, reported the activity of a transketolase able to form tartaric acid semi aldehyde from 5-keto D-gluconic acid, a substrate previously not considered for this class of enzymes. The primary role of transketolase (TK) enzymes is implicated in the catalytic conversion of sugars in the oxidative pentose phosphate pathway (OPPP) (Horecker *et al.*, 1956, Caillau and Quick 2005). They also have dedicated roles in aromatic amino acid biosynthesis, isoprenoid biosynthesis (via the nonmevalonic acid pathway) and glycolytic cycle integration (Henkes *et al.*, 2001). The reaction catalysed by transketolase consists of the reversible transfer of a two-carbon glycoaldehyde fragment from keto-sugars to the C-1 aldehyde of aldo sugars (Schenk *et al.*, 1998). The level of promiscuity to various substrates and level of involvement in basic

cellular processes is not entirely known, but Schenk *et al.* (1998) summarized the donor and acceptor compounds for prokaryotes and eukaryotes as follows: D-xylulose-5-phosphate, D-sedoheptulose-7-phosphate, D-fructose-6-phosphate, D-erythrose-4-phosphate, dihydroxyacetone phosphate, dihydroxyacetone and hydroxypyruvate as donors, and formaldehyde, acetaldehyde, D-ribose-5-phosphate, D-glyceraldehyde-3-phosphate, D-erythrose-4-phosphate and glycoaldehyde as acceptors.

In plants, a small level of transcriptional inhibition of TK enzymes has been shown to have a substantial impact on photosynthesis and plant growth, as well as secondary metabolism (Henkes *et al.,* 2001). This result suggested TKs are enzymatically involved in the poorly understood link between primary and secondary metabolism. In capsicum fruit two transketolase enzymes (CapTKI and CapTKII) were cloned and it was found that they had dedicated functions, one specific for OPPP and the other specific for nonmelavonic acid pathway (Bouvier *et al.,* 1998). TK enzymes from several sources have been isolated from plastids (von Schaewen *et al.,* 1995 Bouvier *et al.,* 1998). But, according to Caillau and Quick (2005) analysis of the Arabidopsis genome reveals that TKs are multigene families composed of both cytosolic and plastid bound enzymes. Evolution of this enzyme class is considered to stem from divergence in organism metabolism via the pentose phosphate and Calvin cycle (Caillau and Quick, 2005). TK class of enzymes, due to their importance in several areas of fundamental cellular metabolism, are well distributed and highly conserved throughout Eukaryote and Prokaryote biota (Schenk *et al.,* 1997). Broadly, TK's occur in mammals (Boren *et al.,* 2005), fungi (Juhnke *et al.,* 1996, Slekar *et al.,* 1996), bacteria (Gosset *et al.*, 1996, Salusjarvi *et al.*, 2004) and plants (Schnarrenberger *et al.*, 1995, Henkes *et al.*, 2001), and are identified by a phylogenetically conserved sequences including a 36 residues transketolase domain (Schenk *et al.*, 1997) and a thiamine diphosphate binding domain (Hawkins *et al.*, 1989). Plants contain one primary isoform of TK, and moreover the plant TK, isolated from spinach chloroplasts is amphibolic for both the Calvin cycle and OPPP (Schnarrenberger *et al.*, 1995).

In plants 5-keto gluconic acid is an uncommon metabolite; its primary occurrence is in the TA biosynthetic pathway from Vitamin C in plants, which was determined by careful radioisotope tracer studies (Saito and Kasai, 1984, Malipiero *et al.*, 1987). Saito *et al.* (1997) suggested that a hydrolase enzyme may be involved in

cleaving the 5-keto gluconic acid compound, this conclusion was based upon ^{18}O and ^{14}C radioisotope tracer studies. The enzyme responsible for catalysing the conversion of 5-keto gluconic acid to TA is as yet unknown. Only one enzyme has been determined in the pathway to TA (Chapter 5) an L-idonate dehydrogenase, which catalyses the NAD+ dependant reversible conversion of idonic acid to 5-keto gluconic acid (DeBolt *et al.,* 2006). Although, 5-keto gluconic acid is uncommon in plant metabolism but readily seen Prokaryote genera, involved in idonate and gluconate metabolism (Bausch *et al.*, 1998, Bausch *et al.*, 2004). In this pathway 5-keto gluconic acid is formed by gluconate breakdown and utilised as a metabolic substrate by bacteria in the gastrointestinal system (Bausch *et al.*, 1998, Salusjarvi *et al.*, 2004). In fact, the pathway for gluconic acid metabolism in bacteria is strikingly similar to the TA biosynthetic pathway in plants (Bausch *et al.*, 1998, Loewus, 1999). Both pathways involve 5-keto gluconic acid, which is reversibly converted to the intermediate L-idonate, another rare sugar acid in plants (Bausch *et al.*, 1998).

Aldehyde dehydrogenase

The penultimate step in TA synthesis involves a compound identified as TA semi-aldehyde (Saito and Kasai, 1984, Loewus, 1999). One of the primary candidates in chapter 3 was succinic semi aldehyde dehydrogenase, which provided a potential mechanism for the oxidation of the TA semi aldehyde compound.

6.2 Methods and materials

Chemicals and enzymes

See chapter 2 for a list of authentic chemical suppliers, enzymes were purchased from the same suppliers

Identification of sequences associated with proposed steps in TA biosynthesis

The amino acid sequences encoding putative transketolase and semi aldehyde dehydrogenase candidates were identified by comparisons with known enzymes using PFAM, NCBI, BRENDA and Interpro protein domain BLAST interfaces (Altschul *et al.*, 1990, Mulder *et al.*, 2005).

Plant material

Refer to methods and materials of Chapters 4 and 5 for plant material

Isolation and PCR amplification of candidate sequences

Full length genes were amplified from pre veraison berry cDNA using primers which contain sticky end restriction sites for directional cloning into the pET expression system (see chapter 5). as follows:

VvTKI:

Forwards-GGGCATATGATGGGGAAAGGAGGCAACTCTG and reverse-CCGGATCCTTAGAGATTAAACATGACCTTG

TSAD:

Forwards-GGCATATGATGGGGATATCGCAGATGG and reverse-GGGGATCCTCAGTTACTGCTTATATTTCC.

Real time PCR analysis of transketolase expression patterns during berry development

Quantitative RT-PCR was conducted on samples collected biweekly during berry development (1-16 weeks post flowering) by isolation of mRNA (standardised at 500 ng. μl^{-1}) and quantitative analysis of transcription as follows. Reaction mixes used 10 µl of BioRad® real time PCR reagent, 1µl (500 ng. μl^{-1}) template cDNA, 8.4 µl dH_2O and , 0.6 µl (1.5 pmol) F/R primer. Internal primers for the two paralogs of TKase identified from sequence comparisons were as follows:

VvTKaseI

Forwards primer CTGTCGATAGACGCAGTGGA and reverse primer CACTTCAACCCCAGGTGTCT

VvTKaseII

Forwards primer AGAAGAGCGCAATGTCAGGT and reverse primer TCTCCAAGCCCAATTGAATC

Standard curves for the expression of VvTKaseI/II were formed by cloned and sequenced VvTKaseI/II used as template at a series of known log scale concentrations. Relative expression is based on a correction factor, which is a calculated based upon the expression of the ubiquitin control gene in all templates.

Molecular cloning and recombinant protein formation

Full-length VvTKI, TSAD and GLCI was amplified from *V. vinifera* RNA obtained from berries sampled 4 weeks post anthesis and cloned via

pTOPO2.1(In*vitro*gen) into pET14b (Novagen) for prokaryotic expression. Sequence alignment, cloning and over expression were as described in chapter 5, with the exception of the induction temperature for VvTKI which rather than 37 °C was 28 °C to maximise recombinant protein translation.

Development of an in *vitro* assay for grapevine transketolase activity

Thiamine pyrophosphate, magnesium cofactor dependent reaction of VvTKI was measured as change in absorbance at 340 nm by assaying the conversion of product interconversions as described below. Assays (150μL) for testing the activity of VvTKI in the OPPP contained 15 μL purified protein extract (ca 0.03 mg/mL) pre-equilibrated to 30°C in 10 mM Tris HCl pH 7.5, thiamine pyrophosphate, erythrose-4P, 100 μM MgCl, 8U phosphoglucose isomerase, 8U glycerol phosphate dehydrogenase, 330 μM NADH and $NAD(P)^+$ in a glass cuvette zeroed at A_{340} nm before addition of substrate being xylulose-5P to a final concentration of 33 mM. The activity of TK in the OPPP leads to fructose-6-phosphate and glyceraldehyde-3-phosphate. Fructose-6-phosphate is converted to glucose-6-phosphate, which is then converted to glycerol 1-5 lactone by the activity of glycerol phosphate dehydrogenase, which requires $NAD(P)^+$ as a cofactor. Also the presence of glyceraldehyde-3-phosphate was tested by reaction chemistry involving trios-phosphate isomerase, which converts glyceraldehyde-3-phosphate to dihydroxyacetone phosphate that is further converted to glycerol-3-phosphate in the presence of NAD+ by the commercially available enzyme α-glycerol-3-phosphate dehydrogenase. Each reaction was followed by change in absorbance at A_{340}nm. The assay to test if 5-keto gluconic acid could act as a substrate for VvTKI involved 15 μL purified protein extract (ca 0.03 mg/mL) pre-equilibrated to 30°C in 100 mM Tris HCl pH 8, thiamine pyrophosphate, erythrose-4-phosphate, 1 mM MgCl, 8U phosphoglucose isomerase, 8U glycerol phosphate dehydrogenase, 330 μM NAD^+ or NADH, in a glass cuvette zeroed at A_{340} nm before addition of substrate being 5-keto gluconic acid to a final concentration of 33 mM.. Controls included, no enzyme, boiled enzyme, no substrate (dH_2O), reaction stopped with TCA, no added NAD^+ and/or no added NADH. Reactions were stopped with 50 μL 1 M HCl, centrifuged at 13,500 *g* for 5 min.

Freezing and thawing stability of the protein was tested as activity over time. The variation of activity with pH was studied for the acceptor substrates, to calculate the ideal pH for VvTKI reactions were measured between pH 5.4 and 8.5 using the following buffers: MES, pH 5.4-6.2; PIPES, pH 6.2-6.6; TRIS, pH 6.5-8.5. Standard assays were carried out as described, with the buffer concentration fixed at 10 mM throughout.

Development of an assay to test for tartaric semi aldehyde dehydrogenase activity

Assay conditions for testing the NAD dependant activity of TSAD were similar to those described for L-IdnDH in chapter 5. The reverse reaction from TA to TA semi aldehyde was tested in the presence of NADH at pH 7.5 (using 100 mM TRIS-HCl). Succinic acid was also tested as a substrate for this recombinant protein.

Sequence comparisons

The deduced amino acid sequence compositions of the VvTKI and partial sequence encoding VvTKII were compared to known and characterised transketolase enzymes using the ClustalW online software package available from European Molecular Biology Protein BLAST database (www.EMBprot.org). Sequences were obtained from Genbank and the UC-Davis genome centre.

6.3 Results

6.3.1 Transketolase

Identification of transketolase candidates from grapevine transcriptome and extraction of full length sequences from cDNA libraries and compiled contig data

Using homology searching in the grapevine compiled contig database **(cgf.ucdavis.edu),** two paralogous grapevine transketolase enzymes were identified as in contig 1028716 and 1012153. Only one of the two paralog sequences encoded a full length sequence and this contig was chosen for further study.

Sequence analysis grapevine transketolases I and II (VvTKI and VvTKII)

Sequence analysis of the two grapevine TK paralogs encoded within contig numbers 1028716 and 1012153 indicated that they shared 86 % identity at the amino acid level (Figure 6.1). Further comparison of the two amino acid sequences suggested that each were isoforms of TKase, both containing at least partial N terminus, central and C terminus TK domain architecture (Lindqvist *et al.*, 1992, Nikkola *et al.*, 1994) including the 36 residue transketolase motif (TK motif) and in VvTKI, the thiamine diphosphate binding motif (TdP binding motif) (not seen in the VvTKII because the clone did not cover the entire ORF) as described (Schenk *et al.*, 1997) (Figure 6.1). The full length ORF for grape VvTKI was 729 amino acids compared with 744, 741 and 741 amino acids of the TK isolated from capsicum, spinach chloroplasts and Arabidopsis respectively (Schnarrenberger *et al.*, 1995, Mendel *et al.*, 1996, Bouvier *et al.*, 1998). Comparing VvTKI sequence with those isolated from capsicum fruit (Bouvier *et al.*, 1998), it was evident that both TK proteins remained well conserved with the other plant TK enzymes such as those isolated from Arabidopsis (Mendel *et al.*, 1996) and spinach chloroplast (Flechner *et al.*, 1996) (Figure 6.2) and all shared greater than 80 % sequence identity. The region where maximal conservation occurred was in the N terminus, central and C terminus

domains as well as the highly conserved TK motif and TdP binding motif. The sequence encoding CapTK2 is also included in the ClustalW alignment and shows much lower sequence identity than with any other of the plant TK's. CapTK2 does not have substantial sequence identity with either VvTKI or the VvTKII, rather CapTK1 has greater than 80% sequence identity with both.

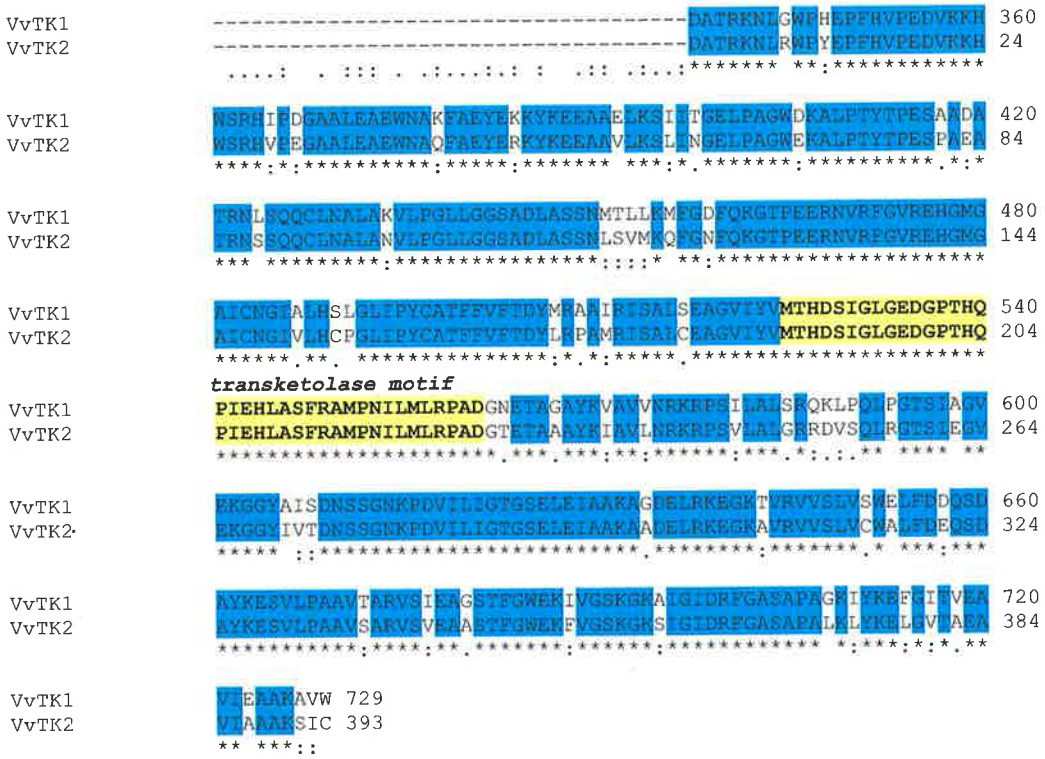

Figure 6.1 Amino acid sequence comparison between VvTKI and VvTKII across the 393 amino acid cloned sequenced region. The bold region in yellow encodes the conserved transketolase domain; the regions highlighted in blue encode identical amino acid sequence in both paralogs.

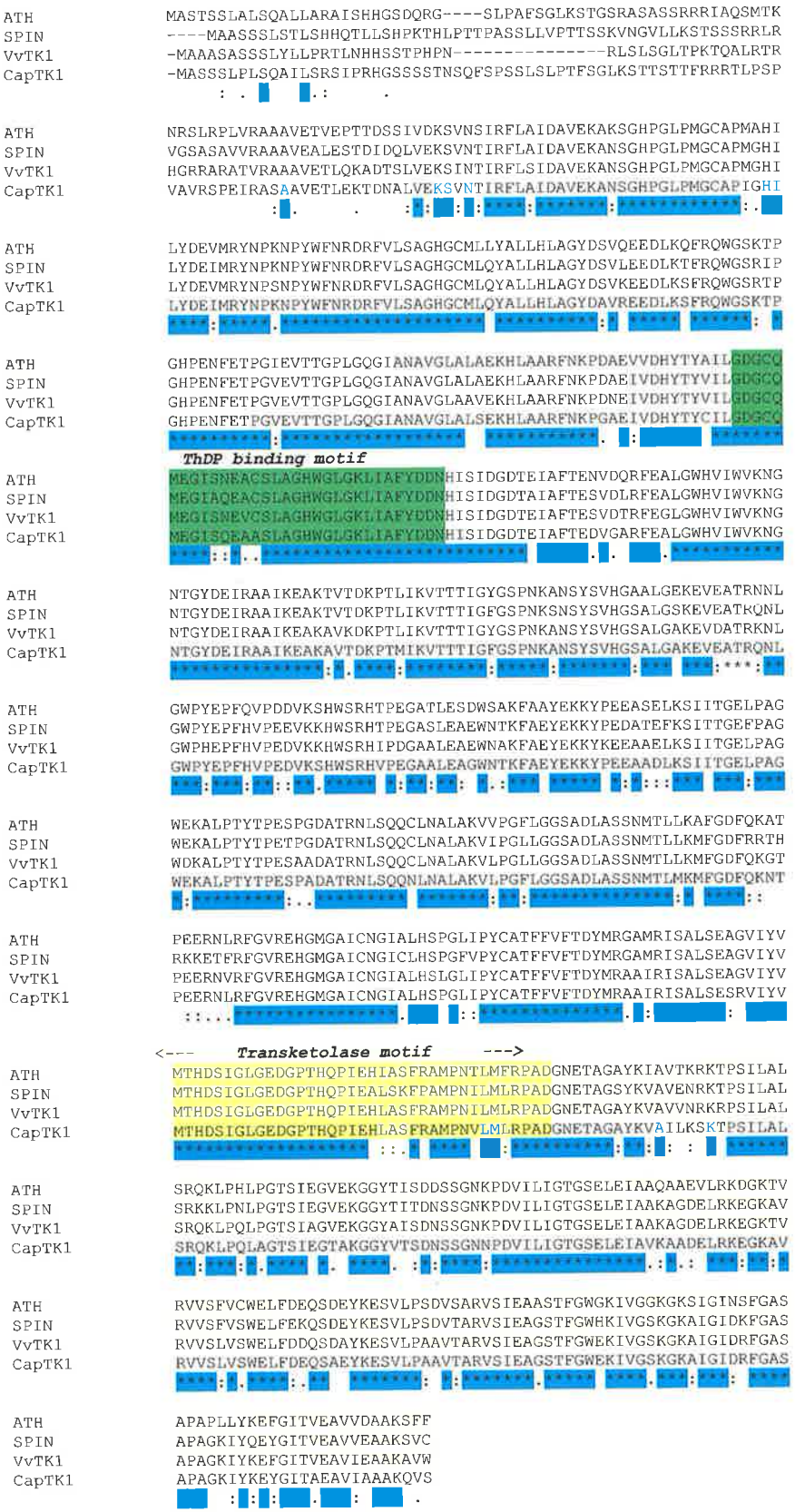

Figure 6.2 Sequence comparison between the four most conserved plant TK's. The yellow highlighted region indicates the conserved tranketolase motif and the green

highlight indicates the TdP binding domain. Regions where the stars at the base of each row are shaded blue indicates 100 % sequence identity in all 4 plant transketolases

Looking more broadly at sequence comparisons including mammalian and prokaryote TK sequences it is clear that although the ThP binding motif and TK domain remain reasonably well conserved among plant species analysed above (according to the sequence parameters outlined by Schenk *et al.*, 1997) the VvTKI sequence does not share strong identity match with mammalian or prokaryote transketolase sequences (Figure 6.3). Mammalian TK remains more diverged from plant genes than the TK from *E. coli*, this is evident when looking at the sequence leading up to and including the TdP binding motif (Figure 6.3). Highlighted in yellow are amino acids conserved between the VvTKI and *E. coli* and human TK's, which shows a much higher level of conservation leading up to the TdP binding motif, in particular a sequence of 12 and 18 amino acids RDRFVLSXGHGC and GVEVTTGPLGQGIANAVG conserved among all plants and the *E. coli* TK (Figure 6.3). In the upstream 60 amino acid sequence flanking the TK motif, there is much less sequence conservation between the VvTKI and *E. coli* sequences (again highlighted in yellow in Figure 6.3), with 25/60 matching amino acids versus 41/60 matching amino acids in sequence leading up to the TdP binding motif region.

```
VvTK1       GHILYDEVMRYNPSNPYWFNRDRFVLSAGHGCMLQYALLHLAGYDSVKEEDLKSFRQWGS 161
VvTK2       ------------------------------------------------------------
CapTK1      GHILYDEIMRYNPKNPYWFNRDRFVLSAGHGCMLQYALLHLAGYDAVREEDLKSFRQWGS 176
SPIN        GHILYDEIMRYNPKNPYWFNRDRFVLSAGHGCMLQYALLHLAGYDSVLEEDLKTFRQWGS 173
ATH         AHILYDEVMRYNPKNPYWFNRDRFVLSAGHGCMLLYALLHLAGYDSVQEEDLKQFRQWGS 173
Ecoli       AEVLWRDFLKHNPQNPSWADRDRFVLSNGHGSMLIYSLLHLTGYD-LPMEELKNFRQLHS  95
Human       MAVLFFHTMRYKSQDPRNPHNDRFVLSKGHAAPILYAVWAEAGFL--AEAELLNLRKISS 105
CapTK2      GSSLGVVELTVALHYVFNAPQDRILWDVGHQSYPHKILTG-------RREKMSTLRQTNG 168
                                .   . . .        :. :    .    . .

VvTK1       RTPGHPENFETPGVEVTTGPLGQGIANAVGLAAVEKHLAARFNKPDNEIVDHYTYVIL   221
VvTK2       ------------------------------------------------------------
CapTK1      KTPGHPENFETPGVEVTTGPLGQGIANAVGLALSEKHLAARFNKPGAEIVDHYTYCILGD 236
SPIN        RIPGHPENFETPGVEVTTGPLGQGIANAVGLALAEKHLAARFNKPDAEIVDHYTYVILGD 233
ATH         KTPGHPENFETPGIEVTTGPLGQGIANAVGLALAEKHLAARFNKPDAEVVDHYTYAILGD 233
Ecoli       KTPGHPEVGYTAGVETTTGPLGQGIANAVGMAIAEKTLAAQFNRPGHDIVDHYTYAFMGD 155
Human       DLDGHPVP-KQAFTDVATGSLGQGLGAACGMAYTGKYFDKASYR---------VYCLLGD 155
CapTK2      -LAGFTKRSESEYDCFGTGHSSTTISAGLGMAVGRDLKGR----------NNNVIAVIGD 217
               . .          :. .   . . . :   .        .. .  .       ..

                 TdP binding motif
VvTK1       GCQMEGISNEVCSLAGHWGLGKLIAFYDDNHISIDGDTEIAFTESVDTR-FEGLGWHVIW 280
VvTK2       ------------------------------------------------------------
CapTK1      GCQMEGISQEAASLAGHWGLGKLIAFYDDNHISIDGDTEIAFTEDVGAR-FEALGWHVIW 295
SPIN        GCQMEGIAQEACSLAGHWGLGKLIAFYDDNHISIDGDTAIAFTESVDLR-FEALGWHVIW 292
ATH         GCQMEGISNEACSLAGHWGLGKLIAFYDDNHISIDGDTEIAFTENVDQR-FEALGWHVIW 292
Ecoli       GCMMEGISHEVCSLAGTLKLGKLIAFYDDNGISIDGHVEGWFTDDTAMR-FEAYGWHVIR 214
Human       GELSEGSVWEAMAFASIYKLDNLVAILDINRLGQSDPAPLQHQMDIYQKRCEAFGWHAII 215
```

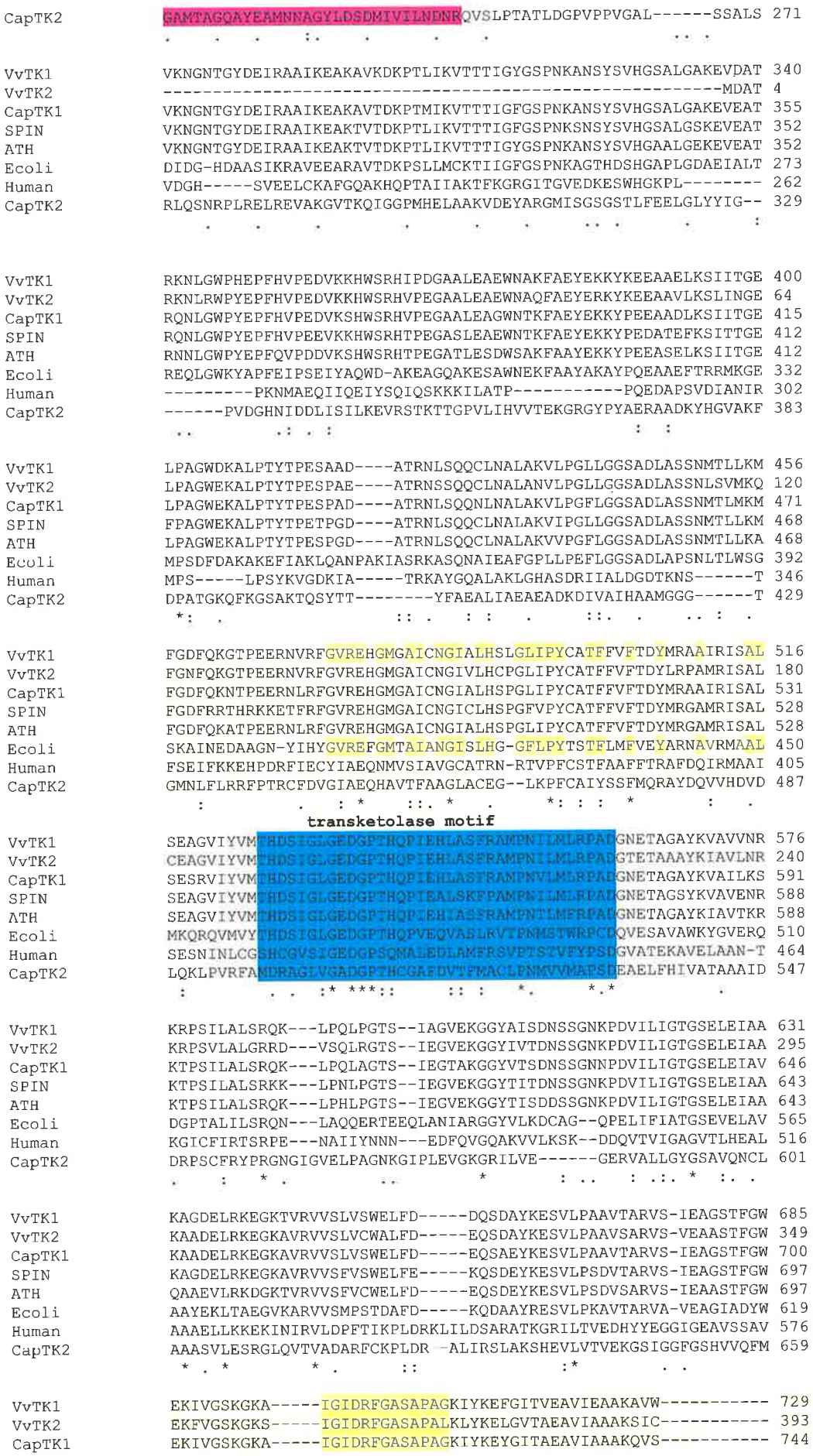
transketolase motif

```
SPIN            HKIVGSKGKA-----IGIDKFGASAPAGKIYQEYGITVEAVVEAAKSVC---------- 741
ATH             GKIVGGKGKS-----IGINSFGASAPAPLLYKEFGITVEAVVDAAKSFF---------- 741
Ecoli           YKYVGLNGAI-----VGMTTFGESAPAELLFEEFGFTVDNVVAKAKELL---------- 663
Human           VGEPGITVTH-----LAVNRVPRSGKPAELLKMFGIDRDAIAQAVRGLITKA-------- 623
CapTK2          ALDGLLDGKLKWRPIVLPDRYIDHGSPADQLAEAGLTPSHIAATVFNILGQTREALEVMT 719
                                :         . .       *.  . : .  .
```

Figure 6.3 Sequence comparison between 1 TK from mammalian and 1 TK from prokaryote sources as outliers and plant TK's shows the level of conservation between plant TK's and mammalian/ prokaryote is low. The TdP binding motif, which is shaded in green (plant), and purple (other) and TK motif, which is shaded in blue and labelled as transketolsae motif, both remain conserved (Schenk *et al.*, 1997). Several regions of conservation exist between *E. coli* TK and plant TKs, which are highlighted in yellow

Amplification of VvTKI

A 2190 bp PCR fragment was cloned from berry tissue and sequence analysis revealed minimal difference (3 amino acids) between the clone and the sequenced gene isolated from the grape (99 % identity at the nucleotide level). Internal primers encoding approximately 831 bp of the ORF were amplified from another grapevine, which makes significant amounts of TA, *Parthenocissus tricuspifolia* (data not shown). This gene was also successfully amplified from *Ampelopsis aconitifolia, A. brevipedunculata, V. californica* as well as *V. vnifera* (data not shown).

Bacterial over-expression, HIS TAG purification and analysis of the recombinant protein

Recombinant transketolase protein was recovered in the soluble fraction prepared from *E. coli* expression vector cell extract via HIS TAG purification (Figure 6.4). An induction temperature of 28 °C was required to make substantial amounts of soluble protein; at 37 °C the level of expression was insufficient for enzymatic assays. An induction temperature of 28 °C was more time consuming but yielded greater protein contents (0.005 at 37 °C versus 0.04 mg/mL at 28 °C). To check that the HIS-TAG bound protein was the protein identified on the Coomassie gel, monoclonal

western blot to the HIS-TAG was used to show that the correct protein had been purified (data not shown). The TK isolated from the grape encoded a ca 74 kDa protein.

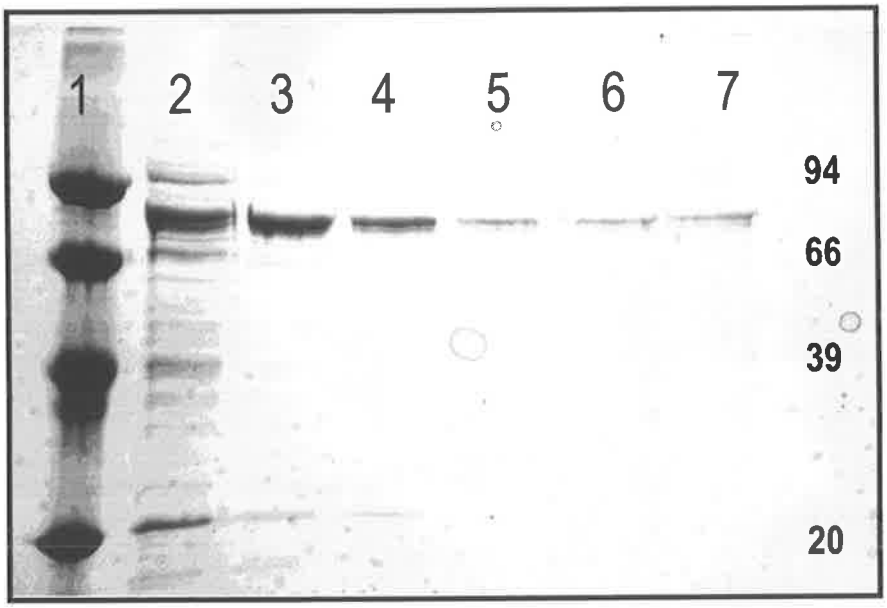

Figure 6.4 Coomassie gel analysis of purified TK from *E. coli* extract reveals an approx. 74 kDa protein encoded by the VvTKI with gel lanes 2-7 containing the elution fractions from HIS TAG purification and lane 1 containing a molecular weight ladder and the corresponding molecular weight values indicated on the right (kDa).

Quantitative real time PCR analysis of VvTKI and VvTKII expression during berry development

To further assess the expression pattern of grapevine transketolase genes, real time PCR analysis was used to examine levels of TK transcription for both isoforms during berry development and to compare these data with known the profile of TA biosynthesis. Real time PCR data was gathered using RNA samples prepared every two weeks during berry development. Results showed that of the two paralogs that appear in the grapevine genome and display an overlapping expression pattern during the grape berry development (Figure 6.5). One TK is expressed predominantly pre veraison, from 2 weeks post flowering until 6 weeks post flowering, after which is down-regulated (Figure 6.6) then the other TK is up-regulated which occurs veraison

to post veraison (Figure 6.5) approximately 8 to 16 weeks post flowering. Importantly, TA biosynthesis occurs pre veraison (see Chapter 3), in line with expression of VvTKI (Figure 6.6). A gap in transcription appears during the veraison period of berry development, around 7 to 8 weeks post flowering (Figure 6.5).

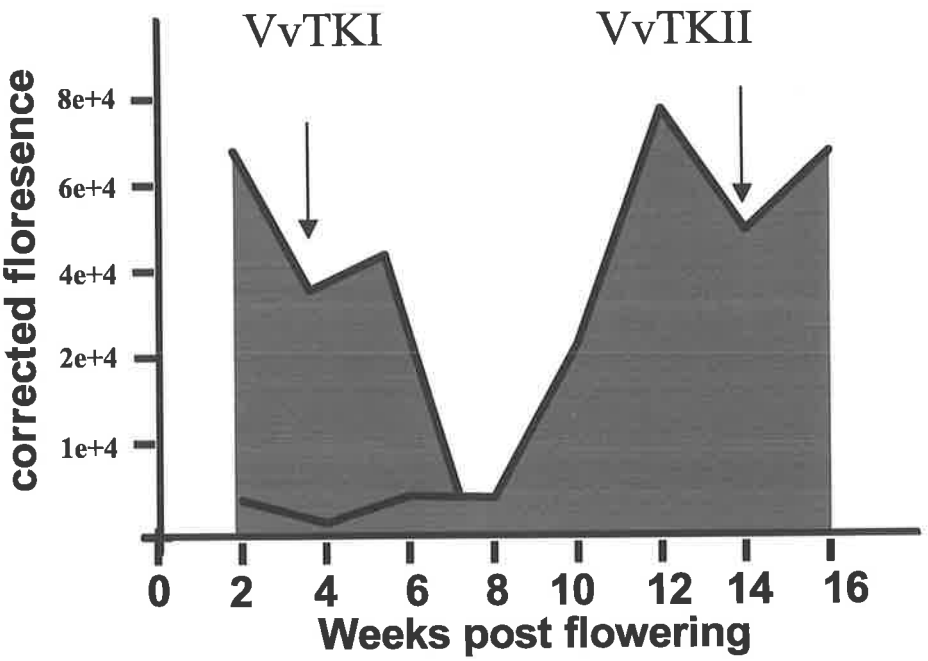

Figure 6.5 Real time PCR analysis shows overlapping expression patterns of the two grapevine transketolase paralogs VvTKI and VvTKII during berry development measured as relative corrected florescence every two weeks post flowering, real time PCR data was calculated as corrected florescence as compared to the expression of control genes ubiquitin in each template sample.

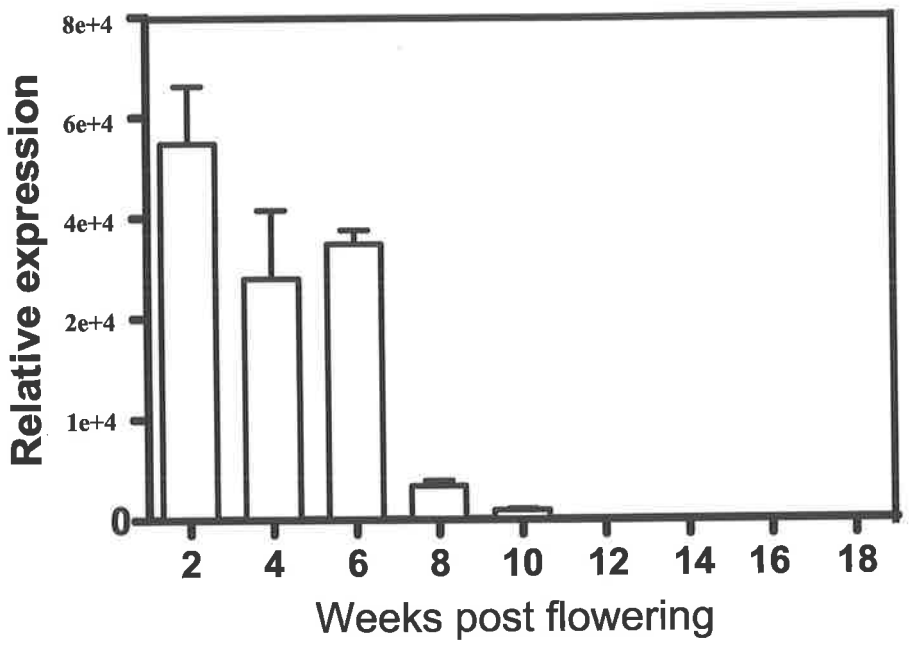

Figure 6.6 Real time expression pattern of VvTKI during berry development measured as relative corrected florescence every two weeks post flowering, real time PCR data was calculated as corrected florescence as compared to the expression of control genes ubiquitin in each template sample

Characterisation of the activity VvTKI in the OPPP and assessment of the involvement of VvTKI in converting 5-keto gluconic acid to tartaric acid, a key step in tartaric acid biosynthesis

Freezing and thawing of VvTKI was found to have a negative impact on protein activity therefore freshly prepared protein was used for all assays. Of the range of pH buffers tested, pH 7.5 was found to provide maximal activity. In order to test the activity of the soluble VvTKI protein, a coupled assay involving the conversion of common sugar intermediates involved in the OPPP was developed. By scrutinizing textbook reactions for transketolase and considering how 5-keto gluconic acid would most likely fit into the scheme, the result was a series of reactions finishing as a coupled reaction measurable as change in absorbance at 340 nm not unlike the reaction system for the OPPP (Equation 6.1 and 6.2). The somewhat

convoluted series of reactions are required as it is not possible to measure the formation of the actual 4 carbon breakdown product of 5-keto gluconic acid as the authentic compounds are not commercially available. Results showed that the recombinant VvTKI was able to complete one of its known reactions in OPPP (described in Equation 6.1; Figure 6.7). Activity was measured using a simple coupled reaction of dihydroxyacetone phosphate to glycerol 3-phosphate by the activity of glycerol 3-phosphate dehydrogenase in the presence of NAD^+, and showed clear reproducible enzymatic activity (Figure 6.7).

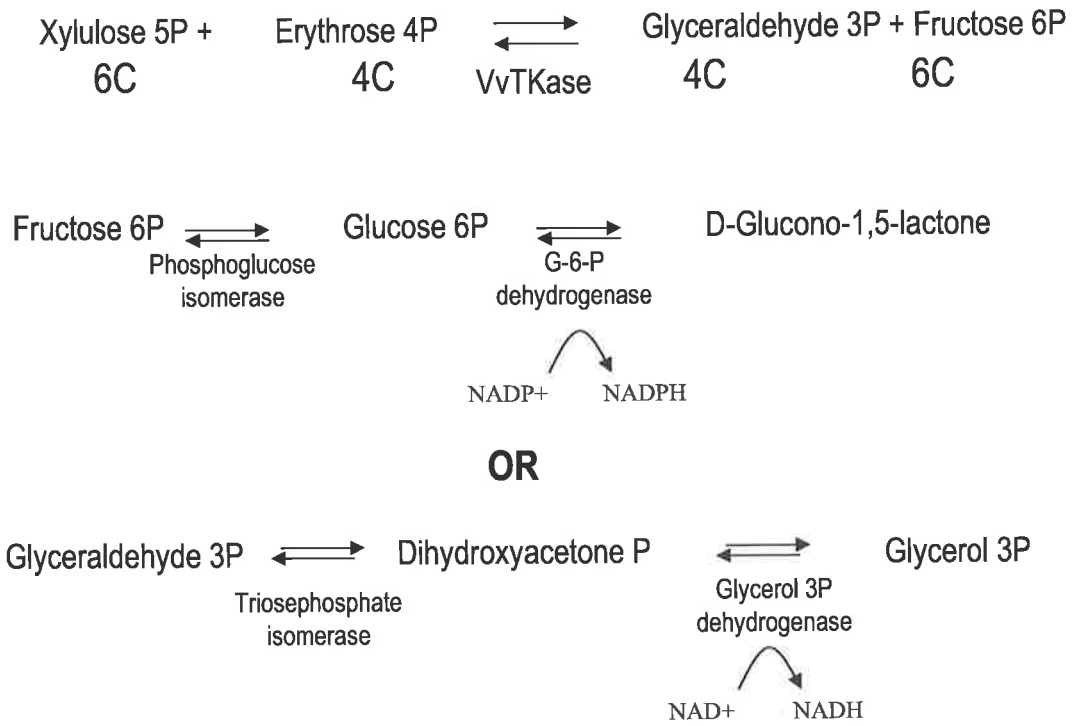

Equation 6.1 The substrates and enzymes involved in the OPPP; the reaction can be monitored using a simple coupled reaction in two ways, one to monitor the breakdown of fructose 6P or two to monitor the breakdown of glyceraldehyde 3P.

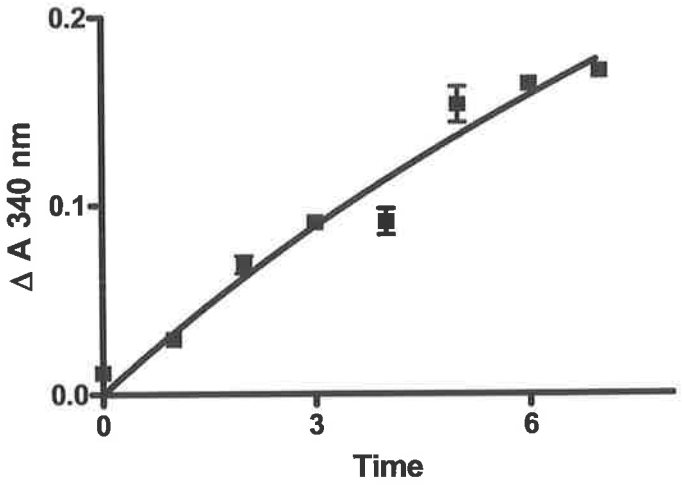

Figure 6.7 The activity of recombinant VvTKI with xylulose 5P and erythrose 4P as substrates measured as the conversion of dihydroxyacetone P to glycerol 3P by the activity of glycerol 3P dehydrogenase (assayed as change in absorbance at 340 nm with the conversion of NAD to NADH). Time is measured in minutes.

To test the ability of VvTKI to use 5-keto gluconic acid as a substrate, acceptor substrates were used in three combinations with 5-keto D-gluconic acid as the donor substrate, including ribulose-6-phosphate, erythrose-4-phosphate and xylulose-5-phosphate. Erythrose 4-phosphate was chosen as it was the only acceptor substrate whose use resulted in detectable enzymatic activity. The reaction was followed by measuring the activity of enzymes involved in the breakdown of fructose-6-phosphate. Phosphoglucose isomerase successfully converted to fructose-6-phosphate to glucose-6-phosphate (Figure 6.8A) and subsequently glucose-6-phosphate dehydrogenase converted glucose-6-phosphate to D-glucono-1,5-lactone (Figure 6.8B); the latter reaction requires $NADP^+$ and was monitored spectrophotometrically as the change at 340 nm.

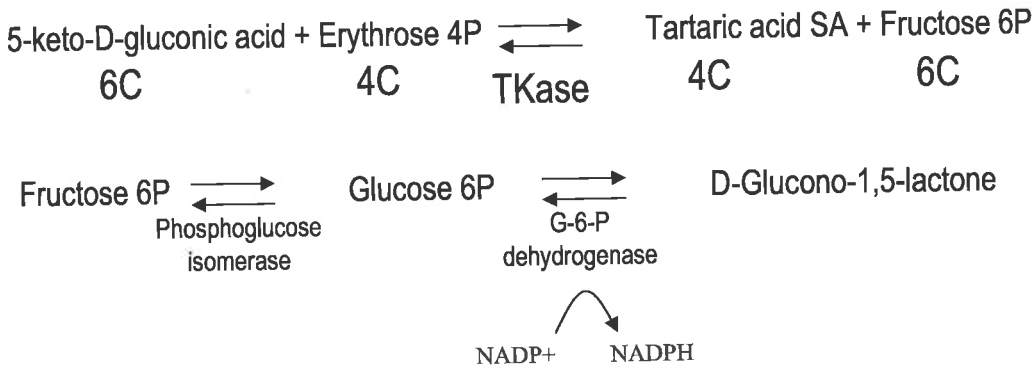

Equation 6.2 Shows the substrates and enzymes involved in the putative conversion of 5-keto gluconic acid; the reaction can be monitored using a simple coupled reaction by monitoring the catabolic breakdown of fructose 6P

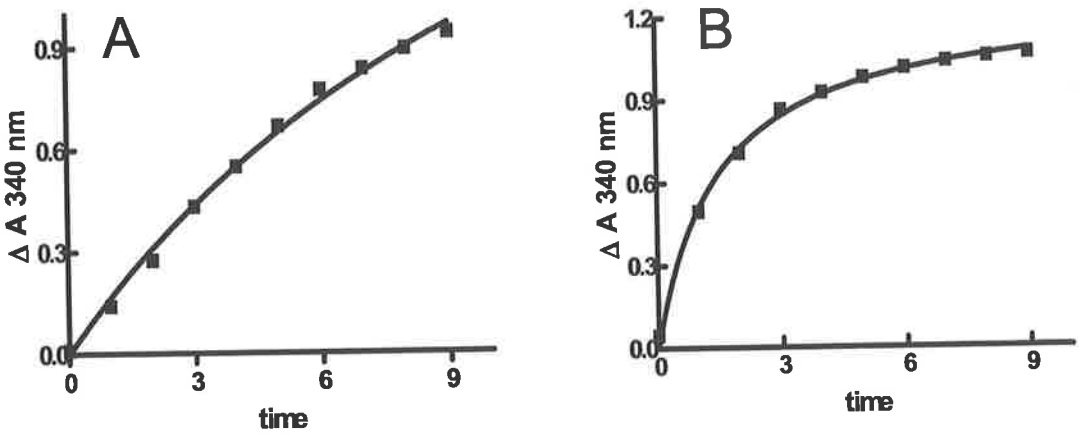

Figure 6.8 Coupled reactions that follow the activity of TK in Equation **6.2 A)** Measures the breakdown of fructose 6P to glucose 6P which is then converted to D-glucono-1,5-lactone and measured as change in absorbance at 340 nm and uses two enzymes, phosphoglucose isomerase, which converts fructose 6P to glucose 6P and then glucose 6P dehydrogenase converts glucose 6P to D-glucono-1,5-lactone. **B)** The activity of the latter reaction just involving the activity of glucose 6P dehydrogenase, which converts glucose 6P to D-glucono-1,5-lactone. Time in minutes.

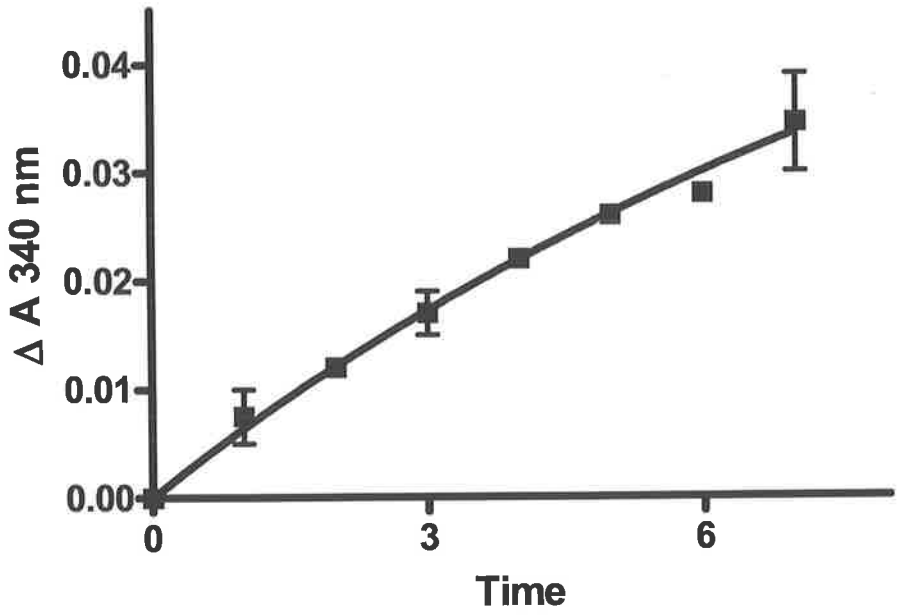

Figure 6.9 The activity of TK (equation 6.2) using 5-keto D-gluconic acid as a substrate by the measurement of the conversion of glucose 6P to D-glucono-1,5-lactone by the activity of glucose 6P dehydrogenase which occurs two steps down from the TK activity (see equation 6.2). Time in minutes.

6.3.2 Tartaric semi aldehyde dehydrogenase (TSAD)

Identification of putative tartaric semi aldehyde dehydrogenase as a likely candidate for the final step of tartaric acid biosynthesis

Contig 1028096 was identified as a key differentially expressed transcript in early berry development; this work was described fully in Chapter 3. Comparison of the conceptual translation product to database sequences indicated close similarity to succinic semialdehyde dehydrogenase, suggested earlier to be a candidate enzyme for the final step in TA biosynthesis. The amino acid sequence showed 99.4 % similarity to the domain architecture of the aldehyde dehydrogenase family of proteins, and 98.9 % similarity with NAD^+-dependant aldehyde dehydrogenase domains, both of which are key components of this class of enzymes (data not shown). The protein encoded

within contig 1028096 was given the provisional name tartaric semi aldehyde dehydrogenase (TSAD).

PCR amplification of and sequence analysis of TSAD

Putative TSAD expression was detailed in chapter 4. To recapitulate, it was expressed during pre veraison development in agreement with TA synthesis (chapter 5 and 7) and *in silico* analysis (chapter 3). Amplification was tested using *V. vinifera*, *V. californica* and *A. aconitifolia* templates and was achieved successfully therein. The resultant full length gene encoding the TSAD ORF was 1593 bp which was confirmed by gel band at approx 1600 bp (Figure 6.10). BLAST analysis revealed the two closest homologs to the grape TSAD gene were Arabidopsis succinic semi aldehyde dehydrogenase, which shared 78 % sequence identity and human succinic semi aldehyde dehydrogenase, which shared 57 % sequence identity. TSAD belongs to the aldehyde dehydrogenase family of proteins.

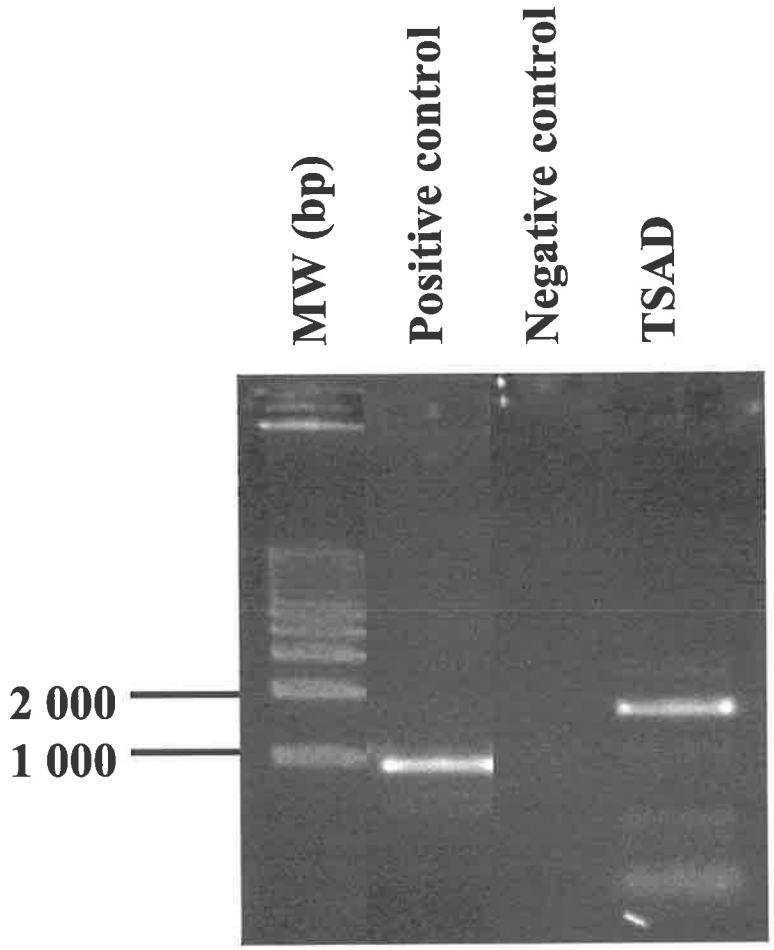

Figure 6.10 PCR amplification of TSAD (gel run by Carole Zimmerman)

Over-expression in prokaryote vector

Recombinant TSAD protein was recovered in the soluble fraction prepared from *E. coli* expression vector cell extract via HIS TAG purification (Figure 6.11). An induction temperature of 37 °C was required to make substantial amounts of soluble protein, yielding an estimated protein content of 0.01 mg/mL. Assessment of the molecular weight of TSAD by comparison with a molecular weight ladder revealed TK isolated from the grape encoded a ca 59 kDa protein (Figure 6.11).

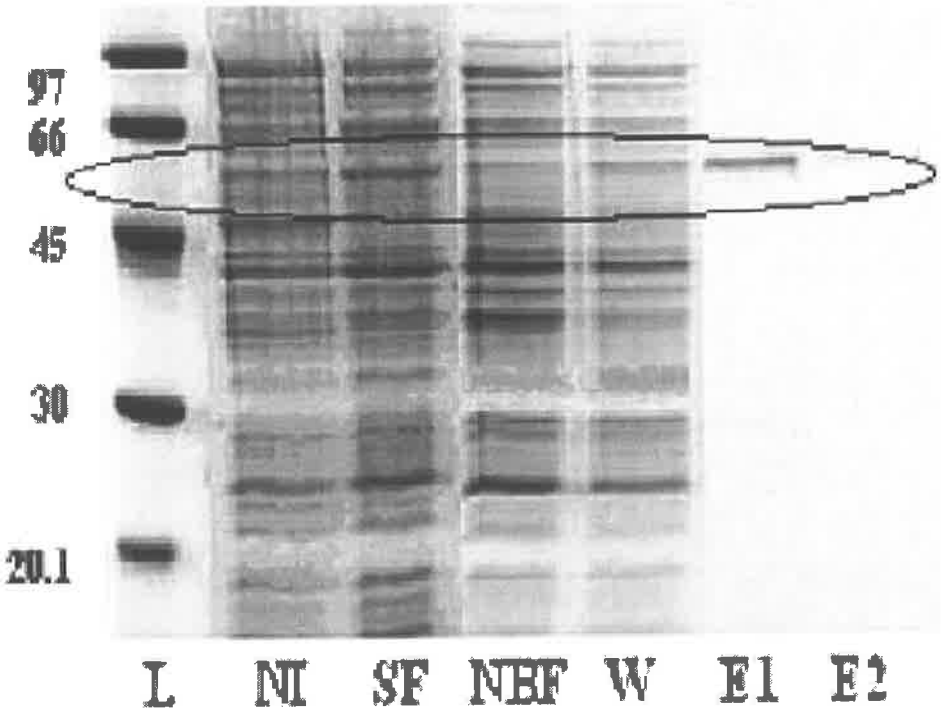

Figure 6.11 Protein gel showing purification of TSAD. (L) denotes molecular weight ladder, (NI) non induced control, (SF) soluble fraction, (NBF) non bound fractions, (W) wash fraction and (E1) is the initial HIS TAG purification elution and (E2) is the second elution fraction. The black outlined area indicates the region where the pure protein elutes

Testing the activity of TSAD in the tartaric acid biosynthetic pathway

Under no experimental conditions did TSAD catalyse the conversion of TA to TA semi aldehyde, nor the conversion of succinic acid to succinic acid semi aldehyde or succinic acid semi aldehyde to succinic acid in the presence of the required combination of cofactors (NAD^+ or NADH) (no data presented).

6.4 Discussion

Research within this chapter describes the cloning, sequence and biochemical analysis of two putative TA biosynthetic candidates. Chapter 5 described the characterisation of L-idonate dehydrogenase, the first enzyme in the direct pathway from AA to TA. However, enzymes and the genes that encode three other steps in TA biosynthesis remain unknown. To address this, two more gene candidates were explored for activity in the TA synthetic pathway. A transketolase homolog, VvTKI, was implicated as a candidate gene to convert 5-keto gluconic acid to TA semi aldehyde. The subsequent conversion of TA semi aldehyde to TA was postulated to be catalysed by a homolog to succinic acid semi aldehyde (TSAD), which led to the exploration of the enzymatic activity of a gene isolated by transcriptional profiling in chapter 3. The activity of TSAD could not be confirmed, perhaps due to an inactive recombinant protein or perhaps due to an alternative function. The activity of VvTKI was far more promising. The results for this protein are discussed in some detail below.

Sequence comparison showed that the full length 729 amino acid sequence encoding VvTKI was highly conserved with other known plant TK's (Flechner *et al.*, 1996, Mendel *et al.*, 1996, Bouvier *et al.*, 1998). VvTKI contained N terminus, central and C terminus transketolase domains (Lindqvist *et al.*, 1992, Nikkola *et al.*, 1994) as well as both the TdP-binding motif and the TK motif (Schenk *et al.*, 1997). Interestingly, the sequence from capsicum fruit, where two dedicated TK's were cloned (Bouvier *et al.*, 1998) being CapTK1 and CapTK2, only CapTK1 showed high sequence identity to the VvTKI and VvTKII sequences. CapTK2 was isolated and claimed to have dedicated activity for a key step in the nonmevalonic acid pathway (Bouvier *et al.*, 1998). Bernacchia *et al.* (1995) demonstrated 3 paralogs in *Craterostigma ssp.* and denoted that two were expressed under rehydration conditions and one was continuously expressed. Interestingly, Bouvier *et al.* (1998) showed that two transketolase enzymes found in capsicum fruits shared just 21.6 % identity at the amino acid level. With CapTKI (involved in the OPPP) sharing greater than 80 % identity with spinach and potato TKs. Both VvTKI and II shared high homology with spinach, Arabidopsis and CapTK1 TK's. CapTKI incidentally was shown to be highly active in the OPPP, its dedicated role as determined by enzymatic assays (Bouvier *et al.*, 1998). But, gene sequence homology does not denote function; homologs result

from divergent evolution (Gerlt and Babbit, 2000), in some cases a progenitor gene is duplicated and the new gene assumes new function. In this chapter the recombinant grapevine VvTKI cloned from stage 1 grape berries has also been shown to have activity in the OPPP (Figure 6.9) being able to use xylulose 5P and erythrose 4P as substrates to form glycoaldehyde 3P and fructose 6P. Just because a recombinant enzyme purified from bacteria was shown to perform a particular function, even with substantial sequence homology evidence (Figure 6.2), does not confirm its *in vivo* function. Therefore these results only provide evidence towards understanding the function of gene candidate VvTKI. Based on sequence comparison to other plant derived TK's and what is known of the characterised enzyme's catalytic function, it appears likely that due to the high sequence identity of VvTKI and VvTKII of 86 % at the amino acid level, they serve the same function, both being primarily involved in the OPPP. Yet, we can not rule out that even with the high homology small changes in amino acid sequence can create significant changes in catalytic activity (Broun *et al.*, 1997; also chapter 5 of this thesis). VvTKI and VvTKII have different expression patterns during berry development; assuming that the OPPP is utilised throughout berry development, these data suggest an example where a gene duplication event has created conditions of dual-functionalisation, in this case paralog genes of identical function with opposing expression patterns rather than deletion or new function in response to selection pressure of the additional gene copy. But moreover, quantitative rtPCR data may be suggested as offering another role for VvTKII, which has not been tested in these experiments.

In addition to sharing homology with the plant derived TK enzyme sequences, VvTKI shared high sequence identity with *E. coli* TK (Figure 6.4). The TK motif and TdP binding motif were highly conserved as was expected but the *E. coli* sequence displayed many regions of sequence conservation with the plant TK enzymes compared with a plant versus mammalian comparison (highlighted in yellow in figure 6.4). Regions of high conservation were particularly noteworthy in the N terminus region leading up to the TdP binding motif, which compared to mammalian TK and CapTK2 (involved in isoprenoid biosynthesis) was much more similar. A crude protein mixture isolated from a species of *Gluconobacter* was effectively able to use 5-keto gluconic acid as a substrate in what was considered to be a transketolase reaction (Salusjarvi *et al.*, 2004). These data provided a rational basis for testing a plant TK for further substrate specificity. Figure 6.9 demonstrates that indeed the

grapevine VvTKI was able, albeit at a low rate, to cleave 5-keto-gluconic acid to form TA. Although little is known about the biosynthetic pathway for TA biosynthesis, one cytosolic enzyme in the pathway (see Chapter 3, 5), and the intermediate compounds involved in the pathway has been determined (Saito and Kasai, 1984, Loewus, 1999 Debolt *et al.*, 2004). Here, results show that a recombinant TK isolated from TA synthesising grape tissue was able to use 5-keto gluconic acid and erythrose 4P as substrates forming TA semi aldehyde and fructose 6P, but at a very low rate of activity. How likely the donor and acceptor substrate are of interacting within the *in vivo* grape cell is not clear, but *in vitro* assays with recombinant protein suggest the catalytic activity is possible. Moreover results showed that while the catalytic activity was possible the activity of the TK was far more active in its dedicated role in the OPPP.

It is commonly considered that organic acids are synthesised in the cytosol before being transported to the vacuole (Terrier and Romieu, 2001). The recent report that in Arabidopsis transketolase (TK) enzymes may be present in the cytosol as well as plastids (Caillau and Quick, 2005) provides further support for their involvement in TA biosynthesis in the specific conversion of 5-keto gluconic acid to TA semi aldehyde. To this end, future work into understanding the subcellular localisation of VvTKI and VvTKII is needed. Not to mention looking for new TK genes, as further isoforms may exist, to date analysis of the grape transcriptome has only extended into approximately two thirds of expressed genes (Goes da Silva *et al.*, 2005, discussed in chapter 3) leaving much gene data wanting from transcriptional analysis. Against TK's being expressed in the cytosol, when two TK paralogs were cloned from capsicum fruits (Bouvier *et al.*, 1998), antibody analysis showed that they localised only in plastids, which is not supportive of TK's involvement in TA synthesis. The transketolase family of proteins have been postulated as forming the vital link between primary and secondary metabolism. Research presented in this chapter has extended the breadth of substrates and pathways that these multi facetted proteins may act within, suggesting a fascinating topic for future research. Primarily, as TA remains metabolically inert in the grape cell throughout development (Iland and Coombe, 1988), the other two carbons cleaved from the 5-keto gluconic acid compound (Saito and Kasai, 1984), under the activity of the TK would have a flux into primary metabolism.

Real time PCR analysis of VvTKI and VvTKII transcription using gene specific primers (methods and materials) during berry development showed an overlapping pattern of expression similar to that observed by Bouvier *et al.* (1998). In more detail, transcription of VvTKII was higher in post veraison fruit than VvTKI, which was specific to pre veraison (Figure 6.5). Whether these two genes encoding TK enzymes are serving the same function is not clear, but they do have highly conserved motifs and share over 86 % identity at the amino acid level. The two TK homologs isolated from capsicum fruit shared only 21.6 % identity (Bouvier *et al.*, 1998), these data were confirmed by very low level of homology to both VvTKI and VvTKII as well as other published sequences (Mendel *et al.*, 1996, Flechner *et al.*, 1996). In addition all sequences that shared strong sequence identity with VvTKI such as several plant TK and the *E. coli* TK have been shown to be active in the OPPP. Based on homolgy, it is likely that both VvTKI and VvTKII are encoding proteins with the potential to serve the same function. Providing an example of where gene duplication has provided two copies of the same gene that are transcriptionally distinct. In *Craterostigma plantagineum* three TK paralogs were found, one was ubiquitously expressed, where as the other two were expressed under rehydration conditions (Bernacchia *et al.*, 1995). Data for the three different species of plant compared in the present work show that TK enzymes have dedicated roles in plants, and have evolved independently at a genus and species levels as well as a plant family level. Only one of the two paralogs of grape transketolase identified in this chapter were over expressed for biochemical analysis because of experimental and time limitations, so although VvTKI was able to use 5-keto gluconic acid as a substrate to a small extent, VvTKII may yet prove to be more specific to 5-keto gluconic acid as a substrate.

In conclusion, data presented within this chapter describes further characterisation of candidate genes surveyed for TA biosynthetic activity. In addition to the two genes described here, a third enzyme, which had a lactone ring cleavage motif, was explored (candidate gene 1 in Chapter 4). It was anticipated that this protein may display enzymatic activity against ascorbic acid, due to the potential of this candidate gene to cleave the lactone ring to form 2-keto L gulonic acid, but this was not the cased. The expected size of this protein was small, approx 20 kDa, and despite substantial effort it was not possible to purify soluble recombinant protein. Characterisation of the other two proteins described here did lead to one active

protein, VvTKI. Exploration of VvTKI's catalytic capacity extends the donor substrate list for the plant tranketolase enzyme family to include 5-keto D-gluconic acid and clearly shows the role of VvTKI in the OPPP. The data does not however provide strong enough evidence to draw the conclusion that VvTKI is involved in TA biosynthesis *in vivo*. Furthermore, that the role of VvTKII may within the TA biosynthetic pathway remains unexplored. Sequence comparisons show that the grapevine paralogs described here are extremely similar in primary sequence, and have greater similarity to CapTKI, *Arabidopsis* and spinach chloroplast transketolases than to CapTKII, which suggests that both proteins are unlikely to be involved in isoprenoid biosynthesis. Tissue specificity and developmental expression data may hold the key to the true function of these enzymes and may yet support a role for one or both in TA biosynthesis.

Chapter 7

The impact of light interference on the accumulation of malic, ascorbic, tartaric and oxalic acids in *Vitis vinifera* reveals a link between light and tartaric acid synthesis

7.1 Introduction

In previous chapters of this thesis, the main focus has been to dissect the pathway for TA biosynthesis in grapes by radioisotope tracer studies (chapter 2), which led to the discovery that oxalic and tartaric acids are the metabolic breakdown products of ascorbic acid in *planta*, then isolate (chapters 3 and 4) and characterise genes and the enzymes they encode involved in tartaric acid biosynthesis (chapters 5 and 6). In the original research proposal, a further aim of this research was to understand the impact of various viticultural practices on organic acid synthesis. To this end, research described in this chapter investigated the impact of shading berry clusters to different degrees on the accumulation of various specific organic acids.

In Vitaceous plants, Loewus and Stafford (1958) showed that no direct conversion of ^{14}C-glucose to TA occurred. Saito and Kasai (1969) subsequently demonstrated than in the light, radioactivity was immediately found in tartaric acid after $^{14}CO_2$-fixation, whereas the same experiment, repeated in the dark, showed that radioactivity was detected in TA only after a delay of 480 min post $^{14}CO_2$-fixation. However, no Calvin-cycle intermediate was found to fulfil a principal role in TA biosynthesis, and neither were any TCA-cycle intermediates or primary sugars biosynthetically active (Saito and Kasai, 1968, 1969). Yet, further supporting the positive correlation between light and TA is the observation of maximal synthesis occurring in parts of the plant where high rates of photosynthesis and cell division are taking place, such as young leaves and young berries (Stafford, 1959, Kliewer 1965). The influence of light on TA synthesis may act not by increasing its rate of synthesis from existing precursor pools, but rather on the levels of its precursor, AA. Evidence to support this hypothesis comes from recent studies with *Arabidopsis thaliana*, where an increase in the AA pool size occurred when leaves were exposed to high light levels (Gatzek *et al.,* 2001). Conversely however, Kasahara *et al.* (2002) reported that when plants are exposed to higher light levels than required for photosynthesis, increased reactive oxygen species are generated in the chloroplasts, and chloroplast avoidance movement occurs to reduce the light intensity reaching chloroplast. In photosystem 1, peroxide is produced via the electron transfer from PSI to oxygen, forming superoxide which in turn leads to peroxide formation by the activity of

superoxide dismutase (Allen, 1977); this process has been correlated with a light dependant reduction of dehydroascorbate, a well characterised mop for reactive oxygen species (Anderson *et al.*, 1983). Moreover, Demmig *et al.* (1987) correlated the high-light inducible conversion between violaxanthin and zeaxanthin, and whose increase suggested as a mechanism for protecting PSII against high light. The Mehler Peroxidase reaction (MP) reaction, which acts as an electron acceptor in PSI (Mehler, 1951), whereby ascorbate peroxidase (APO) catalyses the conversion of peroxide to water, is followed by regeneration of ascorbate by the glutathione coupled DHA system, allows electron flow from PSII to PSI to proceed without net oxygen transfer (Neubauer and Yamamoto, 1992). Neubauer and Yamamoto (1992) present a model that intrinsically links the AA pool to photosynthesis and the impact of excess light. An idea worthwhile testing therefore is whether immature grape berries are vulnerable to high light conditions, and how the AA pool contributes to changes in TA synthesis. We already know that TA synthesis places a high demand on AA pools, reaching 10-15 mg. gm^{-1} berry weight (Iland and Coombe, 1988, Chapter 4), but fundamental answers tying TA in with phenotypic events are needed to understand the positive evolutionary effect of retaining TA biosynthesis and sequestration. As stated above, Chapter 2 described research into biomineralisation in the fleshy pericarp of berries of the grapevine *Vitis vinifera* cv. Cabernet Sauvignon. The needle-shaped raphide crystals, often suggested to be composed of TA salts in *V. vinifera*, were shown by X-ray diffraction and transmission electron microscopy, to in fact be calcium oxalate, in common with raphides from many other plant species. Raphides are commonly encountered as crystalline bundles in specialised cells called idioblasts that develop from mesophyll cells in oxalate-accumulating plants. Grapevines are not commonly thought to accumulate oxalate (OxA), and it was only when the profile of organic acids was examined following extraction under acidic conditions in which any crystalline deposits would be dissolved, that OxA was detected. This raised the intriguing conclusion that within the grape berry, AA was capable of serving as the biosynthetic precursor for both TA and OxA, via distinct pathways, a fate not previously seen in other plants. In this study, a further aim was to measure AA levels, and under acidic conditions measure OxA and TA concentrations to test the catabolic flux from precursor to product over development and under conditions of light interference.

Differences in acid metabolism attributed to the individual effects of light intensity and temperature are somewhat unclear, not only because sunlight is ultimately a combination of both visible and infrared radiation, but also because a lack of research has occurred in this field. MA is expected to decrease with increased light due to increased respiratory and metabolic pressures, for instance, under continuous warm conditions total acid synthesis in the pre veraison berry was reported to decrease (Buttrose *et al.*, 1971) and up to an 81 % loss of MA occurs post veraison (Iland and Coombe, 1988). During pre veraison berry development biosynthesis of MA far outweighs any MA metabolism (Iland and Coombe, 1988), whereas MA utilization is increased with respect to little or no biosynthesis post veraison, which results in a massive reduction in cellular MA concentrations, particularly at temperatures above 30°C (Ruffner and Hale, 1976). But is this change in MA consumption at elevated temperatures a localised event or a whole plant response? The role of MA in the TCA cycle as a metabolic intermediate in cellular respiration means that direct influence of increased temperatures on respiration is positively correlated with MA utilisation, yet other flanking intermediates, fumarate and oxaloacetate are not accumulated in the grape berry cell (Ruffner, 1982). In experiments from the 1960's, it was observed that leaves fed with $^{14}CO_2$ under different temperature and light intensity regimes led change in incorporation of the radiolabel in grape berry organic acids, differences were mainly attributed to MA (Kleiwer, 1964, Kleiwer and Shultz, 1964). Yet understanding the mechanism of MA consumption at a fundamental level is only now being unravelled (Famiani *et al.*, 2000, Famiani *et al.*, 2005).

Research described in this chapter demonstrates the impact of four different treatment effects on the accumulation of AA, TA, MA and OxA in the grape berry over a developmental season. The treatments were box enclosed (BT), shaded (ST), moderately exposed bunches (MET) and highly sun exposed bunches (HET). These data present the first measurements of berry OxA and AA concentrations over development and treatment effects, and suggest that shading and box treatments cause a stress response and large accumulation of OxA late in berry development. Light interference regimes had a significant impact on TA during pre veraison accumulation. MA re-metabolism was maximal under HET, consistent with previous research showing a suite of light induced enzymes associated with its *in vivo* metabolism.

7.2 Methods and materials

Chemicals

Refer to chapter 2 for a list of authentic chemicals

Location and description of experimental site

The vineyard site selected for this study was at Nuriootpa, in the Barossa Valley district of South Australia, approximately 80 km north-east of Adelaide. The climate of the region is described by Dry and Smart (1988) as warm with mean January temperature (MJT) in the range from 21.0 to 22.9°C (Gladstones, 1997). Rainfall is moderate (506 mm) with high summer evaporation and low relative humidity. The soil of the site is classified as a light pass fine sandy loam (Northcote, 1988).

The vines used in the experiment were Shiraz, clone BVRC 12. The trellis system was a single-wire system, cordon trained and spur pruned. Row and vine spacing were 3.0 m and 2.25 m respectively, with the rows orientated in an east-west direction. Vineyard management practices were similar to district practices. All treated vines received irrigation of 1 ML/ha from the same main with fixed sprinklers. The irrigation was twice higher than the district average, but this level of irrigation was necessary to produce vigorous shoot growth which could be manipulated to obtain various degrees of sunlight intensity at the bunch zone. There was no Botrytis or powdery mildew infection of the experimental vines.

Viticultural treatments and experimental design

The experimental design was a product of work by Renata Ristic and Patrick Iland (Ristic, 2004) and consisted of three main treatments which altered bunch exposure to sunlight to achieve shaded bunches, moderately exposed bunches and highly exposed bunches. The treatments were as follows:

- *Shaded treatment (ST).* The vine canopies were wrapped in bird nets to constrict the canopy and to create shaded conditions. Bird nets were positioned immediately after fruit set,
- *Moderately exposed treatment (MET).* No canopy manipulation was undertaken to obtain moderate exposure of bunches to sunlight.
- *Highly exposed treatment (HET).* High posts (2.5m) were placed on the ends of panels with the addition of 3 rows of foliage wires, 50 cm apart. Vine canopies were divided and shoots were trained upwards and downwards. Vertical positioning of shoots, and when required leaf removal around bunches, were carried out periodically during the seasons.
- *Box treatment (BT).* In the 2000/2001 season an additional treatment (box treatment) was applied on vines of HET. Bunches in a zone of highly exposed bunches were enclosed in boxes designed by Mark Downey, The University of Adelaide. The boxes were made from white polypropylene sheeting (0.6mm) painted black on the inside. They were approximately 250 mm in length and 120 mm deep with the front of the box 150 mm wide and the back 210 mm wide. The boxes were designed to eliminate sunlight (>99.5% of ambient) while allowing air-flow around bunches, without creating any temperature difference between bunches inside the boxes and those in the canopy (Downey *et al.*, 2004). Bunches were enclosed in boxes after fruit set, on 24th November 2000.

The treatments were arranged in a randomised block design along one row of vines. There were eight replicates of each treatment, each replicate consisting of a panel of 3 vines. The experiment was conducted in the 2000/2001 season.

Sampling procedure

Samples were collected at regular intervals during berry development starting when berries were pepper-corn size (approximately 3-4 mm in diameter), corresponding to Eichorn and Lorenz (E-L) growth stage 29 (Coombe, 1995) and finishing when berries reached a maturity of 26-27 °Brix, corresponding to E-L growth stage 38. In the season 2000/2001 sampling commenced earlier, on 12th of December 2000 (28 DAF) and finished on 4th of March 2001 (110 DAF). On each

sampling date three randomly selected bunches from each replicate of ST, MET and HET and one bunch from each replicate of the BT treatment were collected. For each treatment replicate all the berries from bunches were combined and then randomly divided into three sub-samples of 50, 30 and 30 berries.

Degree of sunlight intensity at the bunch zone

Sunlight intensity at the bunch zone was determined on a cloudless day between 12 noon and 1 pm using a ceptometer (Decagon Devices, Cambridge, England). Approximately four weeks before harvest readings were made at the fruit zone on both sides of the each vine with the ceptometer positioned parallel to the cordon and pointed upwards. Ambient measures were taken by positioning the ceptometer at the bunch zone height outside the canopy.

Berry sample preparation

Measurements described below were made by Dr. Renata Ristic. Juice total soluble solids (TSS expressed as °Brix) and pH were measured on the juice, obtained by crushing a sub-sample of 50 fresh berries, using a refractometer and a pH meter respectively. Five mL of centrifuged juice was diluted in 20 mL of distilled water, frozen and later, after thawing, titratable acidity (TA) was determined by an automatic compact titrator (Crison, Version III, Spain). TA was expressed as g/L of TA.

HPLC analysis

All HPLC extraction protocols were as described in chapter 2 and the subsequent publication (DeBolt *et al.*, 2004). All extracts were analysed using an Alltech Prevail HPLC column; additionally, all samples except those with appreciable amounts of colour (harvested 17.01.01 and later) were analysed using a Phenomenex Rezex OA column (data not shown). This approach permitted discrimination of all organic acids present in the berries. Detection of the organic acids including oxalic, tartaric, and malic was by UV absorbance (210 nm) with a diode array detector to assess spectral data of elution products (data not shown). Organic acid quantitation

was achieved using standard curves obtained from authentic compounds (data not shown).

Analysis of ascorbic acid (AA) concentration in the grape

Endogenous AA could be determined only from freshly harvested berries. Therefore, since the analyses detailed here were performed using grapes harvested in 2001 and thereafter stored at -20C, a method was developed to allow quantitative determination of AA content of berries through measurement of its stable oxidation products. Oxidised AA was detected as a peak on the HPLC chromatogram, which absorbed maximally at 210 nm and eluted less than 20 seconds after the AA peak. We quantified the levels of AA by creating a correction factor between the two peaks by measuring AA levels in a series of dilutions of fresh berries that were spiked with known amounts of AA and used this measurement to quantify the AA content of frozen grapes throughout development. Measurements of AA were made as mg of AA per 100 of fresh berry weight, due to low concentrations of the metabolite in berries.

Real time PCR analysis of L-IdnDH transcript abundance in HET versus BT

Quantitative RT PCR was conducted using 10 µl of BioRad® real time PCR reagent, 1µl (500 ng.µl^{-1}) template cDNA, 8.4 µl dH_2O and , 0.6 µl (1.5 pmol) F/R primer. Internal primers were as follows: forwards primers 5'AAGTTTGCCTTGTGGGTTTG and reverse primer 5'AAGGCTTCCTCCACATCCTT. A standard curve for expression of L-IdnDH was formed from cloned and sequenced L-IdnDH used as template at a series of known log scale concentrations. Relative expression is based on a correction factor, which is a calculated based upon the expression of the ubiquitin control gene in all templates. Plant material used was gathered during pre veraison development (vis 4 weeks post flowering). Treatment effects for the dark treatments were as previously described for the BT and HET and the cDNA for experiments provided by Ms Nicole Cordon and Dr Simon Robinson (CSIRO Plant Industry, Australia).

7.3 Results

7.3.1 Degree of sunlight intensity at the bunch zone

The degree of sunlight intensity at the bunch zone significantly differed ($P<0.001$) between treatments. Measures of light intensity (PAR) at the bunch zone showed that the fruit of BT received less than 1 % of available light, ST received less than 5% of available light (<100 PPFD). The light intensity at the bunch zone was 10-40% of ambient (300-700 PPFD) for MET and 40-80% of ambient (800-1500 PPFD) for HET.

7.3.2 Measurements of the impact of shading on tartaric acid accumulation

Assuming random heterogeneity, bunches samples across development under the four described treatments were assayed for TA concentration by HPLC. Chemical analysis showed a consistent negative correlation between TA biosynthesis and shade. BT was significantly lower in accumulation of TA than the sun exposed treatment throughout the berries' development. Greatest differences in TA accumulation were seen between the BT and HET. Observed changes began in the initial stages of berry development and remained throughout development (Table 7.2, Figure 7.1). It appears that TA concentration is variable due to berry size during development, for example BT has 15 $mg.gram^{-1}$ FW present 59 DAF and approximately 10 $mg.gram^{-1}$ FW measured at 65-75 DAF. Similar to observations for BT bunches; the ST displayed a marked reduction in TA accumulation at 65-75 DAF and 100 DAF (Figure 7.1) suggestive of a concentration effect.

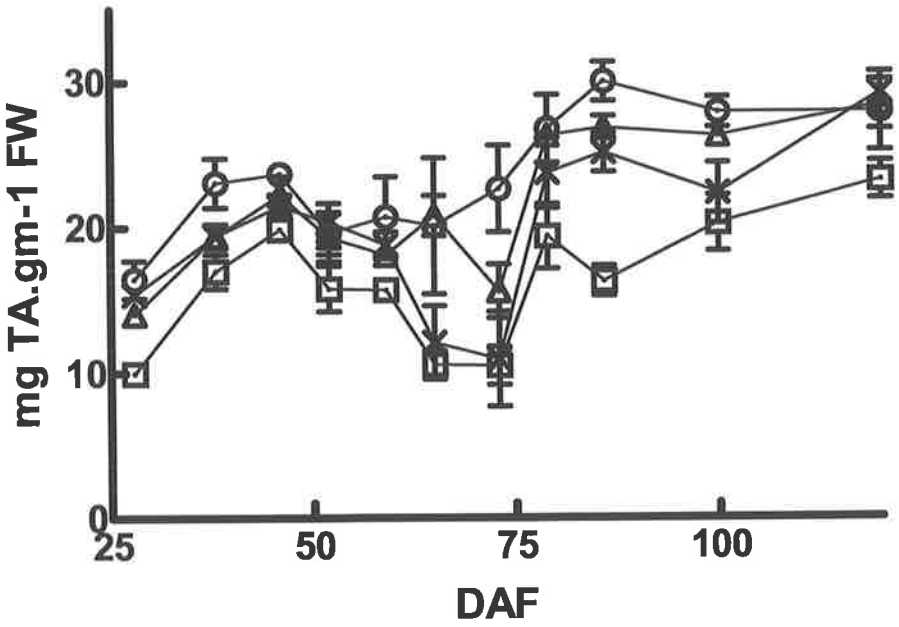

Figure 7.1 Tartaric acid accumulation over berry development compared between four treatments of light interference. (○) Open circle indicates HET, (Δ) open arrow pointing upwards indicates MET, (x) indicates ST and (□) open box indicates BT.

7.3.3 Measurements of the influence of light on other organic acids

Malic acid

Initially (for the first 4-6 weeks) MA accumulation was unaffected by shading, (Figure 7.2): all treatments accumulated close to 20 mg.gram^{-1} FW by 40 DAF. MA accumulation was subsequently staggered between BT and ST compared to the HET and MET where biosynthesis and accumulation continued up to 60 DAF (Table 7.2,

Figure 7.2). The maximal amounts of MA accumulation in the BT and ST were 19.5 and 23.5 $mg.gram^{-1}$ compared with the MET and HET, where measurements showed 29.3 and 27.7 $mg.gram^{-1}$ respectively.

Measurements of MA concentration in the post veraison berries showed that MET and HET MA levels decreased from the values stated above to 7.68 and 6.41 $mg.gram^{-1}$ FW respectively. At ~120 DAF results showed that BT and ST recording 5-10 % greater MA concentrations that the HET fruit (Figure 7.2).

The rate of malate consumption was calculated as the slope of the curve of the post version dissimilation of malate (Table 7.1, Figure 7.3). Results showed that HET and MET treatments had substantial malate loss during the latter half of berry development (Figure 7.2, 7.3). Moreover, BT and ST treatments displayed very low rates of malate loss (Table 7.1). The slope of the curve for malate dissimilation in the BT was not significantly different to 0.

Table 7.1 Malate consumption rate during the latter stages of berry development among (59-120 DAF) the four treatments and the goodness of fit (r^2) to a linear regression

	BT	ST	MET	HET
Slope	-0.1534 ± 0.04833	-0.1867 ± 0.09882	-0.3958 ± 0.07907	-0.3867 ± 0.03200
r^2	0.6685	0.4165	0.8336	0.9669

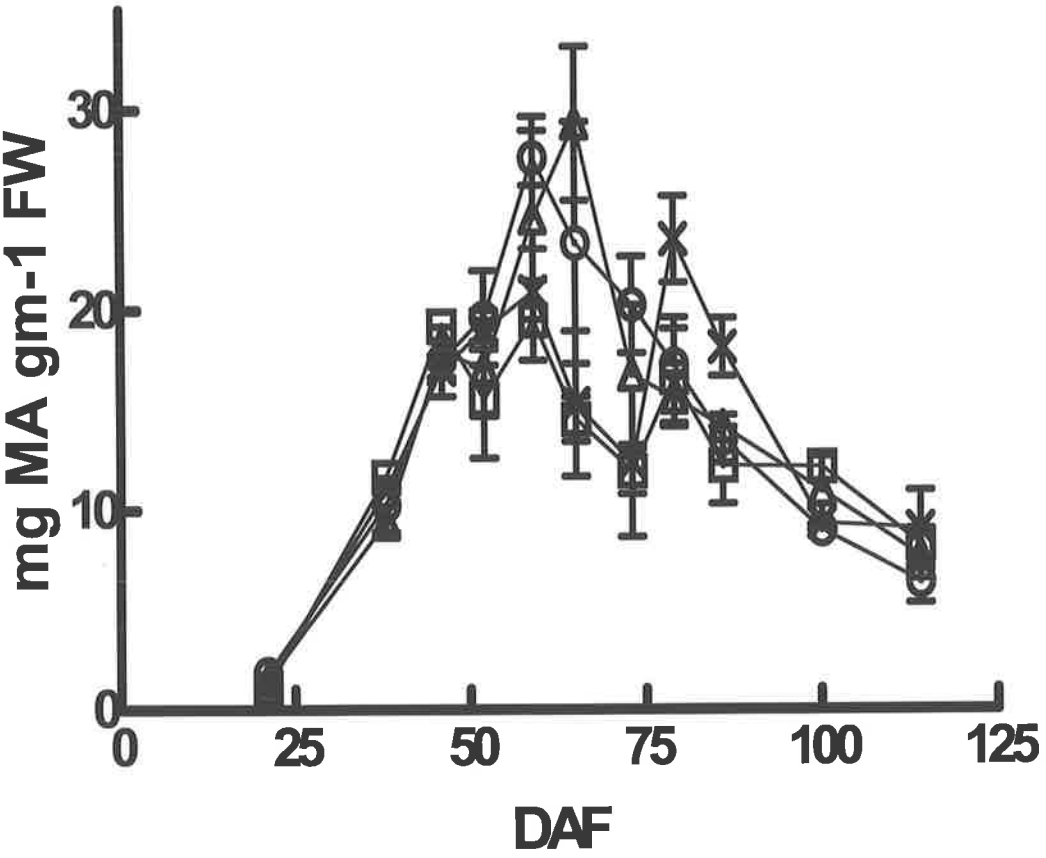

Figure 7.2 Malic acid accumulation during berry development compared between four treatments of light interference. (○) Open circle indicates HET, (Δ) open arrow pointing upwards indicates MET, (x) indicates ST and (□) open box indicates BT.

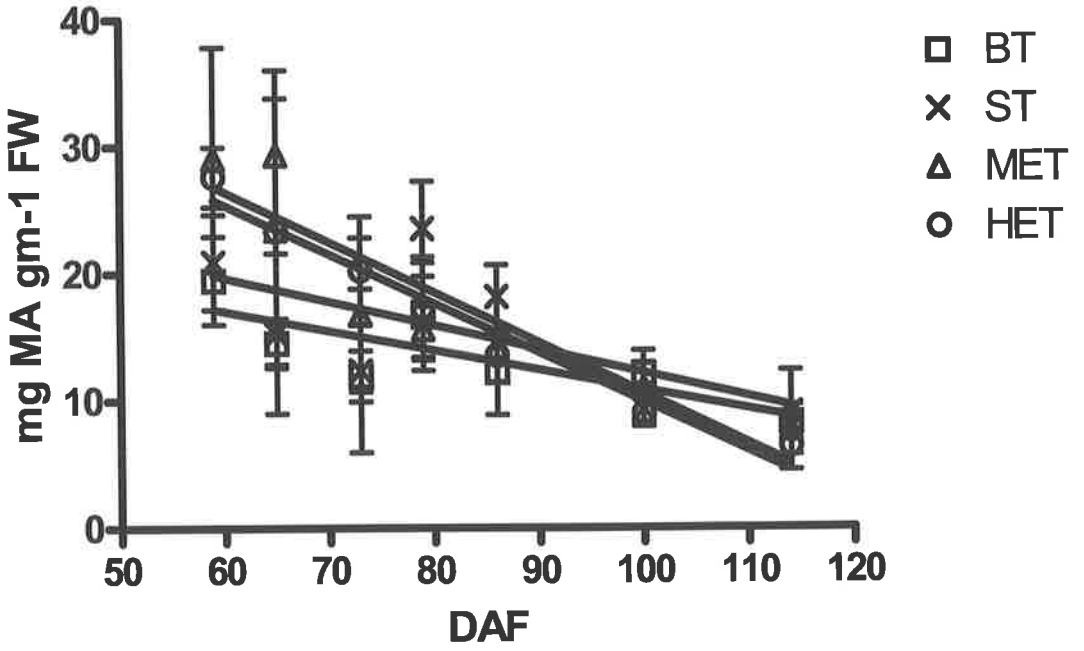

Figure 7.3 Rates of malic acid consumption in post veraison berry development under BT, ST, MET and HET fitted by linear regression (the slope of each curve is displayed in Table 7.2)

Oxalic acid

Oxalic acid (OxA) accumulation in the developing grape was determined following extraction of berries under acidic conditions, and is a measurement of the oxalic acid sequestered in calcium oxalate crystals (DeBolt *et al.*, 2004). OxA occurred throughout development of the berry and appears to be present from the onset (Figure 7.4), and its biosynthesis appears therefore as a proportion of cells present. In the ST and BT fruit a second peak in OxA accumulation followed the pre veraison accumulation. The largest observed OxA concentrations were measured in the BT and ST at time points 9, 10 and 11. A maximum of 3.5 ($mg.gram^{-1}$ FW) was measured in BT, which was more than double that in the HET and MET (1.4 $mg.gram^{-1}$ FW) (Figure 7.4). A peak in OxA accumulation was also present in the HET, although it occurred earlier, was less substantial and decreased thereafter. Apart

from this latter peak in accumulation the concentration of OxA in the berry remained around 1.5 (mg.gram^{-1} FW) (Table 7.2).

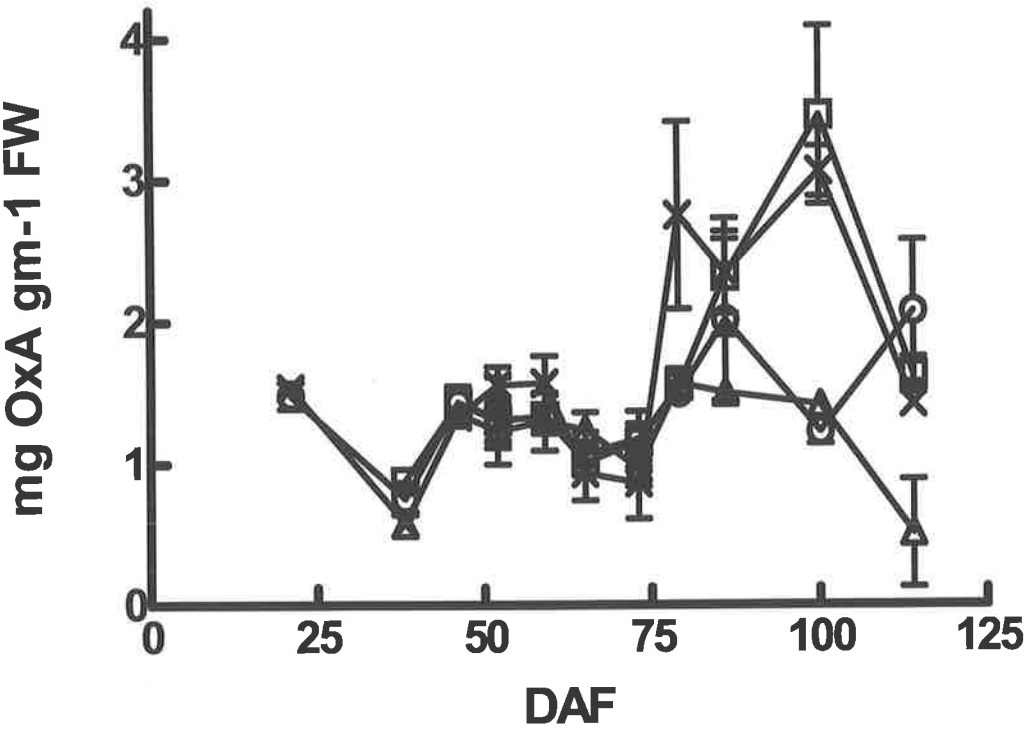

Figure 7.4 Oxalic accumulation over berry development compared between four treatments of light interference. (○) Open circle indicates HET, (Δ) open arrow pointing upwards indicates MET, (x) indicates ST and (□) open box indicates BT.

Ascorbic acid

Ascorbic acid (AA) was expressed as milligrams per 100 gram fresh weight of berries due to substantially lower per berry concentrations compared with TA and MA. Trends in AA accumulation during berry development show that much higher AA levels are present early in berry development. Results show that AA concentration decreased until 75 DAF, after which a small increase was observed

(Figure 7.5). There was a significant treatment effect on the concentration of AA throughout berry development. The greatest differences observed were in the MET, where no canopy manipulation was undertaken to obtain moderate exposure of bunches to sunlight, and BT. MET and HET displayed significantly greater ($P < 0.001$) concentrations of AA than those measured in BT and ST during the initial stages of development (0-50 days) (Figure 7.5), in line with the period of maximal TA synthesis (Figure 7.1). BT remained the lowest accumulator of AA throughout development. Light interference appears to have an impact on the re-metabolism of AA late in berry development, as where HET and MET are decreasing in concentration, BT and ST remain at similar concentrations in the last three time points.

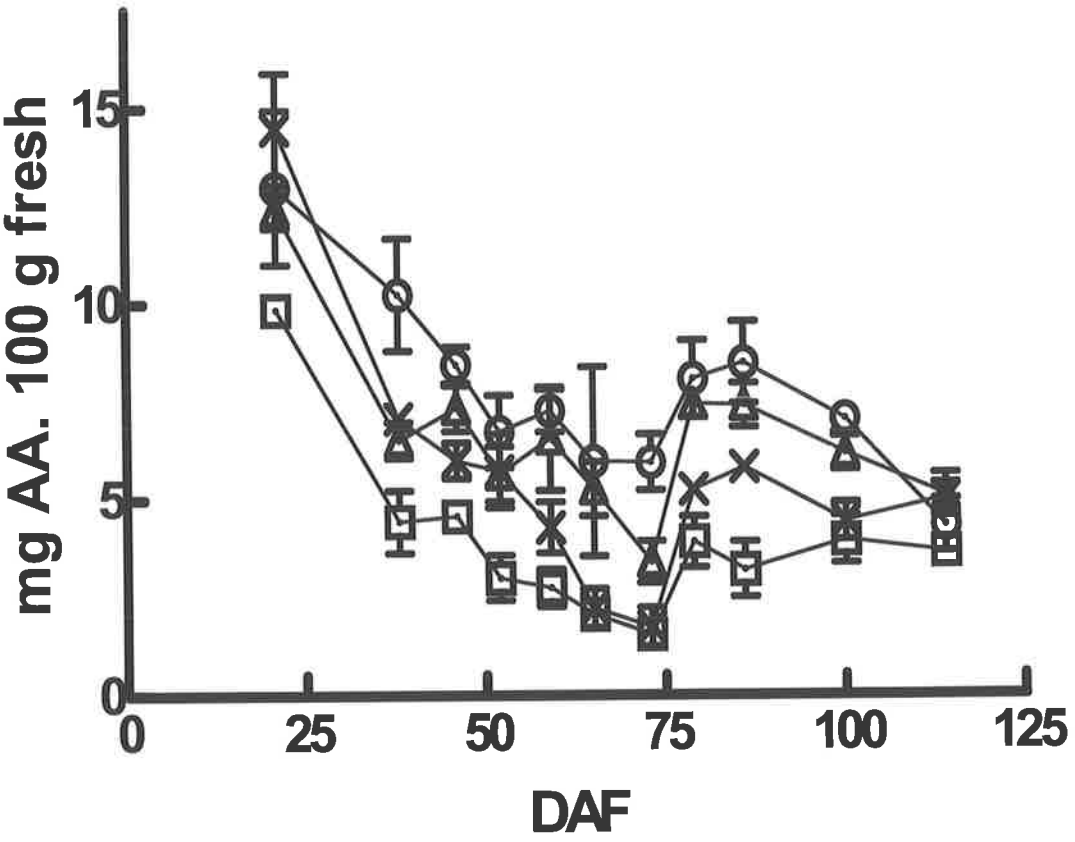

Figure 7.5 Ascorbic acid accumulation during berry development compared between four treatments of light interference. (○) Open circle indicates HET, (Δ) open arrow pointing upwards indicates MET, (x) indicates ST and (□) open box indicates BT error bars indicate standard error from the mean.

Table 7.2. Mean and standard deviation measurement for ascorbic acid and its breakdown products tartaric acid and oxalic acid during berry development under four treatments of light interference

Ascorbic acid

DPF	BT		ST		MET		HET	
	Mean	StDev	Mean	StDev	Mean	StDev	Mean	StDev
0	0.00	0.00	0.00	0.00	0.00	0.00	0.00	0.00
21	9.85	0.58	14.47	2.48	12.39	0.00	12.98	3.43
38	4.44	1.37	7.06	0.19	6.52	0.80	10.23	2.49
46	4.57	0.51	5.99	0.80	7.33	1.01	8.44	0.80
52	3.00	1.00	5.73	1.63	5.65	1.21	6.73	1.60
59	2.74	0.82	4.29	1.13	6.55	2.28	7.27	0.94
65	2.06	0.61	2.22	0.85	5.27	1.20	5.97	4.18
73	1.56	0.18	1.74	0.85	3.40	0.92	5.95	1.24
79	3.91	1.13	5.24	0.57	7.44	0.38	8.07	1.69
86	3.21	1.22	5.81	0.22	7.39	0.97	8.49	1.80
100	3.96	1.05	4.44	0.82	6.17	0.75	7.05	0.60
114	3.65	0.29	5.02	0.67	5.10	0.95	4.32	1.17

Tartaric acid

DPF	BT		ST		MET		HET	
	Mean	StDev	Mean	StDev	Mean	StDev	Mean	StDev
0	0.00	0.00	0.00	0.00	0.00	0.00	0.00	0.00
21	9.97	1.05	15.40	0.66	14.00	0.00	16.44	2.23
38	16.98	2.05	19.41	0.58	19.39	1.43	23.06	2.93
46	19.85	0.63	21.46	1.38	22.20	2.23	23.66	0.10
52	15.77	2.70	20.35	2.27	19.29	2.85	19.58	2.53
59	15.68	1.05	18.75	1.60	18.06	0.11	20.69	4.80
65	10.55	1.67	12.07	4.35	20.78	2.35	20.07	8.08
73	10.49	2.28	10.93	5.62	15.60	3.19	22.63	5.17
79	19.37	3.88	23.73	4.17	26.29	0.78	26.75	4.04
86	16.30	1.79	25.14	2.37	26.85	1.36	30.02	2.32
100	20.26	3.33	22.33	3.60	26.27	1.02	27.90	1.81
114	23.20	2.21	29.18	1.64	28.40	2.94	27.93	4.71

Oxalic acid

DPF	BT		ST		MET		HET	
	Mean	StDev	Mean	StDev	Mean	StDev	Mean	StDev
0	0.00	0.00	0.00	0.00	0.00	0.00	0.00	0.00
21	0.00	0.00	1.53	0.08	0.00	0.00	1.48	0.16
38	0.88	0.07	0.58	0.04	0.57	0.06	0.75	0.20
46	1.43	0.01	1.34	0.13	1.35	0.09	1.43	0.21
52	1.30	0.53	1.56	0.22	1.23	0.22	1.32	0.27
59	1.34	0.12	1.57	0.34	1.30	0.35	1.32	0.06
65	1.01	0.14	0.93	0.33	1.24	0.21	1.07	0.27
73	1.15	0.23	0.86	0.43	0.96	0.22	1.17	0.34
79	1.54	0.15	2.75	1.14	1.56	0.18	1.50	0.06
86	2.32	0.72	2.35	0.50	1.50	0.08	2.01	0.99
100	3.46	1.09	3.06	0.31	1.42	0.09	1.23	0.15
114	1.63	0.22	1.42	0.09	0.51	0.66	2.08	0.87

Table 7.2 (continued) Malic acid measurements during berry development under the influence of four light interference treatments

Malic acid								
DPF	BT		ST		MET		HET	
	Mean	StDev	Mean	StDev	Mean	StDev	Mean	StDev
0	0.00	0.00	0.00	0.00	0.00	0.00	0.00	0.00
21	1.12	0.21	1.31	0.27	1.51	0.11	1.82	0.22
38	11.66	1.22	10.97	0.69	9.41	1.37	10.25	2.32
46	19.21	0.15	17.04	2.38	17.89	2.16	17.48	0.95
52	15.53	5.08	19.01	1.70	17.08	4.17	19.61	4.09
59	19.49	3.47	20.91	3.73	24.60	8.81	27.60	2.36
65	14.54	1.93	15.31	6.30	29.33	6.68	23.36	10.47
73	11.95	1.99	12.36	6.42	16.76	6.06	20.26	4.21
79	16.62	4.24	23.51	3.74	15.58	2.16	17.26	4.06
86	12.22	3.33	18.14	2.50	14.16	1.14	13.55	2.06
100	12.13	0.85	9.32	1.01	10.95	2.99	8.99	0.35
114	8.26	1.40	9.05	3.30	7.68	1.96	6.41	1.88

7.3.4 Real time PCR analysis of L-IdnDH transcript abundance in HET versus BT compared with biosynthesis of tartaric acid

Accumulation of TA was measured at 28 DAF (Figure 7.6A), showing a significantly greater concentration of TA in the HET than the BT. An internal amplicon of L-IdnDH was successfully cloned and sequenced, revealing 100% sequence identity to the corresponding region of full length L-IdnDH (Chapter 5). The levels of transcript amplifying L-IdnDH increased more than two fold under conditions of light compared to dark, from an average of $3.4*10^4$ to $8.7*10^4$ (Figure 7.6B) compared with amplification of the ubiquitin control gene under both treatments. Measurements of MA and oxalic acid at the same time point were not significantly different between BT and HET (Figure 7.6C).

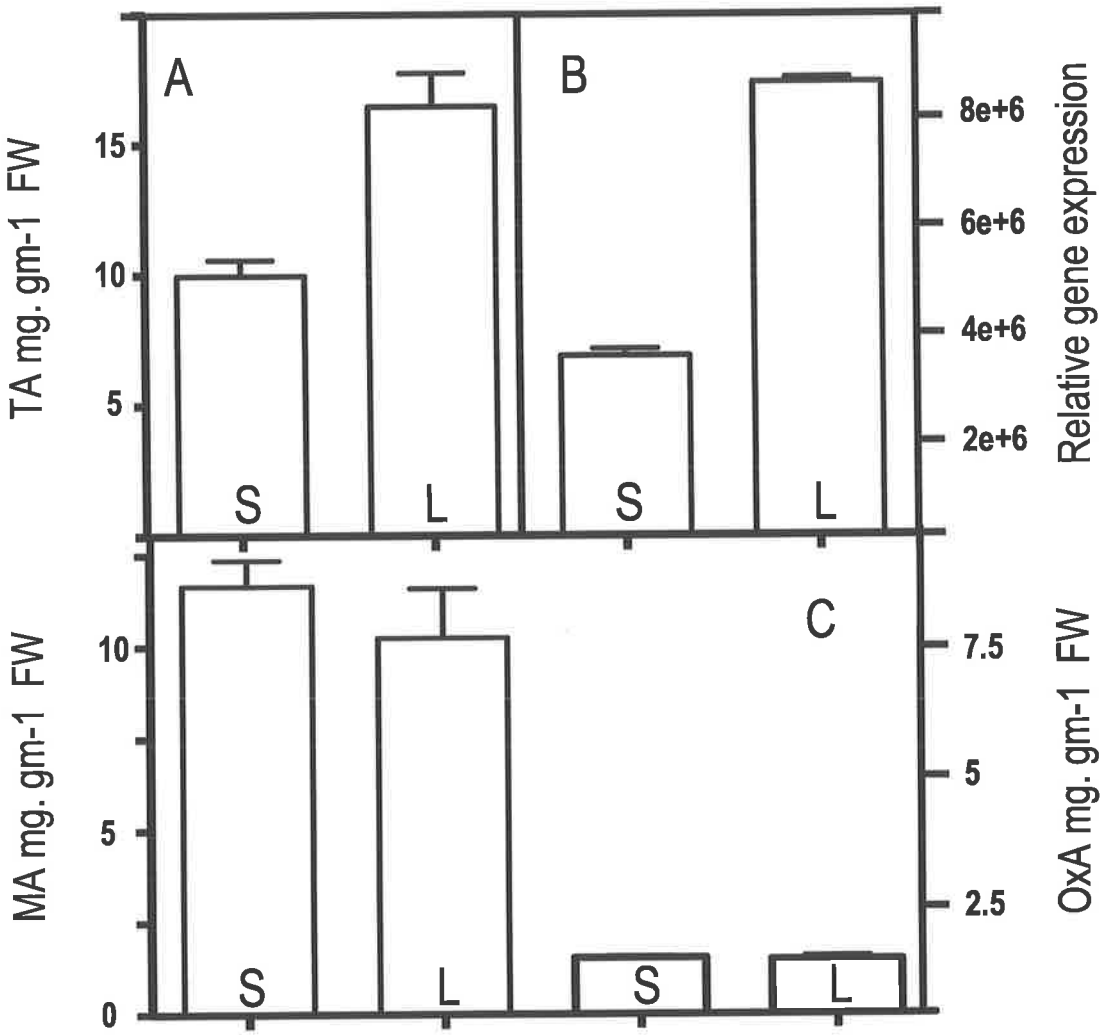

Figure 7.6 Changes in metabolite profile and L-IdnDH transcript abundance at the time of peak TA biosynthesis. S is shading treatment (ST) and L is fully light exposed treatment (HET): A) organic acid levels, B) L-IdnDH transcript levels and C) levels of malate and oxalate, at 4 weeks post flowering (28 DAF)

Discussion

Experiments described in this chapter aimed to assess the impact of various light regimes on the accumulation of specific organic acids during development of the grape berry (*V. vinifera* L cv. Cabernet Sauvignon). *V. vinifera* is arguably the best system for such analysis, relative to other grape genus *Ampelopsis* spp, or *Parthenocissus* spp, for example because a strong background has already been established into the accumulation pattern of organic acids such as TA and MA in the berry skin and flesh (Iland and Coombe, 1988) the developmental pattern (Ruffner, 1982, Terrier and Romieu, 2001) and importantly because *V. vinifera* is the primary species used for table grape and wine grape production world wide (Pretorius *et al.*, 2001). Individual berry clusters were shaded from light. It is important to point out that these experiments were conducted with the intent of informing viticultural practices, where canopy management is used to modulate light penetration to individual clusters. The results are of relevance to the applied practice of viticulture, because they reveal a differential impact of light on specific organic acids, relative to others.

There was natural variation in metabolite measurements between time points due to the effect of change in berry composition and size, most likely due to cell expansion and water accumulation from rain or irrigation effects. TA displayed a pre veraison accumulation pattern, and berry levels consistent with many published reports (summerised by Ruffner, 1982, Iland and Coombe 1988, McCarthy and Coombe, 2000, Terrier and Romieu, 2001). Data for TA treatment effects revealed a consistent trend of increasing levels of TA with increasing exposure to light (Figure 7.1). At time point 100 DAF there was 9 % greater TA in the HET compared to MET and 20 % and 28 % less TA in the ST and BT respectively. But ~2 weeks laterat 120 DAF the amounts of TA in ST, MET, and HET were almost identical (Table 7.1), whereas the BT still displayed 20 % less TA than any other treatment. Decreases in TA accumulation 8-16 weeks post flowering were most pronounced in the BT and ST, suggesting that these treatments suffered the least amount of water loss during the latter stages of ripening. All ST demonstrated a significantly lower accumulation of TA than HET fruit during the initial exponential TA biosynthetic phase.

MA also accumulated in a defined pre veraison pattern, which occurred later in berry development (30-50 DAF) than the peak in TA synthesis (10-30 DAF) (Figure 7.1 7.2), in agreement with previously published reports (Ruffner, 1982, Iland and Coombe, 1988, Terrier and Romieu, 2001, Fernandez *et al.,* 2006). The accumulation pattern of MA displayed a lack of significant difference between treatments during the initial biosynthetic phase, suggesting that in fact treatments on the berry cluster itself have limited impact on cellular MA accumulation. Even in the BT, changes in MA levels between treatments were minimal compared with the changes seen in TA during the biosynthetic phase (Figure 7.6). In all treatments a decrease in MA concentration occurred in the post veraison (Figure 7.3) consistent with published reports (Iland and Coombe, 1988, Terrier and Romieu, 2001). Calculating the rate of dissimilation was achieved by measuring the slope of the curve between the maximal MA synthesis (~60 DAF) and final measurement at harvest ripeness (120 DAF)(Table 7.1). Although MA concentrations decreased in the BT, the slope of the curve was not significantly different to zero, showing very low levels of MA metabolism. By calculating ambient light reaching the fruit under MET (10-40 %) and HET (40-80 %), and assessing the rate of dissimilation, there is very little difference in metabolism of MA between HET and MET, suggesting that light activated enzymes responsible are induced under conditions upwards from 10-40 % ambient light as in MET. In conditions of less than 5 % ambient light, as seen in the ST and BT, there was a significant reduction in MA metabolism (Figure 7.3, Table 7.1). At 120 DAF, measurements showed that MA had fallen approximately 75 %, from a maximum of 29.3 max to 7.7 min ($mg.gram^{-1}$) and 27.7 max to 6.4 min ($mg.gram^{-1}$) in the MET and HET respectively. Whereas the ST and BT fell approx 50-60 % from 23.5 max to 9.1 min and 19.5 max to 8.5 min ($mg.gram^{-1}$) respectively (Table 7.2). Trends observed showed greater concentrations of MA in HET than ST and BT, but the rate of metabolism late in development was increased in the HET. At physiological ripeness (120 DPF) the BT had greater MA concentration than that measured in HET. Re-metabolism of MA is an important aspect of fruit ripening and physiology (Coombe 1976, Ruffner, 1982, Famiani *et al.*, 2000, Famiani *et al.*, 2005), yet its regulation is poorly understood. MA re-metabolism is linked with the TCA cycle and in turn cellular respiration, which is highly correlated with light and temperature. This suggests that the light source, which contains a combination of visible and infrared (heat) radiation, has an impact on temperature and potentially

metabolic enzymes responsible for malate re-metabolism. Ultimately, these data show that metabolism of malate is a localised response, with the effects of temperature and light on the foliar parts (as in ST the foliar parts of the vine and berry clusters were constricted and shaded) of the plant not impacting on MA re-utilisation in the berry. In earlier work, the rate of dissimilation of MA in the ripening grape berry has been quoted at 0.005 μmol min^{-1} g^{-1} FW (Ruffner, 1982, Walker and Chen, 2002), but clearly there is also a significant effect of light, as HET had 30 % less MA than the ST and BT late in berry development. Considering MA is consumed more readily in HET, it is still highly plausible that maximal acidity is achieved with maximal light due to maximal TA, because TA is a stronger acid than MA (pK1 2.98 versus 4.01). Juice pH data (Figure 7.7B) confirms these findings, with the HET displaying the lowest pH at harvest. Moreover, HET shows maximal TSS at harvest (Figure 7.7A), suggesting that quality attributes of the grape are highly correlated with light.

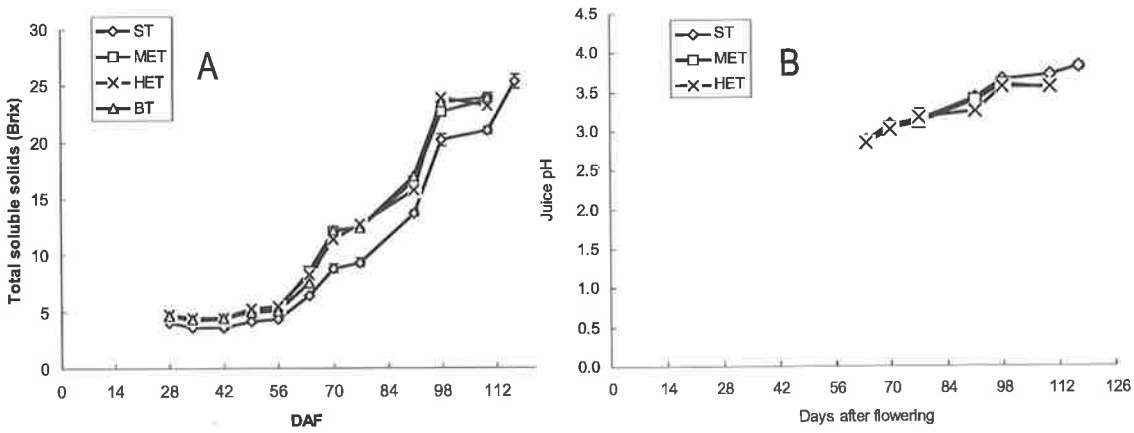

Figure 7.8 Juice pH measurements during berry development (A) and total soluble solids measurements from days 70 to 126 post flowering for all treatments accept BT (B)

Initial measurements of AA content at 28 DAF demonstrated that AA levels are highest in early berry development and steadily decrease thereafter. The present study shows that light plays a significant role in mediating gross cellular AA and TA concentrations in the pericarp of developing grape berries. To quantify the previous point, levels of light required to create a substantial impact on accumulation of these

metabolites lie between 5 and 10 % ambient light, the difference between MET and ST. These data present the first study of AA in grape berry development, and its flow through to its catabolic end products TA (Saito and Kasai, 1969) and OxA (DeBolt *et al.*, 2004). Gaztek *et al.* (2001) has proposed that cellular AA concentrations are increased in response to high light acclimation, due to an increased need for an antioxidant. Moreover, AA in plants has been linked to cell division, cell expansion, photosynthesis and many stress related responses (Smirnoff, 1996). Our data supports this thesis, that light leads to increased temperature and light mediated metabolic processes and the subsequent requirement for AA increases. Although, we have no data supporting whether increased AA is as a requirement for an antioxidant, signal compound, and/or stress related response, it is clear by the low concentration of AA seen in the BT treatment, that light alone has a localised impact on AA accumulation in the grape berry. In the grape, the fate of AA is linked to the accumulation of the main organic acid, TA (Saito and Kasai, 1968, 1969), and we see direct correlations with the effect of light interference and accumulation patterns of AA and TA. Under ST/MET/HET (all of which receive light) the initial AA pool size is bigger than BT (99 % of light blocked)(Figure 7.6). As TA biosynthesis occurs pre veraison, after which remaining biochemically inert in the cell (Iland and Coombe, 1988), it appears that a greater AA concentration provides a greater kinetic drive for TA synthesis under high light conditions. TA accumulates in much larger quantities than AA, Iland and Coombe, (1988) and Gebhardt and Thomas (2002) report levels of TA at 15 mg per gram fresh weight and 10 mg per 100 grams fresh weight respectively, consistent with the data we have presented. Differences between these reports and ours are considered to be seasonal and varietal differences. The differences in AA content in the leaves could be a consequence is variation in respiration, as has been shown in studies in high and low simulated temperatures (Fryer *et al.*, 1998, Flexas *et al.*, 1999).

Aims of this study were directed towards understanding the flux between AA and its degradation products, TA and OxA, which occur via different pathways in neighbouring cells in the grape berry (DeBolt *et al.*, 2004). OxA biosynthesis in plants has been of great interest for many years (summarized in a thorough review: Franceschi and Nakata, 2005), but levels in the grapevine have not previously been measured. Measurements of OxA concentrations across berry development have also been ignored, most likely due to its presence at very low concentrations, and because its detection is possible only under acidic conditions that promote solubilisation of

otherwise insoluble calcium oxalate crystalline forms (DeBolt *et al.*, 2004). Apart from the interest in quantifying OxA *in vivo*, the surprising observation that an accumulation suddenly peaked post veraison in the BT and ST was made. These data showed that almost double the amount of OxA in a four week period occurred (Figure 7.5). Moreover, it is possible that stressed vines produce increased levels of OxA (Mores-Flores, 2001). Two explanations at least for the peak in OxA seen in BT and ST may be proposed. First, increased calcium flux to the berry post veraison (a phenomenon previously measured and published by Rogiers *et al.*, 2001) results in an increased Ca^{2+} sequestration requirement, reflected in in a peak of OxA biosynthesis. To this end, thorough measurements on transport and calcium concentration in the ripening berry are needed, along with a detailed analysis of the regulation of OxA biosynthesis gene expression. Second, that the high degree of light interception imposed by the box treatment (BT) is perceived by the berry as a stress response, resulting in the increased biosynthesis of OxA and subsequent formation of calcium oxalate crystals. The role of calcium oxalate formation in response to stress has been widely reported (Franceschi and Nakata, 2005).

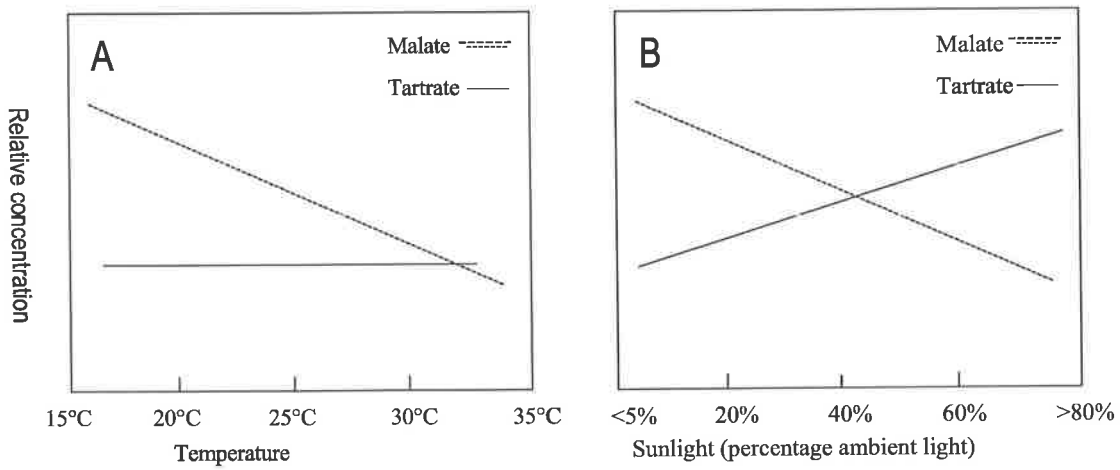

Figure 7.8 The impact of temperature (A) (Coombe, 1987) and light (B) (chapter 7) on malic and tartaric acid in grape berries of *Vitis vinifera*

Combining these data, a mechanism to maintain maximal berry acidity using cultural practices to allow maximal light into the canopy and onto grape bunches would, based on the conclusions of this chapter, allow for maximum TA synthesis, but at the compromise of maximum MA re-metabolism (7.8B), not to mention the effect of temperature on MA metabolism (Coombe, 1987, Figure 7.8A). These data are confirmed by juice pH and TSS data, which reveal that HET had the greatest level of TSS and the lowest juice pH (Figure 7.7). MA metabolism compared to the shaded treatments resulted in minimal difference in overall concentration suggesting that temperature (growing degree days) most likely has the greatest impact on levels at harvest. Therefore shading post veraison would allow for maximal MA synthesis and minimal MA degradation not impacting on TA synthesis. Light appears linked to the achieving maximal TA, which is of greatest benefit to warm climate viticultural and winemaking.

Chapter 8

Conclusions and Future Directions

Conclusions to the presented thesis titled "Tartaric acid biosynthesis in higher plants" will summarise the findings of the results and put into context their significance. As the title suggests, the research presented was towards furthering the understanding of how plants form TA, which is a vital additive to wine and many food processes. No substantial efforts had been made to further understand the TA pathway since Saito and co-workers made inroads between the late 1960's and late 1980's. Their choice of tools was radioisotope tracer studies, which provided strong data that the formation of TA laid outside the oxidative breakdown of primary sugars. In fact it was found, in a landmark paper, that TA was formed via the catabolism of ascorbic acid (AA, vitamin C) (Saito and Kasai, 1969). The pathway has for a long time troubled plant scientists, it offers the breakdown of AA, but it also lies as an inert acid, with no clear metabolic role *in planta*. Moreover, neither enzymes nor the genes that encode them are known for any step in TA biosynthesis. These series of unanswered questions made for a remarkably interesting topic for a PhD researcher. The grapevine is an ideal plant to study TA biosynthesis in because it accumulates up to 15 mg. g^{-1} FW in the berry (Iland and Coombe, 1988) and is a fruit crop of enormous economic value. The primary aims of the research were to confirm the pathway of TA biosynthesis and make inroads into discovering enzymes involved in the pathway. Moreover, due to working with the Cooperative Research Centre for Viticulture, a further aim was to attempt to provide viticulturalists with data towards optimising acids in the vinified product. The following chapter will summarise the successes, failures and future perspectives.

The first results chapter (2) described the identification of crystals in grape berries and crystallographic studies to determine their structure and biosynthetic origin. These were initially discovered (in this research) when attempting to isolate grape protoplasts, which were being pierced by crystal structures. Table 2.1 showed the level of discrepancy in published literature over the past 100 years, the crystals being described as several combinations of calcium, potassium, TA and oxalate. To this end, although good quality protoplasts were never isolated, the use of TEM and X-ray powder diffraction were employed to show definitively that the composition of crystals in the grape is calcium oxalate hydrate, and no evidence for any TA crystals was found. These data corrected a long-held misconception that TA crystals occur in the grape berry mesocarp. Saito and Kasai discovered that in the grape berry, 1-^{14}C-

AA was cleaved at the C4/5 bond to yield carboxyl-labelled TA. Subsequently, another TA accumulator, *Pelargonium crispum* was tested with 1-^{14}C-AA or 6-^{14}C-AA. Here, radio labelled TA arose from cleavage of 6-^{14}C-AA but not 1-^{14}C-AA, suggesting that the carbon chain of AA was cleaved between positions 2 and 3. The first two carbons of 1-^{14}C-AA yielded 1-^{14}C oxalic acid. Chapter two went on to wed these disparate findings through a series of radioisotope tracer studies. Grapevines are not commonly thought to accumulate oxalate, and it was only when the profile of organic acids was examined under acidic conditions in which any crystalline deposits would be dissolved, that oxalate was detected. This raised the intriguing possibility that within the grape berry, AA was capable of serving as the biosynthetic precursor for both TA and oxalic acids, via distinct pathways, a fate not previously seen in other plants. This possibility was addressed by feeding intact bunches of immature grapes with L-[1-^{14}C]AA and examining the profile of organic acids following extraction under acidic conditions. Radiolabel was seen in both oxalic acid and TA, indicating for the first time that AA is cleaved in two distinct patterns within developing grape berries.

Aided by modern molecular tools, and a recent surge of EST data injected into grape research due to the combined efforts of the members of the International Grape Genome Project, the next stage in the research attempted to identify genes involved in TA synthesis. Preliminary biochemical investigations to identify TA-biosynthetic specific enzyme activity in soluble protein extracts prepared from immature grape berries were unsuccessful. It is suggested that despite the use of extraction buffer systems designed to maximise the recovery of enzymatic activity from these tissues (Ford and Høj, 1998), the combination of high organic acid and high phenolic conditions was refractory to the recovery of a measurable amount of soluble protein. Earlier work (data not shown) to isolate glucosyltransferase enzymes from similar tissues was likewise unsuccessful, with only one tenth to one fortieth of the yield of protein observed in extractions from mature berries compared to leaves (Ford and Høj, 1998). Although the ease of transformation in model plant systems such as *Arabidopsis* provides researchers with reverse genetic tools to link genes to phenotypes, many non-model systems, including the grapevine are plagued by long regeneration timeframes and problematic species genetics. Consequently, despite their undisputed economic and cultural importance, the biology of these species remains largely unexplored. With this in mind, a more creative approach was necessary. A

combined approach using transcriptional and metabolic profiling to target a key gene in the biosynthesis of TA in grapevines was adopted. Transcriptional profiling has since been used widely in combination with metabolite analysis (Suzuki *et al.*, 2002) in the search for glucosyltransferase activities in *M. truncatulata* (Achnine *et al.*, 2005), and during fruit development in tomato (Alba *et al.*, 2005). Recent work provided a method for the interrogation of transcript data from a large collection of sequenced and catalogued grapevine cDNAs (Goes da Silva *et al.*, 2005); the research described in chapter 3 was not characterising an entire transcriptome, rather to refine the search for candidate genes expressed in tissues known to be active in TA biosynthesis. Likely involvement in TA biosynthetic reactions was further tested by examining the domain architecture of deduced protein sequences for evidence of oxidoreductase-type reaction domains. A number of potential candidates were identified by this combined approach.

To further test each of these candidate genes and in the absence of a simple transgenic assay system in grapevines, the first large scale survey of the organic acid profiles of 28 members of the family Vitaceae was achieved with the aim of correlating variation in biosynthesis with gene expression. Considerable differences in the accumulation of TA, among other acids, were observed, suggesting that the full metabolomic analysis of grape berry composition will reveal numerous metabolite differences within this plant family that can be applied to future studies. Crucial to the present investigation, one species, namely *A. aconitifolia*, was identified in which TA could not be detected. PCR analysis of berry messenger RNA and genomic DNA indicated that one candidate gene was absent from the *A. aconitifolia* genome. Over expression and enzymological characterisation confirmed the capacity of the encoded enzyme to complete a key step in TA biosynthesis, the conversion of L-idonate to 5-keto D-gluconic acid, providing the first evidence for a biochemical component of this pathway. One of most promising results, apart from aiding the discovery of the first TA biosynthetic gene, was that the species of grape that lacked the ability to form TA formed substantially greater amounts of AA. These data suggest that deletion of components of the TA pathway may create a feedback inhibition leading to accumulation of AA. Furthermore, evidence provided from the examination of precursor uptake experiments allows for the first time in any plant species a glimpse into the intricacies of the role of AA as a biosynthetic precursor, and suggests a rational basis to design grapes, already the world's most important fruit crop,

containing elevated levels of the vital human micronutrient vitamin C. Research into vitamins and nutrigenomics has demonstrated that a delicate balance between the right amount of nutrition and too much nutrition is required so as to avoid detriment to the human diet. To this end, multiyear long experiments are underway for the coming 3-5 years, to generate grapevines with the L-IdnDH gene deleted. Several constructs have been made using the HELLSGATE and KANNIBAL (CSIRO) RNAi vectors targeting various regions of the ORF, which has been shown to have an impact on phenotype knockdown (Halliwell *et al.*, 2001). These results combined to form the basis for a patent and a publication (attached with the thesis).

Much is still to be learnt about the intricacies of the kinetic parameters of the enzyme L-IdnDH. Initial biochemical characterisation indicated that in the reverse direction (catalysing the conversion of 5-keto gluconic acid to L-idonic acid) a degree of cooperativity was occurring (Figure 5.11). Moreover, preliminary size exclusion chromatography suggested that the size of L-IdnDH was larger than a monomer. L-IdnDH appears to be a very interesting enzyme and further work will take place in the Ford lab towards its understanding. The identification of L-IdnDH was the highlight of the thesis, as leading into research on this topic both literature and peers suggested it unlikely that any enzymes in the pathway would be isolated, due to previous efforts and the difficulty of working with the seasonal and genetic constraints of the woody perennial grapevine.

More than discovering the dual metabolic nature of AA in the grape (Chapter 2) and demonstrating the activity of a TA biosynthetic enzyme (Chapter 3, 4 & 5), the study extended to other genes isolated *in silico* (Chapter 6). In chapter 6 the isolation and attempted characterisation of 3 other enzymes was presented, only one of which was active. But the other two revealed several results of importance for TA synthesis. A gene with a lactone ring cleavage domain was over expressed in a prokaryote expression vector but could not be isolated in the soluble fraction for enzymatic assays. This enzyme is nonetheless worth further investigation as it is clearly a membrane bound protein and may have activity against AA, it would be useful to study this gene using reverse genetics in Arabidopsis or a similar such system. The other enzyme was a homolog to an aldehyde dehydrogenase (TSAD). Enzymatic activity of TSAD showed that activity against several substrates tested failed, but future studies using reverse genetics in a model species to gain gene function and assess phenotype may provide significant insight as the potential exists that it could

convert TA semi aldehyde to TA. The enzyme that was active was a homolog to a plant transketolase (VvTKI), and showed some remarkably interesting properties and is an enzyme that warrants much further research. It was found that this enzyme, that classically catalyses the reversible transfer of a two-carbon glycoaldehyde fragment from keto-sugars to the C-1 aldehyde of aldo sugars (Schenk *et al.*, 1998), was able to efficiently function in the OPPP, but also that 5-keto gluconic acid was a weakly compatible substrate for the in *vitro* enzyme. This reaction used 5-keto gluconic acid and eythrose 4P to form fructose 6P and TA semi aldehyde. Further study of transketolase proteins in the grapevine may reveal higher activity. Such a study would involve mining grape cDNA libraries for paraologs, over expressing them in bacteria and assessment of their enzymatic properties. Failing that, isolation of crude protein may show that endogenous protein has properties that the recombinant protein lacks. Currently the protein characterised in this study and one other paralog (VvTKII, also identified in Chapter 6) have been identified, but based on literature, several copies may exist, both in plastids and the cytosol (Caillau and Quick, 2005).

Experiments with the potential to inform viticultural practices were designed specifically to test the impact of various light regimes on the organic acid profile (Chapter 7). The significance of results arising from these experiments was able to provide a model to maximise acidity in the grape based on light exposure. This model involves maximising light exposure to the berry cluster during pre veraison development, which in turn maximises TA biosynthesis. Combining this data with studies by Coombe (1987) on temperature a model for the effects of temperature and sunlight on malic and tartaric acids is proposed (Figure 7.9). Future in-field viticultural experiments are suggested to confirm these models. Limiting the light then during post veraison development, even slightly shading limits malic acid dissimilation and will results the highest amount of acid at harvest. These results are particularly pertinent in warm climate viticulture due to the problems with low acid ripe grapes and significant exogenous additions of TA needed (see Chapter 1).

Results of this thesis have extended the understanding of TA in higher plants by providing the first biochemical evidence of the pathway. In areas where gaps remain in the research, such as characterising all the known transketolase enzymes in the grape, substantial clues have been left towards solving these problems. In several cases data from this thesis has provided future researchers with infrastructure, such as Table 3.1, which described a list of 87 differentially expressed genes in pre veraison

grape berries, Chapter 4 where results demonstrate the first thorough screen of organic acids in the family Vitaceae and in Chapter 7 the impact of light of various organic acids other than TA is described. Moreover, with a growing number of EST project in non-model plant species, where reverse genetics is complicated by the length of regeneration time, the method of isolating differentially expressed transcripts and combining this with metabolomic profiling may bring new light to uncharacterised areas of metabolism.

BIBLIOGRAPHY

Achnine, L., Huhman, D.V., Farag, M. A., Sumner, L.W., Blount, J.W. & Dixon, R.A. (2005) Genomics-based selection and identification of triterpene glycosyltransferases from the model legume *Medicago truncatula. Plant J.* **41**, 875-887.

Agius F., R. Gonzalez-Lamothe, J. L. Caballero, J. Munoz-Blanco, M. A. Botella and V. Valpuesta. (2003) Engineering increased vitamin C levels in plants by overexpression of a D-galacturonic acid reductase. *Nature Biotechnol.* **21,** 177-181.

Aharoni, A., de Vos, C.H., Verhoeven, H.A., Maliepaard, C.A., Kruppa, G., Bino, R.J. and Goodenowe, D.B. Nontargeted Metabolome Analysis by Use of Fourier Transform Ion Cyclotron Mass Spectrometry (2002) *OMICS: J. Integ. Biol.* **6,** 217–234.

Alba, R., Payton, P., Fei, Z., McQuinn, R., Debbie, P., Martin, G.B., Tanksley, S.D. and Giovannoni, J.J. (2005) Transcriptome and selected fruit metabolite analysis reveal multiple points of ethylene regulatory control during tomato fruit development. *Plant Cell* **17**, 2954-2965.

Allen, J. F. (1977) Oxygen – A physiological electron acceptor in photosynthesis. *Curr. Adv. Plant Sci.* **29,** 459-469.

Altschul, S.F., Madden, T.L., Schäffer, A.A., Zhang, J., Zhang, Z., Miller, W., Lipman, D.J. (1997) Gapped BLAST and PSI-BLAST: a new generation of protein database search programs, *Nucleic Acids Res.* **25,** 3389-3402.

Altschul, S.F., Gish, W., Miller, W., Myers, E.W. & Lipman, D.J. (1990) *J. Mol. Biol.* **215**, 403-410.

Amerine, M. A. (1956) The maturation of wine grapes. *Wines and Vines.* **37,** 1-11.

Anderson, J. W., Foyer, C. H. and Walker, D. A. (1983) Light dependant reduction of dehydroascorbate and the uptake of exogenous ascorbate by spinach chloroplasts. *Planta.* **158,** 442-450.

Antcliff, A.J. (1990) Taxonomy –The grapevine as a member of the plant kingdom. In: 'Viticulture, Vol. 1, Resources. Eds. B.G. Coombe and P.R. Dry. Winetitles, Adelaide pp. 107-118.

Arnott, H.J. and Pautard, F.G.E. (1970) Calcification in plants. In: Schraer H. (Ed), Biological calcification: cellular and molecular aspects. Appleton-Century-Crofts, New York pp. 375-420.

Arnott, H.J. and Webb, M.A. (2000) Twinned raphides of calcium oxalate in grape. *Int. J. Plant Sci.* **161**, 133-139.

Asada, A., Kusakawa, T., Orii, H., Agata, K., Watanabe, K. and Tsubaki, M. (2002) Planarian cytochrome b(561): conservation of a six-transmembrane structure and localization along the central and peripheral nervous system. *J. Biochem.* **131,** 175–182.

Banhegyi, G. & Loewus, F. A. (2004) in *Vitamin C. Functions and Biochemistry in Animals and Plants,* eds Asard, H, May, J. M. & Smirnoff, N.) BIOS. Sci. Publ. London and New York, pp33-48.

Bausch C., Peekhaus N., Utz C., Blais T., Murray E., Lowary T. and Conway T. (1998). Sequence Analysis of the GntII (Subsidiary) System for Gluconate Metabolism Reveals a Novel Pathway for L-Idonic Acid Catabolism in Escherichia coli. *J. Bacteriol.* **180,** 3704-3710.

Bausch, C., Ramsey, M., Conway, T. (2004). Transcriptional Organization and Regulation of the L-Idonic Acid Pathway (GntII System) in Escherichia coli. *J. Bacteriol.* 186: 1388-1397

Berg, H.W. and Keefer, R.M. (1958) Analytical determination of tartrate stability in wine. I. Potassium bitartrate. *Am. J. Enol. Vit.* **9**, 180-193.

Bernacchia, G., Schwall, G., Lottspeich, F., Salamini, F and Bartels, D. (1995) The transketolase family of the resurrection plant *Craterostigma plantagineum*; differential expression during rehydration phase. *EMBO J.* **14,** 610-618.

Bennetzen, J. L. and Freeling, M. (1997) The unified grass genome: synergy in synteny. *Genome Research.* **7,** 301-306.

Biemelt, S., Keetman, U. and Albrecht, G. (1998) Re-Aeration following Hypoxia or Anoxia Leads to Activation of the Antioxidative Defense System in Roots of Wheat Seedlings. *Plant Physiol.* **116**, 651–658.

Blokhina O. B., T. V. Chirkova, K. V. Fagerstedt. (2001) Anoxic stress leads to hydrogen peroxide formation in plant cells. *J. Exp. Bot.* **52,** 1179-1190.

Boss, P.K., Sensi, E., Hua, C., Davies, C. and Thomas, M. R. (2002) Cloning and characterization of grapevine (*Vitis vinifera* L.) MADS-box genes expressed during inflorescence and berry development. *Plant Sci.* **162,** 887-895.

Boss, P.K., Sreekantan, L. and Thomas, M. R. (2006) A grapevine TFL1 homolog can delay flowering and alter floral development when overexpressed in heterologous species. *Functional Plant Biol.* **33,** 31-41.

Boss, P.K. and Thomas, M. R. (2002) Association of dwarfism and floral induction with a grape "green revolution" mutation. *Nature* **416,** 847-850.

Boss, P.K., Vivier, M., Matsumoto, S., Dry, I.B. and Thomas, M. R. (2001) A cDNA from grapevine (Vitis Vinifera L.) which shows homology to AGAMOUS and SHATTERPROOF is not only expressed in flowers but also throughout berry development. *Plant Mol. Biol.* **45,** 541-553.

Boulton, R.B., Singleton, V.L., Bisson, L.F. and Kunkee, R.E. (1998) Principles and practices of winemaking. Aspen Publishers, Inc. Maryland. pp 320-322.

Bouvier F., d'Harlingue, A., Suire, C., Backhaus, R.A. and Camara, B. (1998) Dedicated roles of plastid transketolases during the early onset of isoprenoid biogenesis in pepper fruits. *Plant Physiol.* **117,** 1423-1431.

Broun, P., Shanklin, J., Whittle, E. & Somerville, C. (1997) Catalytic plasticity of fatty acid modification enzymes underlying chemical diversity of plant lipids. *Science* **282,** 1315-1317.

Buchs, M.L. (1957) Bibliography of organic acids in higher plants. *U.S.D.A. Agric. Res. Serv.* ARS-73-18.

Burns, J. J. (1967) Ascorbic acid. In, D. M. Greenberg, Metabolic Pathways, Vol 1 (pp. 394) New York: Academic Press, 3rd Edition

Buttrose, M. S., Hale, C. R. and Kliewer, M. W. (1971) Effects of temperature on the composition of "Cabernet Savignon" berries. *Am. J. Enol. Vit.* **22,** 71-75.

Cai, C.Z., Han, L.Y., Chen, X. & Chen, Y.Z. (2003) SVM-Prot: Web-Based Support Vector Machine Software for Functional Classification of a Protein from Its Primary Sequence. *Nucl. Acids Res.* **31**, 3692-3697.

Caillau, M. and Quick, P.W. (2005) New insights into plant transaldolase. *Plant Journal* **43,** 1-16.

Campbell, M. K. (1999) *Biochemistry* (Third edition) Saunders College Publishing. pp 171-178.

Chen, Z., Young, T. E., Ling, J., Chang, S.-C. & Gallie, D.R. (2003) Increasing vitamin C content of plants through enhanced ascorbate recycling. *Proc. Natl. Acad. Sci.* USA. **100**, 3525-3530.

Choi, H-K, Mun, J-H., Kim, D-J., Zhu, H., Baek, J-M., Mudge, J., Roe, B., Ellis, N., Doyle, J., Kiss, G.B., Young, N. D. and Cook, D.R. (2004) Estimating genome

conservation between crop and model legume species. *Proc. Natl. Acad. Sci.* USA. **101**, 15289-15294.

Conklin, P.L. (2001). Recent advances in the role and biosynthesis of ascorbic acid in plants. *Plant, Cell Environ.* **24,** 383-394.

Coombe, B.G. (1960) Relationship of Growth and Development to Changes in Sugars, Auxins, and Gibberellins in Fruit of Seeded and Seedless Varieties of Vitis Vinifera. *Plant Physiol.* **35,** 241-250.

Coombe B. G. (1976) The development of fleshy fruits. *Annual Review of Plant Physiology* **27,** 207–228.

Coombe B. G. (1987) Influence of temperature on composition and quality of grapes. *Acta. Hortic.* **206,** 23-35.

Coombe B. G. (1995) Adoption of a system for identifying grapevine growth stages. *Aust. J. Grape Wine Res.* **1:** 100-110.

Coombe, B.G. and Dry, P.R. (Eds.) (1988) Viticulture. *Winetitle*s, Adelaide, Australia.

Coombe, B.G. and McCarthy, M.G. (2000) Dynamics of grape berry growth and physiology of ripening. *Aust. J. Grape Wine Res.* **6,** 131-135.

Davey, M.W. C. Gilot, G. Persiau, J. Østergaard, Y. Han, G. C. Bauw, M. C. Van-Montagu. (1999) Ascorbate biosynthesis in Arabidopsis cell suspension culture. Ascorbate biosynthesis in Arabidopsis cell suspension culture. *Plant Physiol.* **121,** 535-543.

Davies, C. and Robinson, P. (2000) Differential screening indicates a dramatic change in mRNA profiles during grape berry ripening. Cloning and characterization of cDNAs encoding putative cell wall and stress response proteins. *Plant Physiol* **122,** 803-812.

DeBolt, S., Hardie, J., Tyerman S.D. and Ford, C.M. (2004) Composition and synthesis of raphide and druse crystals in berries of *Vitis vinifera* L. cv. Cabernet Sauvignon: the role of ascorbic acid as the biosynthetic precursor of both oxalic and tartaric acids is revealed by specific radio labelling studies. *Aust. J. Grape Wine Res.* **10,** 134-142.

DeBolt, S., Cook, D.R. and Ford, C.M. (2006) Tartaric acid synthesis from vitamin C in higher plants. *Proc. Natl. Acad. Sci.* USA. **103**, 5608-5613.

Delseny, M. (2004) Re-evaluating the relevance of ancestral shared synteny as a tool for crop improvement. *Curr. Op. Plant Biol.* **7,** 126-131.

Demmig, B., Winter, K., Kruger, A. and Cygan, F-C. (1987) Photoinhibition and zeaxanthin formation in intact leaves. A possible role of xanthophyll cycle in the dissipation of light energy. *Plant Physiol.* **84,** 218-224.

Devos, K. M. and Gale, M. D. (2000) Genome Relationships: The Grass Model in Current Research. *Plant Cell.* **12,** 637-646.

Dixon, R.A. and Steele, C,L. (1999) Flavonoids and isoflavonoids – a gold mine for metabolic engineering *Trends Plant Sci.* **4,** 394-400.

Dry, P.R. and Smart, R.E., (1988) Vineyard site selection: *in* Coombe, B.G. and Dry, P.R. (eds.), Viticulture; Winetitles, Adelaide, Australia.

Dunsford, P. and Boulton, R. (1981) The kinetics of potassium bitartrate crystallization from table wines. I. Effect of particle size, particle surface area and agitation. *Am. J. Enol. Vit.* **32**, 100-105.

Emmerlich, V., Linka, N., Reinhold, T., Hurth, M.A., Traub, E.M. and Neuhaus, H.E. (2003) The plant homolog to the human sodium.carboxylic cotransporter is the vacuolar malater carrier. Proc. Natl. Acad. Sci. USA **100**, 11122-11126.

Esau, K. (1965) Anatomy and cytology of *Vitis* phloem. *Hilgardia* **37**, 17-27.

Ewing, R.M., Ben Kahla, A., Poirot, O., Lopes, F., Audic, S. and Claverie, J-M. (1999) Large-scale statistical analysis of rice ESTs reveal correlated patterns of gene expression. *Genome Res.* **9,** 950-959.

Famiani, F., Walker, R.P., Tesci, L., Chen, Z-H., Proietti, P. and Leegood, R.C. (2000) An immunohistochemical study of the compartmentation of metabolism during the development of the grape *Vitis vinifera* L. berries. *J. Exp. Bot.* **345,** 675-683.

Famiani, F., Cultrera, N., Battistelli, A., Casulli, V., Proietti, P., Standardi, A., Chen, Z-H., Leegood, R.C. and Walker R. P. (2005) Phosphoenolpyruvate carboxykinase and its potential role in the catabolism of organic acids in the flesh of soft fruit during ripening. *J. Exp. Bot.* **56,** 2959-2969.

Fedorova, M., van de Mortel, J., Matsumoto, P.A., Cho, J., Town, C.D., VandenBosch, K.A., Gantt, J.S. and Vance, C.P. (2002) Genome-wide identification of nodule-specific transcripts in the model legume *Medicago truncatula. Plant Physiol* **130,** 519-537.

Fernandez, L., Romieu, C., Moing, A., Bouquet, A., Maucourt, M., Thomas, M.R. and Torregrosa, L. (2006) The grapevine *fleshless berry* mutation. A unique genotype to investigate the difference between fleshy and fleshless fruit. *Plant Physiol.* **140,** 537-547.

Flechner, A., Dressen, U., Westhoff, P., Henze, K., Schnarrenberger, C. and Martin, W. (1996) Molecular characterisation of transketolase (EC 2.2.1.1) active in the Calvin cycle of spinach chloroplasts. *Plant Mol. Bio.* **32,** 475-484.

Flexas, J., Badger, M., Chow, W.S., Medrano, H. and Osmond, C.B. (1999) Analysis of the Relative Increase in Photosynthetic O_2 Uptake When Photosynthesis in Grapevine Leaves Is Inhibited following Low Night Temperatures and/or Water Stress. *Plant Physiol.* **117;** 675–684.

Ford, C. M. and Høj, P. B. (1998) Multiple glucosyltransferase activities in grapevine. *Aust. J. Grape Wine Res.* 4, 48-58.

Fowles, G. W. A. (1992) Acids in Grapes and Wines: A Review. *J. Wine Res.* **3,** 25-41.

Francisco J.P., Villegas, D. and Mejia N. (2002) Ascorbic acid and flavonoid peroxidase reaction as a detoxifying system of H2O2 in grapevine tissue. *Phytochem.* **60,** 573-580.

Franceschi, V.R. and Nakata, P.A. (2005) Calcium Oxalate in Plants: Formation and Function. *Ann. Rev. Plant Biol.* **56,** 41-71.

Fryer, M.J., Andrews, J.R., Oxborough, K., Blowers, D.A. and Baker, N.R. (1998) Relationship between CO_2 Assimilation, Photosynthetic Electron Transport, and Active O_2 Metabolism in Leaves of Maize in the Field during Periods of Low Temperature, *Plant Physiol.* **116**: 571–580

Gatzek S., Wheeler, G. L. and Smirnoff, N. (2001). Antisense suppression of L-galactose dehydrogenase in *Arabidopsis thaliana* provides evidence for its role in ascorbate synthesis and reveals light modulating L-galactose synthesis. *Plant J.* **30,** 541-553.

Gebhardt, S. E., and Thomas, R. G. (2002) The Nutritive Value of Foods. U.S Department of Agriculture, *Agriculture Research Service, Home and Garden Bulletin* 72.

Gerlt, J.A. and Babbit, P.C. (2000) Can sequence determine function? *Genome Biol. Rev.* **1,** 1-11.

Goes da Silva, F., Iandolino, A., Al-Kayal, F., Bohlmann, M. C., Cushman, M. A., Lim, H., Ergul, A., Figueroa, R., Kabuloglu, E. K., Osborne, C., Rowe, J., Tattersall, E., Leslie, A., Xu, J., Baek, J., Cramer, G.R., Cushman, J.C. and Cook, D.R. (2005)

Characterizing the Grape Transcriptome. Analysis of Expressed Sequence Tags from Multiple Vitis Species and Development of a Compendium of Gene Expression during Berry Development. *Plant Physiol.* **139**, 574-597.

Gorestein, S., Zemser, M., Vargasalbores, F. and Ochoa, J.L. (1995) Classification of seven species of cactaceae based on their chemical and biochemical properties. *Biosci., Biotechnol. Biochem.* **59**, 2022–2027.

Green, M.A. and Fry, S.C. (2005) (B) Vitamin C degradation in plant cells via enzymic hydrolysis of 4-O-oxalyl-L-threonate. *Nature.* **433,** 83-87.

Green, M.A. and Fry, S.C. (2005) (A) Apoplastic degradation of ascorbate: novel enzymes and metabolites permeating the plant cell wall. *Plant Biosys.* **139,** 2-7.

Haberlandt, G. (1914) Physiological Plant Anatomy. Macmillan and Co, London, pp 530 – 531.

Hale, C. R. (1962) Synthesis of organic acids in the fruit of the grape. *Nature* **195,** 917-918.

Hale, C. R. (1977) Relation between potassium and the malate and tartrate contents of the grape berry. *Vitis* **16,** 9-19.

Hardie, J. W. (2000) Grapevine biology and adaptation to viticulture. *Aust. J. Grape Wine Res.* **6**, 74-81.

Hardie, J.W., O'Brien, T.P. and Jaudzems, V.G. (1996) Morphology, anatomy and development of the pericarp after anthesis in grape, *Vitis vinifera* L. *Aust. J. Grape Wine Res.* **2,** 97-142.

Harris J. M., Kriedermann, P.E. and Possingham, J.V. (1968) Anatomical aspects of grape berry development. *Vitis* **7**, 106-119.

Helliwell, C.A., Varsha, A, Wesley, S., Wielopolska, A.J. and Waterhouse, P.M. High throughput vectors for efficient gene silencing in plants. *Funct. Plant Biol.* **29,** 1217-1225.

Henikoff, S., Greene, E. A., Pietrokovski, S., Bork, P., Attwood, T. K. & Hood, L. (1997) Gene Families: The Taxonomy of Protein Paralogs and Chimeras. *Science* **278,** 609-614.

Henkes, S., Sonnewald, U., Badur, R., Flachmann, R. and Stitt, M. (2001) A small decrease of plastid transketolase activity in antisense tobacco transformants has dramatic effectson photosynthesis and phenylpropanoid metabolism. *Plant Cell.* **204,** 535-551.

Hough, L. and Jones, K.N. (1956) The biosynthesis of monosaccharides. *Adv. Carb. Chem.* **11**, 185-262 pp. 240

Hunman, D.V. and Sumner, L.W. (2002) Metabolioc profiling of saponins in *Medicago sativa* and *Medicago truncatula* using HPLC coupled to an electrospray ion-trap mass spectometer. *Phytochem.* **59**, 347–360.

Iandolino, A.B., Goes da Silva, F., A., Lim, H., Choi, Williams, L.E. & Cook, D.R. (2004) High quality RNA, cDNA and derived EST libraries from grapevine (*Vitis vinifera* L.). *P. Mol. Bio. Rep.* **22,** 269-278.

Iland, P.G., and Coombe, B.G. (1988) Malate, tartrate, potassium, and sodium in flesh and skin of Shiraz grapes during ripening: Concentration and compartmentation. *Am. J. Enol. Vitic.* **39,** 71-76.

Isherwood, F.A., Chen, Y.T. and Mapson, L.W. (1954) Synthesis of L-ascorbic acid in plants and animals. *Biochem. J.* **56**, 1-15.

Israel, D. W. and Jackson, W.A. (1982) Ion balance, uptake and transport processes in N2-fixation and nitrate and urea-dependant soybean plants. *Plant physiol.* **69**, 171-178.

Jackson, D.I. (1986). Factors Affecting Soluble Solids, Acid, pH, and Color in Grapes. *Am. J. Enol. Vitic.* **37**, 179-183.

Jackson, R.S. (2000) "Wine Science: Principles, Practice, Perception," Academic Press, 2nd ed, pp. 65-87.

Jalal, M.A.F., and Collin, H.A. (1977) Polyphenols of mature plant, seedling and tissue cultures of Theobroma cacao. *Phytochem.* **16,** 1377-1380.

Kasahara, M., Kagawa, T., Oikawa, K., Suetsugu, N., Miyao M. and Wada, M. (2002) Chloroplast avoidance movement reduces photodamage in plants. *Nature.* **420,** 829-833.

Kliewer, W. M. (1965) Changes in the Concentration of Malates, Tartrates, and total free Acids in Flowers and Berries of Vitis vinifera. *Am. J. Enol. Vitic.* **16,** 92-100.

Kliewer, W.M. (1966) Sugars and organic acids of Vitis vinifera. *Plant Physiol.* **41**, 923-931.

Kliewer, W.M. (1967) Annual cyclic changes in the concentration of free amino acids in grapevines. *Am. J. Enol. Vitic.* **18**, 126-137.

Kliewer, W. M. and Schultz, H.B. (1964) Influence of Environment on Metabolism of Organic Acids and Carbohydrates in *Vitis Vinifera.* II. *Am. J. Enol. Vitic.* **15,** 119-129.

Kobayashi, S., Goto-Yamamoto, N. and Hirochika, H. (2004) Retrotransposon-Induced Mutations in Grape Skin Color. *Science (Brevia).* **304**, 982.

Kostman, T.A., Tarlyn, N.M., Loewus, F.A. and Franceschi, V.R. (2001) Biosynthesis of L-ascorbic acid and conversion of carbons 1 and 2 of L-ascorbic acid to oxalic acid

occurs within individual calcium oxalate crystal idioblasts. *Plant Physiol.* **125**, 634-640.

Kostman, T.A. and Koscher, J.R. (2003) L-galactono-γ-lactone dehydrogenase is present in calcium oxalate crystal idioblasts of two plant species. *Plant Physiol. Biochem.* **41**, 201-206.

Leigh, R.A. and Storey, R. (1993) Intercellular compartmentation of ions in barley leaves in relation to potassium. *J. Exp. Bot.* **44**, 755–762.

Li, X., Zhang, D., Lynch Holm, V.M. Okita, T.W. and Franceschi, V.R. (2003) Isolation of a crystal matrix protein associated with calcium oxalate precipitation in vacuoles of specialised cells. *Plant Physiol.* **133**, 549-559.

Lindqvist, Y., Schneider, G., Ermler, U. and Sundstrom, M. (1992) Three dimensional structure of transketolase, a thiamine diphosphate dependant enzyme, at 2.5 A resolution. *EMBO J.* **11,** 2373-2379.

Loewus, F.A. (1999) Biosynthesis and metabolism of ascorbic acid in plants and of analogs of ascorbic acid in fungi. *Phytochem.* **52,** 193-210.

Loewus, F.A. and Stafford, H.A. (1958) Observations on the incorporation of 14C into tartaric acid and the labelling pattern of D-glucose from an excised grape leaf administered L-ascorbic acid 6-14C. *Plant Physiol.* **33**, 155-156.

Malipiero, U., Ruffner, H.P. and Rast, D. M. (1987) Ascorbic to tartaric acid conversion in grapevines. *J. Plant Physiol.* **129,** 33-40.

Mandel, M.A., Feldmann, K.A., Herrara-Estrala, L., Rocha-Sosa, M. and Leon, P. (1996) *CLA1* a novel gene required for chloroplast development, is highly conserved in evolution. *Plant J.* **9,** 649-658.

Mazen, A.M.A., Zhang, D. and Franceschi, V.R. (2003) Calcium oxalate formation in *Lemna minor*: physiological and ultrastructural aspects of high capacity calcium sequestration. *New Phytologist* **161**, 435-448.

Molano-Flores, B. (2001) Herbivory and calcium concentrations affect calcium oxalate crystal formation in leaves of *Sida* (*Malvaceae*). *Ann. Bot.* **88**, 387-391.

Moore, S., Payton, P., Wright, M., Tanksley, S. and Giovannoni, J. (2005) Utilization of tomato microarrays for comparative gene expression analysis in the Solanaceae. *J. Exp. Bot.* **56,** 2885 – 2895.

Mpelasoka, B.B., Schachtman, D.P., Treeby, M.T. and Thomas, M.R. (2003) A review of potassium nutrition in grapevines with special emphasis on berry accumulation. *Aust. J. Grape Wine Res.* **9**, 154-168.

Mulder NJ, Apweiler R, Attwood TK, Bairoch A, Bateman A, Binns D, Bradley P, Bork P, Bucher P, Cerutti L, et al., InterPro, progress and status in 2005 (2005) *Nucleic Acids Res.* **33**, D201-D205.

Mulder NJ, Apweiler, R., Attwood, T. K., Bairoch, A., Bateman, A., Binns, D., Biswas M., Bradley, P., Bork, P., Bucher, P., Copley, R., Courcelle, E., Durbin, R., Falquet, L., Fleischmann, W., Gouzy, J., Griffith-Jones, S., Haft, D., Hermjakob, H., Hulo, N., Kahn, D., Kanapin, A., Krestyaninova, M., Lopez, R., Letunic, I., Orchard, S., Pagni, M., Peyruc, D., Ponting, C. P., Servant, F., and Sigrist, C. J. A. (2002) InterPro: An integrated documentation resource for protein families, domains and functional site. *Briefings in Bioinfo.* **3,** 225-235.

Nakata, P.A. (2003) Advances in our understanding of calcium oxalate crystal formation and function in plants. *Plant Sci.* **164**, 901-909.

Nassar, A. R. and Kliewer, W. M. (1966) Free aminoacids in various parts of *Vitis vinifera* at different stages of development. *Am. Soc. for Hort. Sci.* **89**: 282-294.

Nikkola, M., Lindqvist, Y. and Schneider, G. (1994) Refined structure of transketolase from *Saccaromyces cerevisiae* at 2.0A resolution. *J. Mol. Bio.* **238,** 387-404.

Northcote, K. H. (1988) Soils and Australian Viticulture. In 'Viticulture, Vol. 1: resources' (Eds. B.G. Coombe and P.R. Dry) pp. 61-90. Australian Industrial Publishers, Adelaide.

Pasteur, L. (1860) Recherches sur la Dissymetry Moleculair, *Compt. Rend.* **51**, 298.

Perrson, S., Wei, H., Milne, J., Page, G.P. and Somerville, C.R. (2005) Large scale coexpression analysis reveals novel genes involved in cellulose biosynthesis. *Proc. Natl. Acad. Sci.* USA. **102,** 8633-8638.

Possner D.R.E. and Kleiwer, W.M. (1985) The localisation of acids, sugars, potassium and calcium in developing grape berries. *Vitis*, 24: 229-240.

Pratt, C. (1971) Reproductive anatomy in cultivated grapes-a review. *Am. J. Enol. Vitic.* **22,** 93-109.

Ristic, R. (2004) A study of seed development and phenolic compounds in seeds, skins and wines of Vitis vinifera L. cv Shiraz. *PhD Thesis.* The University of Adelaide, Australia.

Rodriguez-Clemente, R. and Correa-Gorospe, I. (1988) Structural, morphological, and kinetic aspects of potassium hydrogen tartrate precipitation from wines and ethanolic solutions. *Am. J. Enol. Vitic.* **39**, 169-179.

Ronning, C.M., Stegalkina, S.S., Ascenzi, R.A., Bougri, 0., Hart, A.L., Utterbach, T.R,. Vanaken, S.E., Riedmuller, S.B., White, J.A., Cho, J., Pertea, G.M., Lee, Y., Karamycheva, S., Sultana, R., Tsai, J., Quackenbush, J., Griffiths, H.M., Restrepo, S., Smart, C.D., Fry, W.E., van der Hoeven, R., Tanksley, S., Zhang, P., Jin, H., Yamamoto, M.L., Baker, B.J. and Buell, C.R. (2003) Comparative analyses of potato expressed sequence tag libraries. *Plant Physiol* **131**, 419-429.

Ruffner, H.P. (1982). Metabolism of tartaric and malic acids in Vitis: A review. *Vitis.* **21,** 346-358.

Ruffer H. P. and C. R. Hale. 1976. Temperature and enzymic control of malate metabolism in berries of Vitis vinifera. *Phytochem.* **15**, 1877-1880.

Ruffner, H.P. and Kliewer, W.M. (1975) Phosphenolpyruvate carboxykinase activity in grape berries. *Plant Physiol.* **56,** 67-71.

Ruffner, H.P., Possner, D., Brem, S. and Rast, D. (1984) The physiological role of malic enzyme in grape ripening. *Planta* **160,** 444-448.

Saito, K. (1994) Specific transfer of 3H from D-[3-3H]Gluconic acid into L-tartaric acid in vitaceous plants. *Phytochem.* **37**,1017-1022.

Saito, K. and Kasai, Z. (1969) Tartaric acid synthesis from L-Ascorbic acid-C-14 in grape berries. *Phytochem.* **8,** 2177-2182.

Saito, K. and Kasai, K. (1978) Conversion of labeled structures to sugars, cell wall polysaccarides, and tartaric acid in grape berries. *Plant Physiol.* **62**, 215-219.
Saito, K. and Kasai, Z. (1968) Accumulation of tartaric acid in the ripening process of grape. *Plant Cell Physiol.* **9,** 529-537.

Saito, K. and Kasai, Z. (1982) Conversion of L-ascorbic acid to L-idonic acid, L-idono gamma-lactone and 2-keto-L-idonic acid in slices of immature grapes (Vitis labrusca cultivar Delaware). *Plant Cell Physiol.* **23,** 499-508.

Saito, K. and Kasai, Z. (1984) Synthesis of L-(dextro)-tartaric acid from L-ascorbic acid via 5-keto-D-gluconic acid in grapes (Vitis labrusca cultivar Delaware). *Plant Physiol.* **76,**170-174.

Saito, K. and Loewus, F.A. (1979). The metabolism of L-[6-14C]ascorbic acid in detached grape leaves. *Plant Cell Physiol.* **20**,1481-1488.

Saito, K. and Loewus, F.A. (1989a) Formation of L-dextro-tartaric acid in leaves of the bean, Phaseolus vulgaris L.: Radioisotopic studies with putative precursors. *Plant Cell Physiol.* **30,** 629-636.

Saito, K. and Loewus, F.A. (1989b) Formation of tartaric acid in vitaceous plants: Relative contributions of L-ascorbic acid-inclusive and acid-noninclusive pathways. *Plant Cell Physiol.* **30**, 905-910.

Saito, K. and Loewus, F.A. (1989c) Occurrence of dextro-tartaric acid and its formation from D-gluconate or D-xylo-5-hexulosonate in bean leaf (Phaseolus vulgaris L.). *Plant Sci.* **62**,175-180.

Saito, K., Morita, S.I. and Kasai, Z. (1984) Synthesis of L-dextro-tartaric acid from 5-keto-D-gluconic acid in Pelargonium. *Plant Cell Physiol.* **25**, 1223-1232.

Saito, K., Ohmoto, J. and Kuriha, N. (1997) Incorporation of O-18 into oxalic, L-threonic and L-tartaric acids during cleavage of L-ascorbic and 5-keto-D-gluconic acids in plants. *Phytochem.* **44**, 805-809.

Salusjarvi, T., Povelainen, M., Hvorslev, H., Eneyskaya, E. V., Kulminskaya. A. A., Shabalin, K. A., Neustroev, K. N., Kalkkinen, N. and Miasnikov, A. N. (2004) Cloning of a gluconate/polyol dehydrogenase gene from Gluconobacter suboxydans IFO 12528, characterisation of the enzyme and its use for the production of 5-ketogluconate in a recombinant *Escherichia coli* strain. *Appl Microbiol Biotechnol.* **65**, 306-314.

Schenk, G., Layfield, R., Candy, J.M., Duggleby, R.G. and Nixon, P.F. (1997) Molecular evolutionary analysis of the thiamine dependant enzyme, tranketolase. *J. Mol. Evol.* **44,** 552-572.

Schenk, G., Duggleby, R.G. and Nixon, P.F. (1998) Properties and functions of the thiamin diphosphate dependent enzyme transketolase. *Int. J. Biochem. Cell. Biol.* **30,** 1297-1318.

Schnarrenberger, C., Flechner, A. and Martin, W. (1995) Enzymatic evidence for a complete oxidative pentose phosphate pathway in chloroplasts and an incomplete pathway in the cytosol of spinach leaves. *Plant Physiol.* **108,** 609-614.

Seymour, G.B., Taylor, J.E. and Tucker, G.A. (1993) Biochemistry of Fruit Ripening. Chapman and Hall, London

Shigeoka S., Nakano, Y. and Kitaoka, S. (1979) Some properties and subcellular localisation of L-gulono-1,4-lactone dehydrogenase in *Euglena gracilis* z. *Agric. Biol. Chem.* **43**, 2187-2188.

Singla-Pareek, S.L., Reddy, M.K. and Sopory. S.K. (2003) Genetic engineering of the glyoxalase pathway in tobacco leads to enhanced salinity tolerance
Smirnoff N. (2000) Ascorbic acid: metabolism and functions of a multi facetted molecule. *Current Opinion in Plant Biology*. **3,** 229-235. *Proc. Natl. Acad. Sci.* USA. **100,** 14672-14677.

Smirnoff, N. (1996) The function and metabolism of ascorbic acid in plants. *Ann Bot.* **78,** 661-669.

Smirnoff, N. (2000) Ascorbic acid: metabolism and functions of a multi facetted molecule. *Cur. Op. Plant Biol.* **3,** 229-235.

Smith, JL, Zaluzec, E.J., Wery, J.P., Nui, L.W., Switzer, R.L., Zalkin, H. and Satow, Y. (1994) Structure of the allosteric regulatory enzyme of purine biosynthesis. *Science* **264,** 1427-1433.

Somerville, C.R (2006) Cellulose Synthesis in Higher Plants. *Annual Review of Cell and Developmental Biology.* **22,** pages to be advised.

Stafford, H. A. (1959) Distribution of tartaric acid in the leaves of certain angiosperms. *Am. J. Bot.* **46,** 347-352.

Stafford, H. A. (1957) Tartaric acid dehydrogenase activity in higher plants. *Plant Physiol.* **33,** 194-199.

Stekel, D.V., Git, Y. and Falciani, F. (2000) The comparison of gene expression from multiple cDNA libraries. *Genome Res.* **10,** 2044-2061.

Storey, R. (1987) Potassium localization in the grape berry pericarp by energy dispersive X-ray microanalysis. *Am. J. Enol. Vitic.* **38,** 301-309.

Storey, R., Jones, G.W., Schachtman, D.P. and Treeby, M.T. (2003) Calcium-accumulating cells in the meristematic region of grapevine root apices. *Funct. Plant Biol.* **30**, 719-727.

Stumpf D. K. and Burris, R.H. (1979) A micromethod for the purification and quantification of organic acids of the dicarboxylic acid cycle in plants. *Analyt. Biochem.* **95,** 311-315.

Sumner, L., Mendes, P. and Dixon, R.A. (2003) Plant metabolomics: large-scale phytochemistry in the functional genomics era. Phytochemistry. **62,** 817–836.

Suzuki, H., Achnine, L., Xu, R. Matsuda, S.P.T. & Dixon, R.A. (2002) A genomics approach to the early stages of triterpene saponin biosynthesis in *Medicago truncatula. Plant J.* **32**, 1033-1048.

Takagi, Y. (1962) Reduction of 5-keto-D gluconic acid to idonic acid by Fusarium species. *Agr. Biol. Chem.* **26**, 717-718.

Takagi, Y. (1962) A new enzyme: 5-keto glucono-idono-reductase. *Agr. Biol. Chem.* **26**, 719-720.

Takimoto, K., Saito, K. and Kasai, Z. (1976). Diurnal change of tartrate dissimilation during the ripening of grapes. *Phytochem.* 15, 927-930.

Terrier N., C. Deguilloux, F.-X. Sauvage, E. Martinoia and C. Romieu. (1998) Proton pumps and anion transport in Vitis vinifera: the inorganic pyrophosphatase plays a predominant role in energization of the tonoplast. *Plant Physiol. Biochem.* **36**, 367-377.

Terrier, N. and Romieu, C. (2001) Grape berry acidity. In: Molecular Biology and Biotechnology of the Grapevine (Ed: K. A. Roubelakis-Angelakis) pp. 35-54. Kluwer Academic Publishers, Netherlands.

Terrier N., Glissant, D., Grimplet, J., Barrieu, F., Abbal, P., Couture, C., Ageorges, A., Atanassova, R., Leon, C., Renaudin, J.-P., Dedaldechamp, F., Romieu, C., Delrot, S. and Hamdi, S. (2005) Isogene specific oligo arrays reveal multifaceted changes in gene expression during grape berry (*Vitis vinifera* L.) development. *Planta* **222,** 832–847.

Tyerman, SD., Tilbrook, J., Pardo, C., Kotula, L., Sullivan, W. and Steudle, E. (2004) Direct measurement of hydraulic properties in developing berries of Vitis vinifera L. cv Shiraz and Chardonnay, *Aust. J. Grape Wine Res.* **10**, 170-181.

Van der Hoeven, R., Ronning, C., Giovannoni, J., Martin, G. and Tanksley, S. (2002) Deductions about the Number, Organization, and Evolution of Genes in the Tomato Genome Based on Analysis of a Large Expressed Sequence Tag Collection and Selective Genomic Sequencing. *Plant Cell* **14,** 1441-1456.

von Schaewen, A., Lengenkamper, G., Graeve, K., Wenderoth, I. and Scheibe, R. (1995) Molecular characterisation of the plastidic glucose-6-phosphate dehydrogenase from potato in comparison to its cytosolic counterpart. *Plant Physiol.* **109,** 1327-1335.

Wagner, G., and Loewus, F.A. (1973) The biosynthesis of L(+)-tartaric acid in Pelargonium crispum. *Plant Physiol.* **52**, 651-654.

Wagner, G., Yang, J.C. and Loewus, F.A. (1975) Stereoisomeric characterization of tartaric acid produced during L-ascorbic acid metabolism in plants. *Plant Physiol.* **55**, 1071-1073.

Walker R. P. and Chen, Z-H. (2002) Phosphoenolpyruvate carboxykinase, structure, function and regulation. *Adv. Bot. Res.* **38,** 93-189.

Webb, M.A. (1999) Cell mediated crystallization of calcium oxalate in plants. *Plant Cell* **11**, 751-761.

Webb, M.A., Cavaletto, J.M., Carpita, N.C., Lopez, L.E. and Arnott, H.J. (1995) The intravacuolar organic matrix associated with calcium oxalate crystals in leaves of *Vitis*. *Plant J.* **7**, 633-648.

Wheeler G.L., Jones, M.A. and Smirnoff, N. (1998) The biosynthetic pathway of vitamin C in higher plants. *Nature*. **393**, 365-369.

White, P.J. and Broadley, M.R. (2003) Calcium in plants. *Ann. Bot.* **92**, 487-511.

Williams, M., and Loewus, F.A. (1978) Biosynthesis of (+)-tartaric acid from l-[4-14C] ascorbic acid in grape and geranium. *Plant Physiol.* **61**, 672-674.

Williams, M., Saito, K. and F.A. Loewus. (1979) Ascorbic acid metabolism in geranium and grape. *Phytochem.* **18,** 953-956.

Winkler, A.J., Cook, J.A., Kleiwer, W.M. and Lider, L.A. (1962) General Viticulture, pp. 126. The University of California Press, Berkeley.

Winkler, A.J., Cook, J.A., Kleiwer, W.M. and Lider, L.A. (1974) General Viticulture, pp. 138-196. The University of California Press, Berkeley.

Yang J. C. and Loewus, F.A. (1975) Metabolic conversion of L-ascorbic acid to oxalic acid in oxalate-accumulating plants. *Plant Physiol.* **56**, 283-285

Zhang, F., Fangmei, L. and Dabin, G. (1990) Studies on germplasm resources of wild grape species (Vitis spp.) in China. *Vitis* Special issue, *Proceedings of the 5th International Symposium on Grape Breeding*. pp 50-57.